

---

# The Quantum Substructure of Gravity

Sebastian Zell

---



München 2019



---

# The Quantum Substructure of Gravity

Sebastian Zell

---

Dissertation  
an der Fakultät für Physik  
der Ludwig-Maximilians-Universität  
München

vorgelegt von  
Sebastian Zell  
aus München

München, den 14. Mai 2019

Erstgutachter: Prof. Dr. Georgi Dvali

Zweitgutachter: Prof. Dr. César Gómez

Tag der mündlichen Prüfung: 28. Juni 2019

# Contents

<b>Zusammenfassung</b>	<b>vii</b>
<b>Abstract</b>	<b>ix</b>
<b>Publications</b>	<b>xi</b>
<b>1 Introduction</b>	<b>1</b>
1.1 High Energy Physics after Planck, LHC and LIGO . . . . .	1
1.1.1 Challenges . . . . .	1
1.1.2 New Perspectives . . . . .	2
1.2 Conventions . . . . .	4
1.3 Quantumness on Macroscopic Scales . . . . .	4
1.3.1 Black Holes . . . . .	4
1.3.2 De Sitter . . . . .	12
1.4 Entropy Under the Microscope . . . . .	16
1.5 Infrared Physics . . . . .	17
1.6 Outline . . . . .	19
<b>2 Quantum Breaking</b>	<b>21</b>
2.1 General $\hbar$ -Scaling of Timescales . . . . .	22
2.2 A Basic Example . . . . .	24
2.2.1 Classical Solution . . . . .	24
2.2.2 Deviations from the Classical Evolution . . . . .	26
2.2.3 Other Scattering Processes . . . . .	32
2.2.4 Nonrelativistic Model . . . . .	35
2.2.5 Summary . . . . .	38
2.3 Application to Cosmic Axions . . . . .	39
2.3.1 Importance of a Classical Description of Dark Matter Axions	39
2.3.2 Axion Properties . . . . .	40
2.3.3 Quantum Break-Time . . . . .	44
2.3.4 Validity of Our Simplifications . . . . .	45
2.3.5 Undercriticality of Cosmic Axions . . . . .	47
2.3.6 Relationship to Other Work . . . . .	50

2.4	Application to de Sitter . . . . .	52
2.4.1	A Quantum Description of the de Sitter Metric . . . . .	52
2.4.2	Uncovering the Quantum Origin of Classical Evolution . . . . .	63
2.4.3	Gibbons-Hawking Particle Production as Decay of the de Sitter State . . . . .	70
2.4.4	Quantum Break-Time . . . . .	76
2.4.5	Implications for the Cosmological Constant . . . . .	81
2.4.6	Implications for Inflation . . . . .	82
2.5	Implications of Quantum Inconsistency of de Sitter . . . . .	85
2.5.1	Exclusion of Self-Reproduction in Inflation . . . . .	86
2.5.2	Exclusion of de Sitter Vacua . . . . .	88
<b>3</b>	<b>Storage of Quantum Information</b>	<b>95</b>
3.1	Enhanced Memory Capacity in Attractive Cold Bosons . . . . .	96
3.1.1	Storage of Information in Gapless Modes . . . . .	96
3.1.2	Assisted Gaplessness . . . . .	99
3.1.3	Simulating Black Holes and Others in the Laboratory . . . . .	102
3.1.4	The $C$ -Number Method . . . . .	105
3.2	Prototype Model: 3-Mode System . . . . .	113
3.2.1	Introduction of Bose Gas with Dirichlet Boundary Conditions	113
3.2.2	Critical Point with Gapless Mode . . . . .	119
3.2.3	Neural Network Analogue . . . . .	126
3.3	Memory Burden . . . . .	130
3.3.1	General Mechanism . . . . .	130
3.3.2	Application to de Sitter . . . . .	134
3.3.3	Application to Black Holes . . . . .	138
<b>4</b>	<b>Infrared Physics and Information</b>	<b>141</b>
4.1	Review of Infrared Physics . . . . .	142
4.1.1	Tree Level Processes: Soft Theorem . . . . .	142
4.1.2	Charge Conservation . . . . .	144
4.1.3	Loop Corrections: Infrared Divergences . . . . .	147
4.1.4	Taking Emission into Account: Inclusive Formalism . . . . .	149
4.1.5	Modifying Asymptotic States: Dressed Formalism . . . . .	150
4.1.6	Introduction to von Neumann Spaces . . . . .	153
4.1.7	Dressing from Asymptotic Dynamics . . . . .	155
4.1.8	Collinear Divergences . . . . .	157
4.2	Combined Formalism . . . . .	158
4.2.1	Equivalence Classes as Radiative Vacua . . . . .	158
4.2.2	Calculation of Final State . . . . .	160
4.2.3	Large Gauge Transformations and Dressing . . . . .	164
4.3	Reduced Density Matrix . . . . .	165
4.3.1	Well-Defined Tracing . . . . .	165

4.3.2	Generalization to Superposition as Initial State . . . . .	168
4.3.3	Estimate of Amount of Decoherence . . . . .	169
4.3.4	Implications for Optical Theorem . . . . .	172
4.4	Implications for Black Holes . . . . .	173
4.4.1	Information in Soft Modes . . . . .	173
4.4.2	BMS Symmetries and Memory Effect . . . . .	176
4.4.3	Study of BMS Hair . . . . .	182
4.4.4	Black Hole Quantum Hair . . . . .	185
4.4.5	Relationship to Black Hole N-Portrait . . . . .	189
<b>5</b>	<b>Future Perspectives</b>	<b>191</b>
5.1	Summary . . . . .	191
5.1.1	Quantum Breaking . . . . .	191
5.1.2	Storage of Quantum Information . . . . .	193
5.1.3	Infrared Physics and Information . . . . .	194
5.1.4	Overall Conclusions . . . . .	196
5.2	Outlook . . . . .	196
<b>A</b>	<b>Appendix</b>	<b>199</b>
A.1	Concerning Chapter 2 . . . . .	199
A.1.1	Calculation of the Rate of Particle Production . . . . .	199
A.2	Concerning Chapter 3 . . . . .	200
A.2.1	Review of Periodic Bose Gas . . . . .	200
A.2.2	Formulas . . . . .	202
A.3	Concerning Chapter 4 . . . . .	204
A.3.1	Matching in Schwarzschild Coordinates . . . . .	204
A.3.2	Explicit Solution for Goldstone Supertranslation of a Planet . . . . .	205
	<b>Bibliography</b>	<b>211</b>
	<b>Acknowledgments</b>	<b>231</b>



# Zusammenfassung

In dieser Arbeit identifizieren und untersuchen wir verschiedene universelle Quantenphänomene, die insbesondere, aber bei Weitem nicht ausschließlich, relevant für Gravitation sind.

Im ersten Teil beschäftigen wir uns mit der Frage, wie lange ein generisches Quantensystem als klassisch angenähert werden kann. Wir benutzen ein Skalarfeld mit Selbstwechselwirkung als prototypisches Model, um mögliche Skalierungen der Quantenbruchzeit  $t_q$  zu diskutieren, nach der die klassische Beschreibung zusammenbricht. Anschließend wenden wir diese Analyse auf das hypothetische QCD-Axion an. Unser Ergebnis ist, dass die Näherung als klassisch oszillierendes Skalarfeld extrem genau ist. Als Nächstes untersuchen wir de Sitter. Dabei ist unser Ansatz, die klassische Metrik als Multigraviton-Zustand, der auf Minkowski-Vakuum definiert ist, auszulösen. Auf der einen Seite schafft es dieses zusammengesetzte Bild von de Sitter, alle bekannten (semi-)klassischen Eigenschaften zu reproduzieren. Auf der anderen Seite führt es zu einem Zusammenbruch der Beschreibung durch eine klassische Metrik nach der Zeitskala  $t_q = 1/(G_N H^3)$ , wobei  $G_N$  die Gravitationskonstante ist und  $H$  der Hubble-Parameter. Dieses Resultat zieht wichtige Einschränkungen für inflationäre Szenarien nach sich. Aufgrund von Anzeichen, dass Quantenbrechen im Spezialfall von de Sitter zu einer Inkonsistenz führt, formulieren wir außerdem die *Quantenbruchschranke*. Sie besagt, dass jede konsistente Theorie einen quasi-de Sitter-Zustand verlassen muss, bevor Quantenbruch eintreten kann. Folgen dieses Kriteriums sind, dass Selbstreproduktion in Inflation unmöglich ist sowie dass die heute beobachtete dunkle Energie nicht konstant sein kann, sondern sich langsam mit der Zeit verändern muss. Zudem hat die Quantenbruchschranke weitreichende Folgen hinsichtlich Physik jenseits des Standard Modells, da sie jede Erweiterung mit einer spontan gebrochenen diskreten Symmetrie ausschließt sowie die Axion-Lösung zum starken CP-Problem unausweichlich macht.

Im zweiten Teil untersuchen wir, wie ein Quantensystem effizient Information speichern kann. Wir zeigen auf, dass generische bosonische Systeme mit schwacher und attraktiver Wechselwirkung Zustände besitzen, die wegen emergenter nahezu masseloser Freiheitsgrade eine starke erhöhte Speicherfähigkeit aufweisen. Dies ist von großer Bedeutung sowohl für das Speichern von Quanteninformation unter Laborbedingungen als auch für die Simulation anderer Systeme mit erhöhter Spe-

icherfähigkeit, wie z.B. Schwarzer Löcher, de Sitter und neuronaler Netze. Wir untersuchen eine vereinfachte Version eines attraktiven Bosegases mit Dirichlet-Randbedingungen in einer Dimension als prototypisches Beispiel. Schließlich gehen wir näher auf des Phänomen der *Speicherbürde* ein, dessen Kern ist, dass gespeicherte Information generischer Weise eine Rückreaktion auf das System ausübt und es auf diese Weise an seinen Anfangszustand bindet. Für Schwarze Löcher und de Sitter entspricht dies der Beschreibung von Quantenbruch aus der Perspektive von Quanteninformation.

Die herausragende Bedeutung nahezu masseloser Freiheitsgrade führt uns zum dritten Teil, der sich mit Infrarotphysik beschäftigt. Bisher existieren zwei Methoden, um mit Infrarotdivergenzen umzugehen, die in Theorien mit masselosen Teilchen wie QED und Gravitation auftreten: die Inklusion weicher Emission und das Verkleiden asymptotischer Zustände. Unser erstes Ziel ist es, einen kombinierten Formalismus zu entwickeln, der diese beiden Ansätze vereinheitlicht. Seine entscheidende Stärke ist, dass er im Gegensatz zu seinen Vorgängern zu einer sinnvollen Dichtematrix des Endzustands führt, d.h. er ist in der Lage, die kleine aber nichtverschwindende Menge an Dekohärenz zu beschreiben, die sich durch die Spur über unbeobachtete weiche Strahlung ergibt. Hinsichtlich Schwarzer Löcher zeigen wir auf, dass infrarote Strahlung nicht die führende Ordnung der Entropie erfassen kann, sondern nur einen logarithmischen Bruchteil. Wegen der Verbindung des Theorems über weiche Gravitonen mit der BMS-Gruppe asymptotischer Symmetrien untersuchen wir außerdem das Verhältnis von Supertranslationen und der Information eines Schwarzen Loches. Unser Ergebnis ist, dass die erstgenannten natürlicher Weise zur Buchhaltung genutzt werden können, aber dass sie nicht prädiktiv oder einschränkend wirken.

# Abstract

This thesis seeks to identify and investigate various universal quantum phenomena that are particularly, albeit by far not exclusively, relevant for gravity.

In the first part, we study the question of how long a generic quantum system can be approximated as classical. Using a prototypical model of a self-interacting scalar field, we discuss possible scalings of the quantum break-time  $t_q$ , after which the classical description breaks down. Subsequently, we apply this analysis to the hypothetical QCD axion. We conclude that the approximation as classically oscillating scalar field is extremely accurate. Next we turn to de Sitter. Our approach is to resolve the classical metric as a multi-graviton state defined on top of Minkowski vacuum. On the one hand, this composite picture of de Sitter is able to reproduce all known (semi)classical properties. On the other hand, it leads a breakdown of the description in terms of a classical metric after the timescale  $t_q = 1/(G_N H^3)$ , where  $G_N$  and  $H$  correspond to Newton's constant and the Hubble scale, respectively. This finding results in important restrictions on inflationary scenarios. Furthermore, indications that quantum breaking results in an inconsistency in the special case of de Sitter lead us to formulate the *quantum breaking bound*. It requires that any consistent theory must exit a quasi-de Sitter state before quantum breaking can take place. This criterion rules out the regime of self-reproduction for inflation and moreover it implies that the present dark energy cannot be constant but must slowly evolve in time. Additionally, it has far-reaching consequences for physics beyond the Standard Model by ruling out any extensions with a spontaneously-broken discrete symmetry and by making the axion solution to the strong CP problem mandatory.

In the second part, we investigate how a quantum system can efficiently store information. We point out that generic bosonic systems with weak and attractive interaction possess states that exhibit a sharply enhanced memory capacity due to emergent nearly-gapless degrees of freedom. This has important implications both for the storage of quantum information under laboratory conditions and for simulating other systems of enhanced memory capacity, such as black holes, de Sitter and neural networks. As a prototypical example, we study a simplified version of an attractive Bose gas with Dirichlet boundary conditions in one dimension. Finally, we elaborate on the phenomenon of *memory burden*, the essence of which is that stored information generically backreacts on the system and tends to tie it

to its initial state. For black holes and de Sitter, this amounts to the description of quantum breaking from the perspective of quantum information.

The crucial importance of nearly-gapless degrees of freedom leads us to the third part, which revolves around infrared physics. So far, two methods exist to deal with infrared divergences that occur in gapless theories such as QED and gravity: the inclusion of soft emission and the dressing of asymptotic states. Our first goal is to develop a *combined formalism* that unifies these two approaches. Its crucial strength is that unlike its predecessors, it leads to a sensible density matrix of the final state, i.e. it is able to describe the small but nonzero amount of decoherence that arises due to tracing over unobserved soft radiation. With regard to black holes, we conclude that infrared radiation can only account for a subleading logarithmic part of the entropy. Motivated by the relationship of the soft graviton theorem and the BMS group of asymptotic symmetries, we moreover investigate the connection of supertranslations and black hole information. We conclude that the former can be naturally used as a bookkeeping tool, but that they have no predictive or constraining power.

# Publications

This thesis is based on a series of paper [1–10] that have been published or are in publication. As detailed below, they are the result of varying collaborations with Gia Dvali, Cesar Gomez, Marco Michel, Raoul Letschka and Lukas Eisemann. All authors share first authorship and are sorted alphabetically. Although some new aspects were added throughout, the main goal of this work is to present the above-mentioned results in a wider context and to provide a unified picture. Therefore, the present thesis is to a large extent an ad verbatim reproduction (with respect to text, equations and figures) of the papers [1–10]. Unless indicated otherwise, the papers can be attributed to the chapters as follows.

Chapter 2 and appendix A.1 are based on

- [1] G. Dvali, C. Gomez, and S. Zell, “Quantum Break-Time of de Sitter,” *J. Cosmol. Astropart. Phys.* **1706** (2017) 028, [arXiv:1701.08776 \[hep-th\]](#), ©2017 IOP Publishing Ltd and Sissa Medialab,
- [3] G. Dvali and S. Zell, “Classicality and Quantum Break-Time for Cosmic Axions,” *J. Cosmol. Astropart. Phys.* **1807** (2018) 064, [arXiv:1710.00835 \[hep-ph\]](#), ©2018 IOP Publishing Ltd and Sissa Medialab,
- [7] G. Dvali, C. Gomez, and S. Zell, “Quantum Breaking Bound on de Sitter and Swampland,” *Fortsch. Phys.* **67** (2019) 1800094, [arXiv:1810.11002 \[hep-th\]](#), ©2018 WILEY-VCH Verlag GmbH & Co. KGaA, Weinheim,
- [8] G. Dvali, C. Gomez, and S. Zell, “Discrete Symmetries Excluded by Quantum Breaking,” [arXiv:1811.03077 \[hep-th\]](#), to be published,
- [9] G. Dvali, C. Gomez, and S. Zell, “A Proof of the Axion?,” [arXiv:1811.03079 \[hep-th\]](#), to be published.

Chapter 3 and appendix A.2 are based on

- [5] G. Dvali, M. Michel, and S. Zell, “Finding Critical States of Enhanced Memory Capacity in Attractive Cold Bosons,” *Eur. Phys. J. Quantum Technology* **6** (2019) 1, [arXiv:1805.10292 \[quant-ph\]](#), ©2019 The Authors,

- 
- [10] G. Dvali, L. Eisemann, M. Michel, and S. Zell, “Universe’s Primordial Quantum Memories,” *J. Cosmol. Astropart. Phys.* **1903** (2019) 010, [arXiv:1812.08749 \[hep-th\]](#), ©2019 IOP Publishing Ltd and Sissa Medialab.

Chapter 4 and appendix A.3 are based on

- [2] C. Gomez and S. Zell, “Black Hole Evaporation, Quantum Hair and Supertranslations,” *Eur. Phys. J. C* **78** (2018) 320, [arXiv:1707.08580 \[hep-th\]](#), ©2018 The Authors,
- [4] C. Gomez, R. Letschka, and S. Zell, “Infrared Divergences and Quantum Coherence,” *Eur. Phys. J. C* **78** (2018) 610, [arXiv:1712.02355 \[hep-th\]](#), ©2018 The Authors,
- [6] C. Gomez, R. Letschka, and S. Zell, “The Scales of the Infrared,” *J. High Energy Phys.* **1809** (2018) 115, [arXiv:1807.07079 \[hep-th\]](#), ©2018 The Authors.

At the beginning of each chapter, more details are provided as to where material from the papers [1–10] is used.

# Chapter 1

## Introduction

### 1.1 High Energy Physics after Planck, LHC and LIGO

#### 1.1.1 Challenges

Physics has seen great progress in the 21<sup>st</sup> century. A spectacular success consisted in the first direct detection of gravitational waves [11] more than 100 years after they were predicted [12]. Equally important was the discovery of a new particle at the LHC [13, 14] that appears to be the Standard Model Higgs boson, as it was predicted more than 50 years ago [15–17]. If this expectation turns out to be true, this would mark the completion of the Standard Model. Finally, the unprecedented precision with which the Planck-mission has observed the cosmic microwave background has greatly advanced our understanding of the early Universe [18, 19]. In particular, its results are fully consistent with the paradigm of inflation [20]. Nevertheless, outstanding challenges remain, of which we shall name a few important examples.

- First evidence for dark matter was found more than 80 years ago [21], but its microscopic nature is still unclear.
- Likewise, the mechanism behind the accelerated expansion of today's Universe, which was discovered in 1998 [22, 23], needs to be determined. Prominent candidates include a very small but nonzero cosmological constant and a dynamical quintessence field.
- Despite the discovery of a candidate for the Higgs boson, the LHC has defied many theorists' expectations since so far it has found no compelling evidence for any physics beyond the Standard Model (see e.g. [24]).
- While the Planck results are in line with the paradigm of inflation, a great

challenge consists in selecting a concrete scenario among the plethora of proposed models.

- Finally, it remains to be elucidated how the black holes, the mergers of which lead to detectable gravitational waves, were created in the cosmological evolution.

We shall try to extract common themes from the above questions. Needless to say, such an attempt is a matter of interpretation and highly subjective.

**The Importance of de Sitter.** By definition, inflation corresponds to a quasi-de Sitter state, i.e. a cosmological solution that is sourced by an almost-constant vacuum energy. Likewise, the observation of the accelerated expansion of the present Universe implies that it starts to be dominated by vacuum energy. Therefore, it is of great importance to study de Sitter.

**The Reality of Black Holes.** In the past, black holes have often been the arena of theoretical gedankenexperiments. Probably the most prominent example consists in the debate about black hole information [25, 26], to which we shall turn in the subsequent section 1.3.1. Since the observation of black hole mergers, however, understanding their dynamical properties has become even more relevant, also with regard to observations.

**Minimalistic Models.** One could try to interpret all findings to which we referred above in a minimalistic approach, in which the simplest possible theories are selected. For example, the scenario in which dark matter corresponds to a noninteracting scalar field is still viable (see e.g. [27]).<sup>1</sup> Moreover, the LHC has found no degrees of freedom beyond the Standard Model. Finally, simple single-field inflation is still able to explain all Planck-data. The inflaton could even be a particle of the Standard Model, as it is the case in Higgs inflation [30].

## 1.1.2 New Perspectives

The goal of the present work is to investigate if progress on the above-mentioned challenges can be made by viewing them from new perspectives that we shall propose.

**Limitations of Classical Physics.** Mathematically, both black holes and de Sitter correspond to solutions of classical gravity that are derived in the absence of quantum effects. We know, however, that any fundamental description of Nature has to include quantum phenomena. Therefore, it is crucial to investigate the limitations of classical physics, i.e. to study how far it can take us and at what point it breaks down. We will show that quantum effects can become more important

---

<sup>1</sup>One can argue that it would be even more minimalistic if dark matter were explained by right-handed neutrinos since the latter are required in any case due to the observation of neutrino oscillations. This scenario is e.g. realized in the  $\nu$ MSM [28, 29].

than one would naively expect. In particular, they can be relevant for macroscopically large objects. Apart from implications for the challenges mentioned above, this observation is moreover crucial for the question of black hole information. Finally, also for the study of dark matter it is important to determine if the classical approximation is valid or if quantum effects need to be taken into account.

**The Importance of Quantum Information for Gravity.** Once we conclude that the classical approximation of black holes and de Sitter tends to break down due to quantum effects, a very natural follow-up question is what the classical description is replaced by. Whereas it is very hard to find a complete answer, we shall show that quantum information can play a crucial role. In short, the reason is that any microscopic description of black holes or de Sitter has to account for the huge Bekenstein-Hawking [31] or Gibbons-Hawking entropy [32], respectively. Therefore, we will develop a picture that is completely independent of geometry by viewing the gravitational systems from a perspective of information storage. Such an approach can have important observational implications. For example, it leads to inflationary observables that are sensitive to more than the last 60 e-foldings. Moreover, it is conceivable that black hole evaporation slows down due to their high capacity of information storage. If this is true, it would alleviate constraints on small primordial black holes as dark matter candidates (see e.g. [33] for a review).

**Consistency Issue of the Cosmological Constant.** Finally, the study of how long the description of de Sitter in terms of a classical metric is valid will reveal signs of a fundamental conflict. Whereas the cosmological constant is an unchangeable parameter of the theory, quantum effects gradually lead to a complete deviation from de Sitter. This is an indication that de Sitter is inconsistent on the quantum level. Interestingly, this phenomenon is an effect of infrared quantum gravity, i.e. it is fully independent of the UV-completion of gravity. If the cosmological constant indeed leads to an inconsistency, then any consistent theory must exit a quasi-de Sitter state before quantum effects start to dominate. This implies that the present dark energy cannot be constant but must slowly evolve in time and moreover it leads to important restrictions on inflationary scenarios. Additionally, the inconsistency of a metastable de Sitter vacuum would rule out many well-motivated extensions of the Standard Model. The more involved a model is, the more likely it becomes that an inconsistent de Sitter vacuum exists somewhere in phase space. In this way, a fundamental problem of de Sitter in its infrared quantum description could provide a reason why minimalistic theories are observed in experiment.

The purpose of this thesis is to elaborate on the above approaches. Before we come to original work, we shall use the remainder of this chapter to review important results upon which our studies are based.

## 1.2 Conventions

First, we introduce the conventions used in the following. Throughout, we will set  $c = k_B = 1$ , but we keep  $\hbar$  explicit unless states otherwise. The metric signature is  $(+, -, -, -)$ . In order to simplify notations, we will omit numerical prefactors in large parts of chapters 1, 2 and 3. Therefore, except for chapter 4, the symbol “ $\approx$ ” stands for equality up to a numerical prefactor.

We denote Newton’s constant by  $G_N$ . Correspondingly, the Planck mass is  $M_p = \sqrt{\hbar/G_N}$  and the Planck length is  $L_P = \sqrt{\hbar G_N}$ .

## 1.3 Quantumness on Macroscopic Scales

As said, any fundamental description of Nature has to include quantum effects. Nevertheless, the classical approximation is extremely accurate in almost all contexts. In fact, it works so well that quantum physics was not even discovered until the 20<sup>th</sup> century. It appears that the reason why quantum phenomena are so hard to observe is that they are solely relevant on microscopically small scales, i.e. when only a relatively small number of quanta is involved. As systems become macroscopically large, it seems that the importance of quantum effects diminishes. However, this does not always need to be the case, so it is very interesting to look for large systems which nevertheless cannot be described classically. In this regard, systems that are stationary or static on the classical level are especially relevant. For those, quantum effects will always be the dominant source of time evolution, no matter how long it takes until they become important.

### 1.3.1 Black Holes

#### The Puzzle of Black Hole Information

One such class of systems that are static in the classical approximation are black holes. Moreover, they are particularly interesting because of the long-standing debate on what has become known as “information paradox” [26], which is a suspected violation of unitarity by black holes. As we shall elaborate on, however, there is no paradox, so we will use the terminology “puzzle of black hole information”. In short, the upshot will be that the assumption that a black hole of macroscopic size can always be described classically leads to a contradiction. Therefore, it follows by consistency that the classical description must break down on macroscopic scales. Based on earlier suggestions [34–36], this idea that a black hole is a macroscopic quantum object was first put forward in [37].

We will begin by introducing the relevant quantities. The geometry of a black hole of mass  $M$  is described by the Schwarzschild radius

$$r_g \approx MG_N. \tag{1.1}$$

The dimensions of the quantities are  $[r_g] = (\text{time})$ ,  $[M] = (\text{energy})$  and  $[G_N] = (\text{time})/(\text{energy})$ . Furthermore, a black hole possesses the Bekenstein-Hawking entropy [31]

$$S \approx \frac{r_g^2}{\hbar G_N}. \quad (1.2)$$

In its simplest form, it arises from requiring that whenever energy is added to a black hole, the entropy of the black hole must increase in such a way that the entropy of the whole Universe is conserved.

In the classical theory, black holes have two remarkable properties. First, they form an event horizon, i.e. nothing can ever escape them. Secondly, they possess no hair (see e.g. [38] for a review), i.e. all black holes of the same mass have are described by the same metric outside the horizon.<sup>2</sup> Hawking has famously shown [25], however, that the first property changes once quantum effects are taken into account. For the following discussion it is crucial to note that he works in the semiclassical limit, i.e. quantum fields are studied on top of a fixed classical metric. Therefore, by construction, no backreaction on the black hole is taken into account.

In this limit, Hawking has derived that black holes emit quanta the energies of which are distributed thermally with the characteristic energy  $\hbar r_g^{-1}$ . The rate of this particle production is

$$\Gamma \approx r_g^{-1}. \quad (1.3)$$

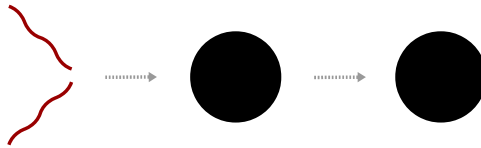
Moreover, the produced particles are in a completely mixed quantum state. Most importantly, since his calculation is only sensitive to the classical black hole metric, all black holes of the same mass emit exactly the same spectrum of particles. Finally, we emphasize that this process of Hawking particle production is a vacuum process, i.e. it is based on the observation that the vacuum for one observer appears as an excited state to another observer.

Additionally, we remark that the semiclassical calculation of black hole evaporation is independent of the UV-completion of gravity. The latter is expected to become relevant when the curvature exceeds the scale  $M_p$ , i.e. on microscopic distances that are smaller than the Planck length  $L_p$ . In contrast, Hawking's calculation only relies on properties of the black hole near the horizon. Since the curvature there is set by the scale  $r_g^{-1}$ , it is small for black hole of large mass, i.e. with  $M \gg M_p$ . Only for black holes of small masses of the order of  $M_p$ , effects of strong gravity become important and Hawking's result can no longer apply.

The fact that in Hawking's computation all black holes of the same mass emit exactly the same spectrum of particles immediately leads to the puzzle of black hole information. In order to illustrate it, we can perform the following gedankenexperiment. We prepare different initial states in such a way that they

---

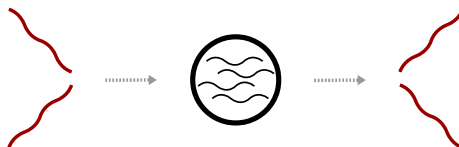
<sup>2</sup>We assume a vanishing electric charge and angular momentum since they are inessential for our discussion.



(a) In the classical limit (1.4), there is no emission.



(b) In the semiclassical limit (1.5), Hawking's calculation of particle production is exact. Since the mass of the black hole is infinite, however, the black hole does not shrink.



(c) In the fully quantum picture, in which both  $G_N$  and  $\hbar$  are finite, the black hole evaporates and can disappear, but Hawking's calculation is no longer exact.

Figure 1.1: Evolution of a black hole in the classical and semiclassical limit as well as in the fully quantum picture. In each case, the initial, intermediate and final state are displayed from left to right. Only in the fully quantum picture, black hole hair becomes visible.

all collapse to black holes of the same mass  $M$ . Subsequently, we wait until they evaporate. By unitarity, we know that the evaporation products must be different in correspondence to the different initial states. However, this appears to contradict Hawking's computation, in which the evaporation products are the same for all black holes of a given mass and any other information about the initial state is lost. We shall show, however, that a paradox can only appear as a result of an inconsistent use of limits. We will study the three relevant cases, which are depicted in Fig. 1.1. The following discussion closely follows [34–37].

**Classical Limit.** First, we can take the classical limit,

$$\hbar \rightarrow 0. \quad (1.4)$$

In this approximation, the classical no-hair-theorem applies, i.e. different initial states indeed form black holes that are indistinguishable for an outside observer. However, this is not a problem since the black holes cannot evaporate in the absence of quantum effects. Therefore, it is consistent to attribute the information about the initial state to the interior of the black hole. We note that the Bekenstein-Hawking entropy (1.2) diverges in the classical limit, i.e. the amount of information contained in a classical black hole is infinite.<sup>3</sup>

<sup>3</sup>This reflects the fact that in a classical theory, infinitesimally small differences between initial

**Semiclassical Limit.** As already mentioned, the crucial point is that Hawking's calculation [25] is performed on top of a fixed classical metric, i.e. it does not take into account any backreaction on the black hole. Therefore, it is only exact in the limit in which the backreaction vanishes. This can be achieved by taking the black hole mass to infinity because then the production of Hawking quanta of finite mass indeed has no effect on the black hole. As the geometry and therefore the Schwarzschild radius have to be kept fixed, we arrive at the following double-scaling limit:

$$M \rightarrow \infty, \quad G_N \rightarrow 0, \quad r_g \text{ fixed.} \quad (1.5)$$

It is important to note that  $\hbar$  is kept finite. For this reason, the scaling (1.5) represents the semiclassical limit, in which the geometry is kept fixed while quantum effects are nonvanishing. In the semiclassical limit, there is no paradox, either. The evaporation products are indeed featureless, i.e. identical for all black holes of the same mass, but the black holes never shrink due to evaporation because of their infinite mass. Thus, just as in the classical limit, it is consistent to attribute the information about the initial state to the interior of the black hole. We note that as in the classical limit, the entropy of the black hole diverges in the semiclassical limit.

**Fully Quantum Picture.** Finally, we turn to the fully quantum picture, in which both  $G_N$  and  $\hbar$  are finite. Correspondingly, also the black hole mass is finite so that black holes can indeed shrink due to evaporation. If Hawking's calculation were still able to describe black hole evaporation in this case, this would lead to a paradox. Namely, then all black holes that have formed from different initial states would lead to the same evaporation products, thereby contradicting unitarity.<sup>4</sup>

Fortunately, Hawking's calculation, which is performed in the limit of infinite entropy  $S$ , is no longer exact for a black hole of finite mass but only represents an approximation. In the most naive estimate, one would expect that corrections appear that scale as  $1/S$ .<sup>5</sup> Already this simplest possible guess indicates that at the latest after on the order of  $S$  quanta have evaporated, the corrections should become important. This corresponds to the timescale

$$t_q \approx Sr_g, \quad (1.6)$$

---

states are still resolvable. Therefore, there are infinitely many ways to form a black hole of a given mass.

<sup>4</sup>We note that even if Hawking's calculation were applicable throughout the whole evaporation process of a black hole of finite mass, it would still not be able to describe very small black holes close to the Planck mass  $M_p$ , for which the curvature on the black hole horizon becomes large. Therefore, no statements can be made about the final stages of evaporation. However, since at that point the mass of the black hole is arbitrarily smaller than it was at the beginning, this uncertainty bears no relevance for the question of unitarity.

<sup>5</sup>One can even arrive at this conclusion using semiclassical arguments about the backreaction of evaporation [39].

after which the semiclassical description would no longer be trustable. As we shall sketch below, more accurate and involved arguments indeed also yield this result. Following [40], we will refer to  $t_q$  as the *quantum break-time*. It will play a prominent role throughout this thesis.

Even beyond the semiclassical limit, energy conservation still has to be fulfilled. To the extent that evaporation takes place, the mass of the black hole must diminish. Because Hawking quanta carry an energy of order  $\hbar r_g^{-1}$ , the quantum break-time (1.6) corresponds to the timescale when the mass of the black hole has diminished significantly. Since Hawking's calculation is performed in the limit of vanishing backreaction, it is clear that there is no reason any more to assume that a black hole still admits a description in terms of a classical metric once the backreaction has become important.<sup>6</sup>

A breakdown of the semiclassical description after the timescale (1.6) may sound surprising at first. The reason is that after losing on the order of half its mass, an initially large black hole is still a macroscopic object,  $r_g \gg L_p$ . Thus, the curvature on the horizon is still expected to be small so that UV-effects of quantum gravity cannot be important. From this perspective, there is no reason why Hawking's calculation should no longer be applicable. The crucial point, however, is that the breakdown of the semiclassical description after the timescale (1.6) is not related to effects of large curvature, which take place on small scales. Instead, it occurs on a macroscopic scale due to a strong backreaction from quantum processes.

We can also formulate the puzzle of black hole information in terms of the purity of states. If one forms a black hole from a pure state, unitarity dictates that the final state of evaporation also has to be pure. In contrast, the emitted quanta in Hawking's computation are in a completely mixed state. During the initial stages of evaporation, however, the emission of quanta in a mixed state does not contradict a unitary evolution since one can imagine that the whole quantum state, i.e. black hole and evaporation products, is in a pure state, but a mixed state for the emission products is obtained after tracing over the black hole. As Page has shown [42], this has to change at the latest after half evaporation, when the Hilbert space of the black hole and the Hilbert space of emitted quanta are of the same size. At this point, the emitted quanta need to purify and information has to be released. Thus, the timescale (1.6) also indicates the point when information has to be released at the latest. In this context, the timescale  $r_g S/2$ , which is analogous to Eq. (1.6), is called Page's time.

We can go one step further and use the above observation concerning the release of information to invert the argument about the validity of a semiclassical description of the black hole. Namely, unitarity implies that after half evapora-

---

<sup>6</sup>As early as in 1980, Page noted the importance of this fact that backreaction already leads to a significant deviation from the semiclassical description when the black hole is still macroscopically big [41].

tion, the total state of all evaporation products needs differ significantly from a completely mixed state. Therefore, a sizable departure from the result of the semi-classical computation has to occur at the latest after the corresponding timescale (1.6). The minimal strength of this deviation is determined by the requirement that it can lead to a significant purification.

Loosely speaking, a paradox arises when we know “too much”, i.e. when we possess two pieces of information that contradict each other. As we have seen, however, the opposite situation is realized in a black hole. When the backreaction due to evaporation has become significant after the timescale (1.6), we know close to nothing about what the black hole has evolved into. In particular, there is no reason any more to assume that it can still even approximately be described by any classical geometry, let alone the metric of a black hole. Except for the fact that the mass has to diminish due to evaporation, it is not even clear if the black hole shrinks in any geometric sense. Likewise, it is completely uncertain how the process of evaporation changes during the evolution of a black hole. After the quantum break-time (1.6), it is equally conceivable that it might slow down, leading to an almost stable object, or speed up, causing a kind of explosion.

### Quantum N-Portrait

As we have seen, the release of information, i.e. deviations from thermality, can only be observed in the fully quantum picture, where both  $\hbar$  and  $G_N$  are finite. Of course, it is very hard to make quantitative predictions beyond the semiclassical limit. To tackle this problem, Dvali and Gomez have proposed the quantum N-portrait [34], which they developed further in [35–37, 40, 43, 44]. Since we will often refer to it throughout this thesis, we will briefly review this corpuscular view of black holes. The key idea is to regard a black hole as an excited multi-graviton state defined on top of Minkowski vacuum. This means that geometry is no longer fundamental but only arises as expectation value of the quantum state of constituent gravitons. Correspondingly, any interaction with the black hole and the time evolution of the black hole arise due to scattering of or with the gravitons of which the black hole is composed.

A strong motivation for this emergent picture of black holes comes from the fact that they can be formed with the help of excitations in flat space. It is clear that one can prepare an initial quantum state on top of Minkowski vacuum in such a way that it subsequently forms a black hole. Although it may be very hard to compute this process explicitly, the mere existence of such a unitary description of collapse suffices for our argument. By evolving the initial state, it leads to a quantum description of the final state, i.e. the black hole, on top of Minkowski. This shows that it must in principle be possible to view a black hole as excited state defined in flat space.

In the quantum N-portrait of a black hole, the wavelength of its constituents

is set by the scale  $r_g$  of the classical geometry, i.e. they have the energy

$$m_g = \hbar r_g^{-1}, \quad (1.7)$$

where we use the unusual symbol  $m_g$  for an easier comparison with later discussions. In order to reproduce the classical energy  $M$  of the black hole, the number of gravitons must be<sup>7</sup>

$$N = \frac{r_g^{-2}}{G_N \hbar}. \quad (1.8)$$

We note that this number is identical to the Bekenstein-Hawking entropy (1.2), but this is a coincidence at this point. Because of the universality of gravitational coupling, the interaction strength between two individual gravitons of energy  $\hbar r_g^{-1}$  is given by

$$\alpha_g = \hbar G_N r_g^{-2}, \quad (1.9)$$

where we consider 4-point interaction for concreteness. We note that  $\alpha_g$  is minuscule for a large black hole,  $M \gg M_p$ . However, the collective coupling, i.e. the strength with which an individual soft graviton couples to the collection of all others, is strong:

$$\lambda_g = \alpha_g N = 1. \quad (1.10)$$

Thus, the constituents of the black hole differ significantly from free gravitons. Finally, we can investigate the classical limit (1.4) and the semiclassical limit (1.5) in this approach. As is evident from Eqs. (1.8) and (1.9), both lead to a diverging number of particles and a vanishing coupling:

$$N \rightarrow \infty, \quad \alpha_g \rightarrow 0, \quad \lambda_g \text{ fixed}. \quad (1.11)$$

Therefore, it is clear why the (semi)classical limit corresponds to a vanishing back-reaction. A state of infinite particle number cannot be changed by any process that only involves a finite number of quanta.

Now we can turn to Hawking particle production in the quantum N-portrait. There, it is no longer a vacuum process, but it arises as a result of ordinary scattering. For example, two of the  $N$  soft gravitons that make up the black hole can scatter and thereby produce a free graviton, i.e. one that is not part of the black hole state. This process is depicted in Fig. 1.2. We can estimate its rate. Since two gravitational 3-point interactions are involved, the amplitude scales as the gravitational coupling  $\alpha_g$  (see Eq. (1.9)) and consequently the rate must contain a factor of  $\alpha_g^2$ . However, this would only be the rate for the scattering of two fixed gravitons. In the state of  $N$  gravitons, it gets enhanced by the possibilities of choosing two out of the  $N$  gravitons,  $\binom{N}{2} \approx N^2$ . Finally, the only quantity that can give the rate its dimensionality of  $[\Gamma] = (1/time)$  is  $r_g^{-1}$ . In total, we obtain

$$\Gamma \approx r_g^{-1} + O(1/N), \quad (1.12)$$

---

<sup>7</sup>As we can absorb numerical prefactors in redefinitions of  $N$  and  $\alpha_g$ , we use exact equalities.

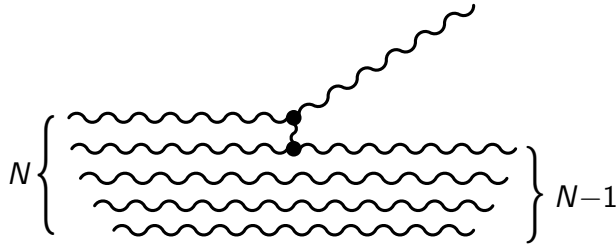


Figure 1.2: Hawking particle production as rescattering of gravitons: Two of the  $N$  gravitons interact and thereby produce a Hawking quantum. (This figure was adopted from [35].)

where we used that  $\lambda_g = \alpha_g N = 1$ . As indicated, this estimate receives corrections that scale as  $1/N$ . In particular, they arise due to the fact that the number of gravitons in the final state of the black hole is different than in the initial one. Thus, the  $1/N$ -corrections encode the backreaction of particle production on the black hole.

The derivation of the rate (1.12) achieves two goals. First, it is able to reproduce Hawking's rate (1.3) in the semiclassical limit  $N \rightarrow \infty$ . Secondly, however, it also gives a handle on computing particle production for finite  $\hbar$  and  $G_N$ .<sup>8</sup> In this case, corrections arise that scale as  $1/N$ . As explained before, we expect on general grounds that such deviations occur beyond the semiclassical limit. That we obtain those corrections is good news since those can lead to the deviations from a featureless thermal evaporation that are required for unitarity. Moreover, we can estimate the timescale of validity of the semiclassical description. Since the process of Hawking particle production now is an ordinary scattering process, which backreacts on the quantum state of the black hole, it leads to a significant deviation from the initial state as soon as on the order of  $N$  gravitons have experienced it. This gives the timescale

$$t_q \approx N r_g, \quad (1.13)$$

which is in full accordance with the previous simple estimate (1.6) of the quantum break-time.

Finally, the quantum N-portrait also provides us with a very natural perspective on black hole formation. We can consider a scattering process of two hard gravitons. In such a case, a black hole can form if the center-of-mass energy is super-Planckian. Once the black hole is viewed as an object composed of  $N$  soft

<sup>8</sup>What makes quantitative computations difficult is the fact that the collective coupling is strong,  $\lambda_g = 1$ . For this reason, tree-level processes in which a large number of gravitons of the initial state scatter are not suppressed. Still, an explicit  $S$ -matrix computation (for the case of black hole formation) has e.g. been performed in [45].

gravitons, one expects that black hole formation should be understandable as process of  $2 \rightarrow N$ -scattering. It was shown in [45] that this is actually the case.<sup>9</sup> (A related calculation can be found in [49].)

### 1.3.2 De Sitter

#### Semiclassical Properties

Apart from black holes, another object that is stationary in the classical approximation is de Sitter space, i.e. the vacuum solution of Einstein's equations in the presence of a positive cosmological constant  $\Lambda$ . We will discuss that it exhibits many similarities to the case of black holes but also crucial differences. The geometry of de Sitter is described by the Hubble radius

$$R_H \approx \sqrt{\frac{1}{\Lambda}}, \quad (1.14)$$

where the respective dimensions are  $[\Lambda] = 1/(\text{time})^2$  and  $[R_H] = (\text{time})$ . In the classical theory, the spacetime possesses an energy density

$$\varepsilon \approx \frac{\Lambda}{G_N}. \quad (1.15)$$

Analogously to the Bekenstein-Hawking entropy of black holes, de Sitter is characterized by the Gibbons-Hawking entropy [32]

$$S \approx \frac{1}{\hbar G_N \Lambda}. \quad (1.16)$$

Also particle production by a black hole has a counterpart in de Sitter, namely Gibbons-Hawking particle production [32]. Again, it will be crucial for our discussion that this phenomenon was derived in the semiclassical limit, i.e. when quantum fields are studied on top of a fixed classical metric. As before, this means that no backreaction on de Sitter space is taken into account. In this limit, Gibbons and Hawking have derived that an observer in de Sitter will see a thermal spectrum of particles with characteristic energy  $\hbar R_H^{-1}$ . The rate of this particle production is

$$\Gamma \approx R_H^{-1}. \quad (1.17)$$

As in the black hole case, this phenomenon arises as a vacuum process in the semiclassical limit.

Again we shall discuss the three relevant limits. As always, the classical limit corresponds to  $\hbar \rightarrow 0$ . In this case, the Gibbons-Hawking entropy (1.16) diverges

---

<sup>9</sup>This calculation is moreover related to the idea that gravity self-completes by classicalization [46–48], i.e. that it manages to self-consistently avoid a strong coupling regime by distributing large energies among many soft quanta.

and the process of particle production shuts off. For the computation of Gibbons-Hawking radiation, the semiclassical limit is relevant, in which the energy density of the spacetime is taken to be infinite while the geometry is kept fixed. From Eqs. (1.14) and (1.15), it is evident that this corresponds to

$$G_N \rightarrow 0, \quad R_H = \sqrt{\frac{1}{\Lambda}} \text{ fixed.} \quad (1.18)$$

In analogy to the semiclassical limit (1.5) for a black hole, the gravitational coupling goes to zero while  $\hbar$  stays finite. Again the entropy (1.15) diverges. In this limit, it is consistent to consider quantum effects that do not backreact on the classical metric.

Finally, we discuss the fully quantum picture, in which both  $\hbar$  and  $G_N$  and consequently also  $S$  are finite. Since Gibbons-Hawking particle production was computed in the limit of infinite  $S$ , one could naively expect that as for black holes, corrections appear that scale as  $1/S$ . Since those become important at the latest after on the order of  $S$  quanta have been produced, the simplest possible guess for the timescale after which the semiclassical description is no longer trustable is

$$t_q \approx SR_H. \quad (1.19)$$

A detailed study of this quantum break-time of de Sitter will be performed in this thesis. As we shall sketch shortly, it will turn out that the estimate (1.19) is indeed justified, in agreement with the previous result in [44].

As for the black hole, the only statement that we expect to remain exact beyond the semiclassical limit is energy conservation. Thus, to the extent that particles are produced, the energy associated to de Sitter has to decrease. Beyond that, it is completely unclear what de Sitter evolves into after the timescale (1.19). In particular, there is no reason any more to assume that it can still even approximately be described by any classical metric. So the most likely scenario is that the de Sitter radius neither increases nor decreases but simply ceases to exist as a geometric notion. Likewise, particle production might equally well speed up or slow down after quantum breaking.

Finally, we want to mention a crucial difference between black holes and de Sitter. The mass  $M$  of a black hole is a parameter of a solution. Thus, in one and the same theory of gravity, multiple black hole solutions corresponding to different masses can exist. For this reason, it is at least in principle conceivable that even though a full classical description of a black hole ceases to be valid after the quantum break-time, it still shrinks in an appropriate sense due to evaporation. In contrast, the cosmological constant is a parameter of the theory. Thus, there is only one single de Sitter solution in a given theory. For this reason, one cannot imagine how the backreaction due to particle production could even approximately be described as a decreasing cosmological constant. As already noted in [44, 50], this conflict between the fixed parameter  $\Lambda$  of the theory and the time evolution

due to quantum effects indicates that quantum breaking could represent a more severe problem in the special case of de Sitter. Section 2.5 of the present thesis will be devoted to the discussion of this point.

### Fully Quantum Picture

Next, we turn to de Sitter beyond the semiclassical limit, i.e. when both  $\hbar$  and  $G_N$  are finite. As suggested in [44] (based on early ideas in [34]), it is possible to develop a fully quantum picture of de Sitter in great analogy to the quantum N-portrait for black holes. In this corpuscular approach, on which parts of this thesis will be based, de Sitter is also viewed as a composite state of many soft gravitons. We will briefly review it.

The first question that arises is what vacuum those gravitons are defined on. Namely, de Sitter is traditionally regarded as a fundamental vacuum of gravity. However, this point of view leads to well-known problems. In particular, the lack of a global time makes it impossible to define an  $S$ -matrix. This creates a big challenge since the  $S$ -matrix formulation is crucial for quantum gravity and string theory. In order to circumvent these problems, Dvali and Gomez have proposed a different point of view [44], in which Minkowski is regarded as the only true  $S$ -matrix vacuum. As soon as de Sitter is treated as an excited state on top of the Minkowski vacuum, it can profit from the well-defined  $S$ -matrix in flat space.

Another motivation for this emergent picture of de Sitter comes from inflation. After reheating, we expect no obstruction in describing the Universe as a collection of particles defined on top of Minkowski vacuum. Then we can make an analogous argument as we did for black holes in section 1.3.1. As long as reheating can in principle be described as a unitary evolution, then also the Universe before reheating, i.e. the quasi-de Sitter state of inflation, must possess a description as quantum state defined on Minkowski vacuum.

Once we view de Sitter as emergent, we can proceed in analogy to the black hole case. First, the wavelength of the constituent gravitons is set by the scale  $R_H$  of the classical geometry, i.e. their energy is

$$m_g = \hbar R_H^{-1}. \quad (1.20)$$

The next requirement is to reproduce the classical energy density (1.15) associated to the cosmological constant. To this end, one has to choose the number of gravitons per Hubble patch as

$$N = \frac{1}{\hbar G_N \Lambda}. \quad (1.21)$$

As in the black hole case, this number coincides with the entropy (1.16) of de Sitter, but again no fundamental reason is apparent to us why this should have to be the

case. The strength of the gravitational coupling among individual constituent gravitons is set by their energy:

$$\alpha_g = \hbar G_N \Lambda. \quad (1.22)$$

Whereas this number is generically very small, the collective coupling, i.e. the strength with which an individual graviton interacts with the collection of all others, yields

$$\lambda_g = \alpha_g N = 1. \quad (1.23)$$

In full analogy to the quantum N-portrait of black holes, the collective interaction is strong and therefore the constituent gravitons of de Sitter have to differ significantly from free gravitons. Finally, we can again investigate the classical limit (1.4) and the semiclassical limit (1.18) in this picture. According to Eqs. (1.21) and (1.22), both correspond to an infinite number of particles and a vanishing coupling:

$$N \rightarrow \infty, \quad \alpha_g \rightarrow 0, \quad \lambda_g \text{ fixed}. \quad (1.24)$$

As is evident from Eq. (1.11), this is fully analogous to the black hole case. Any quantum process that only involves a finite number of particles cannot backreact on the quantum state of de Sitter in the (semi)classical limit.

Next, we turn to Gibbons-Hawking particle production in this composite picture of de Sitter. As for black holes, it no longer corresponds to a vacuum process, but it arises as a result of ordinary scattering. Like before, we can for example consider the case when two of the  $N$  constituent gravitons of de Sitter scatter and thereby produce a free graviton. Fig. (1.2) can equally describe this process. Also the estimate of the rate is fully analogous to the case of Hawking particle production. Because two 3-point interactions of gravitons are involved, the amplitude must contain a single power of  $\alpha_g$  and consequently the rate scales as  $\alpha_g^2$ . Moreover, it is enhanced by a factor of  $\binom{N}{2} \sim N^2$  due to the possibilities of choosing the two gravitons that scatter. Since only  $R_H$  can give the rate its correct dimensionality, we get in total

$$\Gamma \approx R_H^{-1} + O(1/N), \quad (1.25)$$

where we used that  $\lambda_g = \alpha_g N = 1$ . Backreaction, i.e. the fact that the final state of the constituent gravitons is different from the initial one, again leads to corrections that scale as  $1/N$ .

On the one hand, the rate (1.25) reproduces the result (1.17) of Gibbons and Hawking in the semiclassical limit  $N \rightarrow \infty$ . On the other hand, however, it can be used to obtain an estimate for the quantum break-time of de Sitter. Namely, a significant deviation from the initial state of the constituent gravitons occurs as soon as a sizable fraction of them has experienced the scattering process depicted in Fig. 1.2. This leads to the timescale

$$t_q \approx N R_H, \quad (1.26)$$

which agrees with the previous simple estimate (1.19) of the quantum break-time of de Sitter.

## 1.4 Entropy Under the Microscope

Typically, geometry is regarded as the primary characteristic of gravitational systems. This is the case not only on the classical level but e.g. also in the fully quantum pictures of black holes [34] and de Sitter [44] that we have just reviewed. Also there the primary goal is to give a quantum resolution of the geometry.

In the following, we shall suggest an alternative point of view on these systems, which is completely independent of their geometry. Based on early ideas [34], this line of thought was pioneered in [36] and further developed in [51–53] using the example of black holes. The starting point is that both black holes and de Sitter share a remarkable property, namely they satisfy the Bekenstein bound [54] on information storage capacity.<sup>10</sup> This means that among all systems of a given size, black holes and de Sitter can record the most information, where their storage capacity is measured by the Bekenstein-Hawking entropy (1.2) and the Gibbons-Hawking entropy (1.16), respectively. Whereas it is very difficult to give a complete microscopic description of these gravitational systems, a necessary condition that any such theory must fulfill is that it gives an explanation of the entropy. Therefore, we shall suggest to view their maximal capacity of memory storage as key property of black holes and de Sitter.

For this reason, we focus on the question how a generic quantum system can achieve a high capacity of information storage. We will largely follow the arguments presented in [34, 36, 51–53]. To account for a large entropy  $S$ , which could e.g. represent the black hole entropy (1.2) or the de Sitter entropy (1.16), a system must possess an exponentially large number of microstates,

$$\# \text{ microstates} = e^S. \quad (1.27)$$

A very natural way to achieve this is through a big number of lowly-occupied modes that scales as

$$\# \text{ modes} \sim S, \quad (1.28)$$

where we used that  $S$  distinguishable modes with a maximal occupation of  $d$  yield  $S^d$  different states.

The crucial point is that the states (1.27) can only count as microstates if they are nearly-degenerate in energy. Thus, the energy difference between the state in which all of the modes are occupied and the one in which none are must be small. For example, one can require that it is smaller than some fundamental energy gap

---

<sup>10</sup>We note that up to the numerical prefactor, the Bekenstein bound coincides with the previously discovered limit on information storage capacity by Bremermann [55].

$E_{\text{typical}}$  of the system in question. In this case, the energy gap of a single mode must satisfy<sup>11</sup>

$$\Delta E \lesssim \frac{E_{\text{typical}}}{S}, \quad (1.30)$$

where  $E_{\text{typical}} = \hbar r_g^{-1}$  for black holes and  $E_{\text{typical}} = \hbar R_H^{-1}$  for de Sitter. The property (1.30) is remarkable as the resulting energy gaps are arbitrarily smaller than the typical level spacing of the system, provided the entropy is large enough. In summary, we conclude that systems of enhanced memory storage, such as black holes and de Sitter, must possess a large number (1.28) of modes that have an extremely small energy gap (1.30). In other words, a big entropy necessarily requires the existence of many *nearly-gapless* modes.

This observation has two important implications. First, it promises to provide a new way of studying black holes and de Sitter. Since nearly-gapless modes play a crucial role for them, one can look for such nearly-gapless excitations in other systems, which are easier to study both theoretically and experimentally. If this search is successful, one could use those prototype systems to draw conclusions about information storage and processing in the gravitational systems, which are much harder to analyze. Secondly, one can also invert the argument. We know that black holes and de Sitter exhibit a sharply enhanced capacity of information storage. Thus, if we manage to understand how they achieve this property, one can try to imitate their mechanism in order to build devices that can efficiently store quantum information under laboratory conditions, i.e. one could attempt to construct “black-hole-like” storers of quantum information.

## 1.5 Infrared Physics

As we have seen, the large and in fact maximal entropy of black holes and de Sitter requires the existence of a large number of extremely soft modes. Moreover, we know that there is no mass gap in gravity. Because of these two facts, it is very natural to ask if infrared physics, which deals with the infrared divergences that arise in gapless theories, could help to shed light on how black holes and de Sitter store and process information, as was e.g. suggested in [56] for the case of black holes.

---

<sup>11</sup>If we assume that the nearly-gapless modes can have both positive and negative energies, it is also possible to adopt the weaker criterion

$$\Delta E \lesssim \frac{E_{\text{typical}}}{\sqrt{S}}. \quad (1.29)$$

In this case, not all but most states still fit in the elementary gap  $E_{\text{typical}}$ . This suffices to obtain the scaling (1.27) of the number of microstates. For the following discussions, the difference between the criteria (1.30) and (1.29) will be inessential.

The key observation of infrared physics is that in a gapless theory, any small amount of energy suffices to produce an arbitrarily large number of quanta. That this fact has important implications was already realized in the thirties [57] and further studied in the sixties [58, 59]. As a first step, we can consider a generic scattering process in which no soft quanta are emitted. When we compute the amplitude for such a process, we generically find that it vanishes because of divergent loop corrections. This fact is known as “infrared divergence”. It is crucial to note, however, that it does not represent a problem of the theory. Instead, it is a physical result: The probability that no soft modes are emitted in a nontrivial scattering process is zero.

Next, one can include soft quanta in the final state. The number of soft quanta can be arbitrarily large but the total energy contained in them must be small. Then computation shows that the sum over all such final states that include soft quanta gives an infinite contribution. However, when combined with the vanishing contribution due to loop corrections, a finite total rate is obtained [57–59]. Thus, all divergent contributions cancel self-consistently. Moreover, it turns out that the tree level result, which includes neither loops nor soft emission, is a good approximation and infrared physics only gives a small correction to the total rate.

This result could sound like the end of the story, but it is not. Shortly after Weinberg’s computation [59], a different approach to infrared divergences was suggested, in which no soft emission was considered. Instead, charged asymptotic states were modified by adding to each of them, i.e. to both final and initial states, a carefully chosen coherent state of soft photons [60–65]. The physical justification for this modification of asymptotic states is that in a theory with long-range interactions, approximate eigenstates of the asymptotic Hamiltonian can only be formed if the above-mentioned dressing by soft photons is included. Even though the procedure is very different, the combination of all dressing factors approximately results in the same contribution as the one from soft emission and therefore yields a finite total rate.

This finding immediately leads to the puzzle why two seemingly very different procedures should generically yield the same result. Additionally, it is unclear why not both soft emission and soft dressing should be included at the same time. Doing so would lead to a total rate that is infinite and therefore clearly unphysical.

This tension between soft emission and soft dressing has recently been heightened by the study of the density matrix of the final state of scattering. Its diagonal contains the well-known rates, but the off-diagonal elements encode information about the coherence of the final state. This is generically an interesting question since one expects that the tracing over unobserved soft radiation leads to a small but nonzero amount of decoherence. It was found, however, that solely considering soft emission or solely including soft dressing can only lead to full decoherence or full coherence, respectively [66, 67].<sup>12</sup> Therefore, the relationship of soft emis-

<sup>12</sup>It was proposed in [67] that one should also perform a trace over soft dressing. In this case,

sion and soft dressing constitutes an interesting subject of study, which we shall investigate thoroughly in this thesis.

Finally, the question of coherence of the final state leads back to the study of black hole information. Namely, if unobserved soft radiation could lead to a sizable amount of decoherence, then this could be connected to the fact that the result of Hawking's calculation is a mixed state. In this proposal [56], the complete final state, which includes both hard quanta and soft radiation, would be pure and a mixed state would only arise due to tracing over unobserved soft modes. Of course, such an explanation would be very surprising since soft emission occurs in any process of gravity or QED whereas the information puzzle is specific to black holes. Nevertheless, this shows that it is important to clarify the relationship of infrared divergences and quantum coherence, which is one of the goals of this thesis.

## 1.6 Outline

The outline of this thesis is as follows. In chapter 2, we study the question of quantum breaking, i.e. of how long a given system can be approximated as classical. We use simple scaling arguments and the analysis of a prototypical self-interacting scalar field to draw conclusions about quantum breaking in generic systems. Subsequently, we investigate two concrete examples. For hypothetical cosmic axions of QCD, we show that the classical approximation of today's axion field is extremely accurate. Next, we study quantum breaking in de Sitter. First, we construct a concrete model for the corpuscular picture of de Sitter reviewed in 1.3.2, in which the spacetime is resolved as excited multi-graviton state on top of Minkowski vacuum. We show that our model is able to reproduce all known classical and semiclassical properties of de Sitter. Moreover, it allows us to explicitly compute the quantum break-time, after which the description in terms of a classical metric ceases to be valid. Our result is in full agreement with Eq. (1.26). Additionally, we study implications of quantum breaking for the dark energy in today's Universe and for inflationary scenarios. Whereas the discussion up to this point is independent of the question if quantum breaking is a sign of a fundamental inconsistency of de Sitter, we finally discuss some of the important consequences that arise if a consistent theory must not allow for de Sitter quantum breaking. In particular, this makes the existence of a QCD axion mandatory and excludes the self-reproduction regime in inflation as well as any extension of the Standard Model with a spontaneously-broken discrete symmetry.

In chapter 3, our goal is to study gravitational systems from the perspective of quantum information. First, we investigate more generic, i.e. potentially

---

also soft dressing would lead to full decoherence. We will argue in section 4.3.1, however, that both the physical justification and the mathematical soundness of such a trace is questionable.

nongravitational, bosonic systems and show that nearly-gapless modes and therefore states of sharply enhanced memory capacity are a common phenomenon in them, provided weak and attractive interactions exist. We discuss the underlying mechanism, which we shall call *assisted gaplessness*, that leads to the emergence of nearly-gapless modes and provide an analytic procedure for finding them, to which we refer as *c-number method*. Moreover, the fact that simple nongravitational systems already feature states of enhanced information storing capabilities opens up an exciting perspective of simulating other systems of enhanced memory capacity, such as black holes and neural networks, in table-top experiments. Subsequently, we demonstrate assisted gaplessness and the *c-number method* on a concrete prototype model of three interacting bosonic degrees of freedom. We conclude the chapter by studying the phenomenon of *memory burden*, the essence of which is that a large amount of stored information generically backreacts on the system and prevents it from evolving. This observation leads us back to gravity. For both de Sitter and black holes, memory burden turns out to describe the information-theoretic aspect of quantum breaking.

We turn to infrared physics in chapter 4. First, we review known results and comment on the relationship of the soft photon/graviton theorem and charge conservation. Subsequently, we propose a new approach to deal with infrared divergences, which we shall call *combined formalism*. Its purpose is to resolve the tension between the emission of soft radiation and the dressing of asymptotic states by providing a unified description of the two phenomena. Unlike previous approaches, the combined formalism leads to a sensible density matrix that is able to describe the small but nonzero amount of decoherence that arises due to the emission of unobserved soft modes. Finally, we study the implications of infrared physics for black holes. First, we show that the emission of soft radiation can only account for a subleading fraction of the black hole entropy and therefore cannot play a key role for resolving the puzzle of black hole information. Secondly, the connection of the soft photon theorem and the asymptotic symmetries of gravity at null infinity, namely the BMS group [68–70], leads us to study the relationship of BMS symmetries and black hole hair. Our result is that those asymptotic symmetries can be used as a bookkeeper of black hole information, but that they have no predictive or constraining power.

Finally, we conclude in chapter 5 by summarizing our findings and relating them to the challenges introduced in 1.1.1. Moreover, we point out future directions of research.

# Chapter 2

## Quantum Breaking

This chapter is devoted to the study of quantum breaking. Originally introduced in [40], this is the question of how long a given system can be approximated as classical. The corresponding timescale, after which the quantum evolution deviates from the classical description, is the quantum break-time.

First, we show in section 2.1 that simple scaling arguments already tightly constrain what the quantum break-time must generically depend on.

Next, we analyze a prototypical example of a self-interacting scalar field in section 2.2. Following the study of quantum breaking in various regimes, we try to draw conclusions for generic systems.

Subsequently, we study the hypothetical QCD axion in section 2.3. Since it is possible to describe those axions as self-interacting scalar field, we can directly apply the results of the preceding section to infer that the approximation of today's axion field as classical is extremely accurate. Moreover, we critically examine contrary claims made in [71] by emphasizing the distinction between classical and quantum interactions.

In section 2.4, we turn to the investigation of quantum breaking in de Sitter. First, we resolve the classical metric as expectation value of a multi-graviton state defined on top of Minkowski vacuum, thereby providing a concrete model for the corpuscular picture [44] of de Sitter reviewed in 1.3.2. This construction allows us to explicitly compute the quantum break-time, after which the spacetime can no longer be described by a classical metric. The result is in full agreement with previous findings [44]. Finally, we study implications for the dark energy in today's Universe and for inflationary scenarios. Corresponding restrictions arise because observations show no deviation from the description in terms of a classical metric.

In the last section 2.5, we discuss if the consequences of quantum breaking could be even more severe in the special case of de Sitter. Namely, it was suggested in [44, 50] that it could be a sign of a fundamental inconsistency of the spacetime. Therefore, we analyze some of the important constraints that arise if de Sitter quantum breaking indeed must not happen in a consistent theory. In particular,

this rules out the self-reproduction regime in inflation, makes the axion solution to the strong CP problem mandatory and excludes any extension of the Standard Model with a spontaneously-broken discrete symmetry.

This chapter is based on the papers [1, 7–9], which are joint work with Gia Dvali and Cesar Gomez, as well as the paper [3], which is joint work with Gia Dvali.<sup>1</sup> To a large extent, this chapter is an ad verbatim reproduction of these publications. Section 2.2 uses material from both [1] and [3]. Sections 2.1 and 2.3 follow [3]. Section 2.4 follows [1], where section 2.4.6 additionally uses material from [7]. Section 2.5 follows [1], [7], [8] and [9]. Appendix A.1, which belongs to this chapter, follows [1].

## 2.1 General $\hbar$ -Scaling of Timescales

Before computing the quantum break-time in specific models, we will discuss some general features of classicality that are based on scaling properties. A key characteristic of any quantum field-theoretic system is the strength of interaction between its quanta, which can be parameterized by a dimensionless quantity  $\alpha$ . In the quantum language,  $\alpha$  controls the magnitude of scattering amplitudes. Typically, it is convenient to use  $2 \rightarrow 2$ -scattering as a reference point. Of course, the system may possess more than one type of interaction, and correspondingly more than one type of  $\alpha$ . However, for purposes of this discussion, a single  $\alpha$  is sufficient.

We can always normalize fields in such a way that  $\alpha \ll 1$  corresponds to a weak-coupling domain, in which a perturbative expansion in powers of  $\alpha$  can be performed. Correspondingly,  $\alpha > 1$  describes a strong coupling regime, for which perturbation theory in  $\alpha$  breaks down. Throughout we shall restrict ourselves to systems with weak coupling. Even for  $\alpha \ll 1$ , however, the system can become strongly interacting in a *collective* sense. This can happen if the system is put in a state in which the occupation number of interacting quanta  $N$  is large enough. In that case, the strength of interaction is determined by the collective coupling

$$\lambda \equiv \alpha N. \tag{2.1}$$

The regimes of interest can be then split according to whether it is weak ( $\lambda < 1$ ), strong ( $\lambda > 1$ ) or critical ( $\lambda = 1$ ).

We remark that in the case of an extended system,  $N$  refers to the number of particles with which a given particle can interact efficiently. In the case of a constant particle density, a natural choice therefore is to consider the typical wavelength  $\lambda \sim \hbar/E$  of a particle as characteristic size of the volume, where  $E$  is its typical energy. This is the reason why we restrict ourselves to one Hubble patch in the corpuscular picture of de Sitter, which we reviewed in section 1.3.2. Equivalently, it is also possible to consider an arbitrary volume, but then  $\alpha$  needs

---

<sup>1</sup>Important aspects of [1] were moreover published in the proceedings [72].

to be chosen in such a way that it describes the average interaction strength of a pair of particles. If an interaction is short-range, it correspondingly leads to a small value of  $\alpha$ .

We can draw important conclusion by studying how the various quantities scale when we take the classical limit,  $\hbar \rightarrow 0$ , while keeping all the classically-measurable expectation values fixed, i.e. all the parameters in the classical Lagrangian are kept finite. In particular, the collective coupling  $\lambda$  is a classical quantity since it characterizes the strength of classical nonlinearities. Therefore, it is independent of  $\hbar$  and stays finite in the classical limit. Since the quantum coupling vanishes,  $\alpha \rightarrow 0$ , for  $\hbar \rightarrow 0$ , this implies that in the classical limit we have  $N \rightarrow \infty$ . Therefore, states which behave approximately-classically are characterized by a large occupation number of quanta  $N$ . This is in full accordance with our discussion of black holes and de Sitter in section 1.3.

Keeping in mind that we are at large  $N$ , small  $\alpha$  and some fixed  $\lambda$ , we can now perform some dimensional analysis. We assume that the system is well-described classically at some initial time  $t = 0$  and we wish to estimate how long it will take for the classical description to break down. Obviously, this timescale must satisfy the scaling property of becoming infinite in the classical limit  $\hbar \rightarrow 0$ . Then assuming a simple analytic dependence, the quantum break-time should scale to leading order as

$$t_q \approx (\text{fixed classical quantity}) \times N^\beta = (\text{fixed classical quantity}) \times \alpha^{-\beta}, \quad (2.2)$$

where  $\beta > 0$  is an integer and we used that  $\lambda = \alpha N$  is a fixed constant. Already for  $\beta = 1$ , this timescale is huge for macroscopically-occupied weakly-interacting systems.

For completeness, we want to point out that there is another possible functional dependence which fulfills a simple scaling behavior in the classical limit and which requires special attention:

$$t_q \approx (\text{fixed classical quantity}) \times \ln(N) = (\text{fixed classical quantity}) \times \ln(\alpha^{-1}). \quad (2.3)$$

Such a scaling cannot be excluded on the basis of general dimensional analysis. In fact, it was explicitly shown in [40] that it does take place, but under the following conditions:

- 1) the system must be in an overcritical state, i.e. in a state with  $\lambda > 1$ ; and
- 2) the system in this state must exhibit a classical instability, i.e. a Lyapunov exponent which is independent of  $\hbar$ .

Under such conditions, the quantum break-time was found to be given by

$$t_q \approx \Omega^{-1} \times \ln(N), \quad (2.4)$$

where  $\Omega$  is the Lyapunov exponent. In section 2.2.4, we will review the system studied in [40] that can exhibit such a short quantum break-time.

## 2.2 A Basic Example

### 2.2.1 Classical Solution

#### Nonlinearities

Next, we investigate quantum breaking in an explicit example of a scalar field  $\phi$  in  $3 + 1$  dimensions. First, we study it on the classical level where its Lagrangian is

$$\mathcal{L} = \frac{1}{2} \partial_\mu \phi \partial^\mu \phi - \frac{1}{2} \bar{m}^2 \phi^2 + \frac{1}{4!} \bar{\alpha} \phi^4. \quad (2.5)$$

Here  $\bar{m}$  is the classical frequency and  $\bar{\alpha}$  represents a classical coupling constant. We put a bar on these quantities to distinguish them from their quantum counterparts, which we shall discuss shortly. In the classical theory, the dimensions of the parameters are  $[\bar{m}^{-1}] = (\text{time})$  and  $[\bar{\alpha}] = (\text{time}) \times (\text{energy})$  whereas the dimensionality of the field is  $[\phi] = \sqrt{(\text{energy})/(\text{time})}$ . The equation of motion reads

$$(\square + \bar{m}^2) \phi - \frac{1}{6} \bar{\alpha} \phi^3 = 0. \quad (2.6)$$

In the free case, i.e. for  $\bar{\alpha} = 0$ , a solution is given by

$$\phi_0(t) = A \cos(\bar{m}t), \quad (2.7)$$

where  $A$  is the amplitude and we specialized to the spatially homogeneous case.

Our first goal is to study the full classical solution and in particular to determine how long it can be approximated by the free solution (2.7). To this end, we compute the first anharmonic correction  $\phi_1$  to (2.7) in a series expansion in powers of  $\bar{\alpha}$ . Plugging in the split

$$\phi = \phi_0 + \bar{\alpha} \phi_1 \quad (2.8)$$

in (2.6), we obtain the equation of a driven harmonic oscillator:

$$(\partial_t^2 + \bar{m}^2) \phi_1 = \frac{A^3}{6} \cos^3(\bar{m}t). \quad (2.9)$$

Using the identity  $\cos^3(x) = (\cos(3x) + 3 \cos(x)) / 4$ , it is easy to check that

$$\phi_1 = A \frac{A^2}{192 \bar{m}^2} (\cos(\bar{m}t) - \cos(3\bar{m}t) + 12 \bar{m}t \sin(\bar{m}t)) \quad (2.10)$$

is the solution for the initial conditions  $\phi_1(0) = \partial_t \phi_1(0) = 0$ . One could repeat this procedure to iteratively find the full classical solution.

For us, however, only the leading deviation from the free solution will be important. It is caused by the resonant term  $\propto (\bar{m}t)$  and can be neglected as long as

$$\bar{\alpha} \frac{A^2}{\bar{m}^2} \bar{m}t \ll 1. \quad (2.11)$$

This leads to the timescale

$$t_{\text{cl}} \approx \bar{m}^{-1} \frac{\bar{m}^2}{\bar{\alpha} A^2}. \quad (2.12)$$

We will refer to it as *classical break-time* since it determines the point where the approximation in terms of the free solution (2.7) ceases to be valid. The nonlinear corrections that cause this breakdown correspond to an expansion in the dimensionless quantity

$$\lambda \equiv \bar{\alpha} \frac{A^2}{\bar{m}^2}, \quad (2.13)$$

which determines the strength of classical interactions. It will become clear shortly that as notation indicates,  $\lambda$  indeed corresponds to the collective coupling in the quantum theory, as defined in Eq. (2.1). For our conclusions, it will be important that corrections which scale as  $\lambda$  are classical and therefore cannot lead to quantum breaking. Correspondingly, we emphasize that the classical break-time has a fundamentally different meaning than the quantum break-time.

### Classical Versus Quantum Break-Time

The next step will be to find a quantum description of the classical solution. In doing so, the presence of classical nonlinearities leads to an immediate difficulty. This is the problem of identifying the Fock space of creation and annihilation operators  $\hat{c}^\dagger, \hat{c}$  in which the coherent quantum state describing the given classical solution can be defined. If for a given solution nonlinear interactions are important, in general its quantum constituents  $\hat{c}^\dagger, \hat{c}$  differ from the quantum constituents  $\hat{c}_{\text{free}}^\dagger, \hat{c}_{\text{free}}$  which describe the (almost) free waves obtained by solving the classical equations of motions in the same system, but in a weak field limit. The obvious reason for this difference is that in nonlinear waves, interactions are important and the would-be free particles are off-shell. Correspondingly, the dispersion relation of the modes  $\hat{c}^\dagger, \hat{c}$  is in general very different from the one of  $\hat{c}_{\text{free}}^\dagger, \hat{c}_{\text{free}}$ . In other words,  $\hat{c}_{\text{free}}^\dagger$  creates a free quantum whereas  $\hat{c}^\dagger$  creates one which interacts with the other background constituents.

Ideally, one would choose the operators  $\hat{c}^\dagger, \hat{c}$  that take into account all nonlinear interactions in such a way that a coherent state formed out of them leads to the correct classical expectation value for all times, as long as one neglects quantum interactions, i.e. sets  $\hbar = 0$ . For a generic classical solution, however, it is impossible to find such operators. To overcome this problem, our strategy is to approximate the classical solution by the free solution and correspondingly to replace  $\hat{c}^\dagger, \hat{c}$  by  $\hat{c}_{\text{free}}^\dagger, \hat{c}_{\text{free}}$ . This is only possible on timescales that are shorter than the classical break-time  $t_{\text{cl}}$ . Within the validity of this approximation, we will be able to compute quantum effects that lead to a deviation from the classical solution.

The crucial question is what we can learn from this analysis based on the free classical solution about quantum breaking in the full nonlinear case. Clearly, we

will not be able to draw conclusions about the precise way in which quantum effects lead to deviations from the classical description since we have changed the classical solution. It is important to note, however, that our approximation is purely classical: We replace the exact classical solution by a different classical function. For the approximate function, we find an exact quantum-corpuscular resolution in terms of  $\hat{c}_{\text{free}}^\dagger, \hat{c}_{\text{free}}$ . When the description of the classical solution in terms of  $\hat{c}_{\text{free}}^\dagger, \hat{c}_{\text{free}}$  breaks down, this only happens because the approximation of the exact solution on the classical level stops being valid. Thus, we only neglect classical nonlinearities. It is reasonable to expect that taking those into account would not change the overall strength of quantum effects, i.e. the rate at which the classical solution deteriorates. Since the timescale of quantum breaking is only sensitive to the magnitude of quantum effects but not to their precise nature, we will be able to estimate the quantum break-time. We will elaborate on this point in section 2.2.5.

## 2.2.2 Deviations from the Classical Evolution

### A Quantum Picture of the Classical Solution

Now we are ready to give a quantum description of the field  $\phi$ . To this end, we need to switch to the relevant quantum quantities. The classical frequency  $\bar{m}$  determines the mass of the quantum particles and the classical coupling  $\bar{\alpha}$  determines the dimensionless quantum coupling:

$$m = \hbar\bar{m}, \quad \alpha = \hbar\bar{\alpha}. \quad (2.14)$$

We note that the relevant powers of  $\hbar$  can be inferred from dimensional analysis. Because of the importance of the scaling with  $\hbar$ , we will continue to keep it explicit. The quantum Lagrangian that corresponds to the theory (2.5) is

$$\hat{\mathcal{L}} = \frac{1}{2}\partial_\mu\hat{\phi}\partial^\mu\hat{\phi} - \frac{1}{2\hbar^2}m^2\hat{\phi}^2 + \frac{1}{4!\hbar}\alpha\hat{\phi}^4. \quad (2.15)$$

Our overall goal is to investigate corrections which lead to a departure of the true quantum evolution from the classical solution. To this end, the next step is to understand the classical solution as expectation value in an underlying quantum state. As explained, we will neglect interactions in doing so,  $\bar{\alpha} = 0$ . In that case, we can expand the full Heisenberg operator  $\hat{\phi}$  in creation and annihilation operators:<sup>2</sup>

$$\hat{\phi} = \sum_{\vec{k}} \sqrt{\frac{\hbar}{2V\omega_{\vec{k}}}} \left( \hat{c}_{\vec{k}} e^{-ikx} + \hat{c}_{\vec{k}}^\dagger e^{ikx} \right), \quad (2.16)$$

---

<sup>2</sup>We use sums instead of integrals to emphasize that any physical process happens in a finite volume. Correspondingly, we employ dimensionless operators  $\hat{c}_{\vec{k}}^\dagger, \hat{c}_{\vec{k}}$ . This convention also makes it easier to take the nonrelativistic limit. If one considers the idealization of infinite space in order to facilitate computations, this leads to  $\sum_{\vec{k}} \rightarrow V/(2\pi\hbar)^3 \int d^3\vec{k}$ .

where  $V$  is the volume,  $kx \equiv \omega_{\vec{k}}t - \hbar^{-1}\vec{k}\cdot\vec{x}$  and  $\omega_{\vec{k}} = \hbar^{-1}\sqrt{m^2 + |\vec{k}|^2}$ . The creation and annihilation operators satisfy the standard commutation relations,

$$[\hat{c}_{\vec{k}}, \hat{c}_{\vec{k}'}] = [\hat{c}_{\vec{k}}^\dagger, \hat{c}_{\vec{k}'}^\dagger] = 0, \quad [\hat{c}_{\vec{k}}, \hat{c}_{\vec{k}'}^\dagger] = \delta_{\vec{k}, \vec{k}'}. \quad (2.17)$$

Next, we need to fix the quantum state  $|N\rangle$  of the scalar field  $\hat{\phi}$ . It has to fulfill the requirement that the expectation value over it yields the classical harmonic oscillator solution  $\phi_0(t)$  of equation (2.7). Since  $\phi_0(t)$  is translation invariant, we can only use quanta of zero momentum. In this momentum mode, the simplest state that yields the classical solution is a coherent state:

$$|N\rangle \equiv e^{-\frac{1}{2}N + \sqrt{N}\hat{c}_0^\dagger} |0\rangle = e^{-\frac{1}{2}N} \sum_{n=0}^{\infty} \frac{N^{\frac{n}{2}}}{\sqrt{n!}} |n\rangle, \quad \text{with} \quad (2.18)$$

$$N = V \frac{mA^2}{2\hbar^2}. \quad (2.19)$$

In this formula,  $|n\rangle = (\hat{c}_0^\dagger)^n (n!)^{-\frac{1}{2}} |0\rangle$  are normalized number eigenstates of  $n$  quanta with zero momentum. Because of Eq. (2.16), it is easy to see that the state  $|N\rangle$  indeed yields the correct expectation value, i.e. the oscillating solution (2.7):

$$\langle N | \hat{\phi} | N \rangle = A \cos(\bar{m}t), \quad (2.20)$$

where we used that  $\hat{c}_0 |N\rangle = \sqrt{N} |N\rangle$ . Thus, the requirement (2.20) to reproduce the classical expectation value fixes the mean occupation number  $N$  of the coherent state.

We conclude that from the point of view of the noninteracting quantum theory (i.e. for  $\alpha = 0$ ), the oscillating classical field  $\phi_0(t)$  is a coherent state of zero-momentum quanta of mean occupation number density

$$n = \frac{\bar{m}A^2}{2\hbar}. \quad (2.21)$$

In order to obtain a typical total particle number, we need to choose a volume. As explained in section 2.1, it is natural to use the wavelength of particles as reference scale since this corresponds to the distance on which a given particle can interact efficiently. This leads to  $V = \bar{m}^{-3}$  and we obtain

$$N = \hbar^{-1} \frac{A^2}{2\bar{m}^2}. \quad (2.22)$$

As already discussed in section 2.1, we observe that  $N$  scales as  $\hbar^{-1}$ . This means that it becomes infinite in the classical limit  $\hbar \rightarrow 0$ .

Furthermore, we want to study the energy of the coherently oscillating solution (2.7). There are two ways to evaluate it. First, we can compute it on the classical

level, i.e. by plugging the solution in the Hamiltonian derived from the classical Lagrangian (2.5). For  $\alpha = 0$ , we obtain the energy density

$$\rho = \frac{\bar{m}^2 A^2}{2}. \quad (2.23)$$

On the quantum level, there is a second way to determine  $\rho$ . Since the coherent state  $|N\rangle$  has a number density  $n$  and each quantum carries an energy  $m$ , the energy density must be

$$\rho = mn. \quad (2.24)$$

As is evident from Eq. (2.21), this yields the same result. The energy density of the classical solution  $\phi_0(t)$  and of the quantum state  $|N\rangle$  match. We remark that Eq. (2.24) can also be used to derive the occupation number of the coherent state from classical quantities: Given the energy density  $\rho$  and the frequency  $\bar{m}$ , it determines the number density of the quantum state as  $n = \rho/(\hbar\bar{m})$ .

Finally, we conclude that  $\lambda$  has acquired a twofold meaning. First, it controls the strength of classical nonlinearities, as is apparent from Eq. (2.13). Secondly, it follows from expression (2.22) for  $N$  that it corresponds to collective coupling of the quantum theory,  $\lambda = \alpha N$ , in accordance with Eq. (2.1). Thus, classical nonlinearities translate to the quantum theory as collective interactions. We will elaborate on this point in section 2.2.3.

### Construction of the Coherent State

For the sake of completeness, we will outline two procedures to construct the coherent state (2.18). The first one is to look for a state which maximizes the classical expectation value, i.e.

$$\frac{|\langle N|\hat{\phi}|N\rangle|}{\langle N|N\rangle}. \quad (2.25)$$

This condition amounts to realizing the classical result with a minimal quantum input. As shown in [73], this procedure leads to (2.18). Essentially, the reason is that coherent states are eigenstates of the annihilation operator.

A second justification for the use of coherent states would be to follow [74]. There, the idea is to consider a shift of the state  $\phi = 0$ , which corresponds to the classical vacuum, to a different value  $\phi = A$ . In the limit  $\bar{m} \rightarrow 0$ , such a shift  $\phi \rightarrow \phi + A$  by a constant  $A$  would correspond to a symmetry. The corresponding shift-generator  $\hat{Q}$ , which would represent a conserved charge for  $\bar{m} \rightarrow 0$ , has the form:

$$\hat{Q}(t) = \int d^3\vec{x} \partial_t \hat{\phi} = -iq \left( e^{-i\bar{m}t} \hat{c}_{\vec{0}} - e^{i\bar{m}t} \hat{c}_{\vec{0}}^\dagger \right), \quad (2.26)$$

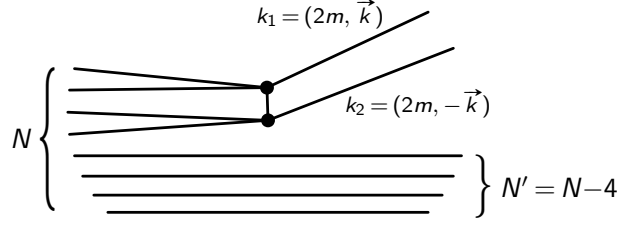


Figure 2.1: Four  $\hat{\phi}$ -particles of the coherent state annihilate into two free particles with nonzero momenta. Their 4-momenta are denoted by  $k_1$  and  $k_2$ .

with  $q = \sqrt{\frac{mV}{2}}$ . Using this generator, we can obtain the coherent state  $|N\rangle$  by shifting the vacuum state  $|0\rangle$  corresponding to  $\phi = 0$ :

$$|N\rangle := \exp\left\{-iA\hat{Q}(t=0)/\hbar\right\}|0\rangle = \exp\left\{\sqrt{N}\left(\hat{c}_{\vec{0}} - \hat{c}_{\vec{0}}^\dagger\right)\right\}|0\rangle, \quad (2.27)$$

with  $\sqrt{N} = Aq/\hbar$ , i.e.  $N = \frac{A^2mV}{2\hbar^2}$  as in (2.19). Note that our states must be time-independent since we are working in the Heisenberg picture. Thus, we have evaluated the charge operator at a fixed time. We could have introduced a constant phase in this way, but for simplicity we set it to 0. Using the Baker-Campbell-Hausdorff formula, we finally obtain (2.18).

### Leading Quantum Process

Now we can come to our main goal, namely the computation of the quantum break-time, which is the timescale when the expectation value of the quantum field will no longer match the classical solution. Because we approximated the classical solution by neglecting classical nonlinearities, we cannot make a statement about what the resulting (“departed”) state will be. Nevertheless, we can estimate the time scale  $t_q$  on which the coherent state approximation and therefore the classical description break down. The implications of our approximations will be further discussed in section 2.2.5.

We are interested in the leading process that is not captured by the classical solution. Generically, the dominant contribution would come from scattering due to four-point coupling. However, in the approximation in which the initial and final particles are treated as free, the rate is suppressed due to momentum conservation: Since both initial and final particles carry vanishing momentum, the phase space for such a process is zero.

Therefore, the lowest order nonvanishing process involves the participation of six  $\hat{\phi}$ -particles. For instance, four particles of the coherent state can annihilate into two particles with nonzero momenta, as is depicted in Fig. 2.1. The final state of such a process can be a tensor product of two one-particles states of 4-momenta  $k_1 = (E_1, \vec{k}_1)$  and  $k_2 = (E_2, \vec{k}_2)$  with a coherent state  $|N - \Delta N\rangle$

of zero momentum particles of reduced mean occupation number  $N - \Delta N$ . We will not fix  $\Delta N$  for now but discuss its meaning shortly. By energy-momentum conservation, we have  $\vec{k}_1 = -\vec{k}_2$  and  $E_1 = E_2 = 2m$ . The tree-level amplitude  $\mathcal{A}$  for the transition  $|N\rangle \rightarrow |N - \Delta N\rangle |k_1\rangle |k_2\rangle$  comes from a process with one internal propagator:

$$\mathcal{A} \approx \alpha^2 \langle N - \Delta N | \langle \vec{k}_1 | \langle \vec{k}_2 | (\hat{c}_{k_1}^\dagger \hat{c}_{k_2}^\dagger \hat{c}_0 \hat{c}_0 \hat{c}_0 \hat{c}_0) | N \rangle \approx \alpha^2 N^2 e^{-\frac{\Delta N^2}{8N}}, \quad (2.28)$$

where the factor  $e^{-\frac{\Delta N^2}{8N}}$  is due to the overlap of coherent states with different mean occupation number.

For large  $N$ , we can approximate it as  $e^{-\frac{\Delta N^2}{8N}} \approx 1 - \Delta N^2/(8N)$ . Thus, as long as  $\Delta N^2 \ll N$ , different choices of the final coherent state lead to the same amplitude, up to  $1/N$ -corrections. This is due to the fact that a coherent state is not a particle number eigenstate, i.e. coherent states with different mean occupation numbers have a nonzero overlap even without any interaction. Our goal is not to consider this non-Hamiltonian effect. Instead, we want to focus on how the coherent state evolves due to interaction of coherent state constituents. Therefore, it is most natural to consider the process which would also be possible if we were to replace the coherent background states by number eigenstates. This leads to  $\Delta N = 4$ . Moreover, this choice of  $\Delta N$  conserves the expectation value of the energy in the limit of vanishing interaction energy. In any case, the precise value of  $\Delta N$  does not matter for our conclusions.

Since we are only interested in the leading contribution to the rate of the scattering process, we will neglect the  $1/N$ -correction that is sensitive to  $\Delta N$  from now on. Then we obtain

$$\Gamma_{4 \rightarrow 2} \approx \bar{m}(\alpha N)^4 = \bar{m}\lambda^4, \quad (2.29)$$

where we used the collective coupling  $\lambda$  as defined in (2.1). Note that the classical frequency  $\bar{m}$  appears, which leads to the correct dimensionality  $[\Gamma_{4 \rightarrow 2}^{-1}] = (time)$ . The rate (2.29) determines how fast the coherent state loses its constituents and *de-classicalizes*.

We point out that one can estimate the rate (2.29) without an explicit  $S$ -matrix computation. Namely, we know that the amplitude consists of two 4-point couplings. Thus, it must scale as  $\alpha^2$  and therefore the rate contains  $\alpha^4$ . However, this would describe a process in which four fixed particles scatter. Because of the degeneracy in the initial state, there are  $\binom{N}{4}$  possibilities to select the four particles that scatter. This leads to an enhancement factor of  $\binom{N}{4} \approx N^4$ . Finally, the only quantity that has the correct dimensionality  $1/(time)$  of a rate is  $\bar{m}$ . Putting together these ingredients, we get a rate  $\Gamma_{4 \rightarrow 2} \approx \bar{m}\alpha^4 N^4$ , in full accordance with Eq. (2.29).

Finally, we remark that for tree-level multi-particle amplitudes with a large enough number of external legs, perturbation theory is expected to break down

due to a factorial growth of the diagrams. This breakdown will not affect our conclusions because nonperturbative arguments indicate that multi-particle quantum processes – e.g. ones in which the coherent state loses order-one fraction of its constituents during one oscillation time – must be exponentially suppressed. This suppression can be explicitly seen by adopting the results of [45], where analogous multi-particle amplitudes have been computed for gravitons. For reading out the exponential suppression, the spin of the particle is inessential. Hence, we can safely conclude that the leading-order process which leads to de-classicalization of the spatially-homogeneous time-dependent field has the rate (2.29).

### Quantum Break-Time

So far, we have computed the timescale  $\Gamma_{4 \rightarrow 2}^{-1}$  during which 4 constituents of the coherent state experience rescattering. However, this is not yet the quantum break-time. A significant deviation from the classical solution only occurs once a significant fraction of the particles in the coherent state has undergone such a process. Since the mean occupation number in the coherent state is  $N$ , quantum rescattering is able to give a significant departure from the coherent state only after a sufficiently large fraction of particles, i.e. of the order of  $N$ , experience rescattering. This process takes the time

$$t_{q,4 \rightarrow 2} \approx N \Gamma_{4 \rightarrow 2}^{-1} = \bar{m}^{-1} \frac{1}{\lambda^3 \alpha}. \quad (2.30)$$

We can verify that  $t_{q,4 \rightarrow 2}$  is indeed a quantum timescale. Whereas  $\bar{m}$  and  $\lambda$  are classical, i.e. independent of  $\hbar$ , the quantum coupling scales as  $\alpha \sim \hbar$ . Therefore, we have  $t_{q,4 \rightarrow 2} \sim \hbar^{-1}$  and the quantum break-time becomes infinite in the classical limit  $\hbar \rightarrow 0$ , as it should. Furthermore, we remark that the result (2.30) is in full accordance with the generic scaling-argument in section 2.1, which led to Eq. (2.2).

### The Classical and Semiclassical Limit

We can investigate the meaning of the classical and semiclassical limit, which we have introduced in section 1.3. In the classical limit  $\hbar \rightarrow 0$ , all quantum effects vanish. This leads to an infinite quantum break-time, as we have just discussed.

Quantum breaking can also be avoided in the semiclassical limit. As we have shown using the examples of black holes (Eq. (1.5)) and de Sitter (Eq. (1.18)), its key idea is to make the energy of the classical solution infinite while keeping the collective coupling fixed. In this way, any backreaction can be avoided. In the present case, it follows from Eqs. (2.13) and (2.23) that the semiclassical limit corresponds to taking

$$A \rightarrow \infty, \quad \bar{\alpha} \rightarrow 0, \quad \bar{\alpha} A^2 \text{ fixed}. \quad (2.31)$$

Thus, we consider a vanishing classical coupling and an infinite classical amplitude while keeping  $\hbar$  finite.

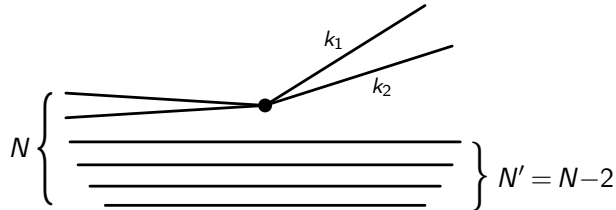


Figure 2.2: Two  $\hat{\phi}$ -particles of the coherent state annihilate into two particles that are not in the coherent state. Their 4-momenta are denoted by  $k_1$  and  $k_2$ . Because of phase space suppression, this process only becomes possible if the constituents of the coherent state have nonzero momenta or if the interaction potential gives a contribution to the asymptotic energies.

Both the classical limit  $\hbar \rightarrow 0$  and the semiclassical limit (2.31) imply on the quantum level that

$$N \rightarrow \infty, \quad \alpha \rightarrow 0, \quad \lambda \text{ fixed}, \quad (2.32)$$

as is evident from Eqs. (2.13), (2.14) and (2.22). This is in full accordance with the analogous limits in the case of black holes (Eq. (1.11)) and de Sitter (Eq. (1.24)). Thus, we uncover a universal mechanism. The (semi)classical limit corresponds to avoiding backreaction by making the number of particles infinite. Correspondingly,  $\alpha \rightarrow 0$  leads to a diverging quantum break-time.

### 2.2.3 Other Scattering Processes

#### Quantum Break-Time due to $2 \rightarrow 2$ -Scattering

So far, we have considered  $4 \rightarrow 2$ -scattering as the leading quantum process. The reason was that  $2 \rightarrow 2$ -scattering is kinematically forbidden in the approximation that initial and final particles are free. In reality, however, the interaction potential gives a small contribution to the asymptotic energy of the particles. This makes the process of  $2 \rightarrow 2$ -scattering possible. Moreover, this process becomes relevant for generic initial states, in which particles in the coherent state have nonzero momenta. Therefore, we give an estimate of the quantum break-time due to  $2 \rightarrow 2$ -scattering.

First, we compute the rate of this process, which is displayed in Fig. 2.2. We will give an upper bound on the rate by assuming that the momenta are comparable to  $m$ , i.e. we ignore any phase space suppression. In that case, we get

$$\Gamma_{2 \rightarrow 2} \approx \bar{m} \lambda^2. \quad (2.33)$$

The corresponding quantum break-time is given by

$$t_{\text{q}, 2 \rightarrow 2} \approx N \Gamma_{2 \rightarrow 2}^{-1} = \bar{m}^{-1} \frac{1}{\lambda \alpha}. \quad (2.34)$$

In the undercritical regime  $\lambda < 1$ , this timescale is shorter than the quantum break-time (2.30) due to  $4 \rightarrow 2$ -scattering. Still it also scales as  $t_{q,2 \rightarrow 2} \sim \alpha^{-1} \sim \hbar^{-1}$ . Thus, it is a quantum timescale and compatible with the scaling relation (2.2). Moreover, we conclude that the collective coupling  $\lambda$  controls which process gives the dominant contribution to quantum breaking.

Using the classical break-time (2.12), we can rewrite Eq. (2.34) as

$$t_{q,2 \rightarrow 2} = \frac{t_{cl}}{\alpha}. \quad (2.35)$$

This shows that even the lower bound on the quantum break-time is larger than the timescale of classical nonlinearities by the big factor  $1/\alpha$ . This observation that quantum effects always grow more slowly than classical ones will be important later.

### Role of Decay

Furthermore, we would like to investigate quantum breaking due to particle decay. To this end, we shall enlarge the theory (2.15) by introducing a coupling of  $\hat{\phi}$  to a new particle species  $\hat{\psi}$  to which  $\hat{\phi}$  can decay. The Lagrangian becomes

$$\hat{\mathcal{L}} = \frac{1}{2} \partial_\mu \hat{\phi} \partial^\mu \hat{\phi} - \frac{1}{2\hbar^2} m^2 \hat{\phi}^2 + \frac{1}{4! \hbar} \alpha \hat{\phi}^4 + i \hat{\psi} \gamma_\mu \partial^\mu \hat{\psi} - \sqrt{\alpha} \hat{\phi} \hat{\psi} \hat{\psi}. \quad (2.36)$$

We take  $\hat{\psi}$  to be a massless fermion, although the spin and the mass are unimportant for this consideration as long as the new particle is light enough to allow for a decay of  $\hat{\phi}$ . In order to make a clear comparison, we have chosen the coupling to fermions to be of the same strength as the bosonic self-coupling. In this way, the amplitudes of both  $2 \rightarrow 2$  scatterings,  $\hat{\phi} + \hat{\phi} \rightarrow \hat{\phi} + \hat{\phi}$  and  $\hat{\phi} + \hat{\phi} \rightarrow \hat{\psi} + \hat{\psi}$ , are controlled by the same coupling  $\alpha$ .

The decay rate for the production of a pair of  $\hat{\psi}$ -quanta is given by

$$\Gamma_{\text{decay}} \approx \bar{m} \alpha N. \quad (2.37)$$

The corresponding macroscopic timescale, after which on the order of  $N$  quanta of the initial coherent state have experienced this decay process, is

$$t_{\text{decay}} \approx \bar{m}^{-1} \frac{1}{\alpha}. \quad (2.38)$$

As in the processes considered before, this timescale is quantum,  $t_{\text{decay}} \sim \hbar^{-1}$ , because of the scaling with  $1/\alpha$ . Comparing Eq. (2.38) with the quantum break-time (2.34) due to  $2 \rightarrow 2$ -scattering of  $\hat{\phi}$ -quanta, we conclude that decay is the dominant quantum process in the regime  $\lambda < 1$ . Nevertheless, the corresponding timescale is still longer than  $t_{cl} = \bar{m}^{-1}/\lambda$ , as it should.

The role of decay is special since it does not affect the coherence of the state of  $\hat{\phi}$ -quanta. The reason is that the part of the interaction Hamiltonian responsible for a two-body decay of  $\hat{\phi}$ -quanta only contains the annihilation operator  $\hat{c}_{\vec{k}}$  of  $\hat{\phi}$ -quanta and the creation operators for  $\hat{\psi}$ -particles. The coherent state  $|N\rangle$ , however, is an eigenstate of  $\hat{c}_{\vec{k}}$  and hence unchanged under its action. Thus, the final state of a pure decay process is still maximally classical. Correspondingly, the evolution can be described by a seemingly classical equation with an additional friction term:

$$\ddot{\phi} + t_{\text{decay}}^{-1} \dot{\phi} + \bar{m}^2 \phi - \frac{1}{6} \bar{\alpha} \phi^3 = 0. \quad (2.39)$$

It is crucial to note, however, that Eq. (2.39) is in fact not classical since  $t_{\text{decay}}$  depends on  $\hbar$ .

This shows that decay represents a border case of quantum breaking. On the one hand, the final state of decay still admits a classical description. On the other hand, the transition to this final state can only be described by a quantum process. A classical observer is completely blind to it. Finally, we remark that the theory (2.36) will eventually also violate coherence. This happens due to rescattering events of the produced  $\hat{\psi}$ -particles since the corresponding interaction term also contains creation operators of  $\hat{\phi}$ -particles.

### Quantum Picture of Classical Processes

We have discussed that the interaction rate gets enhanced by a highly occupied initial state, e.g. in Eq. (2.33) for the case of  $2 \rightarrow 2$ -scattering. A natural question to ask is if it is possible to further enhance the rate if also the final state is highly occupied. Sticking to the example of  $2 \rightarrow 2$ -scattering, we see that the rate gets indeed enhanced by a factor of  $N$  if one of the modes in the final state is also highly occupied:<sup>3</sup>

$$\Gamma_{\text{enhanced}} \approx \bar{m} \lambda^2 N. \quad (2.40)$$

Correspondingly, the timescale after which on the order of  $N$  particles have experienced such a process is much shorter:

$$t_{\text{collective}} \approx N \Gamma_{\text{enhanced}}^{-1} = \bar{m}^{-1} \frac{1}{\lambda^2}. \quad (2.41)$$

The crucial point, however, is that this result is independent of  $\hbar$ . Instead,  $t_{\text{collective}}$  only depends on the classical quantities  $\bar{m}$  and  $\lambda$ . Thus, this process is not quantum, but we have discovered how classical nonlinearities can be described in the quantum language. Obviously, such an interaction cannot lead to quantum breaking.

---

<sup>3</sup>One can wonder why we do not consider a process in which both modes in the final state are highly occupied. The reason is that in such a case, the rate of a process in which initial and final states are exchanged are the same to leading order so that these interactions effectively cancel (see e.g. also [75]).

## 2.2.4 Nonrelativistic Model

### Fast Quantum Breaking

As we have already discussed in section 2.1, it was demonstrated in [40] that a simple system of cold bosons can exhibit a remarkably short quantum break-time in the regime in which the boson gas is overcritical and unstable. In that case, this timescale is determined by the Lyapunov exponent of the classical instability, which the system exhibits in this regime.

In this section, we review the corresponding results from [40]. The system studied there, which was previously analyzed in [76], consists of nonrelativistic bosons of mass  $m$ , which are contained in a periodic  $d$ -dimensional box of radii  $R$  and exhibit a simple attractive interaction. The Hamiltonian has the following form:

$$\hat{H} = \int d^d \vec{x} \hat{\psi}^\dagger \frac{-\hbar^2 \Delta}{2m} \hat{\psi} - \frac{g}{2} \int d^d \vec{x} |\hat{\psi}|^4, \quad (2.42)$$

where the parameter  $g > 0$  controls the strength of the *attractive* interaction among the bosons. The corresponding dimensionless coupling is

$$\alpha = \frac{4gmR^2}{\hbar^2 V}, \quad (2.43)$$

where  $V = (2\pi R)^d$  is the  $d$ -dimensional volume. Note that up to the choice of boundary conditions, the system (2.42) is the nonrelativistic limit of the model (2.15) in the case  $d = 3$ .

We can represent  $\hat{\psi}$  as a classical mean field and the quantum fluctuations,  $\hat{\psi} = \psi_{\text{cl}} + \delta\widehat{\psi}_{\text{q}}$ , where  $\psi_{\text{cl}}$  satisfies the Gross-Pitaevskii equation [77, 78]:

$$i\hbar\partial_t\psi_{\text{cl}} = \left( -\frac{\hbar^2}{2m}\Delta - g|\psi_{\text{cl}}|^2 \right) \psi_{\text{cl}} = \mu\psi_{\text{cl}}. \quad (2.44)$$

The parameter  $\mu$  is the chemical potential, which plays the role of a Lagrange multiplier for imposing the constraint  $\int d^d \vec{x} |\psi_{\text{cl}}|^2 = N$ . We shall focus on the homogeneous solution,

$$|\psi_{\text{cl}}|^2 = -\frac{\mu}{g} = \frac{N}{V}. \quad (2.45)$$

It represents a mean field description of the quantum state in which only the zero-momentum mode is macroscopically occupied. This solution exists for all nonzero values of the parameters. However, beyond a certain critical point it becomes unstable and the system undergoes a quantum phase transition. In the overcritical regime, the instability of the homogeneous solution manifests itself as Lyapunov exponent which is independent of  $\hbar$ .

In order to investigate stability, we go to momentum space:

$$\hat{\psi} = \sum_{\vec{\Gamma}} \frac{1}{\sqrt{V}} e^{i\frac{\vec{\Gamma}}{\hbar}\vec{x}} \hat{a}_{\vec{\Gamma}}. \quad (2.46)$$

Here  $\vec{l}$  is the  $d$ -dimensional wave-number vector, which determines the momentum as  $\vec{k} = \hbar \vec{l} / R$ . The operators  $\hat{a}_{\vec{l}}^\dagger$ ,  $\hat{a}_{\vec{l}}$  are the creation and annihilation operators of bosons of momentum-number vector  $\vec{l}$  and satisfy the usual algebra:  $[\hat{a}_{\vec{l}}, \hat{a}_{\vec{l}'}^\dagger] = \delta_{\vec{l}\vec{l}'}$  and all other commutators zero. Then the Bogoliubov-de Gennes frequencies are given by [79]:

$$\hbar\omega_{\vec{l}} = |\vec{l}| \frac{\hbar^2}{2mR^2} \sqrt{|\vec{l}|^2 - \lambda}. \quad (2.47)$$

They are controlled by the collective coupling  $\lambda = \alpha N$ . All modes with  $|\vec{l}|^2 < \lambda$  become imaginary. Thus, instability sets in for  $\lambda > 1$ , and the number of unstable  $l$ -modes depends on the magnitude of the criticality parameter  $\lambda$ . In the regime in which only the  $|\vec{l}| = 1$ -mode is unstable, the explicit numerical analysis of [40] shows that the quantum break-time scales as

$$t_{\text{q, fast}} \approx \omega_{\vec{l}}^{-1} \ln(N). \quad (2.48)$$

By increasing  $\lambda$ , one can destabilize higher and higher momentum modes and correspondingly make the Lyapunov exponents large. Finally, we note that  $\omega_{\vec{l}}$  are classical quantities because  $m/\hbar$  is classical and represents a zero mode oscillation frequency of an underlying classical field, whose quanta are the bosons in question. Thus, an important message which we take from the results of [40] recounted above is: The quantum break-time can be shortened in the overcritical regime, provided that the initial state exhibits a classical instability, i.e. an instability characterized by an  $\hbar$ -independent Lyapunov exponent.

However, the following clarification is in order. The expression (2.47) creates the impression that we can make the quantum break-time arbitrarily short time if the system is sufficiently overcritical, i.e. if we increase the collective coupling  $\lambda$ , e.g. by keeping all the other parameters fixed and increasing the occupation number of zero-momentum quanta. However, one has to be very careful with this limiting case. Although it is legitimate to take the limit  $\lambda \rightarrow \infty$  in the nonrelativistic model given by the Hamiltonian (2.42), an underlying fundamental relativistic quantum field theory may go out of the validity. For example, in the case of cold bosons, one reason is that they can only be described by the Hamiltonian (2.42) as long as the gas is sufficiently dilute.

### No Quantum Breaking<sup>4</sup>

It is also very interesting to study the model (2.42) in the undercritical regime  $\lambda < 1$ . In that case, it is possible to investigate the model analytically, where we will confine ourselves to  $d = 1$ . We will follow the analysis of [40]. First, we go to

---

<sup>4</sup>Here some material from appendix B.2 of [5] was used.

momentum space by using Eq. (2.46):

$$\hat{H} = \frac{\hbar^2}{2mR^2} \left[ \sum_{l=-\infty}^{\infty} l^2 \hat{a}_l^\dagger \hat{a}_l - \frac{\alpha}{4} \sum_{l,m,n=-\infty}^{\infty} \hat{a}_l^\dagger \hat{a}_m^\dagger \hat{a}_{n+l} \hat{a}_{m-n} \right]. \quad (2.49)$$

Then we use the Bogoliubov approximation [79],  $\hat{a}_0 \rightarrow \sqrt{N}$ , to focus on states in which only the 0-mode is occupied. We obtain

$$\hat{H} = \frac{\hbar^2}{2mR^2} \left[ \sum_{l \neq 0} \left( l^2 - \frac{\lambda}{2} \right) \hat{a}_l^\dagger \hat{a}_l - \frac{1}{4} \lambda \sum_{l \neq 0} (\hat{a}_l^\dagger \hat{a}_{-l}^\dagger + \hat{a}_l \hat{a}_{-l}) \right]. \quad (2.50)$$

Now we perform the Bogoliubov transformation

$$\hat{a}_l = u_l \hat{b}_l + v_l^* \hat{b}_{-l}^\dagger, \quad (2.51)$$

where we choose

$$u_l^2 = \frac{1}{2} \left( 1 + \frac{l^2 - \frac{\lambda}{2}}{\epsilon_l} \right), \quad v_l^2 = \frac{1}{2} \left( \frac{l^2 - \frac{\lambda}{2}}{\epsilon_l} - 1 \right). \quad (2.52)$$

This gives the diagonalized Hamiltonian

$$\hat{H} = \frac{\hbar^2}{2mR^2} \sum_{l \neq 0} \epsilon_l \hat{b}_l^\dagger \hat{b}_l, \quad \epsilon_l = \sqrt{l^2(l^2 - \lambda)}. \quad (2.53)$$

Obviously, the Bogoliubov transformation is only well-defined in the undercritical regime  $\lambda < 1$ . Moreover, since the Bogoliubov approximation neglects corrections that scale as  $1/N$ , it already breaks down close to the critical point, i.e. for  $\lambda \lesssim 1$ .<sup>5</sup> Nevertheless, the Bogoliubov energies agree with the previous result (2.47) both in the undercritical and in the overcritical regime:  $\hbar\omega_l = \hbar^2/(2mR^2)\epsilon_l$ .

In this model, we can study quantum breaking by analyzing the number of depleted particles  $N_d$  in the ground state  $|0_b\rangle$  of the Bogoliubov modes:

$$N_d = \sum_{k \neq 0} \langle 0_b | \hat{a}_k^\dagger \hat{a}_k | 0_b \rangle = \sum_{l \neq 0} v_l^2. \quad (2.54)$$

In the regime  $\lambda \ll 1$ , we get

$$N_d = \frac{\pi^4 \lambda^2}{720}, \quad (2.55)$$

which is smaller than 1. Clearly, this shows that for  $\lambda \ll 1$  significant depletion never happens,  $N_d \ll N$ , i.e. there is no quantum breaking. We note that the dominant contribution to depletion is due to the lowest-lying modes  $l = \pm 1$ . Thus, the absence of quantum breaking is connected to the fact that the phase space for depletion is very small, i.e. only a few modes are accessible. For this reason, we expect that in a generic quantum field-theoretic system, in which many different momentum modes are accessible, quantum breaking also takes place in the undercritical regime.

<sup>5</sup>We remark that the Bogoliubov approximation can be made arbitrarily precise in the double-scaling limit (3.20), which we shall introduce and discuss in section 3.1.4.

### 2.2.5 Summary

We will summarize what we have learned about quantum breaking. The first question is about the validity of our approximations. Namely, we have seen (see e.g. Eq. (2.35)) that the quantum break-time  $t_q$  is generically bigger than its classical counterpart  $t_{cl}$ . Since the linear approximation of the classical solution, on which we base our computation of quantum effects, already breaks down on the timescale of the classical break-time, one is immediately led to wonder whether one can make any statement at all about the quantum break-time of the full nonlinear system.

The answer is positive and the reason is that we determine the quantum break-time in a two-step process. First, we only study the system on timescales shorter than  $t_{cl}$ . In this regime, we can reliably compute quantum effects. The second step is to assume that the overall strength of quantum interactions, i.e. the rate at which the classical approximation deteriorates, stays approximately constant even after  $t_{cl}$ . Since quantum breaking is only sensitive to the magnitude of quantum effects but not their precise nature, this allows us to obtain the quantum break-time by extrapolation.

The reason that we expect this procedure to work is that our approximation solely happens on the classical level. In order to promote our linear approximation to the full solution, the only missing ingredient are classical nonlinearities. Thus, one would have to change the Fock basis by performing an appropriate Bogoliubov transformation and to use the coherent state description in terms of interacting quanta  $\hat{c}^\dagger, \hat{c}$  instead of free ones  $\hat{c}_{free}^\dagger, \hat{c}_{free}$ . In this way, we could increase the classical break-time. The key point is that doing so can solely lead to classical corrections, which only depend on  $\lambda$ . In contrast, the strength of quantum effects that lead to a gradual departure from the classical evolution is still given by the quantum coupling  $\alpha$ . Therefore, the timescale on which these quantum effects become important is of the same order of magnitude as in our linear model.

This fully resonates with our reasoning in section 2.1, which was solely based on scaling arguments. Since the quantum break-time that corresponds to the leading quantum effect must scale as  $\hbar^{-1}$ , it still needs to contain a factor of  $1/\alpha$  in the fully nonlinear theory. By taking into account classical nonlinearities, only corrections that depend on  $\lambda$  may arise. Thus, we can represent the quantum break-time generically as

$$t_q \approx \frac{t_{cl}}{\alpha}, \quad (2.56)$$

where the classical timescale  $t_{cl}$  may be sensitive to classical nonlinearities, i.e. to  $\lambda$ . As already stressed, the key point is that the quantum break-time is generically long due to the small quantum coupling  $\alpha$ .

We must remark that in principle systems can exist for which the estimate (2.56) of the quantum break-time fails. However, this can only happen if the overall strength of quantum effects is drastically changed during the nonlinear evolution of a system. Whereas such a behavior seems very hard to achieve in

general, we have seen in the explicit model (2.42) that quantum breaking may not take place at all. As explained there, we believe that this behavior is caused by the lack of phase space, i.e. the absence of different accessible momentum modes. Therefore, we expect quantum breaking to take place in the relativistic model (2.15). In any case, studying quantum breaking in more detail in such a system constitutes an interesting topic of future research.

Whereas we can obtain the timescale of quantum breaking by extrapolation, it is important to note that we are unable to make a statement about the precise characteristics of quantum effects within our approximation: Since the classical solution already deviates from the full nonlinear theory in our linearized model, we cannot predict in what way the true quantum evolution deviates from the classical description.

Finally, we emphasize that all considerations above pertain to the undercritical regime, i.e. to a collective coupling  $\lambda < 1$ . In the opposite case,  $\lambda > 1$ , we have reproduced the result (2.48) of [40] that quantum breaking can become fast, provided a classical instability exists.

## 2.3 Application to Cosmic Axions

### 2.3.1 Importance of a Classical Description of Dark Matter Axions

Next, we study quantum breaking in a concrete system, namely cosmic axions. The axion [80, 81] is a well-known hypothetical particle which is predicted by the Peccei-Quinn (PQ) solution [82] to the strong CP problem. It is a pseudo-Goldstone boson of spontaneously-broken global chiral PQ symmetry. The explicit breaking of this symmetry by the chiral anomaly through nonperturbative QCD effects results in a nonzero mass of the axion. One of the beauties of axion physics is that its low energy dynamics is extremely constrained due to the Goldstone nature and the power of anomaly. The mass  $m_a$  and the decay constant  $f_a$  of the axion field are related via a nonperturbative scale  $\Lambda_{\text{QCD}}$ :  $m_a = \hbar\Lambda_{\text{QCD}}^2/f_a$ . Note that in any theory in which the sole source of the PQ symmetry breaking is the QCD anomaly, the scale  $\Lambda_{\text{QCD}}$  is entirely determined by the nonperturbative QCD sector and the low-energy parameters of the Standard Model (such as the Yukawa coupling constants of quarks) and is insensitive to the precise embedding of the axion into a high energy theory, i.e. low energy axion physics is insensitive with respect to UV-completion.

Phenomenological constraints put a lower bound on the scale  $f_a$  approximately around  $10^9$  GeV (see e.g. [83–85]). This speaks in favor of so-called invisible axion models [86–89], in which the PQ symmetry can be broken at a very high scale around  $f_a \gtrsim 10^9$  GeV. Such a weak coupling implies that the axion is essentially stable on cosmological scales. This fact makes the axion a very interesting dark

matter candidate. In this scenario, the role of dark matter energy is played by the energy of coherent oscillations of the axion field. Of course, the current energy of the axion field depends on the cosmological epoch of the onset of axion oscillations as well as on its initial amplitude  $A_{\text{in}}$ . Some conservative estimates are based on the assumptions that the axion oscillations first started in the epoch of thermal phase transition of QCD and with the maximal initial amplitude  $A_{\text{in}} \approx f_a$ . This gives the famous cosmological upper bound:  $f_a \lesssim 10^{12}$  GeV [90–92]. We must notice that there exist loopholes [93] which soften this upper bound and allow for much higher values of  $f_a$ . For the present study, however, this change is unimportant and we can safely assume  $f_a$  to be below its conservative upper bound,  $f_a \lesssim 10^{12}$  GeV.

The search for the dark matter axion has been an active field of research since no signs of it have been found so far (see e.g. [94–100] for current experimental efforts). Several of the proposed experiments heavily rely on the approximation of the gas of axions by a coherently oscillating classical scalar field  $a(t)$ . There has been a recent discussion of the axion field on the quantum level (see e.g. [71, 101–103]). Although the main motivation there was astrophysical, it was also suggested that quantum effects can significantly correct the classical description of axions. Obviously, it is important to clarify this issue both from a fundamental as well as an experimental point of view. In doing so, we will not discuss the astrophysical consequences proposed in [71, 101–103]. Instead, we will only be concerned with the general question if the classical description as oscillating scalar field is valid for axions.

Therefore, we will calculate a lower bound on the quantum break-time of the cosmic axion field, i.e. the minimal required timescale before the true quantum evolution of a multi-axion quantum state can depart from its classical mean field description. To this end, we will show that axions can effectively be described by the Lagrangian (2.15). Therefore, after identifying the appropriate parameters, we can simply use the result (2.30) and (2.34) derived before. It will turn out that if for some initial time the approximation of an axion gas by a classical field is good, it remains good – with an extraordinary accuracy – for timescales exceeding the current age of the Universe by many orders of magnitude. Hence, experimental searches relying on the classical field approximation are safe for all practical purposes.

## 2.3.2 Axion Properties

### General Properties

First, we have to specify the theory by which axions can be described. In order to determine their quantum break-time, however, the precise form of their potential, which we denote by  $V(a/f_a)$ , is not so important. For our analysis, it suffices to assume that it is a periodic function of  $a/f_a$ . Only later, for concreteness, we shall use a specific form which is widely used in the literature. In general, the energy

density of a time-dependent classical axion field  $a(t)$  is given by

$$\rho_a = \frac{1}{2}\dot{a}^2 + V(a/f_a). \quad (2.57)$$

So far, all quantities are classical and in accordance with our previous discussions, the fields and parameters in (2.57) have the following dimensions:  $[a] = [f_a] = \sqrt{(\text{energy})/(\text{time})}$  and  $[V] = (\text{energy})/(\text{time})^3$ .

Of course, for a generic nonsingular function  $V(a/f_a)$ , the exact form of  $a(t)$  can be very complicated and the oscillation period  $t_{\text{osc}}$  can have a nontrivial dependence on the amplitude. However, as long as the axion field does not reach the maxima of the potential during its oscillations, the order of magnitude of  $t_{\text{osc}}$  is given by the inverse curvature of potential  $V(a)$  at its minimum, about which the axion oscillates. Without loss of generality, we can set the minimum to be at  $a = 0$ . Then,  $t_{\text{osc}}^{-2} \approx \frac{\partial^2 V(a)}{\partial a^2}|_{a=0} \equiv \bar{m}_a^2$ , where  $\bar{m}_a$  represents the classical frequency of small oscillations (with infinitesimal amplitude).

In the cosmological environment, the coherent oscillations of a homogeneous axion field are described by an equation similar to a damped anharmonic oscillator:

$$\ddot{a} + \gamma\dot{a} + \frac{\partial V(a)}{\partial a} = 0, \quad (2.58)$$

where the friction term  $\gamma$  predominantly comes from the Hubble damping,  $\gamma \simeq 3H$ , due to the expansion of the Universe. The contribution from the axion decay is negligible. Note that for  $\gamma \ll \bar{m}_a$ , which is the case for most of the situations of our interest, we can still identify certain important properties of the time evolution  $a(t)$  without actually knowing the explicit forms of the functions  $V(a)$  and  $a(t)$ . The usual trick to achieve this is to first rewrite equation (2.58) in the following form:

$$\dot{\rho}_a = -\gamma\dot{a}^2. \quad (2.59)$$

Next we can average this expression over a timescale of order  $\bar{m}_a^{-1}$ , on which the variation of  $\gamma$  is negligible and it can be treated as constant. Moreover, if the axion oscillation amplitude is smaller than  $f_a$ , nonlinearities are not important and oscillations are dominated by the mass term. In such a case, the average values over a period of oscillation of the kinetic and potential energies of the axion field are equal and each carry half of the total energy density,  $\frac{1}{2}\overline{\dot{a}^2} = \overline{V(a)} = \frac{1}{2}\overline{\rho_a}$ , so that we can replace  $\overline{\dot{a}^2}$  on the r.h.s. of (2.59) by  $\overline{\rho_a}$ . Finally, applying the resulting average expression for the evolution on timescales longer than the Hubble time  $\gamma^{-1} \gg \bar{m}_a^{-1}$ , we get the following equation describing the time evolution of the axion energy density:

$$\dot{\rho}_a = -\gamma\rho_a, \quad (2.60)$$

where we drop the bar from now on. This can be easily integrated to give

$$\rho_a(t) = \rho_a(t_{\text{in}}) \exp\left(-\int_{t_{\text{in}}}^t \gamma(t') dt'\right), \quad (2.61)$$

where  $t_{\text{in}}$  is some initial time. Taking into account that  $\gamma = 3H$ , we immediately get the well-known result that the axion energy density dilutes as the inverse-cube of the cosmological scale factor, i.e. redshifts just like dust.

Correspondingly, we can use the temperature of the microwave background radiation in the Universe as a useful clock for keeping track of the axion energy density. Thus, we represent the evolution of the axion energy density in the following frequently-used form:

$$\rho_a(T) = \rho_a(T_{\text{in}}) \frac{T^3}{T_{\text{in}}^3}. \quad (2.62)$$

The fact that the classical axion energy density redshifts as dust nicely matches the quantum intuition according to which the time-dependent classical axion field represents a mean field description of a quantum gas of cold bosons.

In the language of the oscillating classical field  $a(t)$ , this means that due to Hubble damping, the amplitude of the axion field reduces as

$$A(t) = A_{\text{in}} \frac{T^{3/2}}{T_{\text{in}}^{3/2}}. \quad (2.63)$$

Since the initial amplitude  $A_{\text{in}}$  is bounded as  $A_{\text{in}} \lesssim f_a$  because of the periodicity of the potential, we conclude that in the cosmological environment, the amplitude quickly satisfies

$$A \ll f_a, \quad (2.64)$$

i.e. oscillations are small due to Hubble damping.

In section 2.3.4, we will show that the friction term, which reduces the density of axions, does not affect the validity of the classical description: The axion evolution is still well-described by a classical solution of damped oscillations. We shall therefore structure our analysis in the following way. First, we will ignore the contribution from the friction term and develop a coherent-state picture of the axion in the absence of dilution. In this setup, we identify the effects which lead to a quantum break-time of the axion field. We show that the timescale is enormous. We shall later take into account the underlying quantum effects which lead to friction in the classical theory and show that the original assumption that they do not contribute to quantum-breaking is consistent at the fundamental level.

### Fundamental Parameters

For concreteness, we model the axion potential by the following widely-considered form

$$V(a/f_a) = \Lambda_{\text{QCD}}^4 (1 - \cos(a/f_a)), \quad (2.65)$$

where the scale  $\Lambda_{\text{QCD}}$  that is set by QCD and quark masses has dimensionality  $[\Lambda_{\text{QCD}}^4] = (\text{energy})/(\text{time})^3$ . A crucial simplification occurs because the amplitude

of oscillations is small due to Hubble damping, i.e. we have  $a/f_a \ll 1$ . Correspondingly, we can expand the axion potential. To leading order, we obtain a Lagrangian of the form (2.5):

$$\mathcal{L} = \frac{1}{2} \partial_\mu a \partial^\mu a - \frac{1}{2} \bar{m}_a^2 a^2 + \frac{1}{4!} \bar{\alpha}_a a^4. \quad (2.66)$$

For the axion, the classical parameters are given as

$$\bar{m}_a = \frac{\Lambda_{\text{QCD}}^2}{f_a}, \quad \bar{\alpha}_a = \frac{\Lambda_{\text{QCD}}^4}{f_a^4}. \quad (2.67)$$

Thus, we can directly apply the whole analysis of section 2.2 to the case of cosmic axions.

First, we turn to classical nonlinearities. They are controlled by the collective coupling

$$\lambda_a = \frac{A^2}{f_a^2}, \quad (2.68)$$

where we plugged in the axion parameters in Eq. (2.13). Thus, the smallness (2.64) of oscillations implies that the collective coupling of axions is small:

$$\lambda_a \ll 1. \quad (2.69)$$

This undercriticality of cosmic axions, which we shall further discuss in section 2.3.5, will be important for our conclusions since it prevents the axions from entering a regime in which fast quantum breaking could take place. Moreover, since the axion field can be well approximated by the free classical solution (2.7), it follows that its energy density is given by

$$\rho_a = \frac{A^2 \Lambda_{\text{QCD}}^4}{2f_a^2}, \quad (2.70)$$

in accordance with Eq. (2.23) discussed before.

On the quantum level, we conclude that the mass  $m_a$  and the dimensionless coupling  $\alpha_a$  are given as before by

$$m_a = \hbar \bar{m}_a, \quad \alpha_a = \hbar \bar{\alpha}_a. \quad (2.71)$$

Consequently, the occupation number in the reference volume  $V = \bar{m}_a^{-3}$  is

$$N = \hbar^{-1} \frac{f_a^2 A^2}{2\Lambda_{\text{QCD}}^4}, \quad (2.72)$$

as is evident from Eq. (2.22). This matches the energy density (2.70).

### 2.3.3 Quantum Break-Time

Having determined the three fundamental parameters of the axion field – the mass  $m_a$  and coupling  $\alpha_a$  of the quantum theory as well as the state-dependent value of  $\lambda_a$  – we can apply our previous analysis of quantum breaking, i.e. we simply need to plug in the values for the axion field in the formulas for the quantum break-time derived before. We will set  $\hbar = 1$  for the remainder of the discussion of axions.

First, we consider the process of  $4 \rightarrow 2$ -scattering depicted in Fig. 2.1.<sup>6</sup> This is the leading process in the limit of small axion momenta. Its rate is given by

$$\Gamma \approx m_a \left( \frac{T_{\text{today}}}{T_{\text{in}}} \right)^{12}, \quad (2.73)$$

where we used the collective coupling (2.68) of the axions as well as the dependence (2.63) of the amplitude on the temperature. When we take  $T_{\text{in}} \approx 100 \text{ MeV}$  as the temperature of the QCD phase transition and also conservatively assume  $A_{\text{in}} \approx f_a$ , we get for today's axion field:

$$\Gamma_{\text{today}} \sim m_a 10^{-144}. \quad (2.74)$$

Thus, the characteristic rescattering time required for a single scattering process, i.e. for reducing the coherence of today's axion field by a factor of order  $1/N$ , already exceeds the age of the Universe by many orders of magnitude.

As we have discussed, quantum breaking can only occur once a significant number of the order of  $N$  scattering processes has taken place. The corresponding timescale is given by  $t_q \approx \Gamma^{-1}N$ , which yields Eq. (2.30):

$$t_q \approx m_a^{-1} \frac{1}{\alpha_a \lambda_a^3} = m_a^{-1} \frac{f_a^8}{m_a^2 A^6}. \quad (2.75)$$

We see that the quantum break-time increases as  $A^{-6}$ . Now we can evaluate it at different epochs. First, we consider it at the onset of oscillations assuming the initial amplitude to be maximal:  $A_{\text{in}} = f_a$ . For example, taking the axion mass  $m_a \approx 10^{-5} \text{ eV}$ , which implies  $f_a \approx 10^{12} \text{ GeV}$ , we get  $t_q \approx 10^{42} \text{ s}$ . Even in this crude estimate, in which we ignore Hubble dilution, the quantum break-time exceeds the current age of the Universe by a factor of approximately  $10^{25}$ .

In order to estimate the quantum break-time (2.75) for the present epoch, we can express it in the form

$$t_q \approx m_a^{-1} \frac{f_a^8 m_a^4}{\rho_a^3}, \quad (2.76)$$

---

<sup>6</sup>In Fig. 2.1, the process of  $4 \rightarrow 2$ -scattering arises due to the exchange of a virtual axion. We remark that instead, it can also come from taking into account the six-point interaction of axions, which follows from keeping the next order in the axion potential (2.65). Both processes lead to a rate of the same order of magnitude.

where we plugged in the energy density (2.70). Using the energy density of dark matter,  $\rho_a \approx (10^{-3} \text{ eV})^4$ , we obtain  $t_q \approx 10^{174} \text{ s}$ , which exceeds the current age of the Universe by a factor of approximately  $10^{157}$ . Thus, the coherent state approximation for describing the axion field in the present epoch is extremely accurate.

### Effect of Nonzero Axion Momenta

So far, we have only considered  $2 \rightarrow 4$ -scattering. In reality, since the classical axion field in the Universe is a distribution over different wavelengths, the  $2 \rightarrow 2$ -rescatterings can also contribute to decoherence. They are displayed in Fig. 2.2. As we have discussed, the process of  $2 \rightarrow 2$ -scattering moreover becomes possible even in the absence of axion momenta because the axion potential gives a small contribution to the asymptotic energy of the particles. The corresponding rate (2.33) gives for the cosmic axions:

$$\Gamma_{2 \rightarrow 2} \approx m_a \frac{A^4}{f_a^4}. \quad (2.77)$$

For today's axion density, we get  $\Gamma_{2 \rightarrow 2} \approx m_a T_{\text{today}}^6 / T_{\text{in}}^6 \approx m_a 10^{-72}$ , which is again minuscule.

As is evident from Eq. (2.34), the corresponding quantum break-time is given by

$$t_{q, 2 \rightarrow 2} \approx m_a^{-1} \frac{f_a^4}{m_a^2 A^2} = m_a^{-1} \frac{f_a^4}{\rho_a}. \quad (2.78)$$

Evaluating this expression at the onset of oscillations with maximal amplitude  $A \approx f_a$ , we get the same result as for the  $4 \rightarrow 2$ -scattering:  $t_{q, 2 \rightarrow 2} \approx 10^{42} \text{ s}$ . On the other hand, if we evaluate the quantum break-time for the current epoch, in which the axion energy density is taken to be the dark matter density, we get  $t_{q, 2 \rightarrow 2} \approx 10^{86} \text{ s}$ , which exceeds the current age of the Universe by a factor of approximately  $10^{69}$ . Thus, the inclusion of  $2 \rightarrow 2$ -scattering due to the distribution of coherent state axions over different momenta does not change our conclusion that the coherent state description for dark matter axions is extremely accurate.

### 2.3.4 Validity of Our Simplifications

In order to conclude our argument, we wish to point out that the simplifying assumptions which we have made in our estimates do not significantly change the result. For example, one could wonder whether particle production, which takes place in an expanding universe, could have any significant effect. In particular, one might be worried about produced free axions, which could scatter off the coherent axion state and lead to decoherence. However, this does not happen since not

enough particles are produced: Because of  $\gamma = 3H \ll m_a$ , particle production is exponentially suppressed by the Boltzmann factor  $\exp(-m_a/H)$ .

A similar argument holds for the effect of the QCD phase transition, which leads to a change of the axion mass. The corresponding transition time  $t_{\text{QCD}}$ , which is of order of the Hubble time around the QCD-temperature,  $t_{\text{QCD}} \approx M_p/\Lambda_{\text{QCD}}^2$ , is much longer than the axion Compton wavelength:  $t_{\text{QCD}} \gg m_a^{-1}$ . Therefore,  $\dot{m}_a \ll m_a^2$ , i.e. the transition is adiabatic. Consequently, the quantum creation of free axions due to the time dependence of the mass is suppressed by  $\exp(-m_a^2/\dot{m}_a)$  and there are not enough produced particles to have a significant effect on the coherence of the axion state.

Of course, axions also interact gravitationally. Considering gravitational interaction in the rescattering process amounts to replacing  $\alpha_a$  by the gravitational coupling strength

$$\alpha_g = G_N m_a^2, \quad (2.79)$$

where  $G_N$  is Newton's constant. So this is equivalent to replacing  $f_a$  by the Planck mass  $M_p = 1/\sqrt{G_N}$ . Hence it is obvious that unless the axion decay constant is trans-Planckian, the gravitational interaction among axions is much weaker than the interaction due to QCD and therefore does not affect the quantum break-time. We remark that the analysis of a gravitationally self-interacting scalar field will be performed in the analysis of de Sitter in section 2.4.

Finally, we turn to the dilution of the axion number density. In a cosmological context, this dilution originates from the Hubble expansion as well as the decay of axions into some lighter particle species, e.g. photons. For realistic values of the axion mass, the decay is a subdominant process. Therefore, we focus on the effect of Hubble friction. Since it describes a classical process, namely the dilution of gas in the background of an expanding universe, we intuitively expect that it does not lead to quantum decoherence.

Our goal, however, is to make this statement more precise. Thus, we generalize Lagrangian (2.66):

$$\hat{\mathcal{L}} = \frac{\mathbf{a}^3}{2} \left( \partial_\mu \hat{a} \partial^\mu \hat{a} - m_a^2 \hat{a}^2 \right), \quad (2.80)$$

where  $\mathbf{a}$  is the scale factor and indices are now raised and lowered with the flat Friedmann-Robertson-Walker-metric,  $g_{\mu\nu} = \text{diag}(1, -\mathbf{a}^2, -\mathbf{a}^2, -\mathbf{a}^2)$ . We do not consider self-interaction of the axion since our present goal is only to investigate possible decoherence due to Hubble friction. The canonically conjugate momentum  $\hat{\Pi}_a = \mathbf{a}^3 \partial_0 \hat{a}$  gives the Hamiltonian

$$\hat{\mathcal{H}} = \frac{\hat{\Pi}_a^2}{2\mathbf{a}^3} + \frac{\mathbf{a}^3}{2} \left( (\mathbf{a} \vec{\partial} \hat{a})^2 + m_a^2 \hat{a}^2 \right). \quad (2.81)$$

Specializing to a spatially homogeneous field, the Heisenberg equation of motion is

$$\ddot{\hat{a}} + \gamma \dot{\hat{a}} + m_a^2 \hat{a} = 0, \quad (2.82)$$

since  $\gamma = 3H = 3\dot{\alpha}/\alpha$ . As the Heisenberg equation is linear, we can apply the Ehrenfest-theorem, i.e, we can take its expectation value to conclude that for any quantum state, the expectation value of the time-evolved quantum operator is equal to the classical solution given by (2.58). Thus, the fact that friction is a linear term suffices to show that it cannot destroy classicality.

For completeness, we will nevertheless explicitly study the quantum time evolution, where we use the calculation of [104]. The former paper contains a derivation of the following eigenvalue equation for an initially coherent state  $|N\rangle$  in the Schrödinger picture:

$$\left( e^{im_a t} \cosh\left(\frac{\gamma t}{2}\right) \hat{c}_{\vec{0}} + e^{im_a t} \sinh\left(\frac{\gamma t}{2}\right) \hat{c}_{\vec{0}}^\dagger \right) |N(t)\rangle = \sqrt{N} |N(t)\rangle, \quad (2.83)$$

where the creation and annihilation operators  $\hat{c}_{\vec{0}}^\dagger, \hat{c}_{\vec{0}}$  are still defined by the mode expansion (2.16) (at  $t = 0$ ). In order to make the formulas more transparent, we wrote down the solution only to leading order in  $\gamma/m_a$  and neglected  $\dot{\gamma}/(m_a\gamma)$ . As explained above, both simplifications are reasonable in a cosmological context. In this limit, (2.83) shows that  $|N(t)\rangle$  is a squeezed coherent state with real squeezing parameter  $s = \gamma t/2$ . The uncertainty is no longer equally distributed,

$$\Delta a \propto e^{-\gamma t/2}, \quad \Delta \Pi \propto e^{\gamma t/2}, \quad (2.84)$$

but still minimal.<sup>7</sup> Thus,  $|N(t)\rangle$  continues to be maximally classical. Including higher terms in  $\gamma/m_a$  does not change these conclusions significantly.<sup>8</sup> This means that also in the presence of classical Hubble friction, the classical description of the free axion field remains valid indefinitely. It does not lead to a quantum break-time.

### 2.3.5 Undercriticality of Cosmic Axions

As we have discussed in section 2.2.4, quantum breaking can be greatly enhanced in the overcritical domain  $\lambda > 1$ , provided a classical instability exists. Obviously, cosmic dark matter axions cannot enter such a regime since they are undercritical.

<sup>7</sup>The emerging physical picture has a straightforward interpretation. In terms of the physical field  $\partial_0 \hat{a}$ , we have

$$\Delta a = \Delta \partial_0 a \propto e^{-\gamma t/2}. \quad (2.85)$$

From this point of view,  $|N(t)\rangle$  is therefore still coherent. Time evolution only reduces the overall uncertainty in physical space. This is in accordance with the commutation relations  $[\hat{a}(t, \vec{x}), \hat{\Pi}_a(t, \vec{y})] = i\delta(\vec{x} - \vec{y})$ , which read in physical space

$$[\hat{a}(t, \vec{x}), \partial_0 \hat{a}(t, \vec{y})] = i\alpha^{-3} \delta(\vec{x} - \vec{y}). \quad (2.86)$$

This means that uncertainty is conformally conserved but dilutes with the physical volume.

<sup>8</sup>In this case, the state  $|N(t)\rangle$  is no longer exactly squeezed at all times, but the deviation of  $\Delta a \Delta \Pi$  from 1 vanishes periodically and is bounded by a constant which scales as  $\gamma^2/m_a^2$ .

In order to obtain a quantitative estimate, we can represent the collective coupling as

$$\lambda_a = \frac{\rho_a}{f_a^2 m_a^2}, \quad (2.87)$$

which follows from (2.68) when we express the amplitude  $A$  in terms of the energy density (2.70). Using the present energy density of dark matter, we get  $\lambda_a = 10^{-44}$ , which is minuscule.

Nevertheless, it is instructive to discuss what an overcritical regime would imply for cosmic axions. First, we consider the truncated theory (2.66). The potential has a minimum at  $a = 0$ , a maximum at  $a_{\text{cr}}^2 = 6m_a^2/\alpha_a = 6f_a^2$  and is unbounded from below for larger values of  $a$ . Thus, the critical value is given by  $\lambda_a = 6$ , i.e. the instability sets in for  $A^2 > 6f_a^2$ . Overcriticality of the axion gas would imply that the amplitude of oscillations  $A$  exceeds  $a_{\text{cr}}$  and the classical field  $a_{\text{cl}}(t)$  grows unbounded. This classical growth is accompanied by an instability of modes with momenta  $|\vec{k}| < \sqrt{\frac{\alpha_a}{2} a_{\text{cl}}(t)^2 - m_a^2}$  so that finally all the modes become unstable. Of course, in such a situation the quantum breaking can be efficient, but it is also meaningless since in this regime the truncated model no longer describes physics of the axion gas correctly. The truncation is only meaningful as long as the amplitude of oscillations does not exceed  $a_{\text{cr}}$ . So the short quantum breaking in a would-be overcritical regime of axion gas is unphysical and is an artifact of an invalid description.

Let us now go to the full axion model with periodic potential (2.65).<sup>9</sup> We can make the axion overcritical, i.e. achieve  $\lambda_a = A^2/f_a^2 \gg 1$ , by assuming a high number density of zero momentum axions. Since  $\rho_a = \lambda_a \Lambda_{\text{QCD}}^4$ , this implies in the classical language that we are looking for a time-dependent solution with energy density  $\rho_a \gg \Lambda_{\text{QCD}}^4$ . In this regime, the solution, up to corrections  $\mathcal{O}(\Lambda_{\text{QCD}}^4/\rho_a)$ , has the form:

$$a_{\text{cl}}(t) = \sqrt{2\rho_a} t. \quad (2.88)$$

This solution has an obvious physical meaning. Since the energy of the axion field exceeds the height of the axion potential, the evolution is the one of a free field with a constant energy density. Let us examine the stability of this solution. The momentum modes of the linearized perturbations around it satisfy the following equation:

$$\ddot{a}_{\vec{k}}(t) + \left( \hbar^{-2} \vec{k}^2 + \bar{m}_a^2 \cos\left(\sqrt{2\lambda_a} \bar{m}_a t\right) \right) a_{\vec{k}}(t) = 0, \quad (2.89)$$

where we have used the collective coupling in the form of Eq. (2.87). Introducing a new variable  $y \equiv \sqrt{\frac{\lambda_a}{2}} \bar{m}_a t$ , we can rewrite (2.89) in the form

$$\partial_y^2 a_{\vec{k}}(y) + \left( B + \frac{2}{\lambda_a} \cos(2y) \right) a_{\vec{k}}(y) = 0, \quad (2.90)$$

---

<sup>9</sup>Naturally, in doing so, we ignore a possible backreaction from the axion field on QCD dynamics.

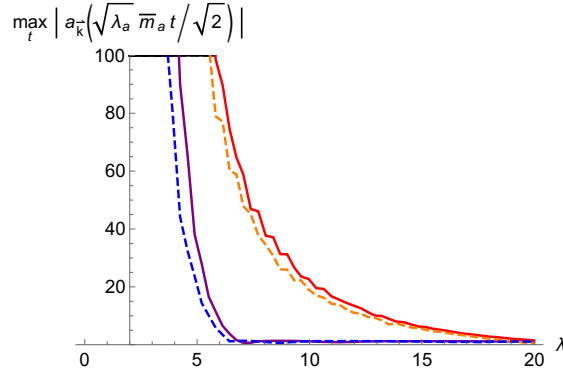


Figure 2.3: Behavior of the solution of (2.90) for fixed  $t$  and  $B$  when the collective coupling  $\lambda_a$  changes. The maximal value of  $a_{\vec{k}}|(\sqrt{\lambda_a/2}\bar{m}_a t)|$  in the interval  $20 \leq \bar{m}_a t \leq 25$  is plotted. The values for  $B$  are 0.85 (purple), 0.95 (red), 1.05 (orange, dashed) and 1.15 (blue, dashed). The closer  $B$  is to the critical value 1, the stronger the instability is and the longer it persists. In each case, the instability disappears for big  $\lambda_a$ .

where  $B \equiv 2\vec{k}^2/(\lambda_a m_a^2)$ .

This is the Mathieu equation, which is known to exhibit instability bands around certain values of  $B$  [105]. However, it is important to remember that we work in the approximation  $\rho_a \gg \Lambda_{\text{QCD}}^4$ , which is equivalent to a large collective coupling:  $\lambda_a \gg 1$ . Therefore, the term  $\propto \cos(2y)$  responsible for generating the instability is suppressed. For this reason, the instability bands get narrower as  $\lambda_a$  increases so that the phase space for the production of the corresponding modes is suppressed.<sup>10</sup>

Additionally, we study the scaling of the timescale of instability. To this end, we investigate how an unstable solution  $a_{\vec{k}}(\sqrt{\lambda_a/2}\bar{m}_a t)$  of (2.90) changes at a fixed  $t$  when we increase  $\lambda_a$ . In doing so, we change  $\vec{k}$  in order to keep  $B$  fixed near an unstable value. Numerical analysis shows that the timescale of instability for a given mode indeed becomes longer as the collective coupling  $\lambda_a$  increases, i.e. the instability disappears for  $\lambda_a \rightarrow \infty$ . This is not surprising since Eq. (2.90) becomes the equation of a free particle in this limit. The result for the dominant instability around  $B = 1$  is displayed in Fig. 2.3. Therefore, we conclude that the increase of stability caused by the narrowing of the instability bands outweighs the reduction of the break-time due to the scaling  $t \propto y/\sqrt{\lambda_a}$ . In summary, this shows that once the full axion potential is taken into account, the quantum break-time cannot be made arbitrarily short even in the overcritical regime.

As a final remark, we note that  $\dot{a}$  cannot be arbitrarily large due to the fact

<sup>10</sup>In this regime, the most relevant instability is the lowest-lying one around  $B = 1$ , i.e. for modes with  $\vec{k}^2 \cong \lambda_a m_a^2/2$ .

that it backreacts on the Peccei-Quinn field. In particular, there is an absolute bound on  $\dot{a}$  given by  $\dot{a} \approx f_a^2$  because at this point, the backreaction from the axion field on the vacuum expectation value of the modulus of the Peccei-Quinn field,  $\Phi_{PQ} \equiv f_a e^{ia/f_a}$ , becomes order one and the axion decay constant  $f_a$  changes. This must be taken into account. So the simple description in terms of a pseudo-scalar  $a$  with a periodic potential breaks down and one has to consider the full theory. For the collective coupling of the axion gas, this restriction translates as the bound  $\lambda < \alpha_a^{-1}$ .

In conclusion, in the overcritical domain the quantum break-time can in principle be made shorter at the expense of Lyapunov instabilities along the lines of the mechanism of [40]. However, this domain is irrelevant for the cosmic axion field because of the following reasons. First, this regime cannot be reached within the validity of axion effective field theory model (2.66), due to backreaction. Secondly, the would-be overcritical domain – in which potentially a fast quantum breaking could occur – is way outside of the realistic parameter space of dark matter axions in our Universe since as explained, the present energy density of dark matter implies a tiny collective coupling. Of course, this does not exclude the possibility that fast quantum breaking can occur for axions that are in special highly localized configurations. However, this can only happen if two conditions are simultaneously fulfilled: There must be an extreme overdensity to reach  $\lambda_a \gtrsim 1$  in some small subregion and moreover the configuration must be classically unstable.

### 2.3.6 Relationship to Other Work

We conclude by discussing in more detail the relationship of our work to the results presented in [71, 101–103]. Also there, the classical axion field is resolved as a multi-particle quantum state. Subsequently, the authors investigate the axionic self-interaction. They do so by calculating the process of  $2 \rightarrow 2$ -scattering, which we also considered. In full agreement with our result, they obtain the quantum break-time (2.78) (see  $\Gamma_s$ , which is defined before equation (8) of [71]). Therefore, they also conclude that the timescale of this process vastly exceeds the age of our Universe and does not play any role for current observations. They proceed, however, to study processes of  $2 \rightarrow 2$ -scattering in which also the final state is macroscopically occupied. In accordance with our discussion in section 2.2.3, they obtain the enhanced rate (2.40) and correspondingly the shorter timescale (2.41):

$$t_{\text{collective}} \approx \bar{m}_a^{-1} \frac{1}{\lambda_a^2}, \quad (2.91)$$

where we restored factors of  $\hbar$  for the present discussion. At the onset of oscillations, it can indeed be short:  $t_{\text{collective}} \approx \bar{m}_a^{-1}$ . They argue that this process leads to Bose-Einstein condensation of the axions, i.e. they increasingly occupy the mode

of zero momentum.<sup>11</sup>

We are, however, not interested in implications of this process. Our key point is that  $t_{\text{collective}}$  is a classical quantity that only depends on the collective coupling  $\lambda_a = \alpha_a N$ . As discussed in section 2.2.3, it corresponds to the timescale of classical nonlinearities. Thus, even if  $t_{\text{collective}}$  is short, it does not jeopardize the classical description of the axion field or lead to a quantum break-time. This agrees with the discussion in reference [75], which is cited in [71]. Also there, it is noted that the process of condensation corresponds to a classical interaction of different momentum modes and can be described as scattering of classical waves.<sup>12</sup>

As a second step, [71,101–103] contains the study of gravitational self-interaction of the axions. Whereas we concluded in section 2.3.4 that it is a subdominant effect in comparison to the axionic self-interaction, it is argued in [71,101–103] that gravitational self-interaction becomes strong at late times. But as for the axionic self-interaction, the key point is that short timescales only appear when classical processes are considered, i.e. ones in which also the final state of scattering is macroscopically occupied.<sup>13</sup> As before, we do not want to make a statement about the potential significance of these classical effects.<sup>14</sup> For us, it is only important that whatever the effect is, it can be described as classical gravitational self-interaction. A quantum treatment is not necessary. In particular, there is no reason why classical simulations of dark matter evolution should fail.

Finally, we want to make a brief remark about the classicality of coherent states, which is relevant beyond the application to axions. In [107], it is claimed that coherent states fail to reproduce a classical evolution even when their occupation number  $N$  is infinite. We want to point out that this observation is only an artifact of an unphysical limit. Namely, the authors of [107] take  $N \rightarrow \infty$  while keeping the coupling  $\alpha$  fixed. This does not correspond to the classical limit but

<sup>11</sup>Our approach is even more radical with respect to the distribution in momentum space. We already start with a fully condensed state in which all axions are in the mode of zero momentum.

<sup>12</sup>That condensation can be described classically was also discussed more recently in [106].

<sup>13</sup>We can explicitly conclude this from equation (11) of [71] when we write the timescale of gravitational interaction as

$$t_{\text{collective, g}} = \bar{m}_a^{-1} \frac{1}{\alpha_g N}. \quad (2.92)$$

Since  $N$  scales like  $\hbar^{-1}$  and the gravitational coupling strength (2.79) is given as  $\alpha_g = \hbar G_N \bar{m}_a^2$ , we conclude that  $t_{\text{collective, g}}$  is independent of  $\hbar$ , i.e. classical.

<sup>14</sup>We would be surprised, however, if the classical gravitational self-interaction were strong. If we look at e.g. the cross section in equation (3.30) of [101],

$$\sigma_g = \frac{G_N^2 m_a^2}{\delta v^4}, \quad (2.93)$$

where  $\delta v$  is the spread of speed of the axions, we note that it only diverges as a result of the forward scattering pole  $\delta v \rightarrow 0$ . It is not clear how this leads to a physical effect. Moreover, if any effect due to gravity exists, it is not evident to us why it should only occur for axions and not also for other potential forms of light dark matter.

to an infinite amplitude of oscillations:  $A \rightarrow \infty$ . As is clear from Eq. (2.1), this limit  $N \rightarrow \infty$  with fixed coupling  $\alpha$  corresponds to an infinite collective coupling:  $\lambda \rightarrow \infty$ , i.e. to an *infinite* overcriticality. When we write the quantum break-time due to  $2 \rightarrow 2$ -scattering (2.34) as

$$t_q \approx \bar{m}^{-1} \frac{1}{\alpha^2 N}, \quad (2.94)$$

we see that the limit of infinite amplitude implies that  $t_q \sim 1/N$ .<sup>15</sup> This is the scaling also observed in [107] (see Fig. 2 there). In particular, the instabilities developed in the artificial limit  $\lambda \rightarrow \infty$  are irrelevant for axion physics since as we have shown in section 2.3.5, this domain is not applicable for the realistic axion field, which is safely subcritical:  $\lambda_a \ll 1$ .

As discussed in section 2.1, one obtains the correct form of the classical limit by taking  $\hbar \rightarrow 0$ . In this case, we have  $N \rightarrow \infty$  while the collective coupling  $\alpha N$  stays fixed. Since this implies that  $\alpha \sim 1/N$ , equation (2.94) leads to the scaling  $t_q \sim N$ . Thus, the classical description stays valid indefinitely in the classical limit  $N \rightarrow \infty$ .

## 2.4 Application to de Sitter

So far, we have studied quantum breaking for a simple self-interacting scalar field in section 2.2. Moreover, we have shown in section 2.3 that this analysis has immediate implications for cosmic axions. In the present section, we turn to a more involved system by investigating quantum breaking in de Sitter. As for the scalar field, we proceed in two steps. First, we have to find a quantum description of the classical solution. Secondly, we determine the quantum break-time by studying quantum effects that are not captured by the classical solution. The first step turns out to be more complicated in the case of de Sitter whereas the second one is largely analogous to the scalar field example.

### 2.4.1 A Quantum Description of the de Sitter Metric

In the introduction 1.3.2, we have reviewed the quantum picture of de Sitter proposed in [44]. In this approach, de Sitter does not correspond to a fundamental vacuum, but it is obtained as expectation value of an excited state that is defined on top of Minkowski vacuum.<sup>16</sup> Since Minkowski has a well-defined  $S$ -matrix, one of the main advantages of such a construction is that all problems that arise due to the lack of an  $S$ -matrix in de Sitter can be avoided. Our first goal is to make the above quantum picture of de Sitter more explicit, i.e. to find a concrete quantum

<sup>15</sup>See [108] for a suggestion to extend the validity of the classical solution in the overcritical regime by averaging over a set of random initial conditions.

<sup>16</sup>More studies of this corpuscular picture of de Sitter can be found in [109–111].

theory for the constituent gravitons that is able to reproduce the classical metric description. Thus, we take a constructive approach towards the idea to regard de Sitter as a multi-graviton state on top of Minkowski by showing that this can indeed be achieved in a suitable approximation.

Since we are not able to give a quantum description of the full nonlinear solution, we will proceed as for the scalar field by linearizing the classical equations of motion. However, even the linearized solution still does not admit a straightforward quantum description. Therefore, we will replace the cosmological constant source of the linear theory by a graviton mass in such a way that both theories – the one with the cosmological constant and the one with the graviton mass – have the same solution. In this deformed theory, we will give a quantum description of the linearized classical solution. In determining these classical solutions, we will largely follow [112].<sup>17</sup>

### Linearizing the Classical Solution

First we work on the classical level and linearize the Einstein equations *on top of the Minkowski metric*  $\eta_{\mu\nu}$ :

$$\epsilon_{\mu\nu}^{\alpha\beta} \tilde{h}_{\alpha\beta} = -2\Lambda \eta_{\mu\nu}, \quad (2.95)$$

with the linearized Einstein tensor defined as  $\epsilon_{\mu\nu}^{\alpha\beta} \tilde{h}_{\alpha\beta} \equiv \square \tilde{h}_{\mu\nu} - \eta_{\mu\nu} \square \tilde{h} - \partial_\mu \partial^\alpha \tilde{h}_{\alpha\nu} - \partial_\nu \partial^\alpha \tilde{h}_{\alpha\mu} + \partial_\mu \partial_\nu \tilde{h} + \eta_{\mu\nu} \partial^\alpha \partial^\beta \tilde{h}_{\alpha\beta}$ . The gauge symmetry is,

$$\tilde{h}_{\mu\nu} \rightarrow \tilde{h}_{\mu\nu} + \partial_\mu \xi_\nu + \partial_\nu \xi_\mu, \quad (2.96)$$

where  $\xi_\nu$  is a gauge-transformation parameter. In de Donder gauge,  $\partial^\mu \tilde{h}_{\mu\nu} = \frac{1}{2} \partial_\nu \tilde{h}$ , the equation takes the following form:

$$\square \left( \tilde{h}_{\mu\nu} - \frac{1}{2} \eta_{\mu\nu} \tilde{h} \right) = -2\Lambda \eta_{\mu\nu}. \quad (2.97)$$

Here  $\tilde{h}_{\mu\nu}$  is dimensionless and denotes a small departure from the Minkowski metric caused by the presence of a constant source  $\Lambda$ . In the full nonlinear de Sitter solution,  $\Lambda$  would correspond to the de Sitter Hubble parameter,  $\Lambda = 3H^2$ . It determines the curvature radius  $R_H = H^{-1}$ , as already stated in Eq. (1.14).

It is very important not to confuse  $\tilde{h}_{\mu\nu}$  with the linear metric perturbation on top of a de Sitter metric:  $\tilde{h}_{\mu\nu}$  is a short-time approximation of the de Sitter metric itself, not a fluctuation on top of it.

<sup>17</sup>Note that we corrected minor numerical factors as compared to [112].

Following the results of [112], the equations of motion (2.97) are solved by

$$\tilde{h}_{00} = \Lambda t^2, \quad (2.98a)$$

$$\tilde{h}_{0i} = -\frac{2}{3}\Lambda t x_i, \quad (2.98b)$$

$$\tilde{h}_{ij} = -\Lambda t^2 \delta_{ij} - \frac{\Lambda}{3} \epsilon_{ij}, \quad (2.98c)$$

where  $\epsilon_{ij} = x_i x_j$  for  $i \neq j$  and 0 otherwise. Still following [112], we apply a diffeomorphism to obtain

$$ds^2 = dt^2 - \left(1 + \frac{1}{3}\Lambda t^2\right) \delta_{ij} dx^i dx^j - \frac{1}{3}\Lambda x_i x_j dx^i dx^j, \quad (2.99)$$

which is an approximation of a de Sitter Universe in closed Friedmann-Robertson-Walker slicing:

$$ds^2 = dt^2 - \cosh^2\left(\sqrt{\Lambda/3} t\right) \left(\frac{dr^2}{1 - \Lambda r^2/3} + r^2 d\Omega^2\right). \quad (2.100)$$

To first order in the  $\Lambda t^2$ - and  $\Lambda r^2$ -expansion, it is clear that (2.100) reproduces (2.99). We conclude that our approximation of weak gravity is valid as long as  $t \ll \Lambda^{-\frac{1}{2}}$  and  $x \ll \Lambda^{-\frac{1}{2}}$ . This yields the classical break-time

$$t_{\text{cl}}^{(0)} \approx \Lambda^{-\frac{1}{2}}. \quad (2.101)$$

It is instructive to confront expression (2.101) for the classical break-time of de Sitter with its counterpart (2.12) for the self-interacting scalar field. The classical oscillations of the scalar field are defined by three parameters: frequency  $\bar{m}$ , amplitude  $A$  and the strength of classical nonlinear interaction  $\bar{\alpha}$ . We can define the corresponding parameters for the classical de Sitter space at short times. The characteristic frequency is defined by the Hubble scale,  $\bar{m}_g = \sqrt{\Lambda}$ . Secondly, the amplitude of the canonically normalized graviton field beyond which nonlinearities become crucial is given by the inverse square root of Newton's constant,  $A_g = 1/\sqrt{G_N}$ . Finally, the strength of gravitational nonlinearities in de Sitter is defined by  $\bar{\alpha}_g = \Lambda G_N$ . Replacing in the expression for the classical break-time of the anharmonic scalar field (2.12) the parameters  $\bar{m}$ ,  $A$  and  $\bar{\alpha}$  by their gravitational counterparts  $\bar{m}_g$ ,  $A_g$  and  $\bar{\alpha}_g$ , we get exactly expression (2.101), which we had obtained by comparing the metrics (2.99) and (2.100). Despite the fact that the anharmonic scalar field and de Sitter are very different systems, their classical break-times obey the universal relation (2.12). The difference is that in gravity, unlike in the scalar field case, only two out of the three parameters are independent. Correspondingly, we do not have the flexibility of making the classical break-time longer than  $1/\sqrt{\Lambda}$ .

### Mapping the Cosmological Constant on a Graviton Mass

Our subsequent task is to provide a quantum-corpuscular description of (2.98) in form of a coherent state. To this end, we slightly deform the linearized theory by promoting it into a similar theory, which has exactly the same metric description for the relevant timescales, but for which the coherent state description is much more straightforward. The choice of deformation for the linear theory is unique. It is given by the only existing ghost-free linear theory of a spin-2 field beyond linearized Einstein gravity: Pauli-Fierz theory of massive spin-2 [113]. We denote the graviton mass by  $m_g$ . Because we are still in a classical theory, however, only the graviton frequency  $\bar{m}_g = m_g/\hbar$  is relevant. We will use the terms frequency and mass interchangeably although we keep  $\hbar$  explicit for now.

But what are the reasons for adding a mass? First, as observed in [112], this deformation leads to a solution which reproduces the de Sitter metric for times  $t \ll \bar{m}_g^{-1} = 1/\sqrt{\Lambda}$  even in the absence of the cosmological constant term. For short timescales, the graviton mass consequently has the same effect as the cosmological term. This means that for short timescales, observers coupled to such a gravitational field cannot tell whether they live in a de Sitter metric of Einstein theory or in a coherently oscillating field of a massive Fierz-Pauli graviton on top of a flat Minkowski vacuum. Since we want to map the cosmological constant to a graviton mass, we already expect at this point that

$$\bar{m}_g \approx \sqrt{\Lambda}. \quad (2.102)$$

We will elaborate on this relation later but keep  $\bar{m}_g$  arbitrary for now.

Secondly, such a deformation allows for a simple coherent state interpretation of the de Sitter metric: It is much more straightforward to describe a coherently-oscillating free massive spin-2 field as coherent state than its massless counterpart sourced by a cosmological term.

In addition, it matches the physical intuition that if de Sitter space allows for a sensible corpuscular resolution in form of a coherent state, the constituents must have frequencies given by the Hubble parameter since this is the only scale of the classical geometry. Thus, these constituents can be viewed as some sort of *off-shell* gravitons of nonzero frequencies set by  $H$ . The mass term is the simplest term which provides such an effective off-shell dispersion relation. Thus, for a sufficiently short time-interval,  $t \ll t_{\text{cl}}$ , we can think of the gravitons of the massless theory which are put off-shell by nonlinearities as on-shell massive gravitons of a free theory. This mapping allows for a coherent state interpretation of the de Sitter metric for sufficiently small times. Although the approximation breaks down after  $t_{\text{cl}}$ , it suffices to “fish out” the  $1/N$ -quantum effects which lead to a departure from the classical solution.

We therefore modify our theory by adding a graviton frequency  $\bar{m}_g$  and removing the cosmological constant source. To linear order, the massive graviton, which

we shall denote as  $h_{\mu\nu}$ , obeys:

$$\epsilon_{\mu\nu}^{\alpha\beta} h_{\alpha\beta} + \bar{m}_g^2 (h_{\mu\nu} - \eta_{\mu\nu} h) = 0, \quad (2.103)$$

with the linearized Einstein tensor given as above. Additionally, it must satisfy the Fierz-Pauli constraint

$$\partial^\mu (h_{\mu\nu} - \eta_{\mu\nu} h) = 0, \quad (2.104)$$

which shows that it propagates five degrees of freedom. Following [112, 114], these degrees of freedom can be split according to irreducible massless representations of the Poincaré group into three different helicity components: helicity-2  $\tilde{h}_{\mu\nu}$ , helicity-1  $A_\mu$  and helicity-0  $\chi$ :

$$h_{\mu\nu} = \tilde{h}_{\mu\nu} + \frac{1}{\bar{m}_g} (\partial_\mu A_\nu + \partial_\nu A_\mu) + \frac{1}{6} \eta_{\mu\nu} \chi + \frac{1}{3} \frac{\partial_\mu \partial_\nu}{\bar{m}_g^2} \chi. \quad (2.105)$$

This decomposition is unique in the sense that in this basis, the kinetic mixing among different helicities is absent and in the limit  $\bar{m}_g \rightarrow 0$ , the field  $h_{\mu\nu}$  “disintegrates” into three independent massless representations of the Poincaré group: spin-2, spin-1 and spin-0. Note that the gauge redundancy (2.96) of the massless theory is not lost. The gauge shift (2.96) is compensated by a corresponding shift of  $A_\mu$ ,

$$A_\mu \rightarrow A_\mu - \bar{m}_g \xi_\mu. \quad (2.106)$$

Hence,  $A_\mu$  acts as Stückelberg-field, i.e. we can continue enjoying the gauge freedom for fixing the gauge of the  $\tilde{h}_{\mu\nu}$ -component. This is particularly useful, since following [114], we can integrate out the additional helicities and write down an effective equation for  $\tilde{h}_{\mu\nu}$ .

This equation in de Donder gauge,  $\partial^\mu \tilde{h}_{\mu\nu} = \frac{1}{2} \partial_\nu \tilde{h}$ , is a massive wave equation:

$$(\square + \bar{m}_g^2) \left( \tilde{h}_{\mu\nu} - \frac{1}{2} \eta_{\mu\nu} \tilde{h} \right) = 0. \quad (2.107)$$

One solution is given by

$$\tilde{h}_{00} = -\frac{2\Lambda}{\bar{m}_g^2} \cos(\bar{m}_g t), \quad (2.108a)$$

$$\tilde{h}_{0i} = \frac{-2\Lambda}{3\bar{m}_g} \sin(\bar{m}_g t) x_i, \quad (2.108b)$$

$$\tilde{h}_{ij} = \frac{2\Lambda}{\bar{m}_g^2} \cos(\bar{m}_g t) \delta_{ij} - \frac{\Lambda}{3} \cos(\bar{m}_g t) \epsilon_{ij}, \quad (2.108c)$$

where the additional helicity-0 part assumes the following form:

$$\chi = -\tilde{h} = \frac{8\Lambda}{\bar{m}_g^2} \cos(\bar{m}_g t). \quad (2.109)$$

This formula is a manifestation of the fact that  $\chi$  and  $\tilde{h}$  are not independent but mix through the mass term and undergo simultaneous coherent oscillations. Correspondingly, the oscillating classical field represents a coherent state composed out of quanta which reside both in  $\chi$  and  $\tilde{h}$ .

For  $t \ll \bar{m}_g^{-1}$ , the oscillating solution (2.108) of the massive theory without any cosmological constant fully reproduces – up to an additive constant – the de Sitter solution (2.98) of the massless theory with a cosmological constant as source:

$$\tilde{h}_{\mu\nu}^{(\bar{m}_g \neq 0, \Lambda=0)} = \tilde{h}_{\mu\nu}^{(\bar{m}_g=0, \Lambda \neq 0)} - \eta_{\mu\nu} \frac{2\Lambda}{\bar{m}_g^2}. \quad (2.110)$$

Due to the normalization of the amplitude  $2\Lambda/\bar{m}_g^2$ , this relation holds irrespective of the graviton mass.<sup>18</sup> Obviously, the classical break-time after which the oscillating field no longer approximates the massless solution (2.98) is

$$t_{\text{cl}} \approx \bar{m}_g^{-1}. \quad (2.111)$$

Finally, we choose  $\bar{m}_g$  such that the classical break-times of linearized solutions in the two theories are the same: In nonlinear massless gravity, the classical break-time is reached when the variation of the dimensionless metric  $\tilde{h}_{\mu\nu}$  becomes of order one. This is equivalent to the statement that the linearized approximation breaks down when the canonically-normalized field  $\tilde{h}_{\mu\nu}$  becomes of order of the Planck mass  $M_p$ . Applying the same criterion to the oscillating solution of the linearized massive theory, we must set

$$\bar{m}_g = \sqrt{\Lambda}. \quad (2.112)$$

With this choice, the classical break-times in the two theories match: the timescale (2.101) of the breakdown – due to classical nonlinearities – of the linearized de Sitter solution (2.98) of a massless Einstein theory and the timescale (2.111) of the breakdown of the same solution (2.108) – due to the mass term – in the linear Pauli-Fierz massive theory. This means that the classical nonlinearities in Einstein gravity and the mass term in the free Pauli-Fierz theory are doing the same job of putting the solution (2.98) out of business. Of course, this argument would allow for a constant prefactor in Eq. (2.112). It will become apparent in section 2.4.1 why it has to be 1. We will adopt the choice (2.112) from now on.

We conclude that we have accomplished our first goal of finding an appropriate approximation to the exact classical solution. Its classical break-time is

$$t_{\text{cl}} \approx \Lambda^{-\frac{1}{2}}. \quad (2.113)$$

---

<sup>18</sup>We note, however, that the massive solution (2.108) diverges in the limit  $m_g \rightarrow 0$ . This shows why it is not convenient to use a free massless field for the quantum description of linearized de Sitter.

Thus, for short timescales  $t < t_{\text{cl}}$ , the graviton mass fully replaces the effect of the cosmological term. This fact shall allow us to give a well-defined coherent state representation of de Sitter space during that time span.

We would like to stress that although we borrow the setup of [112], we do not use its approach of killing (i.e. de-gravitating) the cosmological constant by means of the graviton mass. Instead, we manufacture the de Sitter metric by replacing the cosmological constant by a graviton mass.

In this respect, the idea of our simple model is also reminiscent of the idea of *self-acceleration* [115] in which a de Sitter-like solution is achieved without the cosmological constant source, due to modification of the graviton dispersion relation. More recently, such solutions were obtained [116–118] in the theory of massive gravity of [119]. Since our focus is not on a modification of Einstein theory but rather the creation of a simple setup which allows for a composite interpretation of the de Sitter metric, the graviton mass is merely a computational device which replaces the effect of nonlinearities. In other words, we map the interacting off-shell massless gravitons onto free massive ones. Hence, we shall not be concerned with nonlinear completions of the massive theory.<sup>19</sup>

### The Basic Classical Model

Let us summarize the basic model we shall be working with in the following: We replace the linearized massless theory of an Einstein graviton  $\tilde{h}^{\mu\nu}$  coupled to a cosmological constant source  $\Lambda$ ,

$$\mathcal{L}_E = \frac{1}{16\pi} \left( \frac{1}{2} \tilde{h}^{\mu\nu} \epsilon_{\mu\nu}^{\alpha\beta} \tilde{h}_{\alpha\beta} + \frac{2}{\sqrt{G_N}} \tilde{h} \Lambda + 16\pi \sqrt{G_N} \tilde{h}_{\mu\nu} T^{\mu\nu}(\Psi) + \dots \right), \quad (2.114)$$

by a linear theory of a Fierz-Pauli graviton of mass  $\bar{m}_g = \sqrt{\Lambda}$ :

$$\mathcal{L}_{\text{FP}} = \frac{1}{16\pi} \left( \frac{1}{2} h^{\mu\nu} \epsilon_{\mu\nu}^{\alpha\beta} h_{\alpha\beta} + \frac{1}{2} \Lambda (h_{\mu\nu} h^{\mu\nu} - h^2) + 16\pi \sqrt{G_N} \tilde{h}_{\mu\nu} T^{\mu\nu}(\Psi) + \dots \right). \quad (2.115)$$

This is the theory on which we will base our analysis. It is crucial to note that it does not include a cosmological constant. Instead, it only contains the Fierz-Pauli mass term  $(h_{\mu\nu} h^{\mu\nu} - h^2)$ .

Again, by no means should one think that the cosmological term gives the graviton a fundamental mass. This is not the case as it is obvious already from counting the number of degrees of freedom. We use the fact that the Einsteinian spin-2 helicity component  $\tilde{h}_{\mu\nu}$  of the Fierz-Pauli massive graviton *without* cosmological term has the same form as it would have in a massless theory with cosmological constant.

---

<sup>19</sup>It could nevertheless be an interesting independent project to extend our quantum analysis to a full nonlinear massive theory of the type [119].

In both Lagrangians, we moved to canonically normalized classical fields by dividing by  $\sqrt{G_N}$ . Therefore, both  $h_{\mu\nu}$  and  $\tilde{h}_{\mu\nu}$  as well as the  $A_\mu$ - and  $\chi$ -components of  $h_{\mu\nu}$  have dimensionality of  $\sqrt{(\text{energy})/(\text{time})}$ . Correspondingly, the helicity decomposition of  $h_{\mu\nu}$  continues to have the form given by (2.105).  $T^{\mu\nu}(\Psi)$  denotes the energy momentum tensor of all modes  $\Psi$  which do not belong to the mode-decomposition of the background de Sitter solution, i.e. the quanta which in the quantum picture are not part of the coherent state description of the de Sitter metric. We only keep the lowest order dependence of  $T^{\mu\nu}(\Psi)$  on the fields.

For definiteness, we assume that  $T^{\mu\nu}$  is the stress-energy tensor of some external particles and does not contain a graviton part. Including  $h_{\mu\nu}$  into  $T^{\mu\nu}$  would result in nonlinear self-interactions of  $h_{\mu\nu}$ , which would contribute to both classical and quantum break-times. Since our approach is to replace the effect of the self-coupling by an effective graviton mass, we will not include gravitons in  $T^{\mu\nu}(\Psi)$ . In addition to that, it is convenient to couple gravity exclusively to external particles with initial occupation number equal to zero because such particles manifest themselves only via quantum processes and this is precisely what we are after.

Moreover, we couple  $T^{\mu\nu}(\Psi)$  only to the Einstein spin-2 helicity component  $\tilde{h}_{\mu\nu}$  in the Lagrangian (2.115). The reason why we do not couple the  $\chi$ -component to external sources is that we want the external particles  $\Psi$  to experience – in the classical limit and during the timescale of validity of (2.108) – “life” in an effective de Sitter metric.<sup>20</sup> As explained above, the solution (2.108) for the helicity-2 part  $\tilde{h}_{\mu\nu}$  alone suffices for that since it is equivalent to the de Sitter solution (2.98) of a linearized massless theory for  $t < t_{\text{cl}}$ .

Finally, we further split the helicity-2 component  $\tilde{h}_{\mu\nu}$  according to the symmetries of the Poincaré group. The scalar part, on which we shall focus in the following, corresponds to the trace of the helicity-2 component  $\tilde{h}_{\mu\nu}$ :<sup>21</sup>

$$\tilde{h}_{\mu\nu}^s = -\sqrt{16\pi} \phi \eta_{\mu\nu}, \text{ where} \quad (2.116)$$

$$\phi = \frac{1}{\sqrt{4\pi G_N}} \cos(m_g t). \quad (2.117)$$

From Eq. (2.109) it is clear that  $\phi$  also describes  $\chi$ :

$$\chi = 8\sqrt{4\pi} \phi. \quad (2.118)$$

Thus, the field  $\phi$  represents the scalar degree of freedom which simultaneously resides both in the trace of the helicity-2 component  $\tilde{h}_{\mu\nu}$  and in the helicity-0 component  $\chi$ .

In the following, we restrict ourselves to the scalar part (2.116) and disregard the off-diagonal elements of  $\tilde{h}_{\mu\nu}$ . Doing so can be regarded as a last deformation

<sup>20</sup>Notice that the coupling of the helicity-1 component  $A_\mu$  to  $T_{\mu\nu}$  automatically vanishes due to the conservation of the source:  $\partial^\mu T_{\mu\nu} = 0$ .

<sup>21</sup>The numerical prefactor was chosen to cancel the factor of  $1/(16\pi)$  in the Lagrangian (2.115). This choice, however, is arbitrary.

of the theory. We will show that despite its great simplicity, this model of the scalar component of the graviton suffices to capture all essential properties of de Sitter.<sup>22</sup> In summary, we consider the effective theory

$$\mathcal{L} = \frac{1}{2} \partial_\mu \phi \partial^\mu \phi - \frac{1}{2} \bar{m}_g^2 \phi^2 + \sqrt{G_N} \phi T_\mu^\mu(\Psi), \quad (2.119)$$

where we absorbed a factor of  $\sqrt{16\pi}$  in a redefinition of the energy-momentum tensor  $T_{\mu\nu}(\Psi)$ . The classical frequency is given by

$$\bar{m}_g = \sqrt{\Lambda}. \quad (2.120)$$

Moreover, the amplitude that corresponds to the solution (2.117) is

$$A_g = \frac{1}{\sqrt{4\pi G_N}}. \quad (2.121)$$

Finally, we remark that obtaining  $\phi$  as in (2.117) is only possible with a particular choice of gauge. We selected it for simplicity: It enables us to study linearized de Sitter in terms of only one scalar degree of freedom. We have this gauge freedom at our disposal since the Lagrangian (2.115) is manifestly gauge-invariant. Had we chosen a different gauge, the analysis would generically become more complicated as a single scalar degree of freedom would no longer suffice to describe the de Sitter metric.

### The Quantum State of de Sitter

Having given an effective model of de Sitter in terms of the scalar field  $\phi$ , it is straightforward to describe it on the quantum level. We can proceed in full analogy to the prototypical theory studied in section 2.2.2. The results that we find in our concrete model will completely match the generic scaling relations of the corpuscular approach to de Sitter, which we reviewed in section 1.3.2. First, the classical frequency  $\bar{m}_g$  determines the mass of the field as

$$m_g = \hbar \sqrt{\Lambda}, \quad (2.122)$$

as is required in the Fierz-Pauli theory (2.115).<sup>23</sup> This agrees with Eq. (1.20).

---

<sup>22</sup>In contrast, numerical prefactors, in which we are not interested, might change due to this deformation.

<sup>23</sup>We note that the limit  $m_g \rightarrow 0$  was used in [74] to obtain a coherent state description of Minkowski space in terms of zero energy gravitons. This connection makes a fundamental difference between the two spacetimes evident: The quantum constituents of de Sitter must carry nonzero energies.

Next we can construct the coherent state  $|N\rangle$  of gravitons as in Eq. (2.18), where the mode operators are defined in terms of the expansion (2.16).<sup>24</sup> Then the mean number of gravitons in a volume  $V$  turns out to be

$$N = \frac{V\bar{m}_g}{8\pi\hbar G_N}, \quad (2.123)$$

where we plugged in the amplitude (2.121) in Eq. (2.19). In one Hubble volume,  $V \sim \Lambda^{-3/2}$ , we get

$$N = \frac{1}{\hbar G_N \Lambda} \quad (2.124)$$

gravitons, in accordance with Eq. (1.21).<sup>25</sup>

At this point, we can also analyze the energy of de Sitter. In our quantum description, its expectation value per volume  $V$  is given by a product of the graviton rest mass and their average occupation number in a coherent state:

$$E = m_g N. \quad (2.125)$$

Taking into account Eq. (2.123), we conclude that the quantum description indeed yields the correct classical energy (1.15).<sup>26</sup> The matching of energy is also the reason why the numerical coefficient of the graviton mass has to be 1 in Eq. (2.112).

Finally, we can estimate the quantum coupling of the coherent state gravitons. Despite the fact that the classical solution was obtained in the approximation of ignoring the self-coupling of gravitons, the strength of their coupling is universally fixed by general covariance. To first nonlinear order, the graviton self-coupling can be estimated by taking into account the coupling of gravitons to their own energy-momentum tensor  $T_{\mu\nu}(\tilde{h})$  evaluated to bilinear order in  $\tilde{h}$ . Even without presenting the explicit long expression for  $T_{\mu\nu}(\tilde{h})$ , it is clear that for coherent state gravitons of energy  $m_g$ , the strength of the effective four-point coupling is given by

$$\alpha_g = \hbar\bar{m}_g^2 G_N, \quad (2.126)$$

in accordance with Eq. (1.22). Taking into account formula (2.124) for the number of gravitons per Hubble patch, we conclude as in Eq. (1.23) that the collective

<sup>24</sup>This means that we define the quantum state of  $\tilde{h}_{\mu\nu}$  by defining a quantum state for each symmetry component. Subsequently, we can view the full graviton state  $|N_{\tilde{h}}\rangle$  as tensor product of them:  $|N_{\tilde{h}}\rangle = |N\rangle \otimes_i |0_{h_i}\rangle$ , where  $|0_{h_i}\rangle$  are the vacua for the other components.

<sup>25</sup>Note that in any case we need to work with volumes  $V \lesssim \Lambda^{-3/2}$  for the validity of our first-order approximation.

<sup>26</sup>We remark that we deal with two different notions of energy. The classical energy is associated to the source  $\Lambda$ . The energy of the massive gravitons originates from the gravitational field. We could compare this to the situation for a shell of mass  $M$  and radius  $R$ : In that case,  $M$  is the energy of the source whereas  $M^2 G_N / (2R)$  is the energy of the gravitational field.

coupling  $\lambda_g = \alpha_g N$  is strong:

$$\lambda_g = 1. \quad (2.127)$$

This fact immediately demonstrates the consistency between Eqs. (2.101), (2.111) and (2.113) for the classical break-time of de Sitter and the general formula (2.12): The classical break-time is equal to the de Sitter Hubble radius because the collective coupling  $\lambda_g$  is of order one. Finally, we remark that we will not consider the self-coupling of gravitons in the following but solely focus on interactions with external particles.

### Summary of Approach

We can summarize our approach. On the mathematical level, we consider a theory of free massive gravity, in which we fix a coherent state of  $N$  gravitons at some initial time. After that, it evolves according to its free time evolution. During the whole regime of validity of the first order approximation, i.e. for  $t < t_{\text{cl}}$  (see (2.113)), the expectation value over this state reproduces the classical de Sitter solution of a massless theory.

Consequently, the following physical picture emerges: At the fundamental level, we deal with a theory of massless gravity with the constant source  $\Lambda$ . It leads to the formation of a multi-particle state which represents a quantum description of the de Sitter metric. The characteristic features of this state are:

- 1) the gravitons are off-shell due to the collective coupling;<sup>27</sup> and
- 2) the strength of this collective interaction is critical:  $\alpha_g N = 1$ .

Thus, this state is not accessible within the standard perturbation theory, i.e. by expansion in operators  $\hat{a}_{\text{free}}^\dagger, \hat{a}_{\text{free}}$  of free massless gravitons.<sup>28</sup> However, following [44], we propose that it is possible to “integrate out” the effect of the cosmological constant source as well as of collective interaction and replace it by an effective graviton mass. In other words, for a short time we can model the effect of collective interaction – putting massless gravitons off-shell – by means of a mass term in a free theory. Hence, we can approximate the interacting massless gravitons by free massive gravitons, described by the Fock space of  $\hat{a}^\dagger, \hat{a}$ .

The first evidence which supports the validity of such a modeling is that the state of free massive gravitons reproduces the correct classical expectation value. Of course, this argument does not suffice, since one can realize a given expectation value in a multitude of ways. Therefore, we will collect further evidence by demonstrating that our framework is constructed such that it automatically reproduces all semiclassical results in de Sitter. We shall accomplish this by coupling

---

<sup>27</sup>This off-shellness is real in the sense that a detector would measure a particle of nonzero energy and zero momentum.

<sup>28</sup>For reasons that will become apparent shortly, we denote creation and annihilation operators by  $\hat{a}^\dagger, \hat{a}$  from now on.

the “constituent” gravitons of the coherent state to external quantum particles via the universal gravitational coupling and studying quantum processes due to this interaction.<sup>29</sup> After making sure that these quantum processes correctly account for the known phenomena, we use the example of particle production to show that they also lead to an inevitable deviation from the description in terms of a classical metric and correspondingly a finite quantum break-time of de Sitter space.

## 2.4.2 Uncovering the Quantum Origin of Classical Evolution

### The Semiclassical Limit in the Coherent State Picture

At this point, we have obtained a consistent coherent state description of linearized de Sitter, which – for a short enough time interval – reproduces the classical metric (2.98) as expectation value of the graviton field. The resolution of the background metric in form of a quantum state allows us to achieve the following goals:

- 1) to understand standard classical and semiclassical processes – such as the propagation of a probe particle in a background metric and particle creation by a time-dependent classical metric – in the language of underlying *fully quantum* dynamics; and
- 2) to identify new corrections originating from this quantum dynamics which the standard semiclassical treatment is unable to capture.

In this section, we shall deal with the first point. We will focus on the semiclassical description, in which all fields other than the background metric are treated as quantum, and establish how it emerges as limiting case of our quantum description. From this semiclassical picture it is trivial to obtain the classical limit, in which only classical fields exist. Our starting point is the quantized version of the Lagrangian (2.119). After taking into account the coupling to an external field  $\hat{\Psi}$ , it reads

$$\hat{\mathcal{L}} = \frac{1}{2} \left( \partial_\mu \hat{\phi} \partial^\mu \hat{\phi} - m_g^2 \hat{\phi}^2 + \partial_\mu \hat{\Psi} \partial^\mu \hat{\Psi} - m_\Psi^2 \hat{\Psi}^2 \right) + \frac{\hat{\phi}}{M_p} \hat{T}^\mu_\mu(\hat{\Psi}). \quad (2.128)$$

For simplicity, we chose  $\hat{\Psi}$  as a scalar field of mass  $m_\Psi$ . Its stress-energy tensor is  $\hat{T}^{\mu\nu}(\hat{\Psi}) \equiv -\sqrt{16\pi'} \left( \partial^\mu \hat{\Psi} \partial^\nu \hat{\Psi} - \frac{1}{2} \partial^\alpha \hat{\Psi} \partial_\alpha \hat{\Psi} \eta^{\mu\nu} + \frac{1}{2} m_\Psi^2 \hat{\Psi}^2 \eta^{\mu\nu} \right)$ , where we use the unconventional normalization  $-\sqrt{16\pi'}$  in order to simplify notations. Moreover, we set  $\hbar = 1$  from now on. Correspondingly, we switch to the Planck mass  $M_p = 1/\sqrt{G_N}$ .

In general, the semiclassical treatment corresponds to quantizing weak field excitations on top of a fixed classical background metric, i.e. ignoring any backreaction to the metric from the creation and propagation of quantum particles. In

<sup>29</sup>In marked difference to other theories, the choice of coupling is unique. This might explain why the corpuscular approach is particularly suited for gravity.

our model, this amounts to quantizing the  $\hat{\Psi}$ -field in an effective de Sitter space-time created by the classical  $\phi$ -field. Thus, we can derive the standard semiclassical evolution of a probe particle  $\hat{\Psi}$  in the background classical metric by the effective Lagrangian

$$\hat{\mathcal{L}}_{\hat{\Psi}}^{(\text{eff})} = \frac{1}{2} \left( \partial_{\mu} \hat{\Psi} \partial^{\mu} \hat{\Psi} - m_{\hat{\Psi}}^2 \hat{\Psi}^2 \right) + \frac{\phi_{\text{cl}}}{M_p} \hat{T}_{\mu}^{\mu}(\hat{\Psi}), \quad (2.129)$$

which can be obtained from (2.128) when we replace the quantum field  $\hat{\phi}$  by the classical solution,  $\hat{\phi} \rightarrow \phi_{\text{cl}}$ . Here  $\phi_{\text{cl}}$  is given by (2.117). In such a treatment, the only relevant asymptotic quantum states are the initial states  $|i_{\Psi}\rangle$  and the final states  $|f_{\Psi}\rangle$  of the  $\hat{\Psi}$ -field since the background metric is a  $c$ -number.

As discussed in the section 1.3.2, treating  $\phi_{\text{cl}}$  as a fixed classical background is only consistent in the semiclassical limit (1.18):

$$\Lambda = \text{fixed}, \quad M_p \rightarrow \infty. \quad (2.130)$$

In that case, any backreaction from the dynamics of  $\hat{\Psi}$  can be ignored and we can treat  $\phi_{\text{cl}}$  as an *eternal* classical background. As already stated in Eq. (1.24), the semiclassical limit implies for the fully quantum picture of de Sitter that

$$\Lambda = m^2 = \text{fixed}, \quad N \rightarrow \infty, \quad (2.131)$$

which is evident from Eq. (2.124). The absence of backreaction is therefore achieved by considering an infinite mean occupation number of gravitons. It is important to note that we keep  $\hbar$  fixed in both limits.

As we have seen, the replacement  $\hat{\phi} \rightarrow \phi_{\text{cl}}$  suffices to obtain the semiclassical limit. However, we are asking for more. In our theory, this approximation must emerge as a result of fully quantum interactions between the metric-quanta and external particles  $\hat{\Psi}$ . This means that we would like to understand this replacement not as an external prescription, but as a result of taking the limit (2.131) in the full quantum evolution.

In order to achieve this, let us first describe the evolution of a  $\hat{\Psi}$ -field in the effective semiclassical theory (2.129) in the language of an  $S$ -matrix evolution operator. The nontrivial quantum evolution is due to the last term, which represents the off-diagonal part of the Hamiltonian density:

$$\hat{\mathcal{H}}_{\text{int}}^{(\text{eff})}(x) = \frac{\phi_{\text{cl}}}{M_p} \hat{T}_{\mu}^{\mu}(\hat{\Psi}). \quad (2.132)$$

We can derive the quantum evolution in a weak-field perturbation theory in the expansion parameter  $\phi_{\text{cl}}/M_p \ll 1$ . To first order in this expansion, we define the effective  $S$ -matrix evolution operator

$$\hat{S}^{(\text{eff})} = -i \int d^4x \mathbf{T} \left\{ \hat{\mathcal{H}}_{\text{int}}^{(\text{eff})}(x) \right\}. \quad (2.133)$$

The quantum evolution of  $\hat{\Psi}$  is then described by the matrix elements between different initial and final states:

$$\mathcal{A} = \langle f_{\Psi} | \hat{S}^{(\text{eff})} | i_{\Psi} \rangle . \quad (2.134)$$

Of course, since the effective Hamiltonian is explicitly time-dependent, the evolution described by the effective  $S$ -matrix is in general nonunitary. This leads to subtleties in defining the relevant initial and final  $S$ -matrix states on such a time-dependent background. This complication is completely standard and is a consequence of taking the zero backreaction limit.

Our immediate goal is not to enter in these well-known issues, but rather to understand the effective semiclassical evolution as the limit of the underlying fully quantum one. For this it is enough to recall that the coherent state  $|N\rangle$  is defined in such a way that it reproduces the classical metric in form of the expectation value:

$$\phi_{\text{cl}} = \langle N | \hat{\phi} | N \rangle . \quad (2.135)$$

Consequently, the effective semiclassical  $S$ -matrix operator can be written as

$$\langle f_{\Psi} | \hat{S}^{(\text{eff})} | i_{\Psi} \rangle = (\langle f_{\Psi} | \otimes \langle N |) \hat{S} (|N\rangle \otimes |i_{\Psi}\rangle) , \quad (2.136)$$

where  $\hat{S}$  is the full quantum  $S$ -matrix evolution operator

$$\hat{S} = -i \int d^4x \mathbf{T} \{ \hat{\mathcal{H}}_{\text{int}}(x) \} \quad (2.137)$$

defined by the full quantum interaction Hamiltonian

$$\hat{\mathcal{H}}_{\text{int}}(x) = \frac{\hat{\phi}}{M_p} \hat{T}_{\mu}^{\mu}(\hat{\Psi}) . \quad (2.138)$$

This means that the initial state in the fully quantum picture does not only consist of the external particles  $|i_{\Psi}\rangle$ . Instead, we use the coherent state (describing de Sitter) with external particles on top of it:  $|N\rangle \otimes |i_{\Psi}\rangle$ . Likewise, the final state is  $|N\rangle \otimes |f_{\Psi}\rangle$ .

Of course, the true quantum evolution inevitably implies transitions to final graviton states  $|N'\rangle$  which differ from the initial coherent state  $|N\rangle$  and in general are not even coherent. Such transitions are not equivalent to simply replacing the graviton field by its expectation value and lead to departures from semiclassicality. Therefore, Eq. (2.136) makes the quantum meaning of the semiclassical limit apparent: It corresponds to setting  $|N'\rangle = |N\rangle$ , i.e. ignoring any backreaction to the graviton state. Thus, the semiclassical  $S$ -matrix elements, which reproduce the motion of an external  $\hat{\Psi}$ -particle in the classical metric, are the subset of fully quantum  $S$ -matrix elements in which the quantum field  $\hat{\phi}$  is taken in the same initial and final state  $|N\rangle$ .

Notice that this selection of matrix elements is automatic in the limit (2.131), due to standard properties of coherent states. This is true since the overlap of coherent states yields the factor

$$\langle N + \Delta N | N \rangle = \exp\left(\frac{-\Delta N^2}{8N}\right), \quad (2.139)$$

which was already used in Eq. (2.28). We conclude that  $\langle N + \Delta N | N \rangle \approx \langle N | N \rangle = 1$  for  $N \rightarrow \infty$ . In that case, we can set  $|N'\rangle \approx |N\rangle$ . This consistently explains why this limit corresponds to a zero backreaction. A similar argument holds for transitions from the initial coherent state to noncoherent ones.

Finally, we note that establishing the connection between the semiclassical and the quantum  $S$ -matrix evolutions sheds new light on the standard difficulties of defining in- and out-states of the semiclassical  $S$ -matrix in a time-dependent external metric, such as de Sitter. The reason is the *eternal* nature of the background metric. As we have seen, in the quantum language this *eternity* translates to the approximation in which the initial and final states of gravitons can be taken as the same *undisturbed* coherent state  $|N\rangle$ . But for finite  $N$ , this approximation is good only for a finite time: For finite  $N$ , the coherent state cannot be eternal. As we shall see, precisely because of backreaction to it, the coherent state has a characteristic lifetime, which defines the quantum break-time of the system. This time scales as  $N$ . Consequently, the coherent state can be treated as truly *eternal* only in the limit (2.131), i.e. for infinite  $N$  and zero coupling. This makes the whole story self-consistent, at least at the level of the approximate toy model which we possess. Despite its simplicity, this model allows us to capture the key essence of the semiclassical problem as well as of its quantum resolution. In short, we do not need to worry about defining final  $S$ -matrix states on top of de Sitter in the light of the fact that the coherent state  $|N\rangle$  itself has a finite lifetime. Still, an effective  $S$ -matrix evolution can be applied as a valid approximation for processes which happen on timescales shorter than this lifetime.

### Redshift as Induced Graviton Emission

We have established the connection between the semiclassical and fully quantum  $S$ -matrix descriptions. Before turning to concrete examples, we will switch to a different convention for the mode operators. Instead of the dimensionless  $\hat{c}_{\vec{k}}^\dagger, \hat{c}_{\vec{k}}$ , we use

$$\hat{a}_{\vec{k}} := \sqrt{\frac{V}{(2\pi)^3}} \hat{c}_{\vec{k}}. \quad (2.140)$$

Correspondingly, the commutation relations (2.17) become

$$[\hat{a}_{\vec{k}}, \hat{a}_{\vec{k}'}] = [\hat{a}_{\vec{k}}^\dagger, \hat{a}_{\vec{k}'}^\dagger] = 0, \quad [\hat{a}_{\vec{k}}, \hat{a}_{\vec{k}'}^\dagger] = \delta^{(3)}(\vec{k} - \vec{k}'), \quad (2.141)$$

and the mode expansion of the field reads

$$\hat{\phi} = \int d^3 \vec{k} \frac{1}{\sqrt{2(2\pi)^3 \omega_{\vec{k}}}} \left( \hat{a}_{\vec{k}} e^{-ikx} + \hat{a}_{\vec{k}}^\dagger e^{ikx} \right). \quad (2.142)$$

Further discussions of the connection of discrete and continuous momentum variables can be found in appendix A of [73].

As a first concrete example, we will discuss the redshift which a probe particle experiences in a classical de Sitter metric. Even though redshift can also be described classically, we will study it in the semiclassical  $S$ -matrix description, in which this process corresponds to an initial state  $|i_\Psi\rangle = \hat{b}_{\vec{p}}^\dagger |0\rangle$  of 4-momentum  $p = (p_0, \vec{p})$  that has a higher energy than the final state  $|f_\Psi\rangle = \hat{b}_{\vec{p}'}^\dagger |0\rangle$  of 4-momentum  $p' = (p'_0, \vec{p}')$ . Here we denote the creation operators of  $\hat{\Psi}$  by  $\hat{b}_{\vec{p}}^\dagger$ . The corresponding amplitude is

$$\mathcal{A} = \langle 0 | \hat{b}_{\vec{p}'} \hat{S}^{(\text{eff})} \hat{b}_{\vec{p}}^\dagger | 0 \rangle. \quad (2.143)$$

A complication arises since the external particle does not propagate on a Minkowski background, but in a time-dependent de Sitter metric so that true noninteracting out-states, which would be required for the  $S$ -matrix calculation, do not exist.<sup>30</sup> This problem does not concern us since it only pertains to the semiclassical treatment. What we are only interested in is mapping the fully quantum calculation to the semiclassical one.

By the correspondence (2.136) we discussed before, the fully quantum amplitude is

$$\mathcal{A} = \langle N' | \hat{b}_{\vec{p}'} \hat{S} \hat{b}_{\vec{p}}^\dagger | N \rangle. \quad (2.144)$$

For the purpose of later generalization, we kept  $|N'\rangle$  arbitrary, but we will soon specialize to  $|N'\rangle = |N\rangle$ . Plugging in the full  $S$ -matrix operator (2.137), we obtain

$$\mathcal{A} = \mathcal{K}(p, p') \int d^4 x e^{-i(p-p')x} \langle N' | \hat{\phi} | N \rangle, \quad (2.145)$$

where the gravitational field solely appears in  $\langle N' | \hat{\phi} | N \rangle$  and the kinematical factor  $\mathcal{K}(p, p')$  only depends on the external particles. We do not need its explicit form in the present discussion but write it down for the purpose of later use:

$$\mathcal{K}(p, p') = i \frac{\sqrt{16\pi}}{M_p} \zeta_\Psi(p) \zeta_\Psi(p') (p \cdot p' - 2m_\Psi^2), \quad (2.146)$$

---

<sup>30</sup>As the de Sitter metric is only invariant under spatial but not under time translations, solely the momentum of the external particle is conserved, unlike its energy. This means that the dispersion relation of a  $\hat{\Psi}$ -particle is not Poincaré-invariant but depends on time because also asymptotically, it never stops interacting with the effective background metric. Therefore, noninteracting asymptotic states do not exist. A strategy to overcome this difficulty could be to approximate the initial and final dispersion relations as different but constant. Since the time-dependent change of the dispersion relation scales with the Hubble energy  $m_g$ , we expect this to be possible if we restrict ourselves to  $p_0, p'_0 \gg m_g$ .

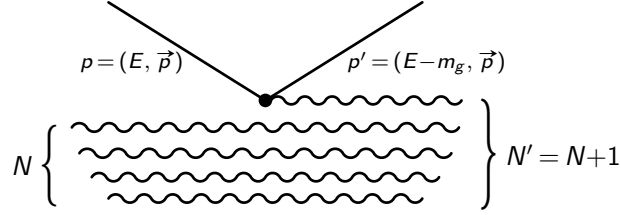


Figure 2.4: Redshift as stimulated graviton emission: An external particle of initial 4-momentum  $p$  deposits a graviton in the background state of  $N$  gravitons. The final 4-momentum of the external particle is  $p'$ .

with the abbreviation  $\zeta_{\Psi}(p) = ((2\pi)^3 2p_0)^{-1/2}$ .

As already discussed, we see explicitly that we can achieve the semiclassical limit  $\hat{\phi} \rightarrow \phi_{\text{cl}}$  by setting  $|N'\rangle = |N\rangle$ . Plugging this in as well as the mode expansion (2.142), we obtain

$$\mathcal{A} = \frac{(2\pi)^4}{\sqrt{2m_g}} \mathcal{K}(p, p') \delta^{(3)}(\vec{p} - \vec{p}') \left( \delta(-p_0 + p'_0 + m_g) \sqrt{\frac{N'}{V}} + \delta(-p_0 + p'_0 - m_g) \sqrt{\frac{N'}{V}} \right). \quad (2.147)$$

This formula makes the quantum dynamics of this process transparent. The external particle emits (contribution  $\propto \delta(-p_0 + p'_0 + m_g)$ ) or absorbs (contribution  $\propto \delta(-p_0 + p'_0 - m_g)$ ) a background graviton. The emission of a graviton, during which the external particle loses energy, corresponds to redshift whereas the absorption of a graviton leads to an increased energy, i.e. blueshift.<sup>31</sup> In the case of redshift, we furthermore observe that we deal with a process of induced emission which is enhanced by the  $N$  already existing gravitons. In the fully quantum  $S$ -matrix language, redshift therefore corresponds to the induced emission of a graviton, as already suggested in [44]. We depict this process in Fig. 2.4.

It is important to note that the final 4-momentum of the emitted graviton is completely fixed in this process of induced emission. Therefore, also the 4-momentum of the external particle is uniquely determined.<sup>32</sup> In this way, our fully quantum computation is able to reproduce the classical redshift.

As already discussed, we deal with a process of induced emission, which is enhanced by the  $N$  already existing gravitons. Consequently, we can obtain the amplitude  $\mathcal{A}_{\text{spont}}$  of spontaneous emission in the de Sitter background by removing this enhancement:  $\mathcal{A}_{\text{spont}} = \mathcal{A}/\sqrt{N'}$ . This relation is particularly interesting in

<sup>31</sup>From our perspective of short timescales, these two processes are indistinguishable. We expect that the boundary conditions of the expanding de Sitter branch select redshift.

<sup>32</sup>Namely, we have  $p' = (p_0 - m_g, \vec{p})$ . This shows that the dispersion relation of the  $\hat{\Psi}$ -particle has to change, as we already pointed out.

the semiclassical limit (2.131), which corresponds to  $N = \infty$ . Since the amplitude  $\mathcal{A}$  of redshift is finite, we conclude that the coherent state representation of the geometry produces the classical redshift although the amplitude of spontaneous emission  $\mathcal{A}_{\text{spont}}$  is zero in this limit. This is the essential difference between redshift and standard loss of energy by gravitational radiation.<sup>33</sup> In the corpuscular resolution of de Sitter, the classical process of redshift is therefore fully analogous to a phenomenon of a nonvanishing stimulated emission with zero spontaneous emission. This phenomenon takes place due to the representation of the graviton background as coherent graviton state whose mean occupation number is infinite in the semiclassical limit (2.131).

Heuristically, the process of redshift is analogous to the transitions between energy levels in an atom. In this picture, the initial “atom”  $\hat{\Psi}$  emits a graviton under the influence of a coherent state gravitational “radiation” and gets deexcited to a lower energy state  $\hat{\Psi}'$ . Clearly, the mass of the atom has to change in the course of this process. The difference between the atom in a radiation field and a particle in de Sitter is that the atom possesses different energy levels even without radiation whereas there are no energy levels for a particle in Minkowski.<sup>34</sup>

### Dilution of Gas as Conversion Process

To conclude this section, we want to briefly point to another process, namely the dilution of a gas of massive neutral particles in a de Sitter background, which at the classical level is described by a coherently oscillating real scalar field with Hubble friction term.<sup>35</sup>

$$\ddot{\Psi} + \sqrt{3\Lambda}\dot{\Psi} + m_{\Psi}^2\Psi = 0. \quad (2.148)$$

We restrict ourselves to the regime where the gas only leads to a small perturbation of the pure de Sitter metric. In the standard classical treatment, one would attribute the dilution to the Hubble damping given by (2.148) (see also the discussion in 2.3.4).

In our fully quantum treatment, a different picture emerges. Just like the de Sitter metric, also the gas has a quantum description as coherent state of  $\hat{\Psi}$ -particles. The coupling of  $\hat{\Psi}$  to gravity makes possible a process of induced decay, which is depicted in Fig. 2.5. For simplicity, we restricted ourselves to  $m_{\Psi} = n m_g/2$ , with  $n$  integer. In that case, two  $\hat{\Psi}$ -particles can annihilate into  $n$  gravitons. In this manner, the mean number of  $\hat{\Psi}$ -particles and therefore the density of the gas decreases. The classical condition that the gas only leads to a

<sup>33</sup>Of course, as all other processes in our picture, the classical redshift is corrected by quantum  $1/N$ -effects.

<sup>34</sup>This means that the particle is analogous to an atom with degenerate energy levels which only split in the presence of external radiation.

<sup>35</sup>Note that in the presence of a chemical potential, the story is a bit more involved and will not be considered here.

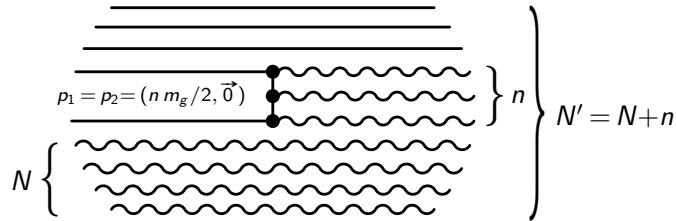


Figure 2.5: Dilution of gas as conversion of the gas particles: Two gas particles of 4-momentum  $p_1$  and  $p_2$ , which are at rest, annihilate into  $n$  gravitons. In this process, both the graviton and the gas state are coherent.

small perturbation from pure de Sitter amounts to a small backreaction on the quantum level, i.e. to the condition that the change of the graviton state  $|N\rangle$  is negligible. This is the case if  $m_\Psi N_\Psi \ll m_g N$ , where  $N_\Psi$  is the mean occupation number of the coherent  $\hat{\Psi}$ -state. In summary, at the quantum level, the dilution of gas is caused by a real conversion process between  $\hat{\Psi}$ - and  $\hat{\phi}$ -quanta.

### 2.4.3 Gibbons-Hawking Particle Production as Decay of the de Sitter State

#### Fully Quantum $S$ -Matrix Calculation

Next, we study the process of Gibbons-Hawking particle production. In doing so, our goal is twofold. As in the previous section, we first want to explicitly discuss how the standard semiclassical treatment can be obtained as limiting case of our fully quantum description. Secondly, we shall discuss what new quantum effects arise if no semiclassical limit is taken. Those lead to a finite quantum break-time of de Sitter.

How Gibbons-Hawking particle production arises in the semiclassical limit, in which quantum fields are studied on top of the undisturbed classical metric background, was already reviewed in section 1.3.2. In this picture, particle production arises as a *vacuum process*: Since the vacua of quantum fields depend on time in the evolving de Sitter metric, their early-time vacuum contains particles from the point of view of a late-time observer. As already emphasized several times, the crucial point is that by construction, there is no backreaction in the semiclassical limit, i.e. particle production does not change the classical de Sitter metric.

In our fully quantum description of the de Sitter metric, particle production emerges as a Hamiltonian process of scattering and decay of the gravitons which compose the coherent state. Once we take into account the coupling of gravitons to other species and to each other, inevitably quantum processes emerge in which part of the coherent state gravitons gets converted into free quanta (both in gravitons and in other species). The final states of these decay and scattering processes

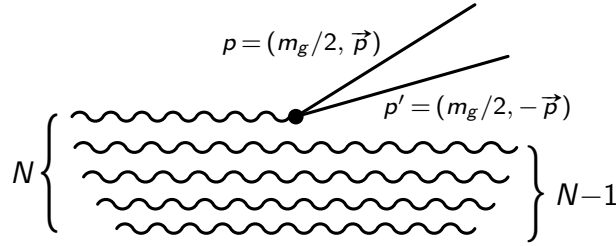


Figure 2.6: Particle production as graviton decay: One of the  $N$  initial gravitons decays and produces 2 external particles of 4-momentum  $p$  and  $p'$ .

correspond to the Gibbons-Hawking quanta, which arise in the usual semiclassical treatment.

We remark that in this context, “free” quanta are those with dispersion relations of particles propagating on top of a classical de Sitter background. As we are working to linear order in the de Sitter metric, the free quanta will have dispersion relations of Minkowski quanta to the leading order, with the de Sitter metric being a small correction. Due to the limitations of our approach, it only makes sense to take into account leading-order effects.

For illustrating the point, we limit ourselves to studying decay processes of background gravitons into external particle species. Due to the universality of graviton coupling, the process of graviton production has a similar rate. The simplest process contributing to particle production via decay is given by a transition from the initial state  $|N\rangle$  to a final state which contains two particles other than gravitons. It is depicted in Fig. 2.6. The corresponding amplitude is determined by the one of redshift (2.145), after the substitution  $p \rightarrow -p$  (where now both  $p$  and  $p'$  correspond to outgoing external particles):

$$\mathcal{A} = \langle N' | \hat{b}_{\vec{p}} \hat{b}_{\vec{p}'} \hat{S} | N \rangle = \mathcal{K}(-p, p') \int d^4x e^{i(p+p')x} \langle N' | \hat{\phi} | N \rangle. \quad (2.149)$$

As already explained in the previous section, the crucial novelty of our approach is that it uncovers the existence of quantum processes in which the final state  $|N'\rangle$  of background gravitons is different from the initial one  $|N\rangle$ . These processes correspond to  $1/N$ -corrections and therefore are fundamentally invisible in the semiclassical picture which in our framework is reproduced in the limit  $N \rightarrow \infty$ . In particular, the final state  $|N'\rangle$  obtained as a result of particle production in the quantum theory does not even have to be a coherent state. This deviation from coherence causes a gradual departure from classicality and eventually leads to quantum breaking.

However, for the case of de Sitter even the transitions among coherent states with different occupation numbers are sufficient for capturing the departure from the classical evolution since classically de Sitter is an eternal state and simply

cannot change. Any quantum process which changes the characteristics of de Sitter space marks a fundamentally new phenomenon not visible in the semiclassical theory. Therefore, for illustrating this point we shall consider transitions to a coherent state, but with different mean occupation number  $N' \neq N$ . As explained in section 2.2.2, it is most natural to consider a process in which the expectation value of the energy is conserved. Since we consider the decay of a particle, this leads to  $\Delta N = N' - N = -1$ . In any case, the precise value of  $\Delta N$  does not matter for our conclusions.

Using  $\Delta N \ll N$ , we obtain the matrix element:

$$\langle N' | \hat{\phi} | N \rangle = \frac{1}{\sqrt{2m_g V}} \left( e^{im_g t \sqrt{N'}} + e^{-im_g t \sqrt{N}} \right) \left( 1 - \frac{\Delta N^2}{8N} \right), \quad (2.150)$$

where the  $1/N$ -correction comes from the overlap of different coherent states. It vanishes in the semiclassical limit. The  $S$ -matrix element subsequently becomes:

$$\begin{aligned} \mathcal{A} = & \frac{(2\pi)^4}{\sqrt{2m_g V}} \mathcal{K}(-p, p') \delta^{(3)}(\vec{p} + \vec{p}') \left( 1 - \frac{\Delta N^2}{8N} \right) \\ & \left( \delta(p_0 + p'_0 - m_g) \sqrt{N'} + \delta(p_0 + p'_0 + m_g) \sqrt{N} \right). \end{aligned} \quad (2.151)$$

After the substitution  $p \rightarrow -p$ , the matrix element reduces to the result (2.147) for redshift in the limit  $N' = N$ , as it should. The amplitude of particle production consists of two parts. The first one describes a process where a graviton leaves the bound state and the second one corresponds to adding a graviton to the bound state. In contrast to the case of redshift, the second process cannot occur because of energy conservation so that the term will be dropped.

As is derived in appendix A.1.1, the rate of particle production is

$$\Gamma = \frac{2\sqrt{\frac{m_g^2}{4} - m_\Psi^2} N}{M_p^2 m_g^2} \left( \frac{m_g^2}{2} + m_\Psi^2 \right)^2 \left( 1 - \frac{\Delta N^2 - 4\Delta N}{4N} \right). \quad (2.152)$$

We observe that particle production to first order only takes place for light particles,  $m_\Psi < m_g/2$ , as we expect it. In order to simplify the discussion, we specialize to massless external particles ( $m_\Psi = 0$ ):

$$\Gamma = \frac{Nm_g^3}{4M_p^2} \left( 1 - \frac{\Delta N^2 - 4\Delta N}{4N} \right) = \frac{\Lambda^2 V}{32\pi} \left( 1 - \frac{\Delta N^2 - 4\Delta N}{4N} \right). \quad (2.153)$$

For dimensional reasons, this result does not come as a surprise. The rate must be proportional to the volume  $V$ . Since particle production can also be derived in the semiclassical treatment, i.e. in the limit  $M_p \rightarrow \infty$ , the Planck mass should not appear so that we can only use  $\Lambda$  to obtain the correct mass dimension.

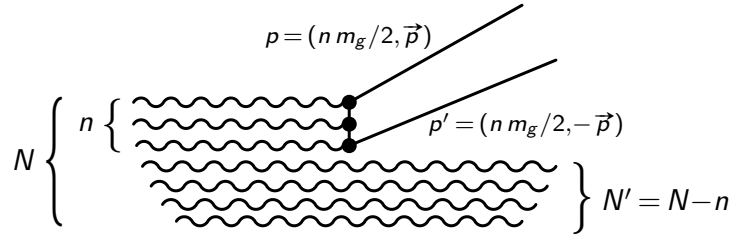


Figure 2.7: Leading-order process for the production of particles with high total energy  $E \gg m_g$ . At least  $n > E/m_g$  of the initial  $N$  gravitons have to decay to produce the two external particles of 4-momentum  $p$  and  $p'$ .

### Glimpses of Gibbons-Hawking Temperature

Before we proceed to our main result, the quantum break-time, we want to check to what extent our approach is consistent with the semiclassical result. To this end, we estimate the power of produced particles. As a pair of produced particles has the energy  $\hbar\sqrt{\Lambda}$ , our quantum result for the decay rate (2.153) leads to

$$P_q \approx \hbar\Lambda, \quad (2.154)$$

where we restored powers of  $\hbar$  for a moment. As it should, particle production vanishes in the classical limit  $\hbar \rightarrow 0$  but is finite in the semiclassical limit  $M_p \rightarrow \infty$ . The power (2.154) matches the semiclassical treatment, in which the Hubble horizon radiates like a black body of temperature  $T \approx \hbar\sqrt{\Lambda}$  because the Stefan-Boltzmann law yields the emitted power  $P \approx T^4 A$ , where  $A \approx \Lambda^{-1}$  is the area of the horizon.

Having concluded that the total power of produced particles is of the right order of magnitude, we investigate the distribution of produced particles. To first order, they are not distributed thermally, but all have the same energy  $m_g/2$ . As soon as one goes to higher orders so that more than one background graviton participate in the scattering process, this  $\delta$ -distribution will be smeared out. Furthermore, we expect at least qualitatively that the resulting distribution is thermal.

For example, one of the key features of the Gibbons-Hawking thermal spectrum is the Boltzmann suppression of the production rate of particles of energy  $E$  higher than the de Sitter Hubble parameter  $\sqrt{\Lambda}$ :

$$\Gamma \propto e^{-E/\sqrt{\Lambda}}. \quad (2.155)$$

Our quantum description of de Sitter space gives a very interesting microscopic explanation of this suppression. The production of particles is a Hamiltonian process in which the background coherent state gravitons get converted into free quanta. Since the frequencies of background gravitons are given by  $m_g = \sqrt{\Lambda}$ , the production of states with energies  $E \gg m_g$  requires the annihilation of  $n$

background gravitons, with  $n > E/m_g$ . The leading-order contribution to this process is schematically expressed in Fig. 2.7, which depicts the annihilation of  $n$  gravitons into a pair of  $\Psi$ -quanta with total energy  $E = nm_g$ . The probability of such a process is highly suppressed due to the participation of a large number of soft gravitons in it: Each soft vertex contributes a factor  $\alpha = 1/N$  to the rate.

For estimating this suppression, we can directly use the results of [45], where multi-graviton transition amplitudes have been calculated (see [49] for a related discussion). Accounting for the fact that there are  $\binom{N}{n}$  possibilities to choose the  $n$  annihilating gravitons, we obtain the rate:

$$\Gamma \propto \left(\frac{1}{N}\right)^n n! \binom{N}{n}. \quad (2.156)$$

Using Stirling's formula twice, which is valid for  $N \gg 1$  and  $N - n \gg 1$ , we get

$$\Gamma \propto e^{-n} \left(\frac{N}{N-n}\right)^{N-n}. \quad (2.157)$$

Before we discuss the exponential suppression, we analyze the additional factor  $\left(\frac{N}{N-n}\right)^{N-n}$ . Defining  $l = N/(N-n)$ , we can rewrite it as  $l^{N/l}$ . It is 1 for  $l = 1$  and  $l \rightarrow \infty$ .<sup>36</sup> Its maximum is at  $l = e$  and gives  $e^{N/e}$ . At this point, the rate is still exponentially suppressed:

$$\Gamma_{\max} \propto e^{-\frac{e-2}{e-1}n}. \quad (2.158)$$

Thus, we conclude that

$$\Gamma \propto e^{-c(n)n}, \quad (2.159)$$

with  $c(n) \approx 1$  and  $c(N) = 1$ . Since we have  $n = E/m_g$  and  $m_g = \sqrt{\Lambda}$ , the above expression reproduces the exponential suppression of the Boltzmann factor (2.155) for the thermal bath. For  $n = N$ , this correspondence even becomes exact. It is remarkable that the analysis of multi-graviton scattering suffices to obtain a thermal behavior.

Having studied produced particles of high energies, we note that smearing out of the energy spectrum also takes place on the infrared side. Indeed, we can produce arbitrarily soft quanta in processes of decays or annihilations of the background gravitons by redistributing the rest of the energy among the remaining background gravitons in form of a recoil. For example, one of the background gravitons can decay into a pair of  $\hat{\Psi}$ -particles of energy  $E \ll m_g$  while transferring the energy difference  $\Delta E = m_g - E$  to the remaining  $N - 1$  gravitons. The process

<sup>36</sup>The approximation (2.157) is no longer valid for  $l \rightarrow \infty$ , i.e.  $n = N$ , but we can directly read off from (2.156) that the additional factor is one:  $\Gamma \propto e^{-N}$ .

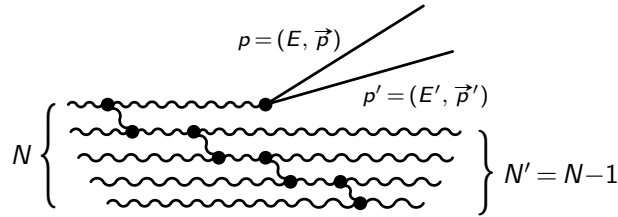


Figure 2.8: Higher order process of particle production, in which the produced particles recoil against all remaining gravitons. In particular, this allows for produced particles of low energies  $E, E' \ll m_g/2$ .

is schematically depicted in Fig. 2.8. Unlike the case of  $E \gg m_g$ , the processes with  $E \ll m_g$  are not exponentially suppressed.

It would not be very informative to give a more precise estimate of processes with the production of deep-infrared quanta of energy  $E \ll m_g$  since the wavelength of such particles exceeds the size of the de Sitter Hubble patch and thus the timescale of validity of our model. So in the discussion of very low energy particle production, we will be satisfied with qualitative arguments, which clearly show that – even ignoring classical nonlinearities and formally extrapolating our model for longer times – the production of very soft modes is possible due to multi-graviton processes.

We thus see that by taking into account multi-graviton contributions to particle production, the  $\delta$ -distribution gets smeared out. Its peak is still at  $E \approx m_g$ , but the region  $E \gg m_g$  is exponentially suppressed by a factor that is strikingly similar to a thermal Boltzmann suppression factor (2.155). It is remarkable that the thermal-like distribution of the produced particles can arise in the microscopic theory as a result of the structure of soft multi-graviton amplitudes without any need of the notion of temperature.

In summary, we have managed to reproduce essentially all key short-distance features of Gibbons-Hawking particle production, i.e. those features that deal with timescales within the validity of our approximation. We have achieved all this within a simplest framework in which the classical part of de Sitter is mapped on a coherent state of gravitons of a linear theory. The quantum effects of de Sitter – such as Gibbons-Hawking radiation – result from quantum interactions of these gravitons. Of course, we do not expect that this simple theory can quantitatively capture all the properties of de Sitter, but it already took us surprisingly far.

### Consistency Check: Gauge Invariance

As a final consistency check, we consider a brief example of how the rate of particle production transforms under gauge transformations. To this end, we study the first order of the transformation from conformal time  $t$  to physical time  $t'$ :  $dt = a(t)dt'$ ,

where  $a(t) \propto \cosh(\sqrt{\Lambda/3} t)$  is the scale factor. Since  $a(0) = 1$ , we expect this not to have any influence on the decay rate in the semiclassical treatment. Our goal is to show how this gauge invariance arises in our framework. Since the leading order of the gauge transformation changes the metric as  $g'_{00} - g_{00} \propto \Lambda t^2$ , our first order perturbation generalizes to

$$\tilde{h}'_{00} = c \tilde{h}_{00}, \quad (2.160)$$

where  $c = 1$  yields the untransformed value.<sup>37</sup> For the quantum description in terms of interacting gravitons,  $c \neq 1$  means that we have to introduce two different scalar function for  $h_{00}$  and the spatial diagonal perturbations.

Generalizing our calculation of the first order matrix element, we observe that only the kinematical factor (2.146) changes:

$$\begin{aligned} \mathcal{K}'(-p, p') &= i \frac{\sqrt{16\pi}}{M_p} \zeta_\Psi(p) \zeta_\Psi(p') \\ &\quad \left( -\left(-\frac{1}{2}c + \frac{3}{2}\right) p_0 p'_0 + \left(\frac{1}{2}c + \frac{1}{2}\right) \vec{p} \cdot \vec{p}' - \left(\frac{1}{2}c + \frac{3}{2}\right) m_\Psi^2 \right). \end{aligned} \quad (2.161)$$

Plugging in the kinematics of a decay, we conclude that the kinematical factor and thus also the rate are indeed gauge-invariant:<sup>38</sup>

$$|\mathcal{K}'(-p, p')|^2 = \left( \frac{m_g^2}{2} + m_\Psi^2 \right)^2. \quad (2.162)$$

#### 2.4.4 Quantum Break-Time

As we have explained in section 2.2.3, a decay process leads to a fully coherent final state, as long as rescattering events of the produced quanta are not taken into account. Nevertheless, it causes quantum breaking since the transition process is quantum, i.e. it is invisible in the classical theory. This point becomes particularly clear in the case of de Sitter. Even if hypothetically we were allowed to maintain

<sup>37</sup>This corresponds to the infinitesimal transformation  $\xi^\mu \propto \delta_0^\mu c \Lambda t^3$ . It destroys de Donder gauge, but the resulting metric still is a solution of the ungauged equations of motion.

<sup>38</sup>This result also determines how the decay rate changes under rescaling of the spatial components,

$$\tilde{h}'_{11} = \tilde{h}'_{22} = \tilde{h}'_{33} = b \tilde{h}_{11}.$$

Since we have shown that a change of  $h_{00}$  has no effect, the spatial transformation is equivalent to a rescaling of all perturbations,  $\tilde{h}'_{\mu\nu} = b \tilde{h}_{\mu\nu}$ . This can be absorbed by the redefinition

$$\Lambda' = b \Lambda.$$

Both in the classical and the quantum description, all results will change according to a modified cosmological constant.

only processes which preserve the coherence of the state of background gravitons, this would still lead to a quantum evolution which has no counterpart in the semiclassical picture: Semiclassically, de Sitter is an eternal state with no clock. Therefore, even a “clean” transition between the two different coherent states  $|N\rangle$  and  $|N'\rangle$  gives an intrinsically quantum evolution of the state which cannot be matched by anything in the classical theory.

Notwithstanding the above, we expect that coherence of the graviton state is not preserved after  $t_q$ . The reason is that the collective interaction is strong,  $\alpha_g N = 1$ . Therefore, a higher-order process such as  $2 \rightarrow 2$ -interaction, which is depicted in Fig. 1.2, has the same rate as decay. This is evident from Eq. (1.25). Even in our model, which does not include self-interaction of gravitons, the exchange by virtual  $\hat{\Psi}$ -particles will lead to their rescattering and subsequent decoherence, albeit on a longer timescale.

In summary, we have found a crucial difference to the semiclassical treatment: In our quantum description of de Sitter, the backreaction of particle production on the spacetime leads to a change of the coherent state  $|N\rangle$  into  $|N'\rangle$ , which is either a different coherent state or a decohered one. On the order of one background graviton leaves the coherent state each Hubble time, due to decay into free quanta or due to rescattering.

After a macroscopic number of gravitons  $\Delta N$  of the order of  $N$  has decayed, the resulting quantum state  $|N - \Delta N\rangle$  can no longer – even approximately – reproduce the initial de Sitter metric. Consequently, we obtain the quantum break-time

$$t_q \approx \Gamma^{-1} N = \frac{N}{\sqrt{\Lambda}}. \quad (2.163)$$

Rewriting in terms of more conventional parameters, we get

$$t_q \approx \frac{M_p^2}{\Lambda^{3/2}}. \quad (2.164)$$

As discussed in section 2.2.5, this timescale is physically meaningful even though  $t_q > t_{cl}$ . The reason for this is that  $t_{cl}$  could be increased by a better choice of operators  $\hat{a}^\dagger, \hat{a}$ , which take into account classical nonlinear interactions. But for any choice of operators, the decoherence mechanism will continue to work and lead to a significant deviation from the classical solution after  $t_q$ . Thus, at the latest after the timescale (2.164), the classical description of de Sitter breaks down. This quantum break-time constitutes the main result of the present section.

Since the timescale (2.164) fully agrees with the earlier result (1.26) of [44], which we reviewed in section 1.3.2, we want to comment on the relationship of the two approaches. In [44], a model-independent perspective was adopted, i.e. no concrete theory of the constituent gravitons of de Sitter was provided. Instead, generic scaling relations were derived that any model of de Sitter has to fulfill. The fact that such general arguments already suffice to determine the quantum

break-time is a great strength of this approach. This universality of the quantum break-time matches the fact that the result (2.164) fulfills the universal dependence (2.56), in which the quantum break-time is set by  $1/\alpha$ . This is true since the classical timescale is  $t_{\text{cl}} \approx H^{-1}$  (in turn, this follows from  $\lambda_g = 1$ ) and the quantum coupling is  $\alpha_g = 1/N$ .

In contrast, we have employed the explicit model (2.115) in the present work. In this way, we have managed to confirm the generic predictions of [44] in a concrete scenario. Thus, it is the combination of the general argument of [44] and the results in the explicit model (2.115) that make the prediction (2.164) of the quantum break-time especially robust. In particular, it is important to emphasize that the quantum break-time is not tied to the specific scenario (2.115) and its shortcomings, but we expect it to hold in a more generic setting because of the general scaling arguments.

### Relationship to Other Work on de Sitter

There are manifold studies of the backreaction of particle production on de Sitter. In particular, it was proposed that due to energy conservation, the vacuum energy should decrease [120, 121].<sup>39</sup> In contrast to our approach, however, the assumption was made that this process can still be described by a classical metric, i.e. by an effectively decreasing cosmological constant. In this picture, the cosmological constant would dynamically relax to zero.<sup>40</sup> There is, however, no reason to assume that the gravitational state of reduced energy can still be described by a classical metric. In the case of black holes, precisely this assumption would lead to the information paradox. Whereas the question of information is less clear for de Sitter,<sup>41</sup> the proposal of a decreasing cosmological constant is much more problematic than that of a shrinking black hole mass. As also discussed in section 1.3.2, the reason is that unlike in the black hole case, the source  $\Lambda$  is a fixed and eternal parameter of the theory and therefore can never change. Consequently, we will not follow the idea of an evolving cosmological constant.

The timescale (2.164) also appears in a second independent line of research, in which de Sitter is treated as a fixed background metric. The central question is how long perturbation theory can be valid on top of this classical metric. Exploiting analogies to the black hole case, it was put forward in [129] and shortly afterwards made more explicit in [130] that this also leads to Eq. (2.164), i.e. a perturbative expansion on a de Sitter background ceases to be valid after this timescale. Numerous calculations in various different setups have since confirmed this

<sup>39</sup>This idea bears similarities to the instability of de Sitter space put forward in [122–124].

<sup>40</sup>An explicit realization of this approach can e.g. be found in [125–127], where Eq. (2.164) acquires the meaning of the timescale on which the cosmological constant changes significantly.

<sup>41</sup>Nevertheless, the timescale (2.164) can also be derived from considerations of information in de Sitter [128].

finding. Examples include [131–133] and [134] summarizes more recent results.<sup>42</sup> It is important to emphasize, however, that all the above findings only point to a breakdown of perturbation theory. This does not exclude the possibility that a resummation or a nonperturbative calculation could successfully be performed on top of the de Sitter metric.

In contrast, we come to a much more dramatic conclusion in our corpuscular picture of de Sitter. The whole notion of a metric ceases to be valid after the quantum break-time (2.164). This breakdown is fundamental and no calculation performed on top of a classical metric can overcome it. For us, the breakdown of perturbation theory on top of the fixed metric therefore gives an indication of quantum breaking, but its implications are more severe than can become visible in a semiclassical study. Not only perturbation theory breaks down but the whole classical metric.

### Emergent Nature of de Sitter Symmetry and Breaking Thereof

We would like to briefly comment on symmetry properties of the  $1/N$ -effects which lead to a quantum break-time of de Sitter. Obviously, since these effects cause a departure from the semiclassical evolution, they are obliged not to respect the de Sitter invariance.

The above fact is fully consistent with our quantum approach. In the standard treatment of gravitational backgrounds, spacetimes with different values of the cosmological constant are considered as different vacua. The corresponding symmetries of such classical backgrounds are thus viewed as *vacuum symmetries*. The novelty of our picture is to treat the de Sitter state associated to a certain value of the cosmological constant as a particular quantum state constructed in a Fock space with a unique fundamental Minkowski vacuum. In our approach, de Sitter therefore is an excited multi-particle state.

Once we “demote” de Sitter from the rank of a vacuum into an ordinary coherent state, its symmetry acquires the meaning of an emergent symmetry: It is not a symmetry of the vacuum, but a symmetry of an expectation value over a particular state. In such a situation, an arbitrary process which affects the expectation value is expected to violate this emergent symmetry. This is exactly what is achieved by  $1/N$ -effects which change the de Sitter coherent state and lead to a finite quantum break-time.

### Relationship to Black Holes

As we have explained in section 1.3, the break-time (2.164) of de Sitter and the break-time (1.13) of black holes are analogous in the sense that they correspond to the timescale after which backreaction of particle production becomes significant.

---

<sup>42</sup>An interesting connection of this breakdown of perturbation theory in de Sitter and asymptotic symmetries, which are the subject of section 4.4.2, was established in [135].

In both cases, the description in terms of a classical metric ceases to be valid at this point. For black holes, the timescale (1.6) corresponds to the half lifetime and it is moreover known as Page's time [42] in the context of the puzzle of black hole information.

Whereas the breakdown of the classical description takes place in the whole volume for de Sitter, we should distinguish between the exterior and the interior region for black holes. The latter are asymptotically flat, i.e. the influence of the localized black hole on the spacetime far away from the horizon is always small. Therefore, a classical geometry should continue to exist even after quantum breaking. Only near the horizon and in the interior of the black hole, the description in terms of a classical metric breaks down completely.

It would be very interesting to study this phenomenon of quantum breaking in more detail by generalizing the present study of de Sitter to the black hole case. This means that one would have to find an explicit implementation of the quantum N-portrait of black holes [34], which we reviewed in section 1.3.1.<sup>43</sup> If such a quantum model can be found that is able to reproduce the classical mean field description for initial times, this would allow for an explicit computation of the quantum break-time along the lines presented here.

### Bound on Number of Particle Species

It is known [150–152] that semiclassical black hole physics puts a strict upper bound on the number of particle species  $\mathcal{N}_{\text{sp}}$  in terms of the gravity cutoff scale  $L_*$ :

$$\mathcal{N}_{\text{sp}} < \frac{L_*^2}{L_P^2}. \quad (2.165)$$

That is, the fundamental cutoff length of gravity  $L_*$ , in the presence of species, is no longer given by the Planck length  $L_P$ , but becomes larger and is given by  $L_* = L_P \sqrt{\mathcal{N}_{\text{sp}}}$ . This bound originates from the fact that the rate of Hawking radiation is proportional to  $\mathcal{N}_{\text{sp}}$ . Consequently, the evaporation of black holes of size smaller than  $L_P \sqrt{\mathcal{N}_{\text{sp}}}$  cannot be thermal – even approximately – due to a very strong backreaction from the decay. Thus, black holes beyond this size are in conflict with basic properties of Hawking radiation and cannot be treated semiclassically. Therefore, the scale  $L_*$  marks the boundary of applicability of semiclassical Einstein gravity. This results in the bound (2.165).

It is interesting to study the effect of the number of species on the de Sitter quantum break-time. So we assume in our simple model that the graviton is coupled to a large number of particle species  $\hat{\Psi}_j$ ,  $j = 1, 2, \dots, \mathcal{N}_{\text{sp}}$ . The presence of more species opens up more channels for Gibbons-Hawking particle production

---

<sup>43</sup>Further work on the corpuscular picture of black holes can be found in [35–37, 40, 43–45, 136–149].

so that the rate increases by a factor of  $\mathcal{N}_{\text{sp}}$ . Correspondingly, the quantum break-time becomes shorter and Eq. (2.164) takes the form:

$$t_{\text{q}} \approx \frac{1}{\sqrt{\Lambda}} \left( \frac{1}{\mathcal{N}_{\text{sp}}} \frac{M_p^2}{\Lambda} \right). \quad (2.166)$$

This relation reveals a very interesting new meaning of the black hole bound on species (2.165) in the context of de Sitter. Namely, when the number of species exceeds the critical value

$$\mathcal{N}_{\text{cr}} \approx \frac{M_p^2}{\Lambda}, \quad (2.167)$$

the quantum break-time becomes shorter than the Hubble time  $1/\sqrt{\Lambda}$ . At the same time, the de Sitter radius  $R_H$  becomes shorter than the gravity cutoff length  $L_*$ .

Moreover, notice that  $\mathcal{N}_{\text{cr}} = N$ . Thus, the maximal number of particle species allowed in any theory which can provide a de Sitter metric as a trustable classical solution cannot exceed the mean occupation number of the de Sitter coherent state. If we violate this bound, everything goes wrong: The quantum break-time of de Sitter becomes shorter than the Hubble time and the de Sitter radius becomes shorter than the quantum gravity cutoff.

We see that, first, there is a nice consistency between the bounds derived from very different considerations: Two seemingly different requirements – namely that the de Sitter radius on the one hand and the quantum break-time on the other hand should not exceed the gravity cutoff – lead to the same conclusion. Secondly, the corpuscular picture of de Sitter gives a very transparent meaning to the species bound: With too many particle species available, the constituent gravitons would decay so rapidly that de Sitter would not last even for a time equal to its radius. Of course, this would make no sense. The theory protects itself from entering such a nonsense regime, which would require the *classical* de Sitter space to have a curvature radius shorter than the quantum gravity length  $L_*$ , which is impossible.

### 2.4.5 Implications for the Cosmological Constant

The concept of quantum breaking provides a new perspective on the cosmological constant problem. Because we know from experience that the present Universe can be described classically, we conclude that quantum breaking has not yet happened. Since any patch with a given value of the Hubble parameter  $H = \sqrt{\Lambda}$  can be described classically at most during the time  $t_{\text{q}} \approx (H^{-1}/\mathcal{N}_{\text{sp}})(M_p^2/H^2)$  (see Eq. (2.166)), this puts an upper bound on the dark energy in our Universe in the case that it is explained by a cosmological constant. The older our Universe is and the more species it contains, the lower this bound becomes.

First, we can study quantum breaking for the observed value of the cosmological constant  $\sqrt{\Lambda} = 10^{-42}$  GeV. Currently, the phenomenologically acceptable number

of hidden sector species is bounded by  $\mathcal{N}_{\text{sp}} \approx 10^{32}$  because a larger number of species would lower the gravity cutoff below the TeV-scale, which is excluded by current collider data [150–152]. Assuming this number, the observed value of the cosmological term would saturate the quantum break-time bound if our Universe were approximately  $10^{100}$  years old. This age should not be confused with the Hubble time or the Hubble radius. It pertains to the entire duration of the classically describable history of our patch.

We can also apply the constraint in the other direction: Knowing the classical age of a given universe and the number of species, we can deduce an upper bound on  $\Lambda$ . For the present age  $t_{\text{u}}$  of our Universe, we obtain  $H_{\text{max}} \approx (M_p^2/t_{\text{u}})^{1/3} = 10^{-1} \text{ GeV}$ , where we set  $\mathcal{N}_{\text{sp}} = 1$  to obtain a more robust bound. This means that the energy density associated to the cosmological constant,  $\rho \approx H^2 M_p^2$ , can be at most  $10^{-40}$  of the Planckian energy density.<sup>44</sup> On the one hand, we cannot explain why the cosmological constant is as small as it is. On the other hand, however, the cosmological constant has to be small for consistency.

## 2.4.6 Implications for Inflation

### Bound on Inflaton Potential

Next we apply our results to inflation [20] and especially its slow-roll version [153]. Since the quantum break-time becomes shorter for higher values of the Hubble scale (see e.g. Eq. (2.164)), it is very interesting to study quantum breaking during inflation when the corresponding Hubble parameter was much higher than it is today.<sup>45</sup> All predictions that we can derive from inflation are based on the semiclassical treatment (see e.g. [155] for a review), in which the notion of a classical metric is meaningful. Thus, an inflationary scenario is only predictive if it avoids quantum breaking. This condition and several of its consequences, to which we shall turn shortly, were already discussed in [44]. Moreover, since all results derived in the semiclassical limit appear to agree with observations, it is very unlikely that an inflationary scenario that undergoes quantum breaking can be viable. For this reason, we arrive at the requirement of avoiding quantum breaking:

$$t_{\text{esc}} \lesssim t_{\text{q}}. \quad (2.168)$$

The quantum break-time must be longer than the time it takes for the system to escape from the quasi-de Sitter state, i.e. longer than the total duration of inflation.

In inflation, generically several degrees of freedom with different interactions exist. Then  $t_{\text{q}}$  is the shortest timescale before any subsystem quantum breaks.

<sup>44</sup>Including  $N_{\text{sp}} \approx 10^{32}$  would lead to  $H_{\text{max}} \approx 10^{-12} \text{ GeV}$  and an energy density of at most  $10^{-62}$  of the Planckian value.

<sup>45</sup>More studies of corpuscular inflation can be found in [110, 111, 154].

Therefore, we can represent the quantum break-time as

$$t_q \approx H^{-1} \frac{1}{\alpha_>}, \quad (2.169)$$

where we used the general relation (2.56) for the quantum break-time. Here  $\alpha_>$  is the strongest interaction that exists in the system and we roughly approximated the classical timescale as  $t_{\text{cl}} \approx H^{-1}$ . Since the number  $\mathcal{N}$  of  $e$ -foldings determines the duration of inflation as  $t_{\text{esc}} = H^{-1}\mathcal{N}$ , condition (2.168) leads to a maximal number of  $e$ -foldings given by

$$\mathcal{N}_{\text{max}} \approx \frac{1}{\alpha_>}. \quad (2.170)$$

Thus, the stronger the coupling is in the system, the more severe the requirement (2.168) of avoiding quantum breaking becomes.

Because gravitational interaction always exists, a model-independent upper bound on the quantum break-time is given by the break-time (2.166) due to pure gravity:

$$t_q < H^{-1} \frac{M_p^2}{\mathcal{N}_{\text{sp}} H^2}. \quad (2.171)$$

Note that we obtain this relation when we plug the effective gravitational coupling  $\alpha_g = \mathcal{N}_{\text{sp}} H^2 / M_p^2$  in the general formula (2.169). This leads to the absolute upper bound on the number of  $e$ -foldings:<sup>46</sup>

$$\mathcal{N}_{\text{max}} < \frac{1}{\mathcal{N}_{\text{sp}}} \frac{M_p^2}{H^2}, \quad (2.172)$$

which must hold in any inflationary scenario.

The condition (2.168) of avoiding quantum breaking can be translated as a constraint on the inflaton potential  $V(\psi)$ , where  $\psi$  is the inflaton. Namely, the change of the potential  $\Delta V$  over some time  $\Delta t \approx t_q$  must satisfy  $|\Delta V| \gtrsim V$ . Approximating  $\Delta V \sim V' \dot{\psi} \Delta t$  and assuming that slow roll is satisfied,  $\dot{\psi} \sim -V'/H$ , we get  $\Delta V \sim -V'^2 \Delta t / H$ . Plugging in Eq. (2.169), we arrive at the following bound:

$$\frac{M_p |V'|}{V} \gtrsim \sqrt{\alpha_>}. \quad (2.173)$$

Again, we observe that the constraint becomes more stringent as the coupling  $\alpha_>$  increases. If the coupling is stronger, the quantum break-time gets shorter and the system needs to move faster to avoid it.

<sup>46</sup>In [44] it was also suggested that inflaton-graviton scattering could lead to a second bound  $\mathcal{N}_{\text{max}} = (M_p/H)^{4/3}$ . However, here we adopt the model-independent gravitational bound (2.172). Furthermore, as discussed in section 2.4.4, we note that bounds on the number of  $e$ -foldings analogous to Eq. (2.172) have been derived earlier in numerous semiclassical studies of perturbation theories on top of a fixed de Sitter metric. The earliest examples (without the consideration of the species effect) can be found in [129, 130].

Additionally, we note that the bound (2.173) has the form conjectured in [156]. For us, however, the r.h.s. is not a fixed constant but can depend on  $\psi$  and  $V$ . Therefore, it does not need to be of order 1 but can be much smaller. For example if the strongest coupling is gravitational, we get  $\sqrt{\alpha_g} = \sqrt{\mathcal{N}_{\text{sp}}} H/M_p$ . We will elaborate on the connection to [156] in section 2.5.1, as was already done in [157] shortly after [156] appeared.<sup>47</sup>

Finally, we emphasize that so far, our discussion of inflation is independent of whether or not quantum breaking in de Sitter leads to an inconsistency. We will discuss this question in section 2.5. Instead, our only requirement is that a semiclassical description of inflation exists since otherwise it is not a predictive scenario. Thus far, we therefore only require that quantum breaking must not take place in the Hubble patch that we observe. Consequently, eternal inflation [158, 159] is not yet excluded at this point.

### Inflationary Observables<sup>48</sup>

On the one hand, quantum breaking can constrain inflationary models. On the other hand, it can lead to new observables for those scenarios that are not excluded. In the semiclassical picture of inflation, only data from the last 60 e-foldings is accessible. All preexisting information is erased. As already explained in [44], the situation is different in the corpuscular picture of de Sitter. The reason is that the  $1/N$ -effects, which lead to a deviation from the classical metric description, cannot be washed out. Therefore, they provide a *quantum clock* that encodes information about the total duration of inflation. In this way, the perturbations produced at different epochs are no longer identical and the age of de Sitter becomes a physical observable.

It is important to note that this difference is unrelated to the standard time variation of the Hubble parameter due to a classical slow-roll of the inflaton. Instead, it comes from the fact that the de Sitter background *ages* due to its quantum decay. In other words, the backreaction that is measured by  $1/N$ -effects violates the de Sitter invariance in the same way as the evaporation of water from a finite volume tank violates the time-translation invariance. Even if the rate of the process is constant, the water level in the tank changes and this is an observable effect. Determining how these new effects that contain information about the total duration of inflation can be measured constitutes an interesting topic of future research. What is clear, however, is that the effects are stronger if inflation lasted longer. Therefore, those scenarios that are maximally close to quantum breaking are the most interesting.

---

<sup>47</sup>We note that the bound (2.173) is stronger than the one presented in [157] by a factor of  $1/\sqrt{\alpha_g}$ .

<sup>48</sup>The following paragraphs use material from [10].

## 2.5 Implications of Quantum Inconsistency of de Sitter

As we have explained, quantum breaking is about the breakdown of an approximation. After the quantum break-time, the true quantum evolution deviates significantly from the classical solution. In order to describe the system after this point, one has to take into account quantum effects.

In the special case of de Sitter, there are indications that the consequences of quantum breaking could be much more severe. Namely, it could lead to an inconsistency [44, 50]. The argument goes as follows [50]: What sets de Sitter apart from all other gravitational solutions is the fact that its source is intrinsically classical, namely a parameter of the theory. For this reason, quantum effects in the state of de Sitter cannot be matched by any evolution of the cosmological constant. Whereas the gravitational field inevitably departs from de Sitter, the cosmological constant is eternally tied to it. This conflict indicates that de Sitter is inconsistent on the quantum level.

We emphasize that for other systems, quantum breaking cannot lead to an inconsistency because also the source of the gravitational solution possesses an underlying quantum description. Therefore, quantum effects in the gravitational field can be matched consistently by quantum effects of the source.

Moreover, we must stress that the question if de Sitter quantum breaking is inconsistent remains open and constitutes an interesting topic of future research. If it does not lead to an inconsistency, this would mean that some exotic future-eternal state exists past the quantum break-time, the mean field description of which no longer matches any reasonable classical metric solution of general relativity. Such a scenario was termed as *quantum eternity* in [44].

In the following, we will not further discuss whether de Sitter quantum breaking is inconsistent. Instead, our goal is to explore some of the implications that arise if quantum breaking indeed leads to an inconsistency for the special situation of de Sitter. In that case, it must not happen in any consistent theory. Therefore, whenever there is a positive energy density, a degree of freedom must exist that relaxes it on a timescale  $t_{\text{esc}}$  that is shorter than the quantum break-time:

$$t_{\text{esc}} \lesssim t_{\text{q}}. \quad (2.174)$$

This condition, which we shall call *de Sitter quantum breaking bound*, looks identical to the one discussed previously in Eq. (2.168), but now it acquires a different meaning. It is no longer about the existence of a (semi)classical description and therefore about predictivity. Instead, it concerns the fundamental consistency of a theory, completely unrelated to the breakdown of any computation techniques or classical approximation.

As already discussed in [44, 50], an immediate consequence of the de Sitter quantum breaking bound is that the currently observed dark energy cannot be

constant but must change in time. Namely, a degree of freedom must exist that drives our Universe towards Minkowski vacuum within a time that is shorter than  $t_q$ . However, this represents an extremely mild restriction. The reason is that for the current phase, the quantum break-time from gravity is enormous,  $t_q \sim 10^{132}$  y (see section 2.4.5).<sup>49</sup> Nevertheless, this point of view promotes the cosmological constant problem from a question of naturalness to an issue of consistency.

### 2.5.1 Exclusion of Self-Reproduction in Inflation

#### Bounds on the Potential

In the case of inflation, the quantum breaking bound can lead to more severe restrictions. For slow roll, we have already investigated the implications of condition (2.174). It leads to the bound (2.173) on the first derivative of the inflaton potential.

Next, we can consider extrema.<sup>50</sup> First, we study the case in which the extremum is unstable – it can either be a local maximum or a tachyonic direction around a saddle point with a negative curvature – and additionally the curvature  $|V''|$  is much larger than the Hubble parameter  $H^2 = V/M_p^2$ . Then the field leaves the neighborhood on a timescale  $t_{\text{esc}} \approx |V''|^{-1/2}$ , which is much shorter than the Hubble time  $H^{-1}$ . Therefore, the system has no chance to suffer from de Sitter quantum breaking.

In the opposite case, in which the curvature is small,  $|V''| \ll H^2$ , the sign of  $V''$  plays no role. The field behaves as effectively-massless and experiences a random walk with variation  $\delta\psi \sim H$  per Hubble volume per Hubble time. These quantum excursions lead to a self-reproduction of the de Sitter phase [158, 159]. Whereas inflation ends in some Hubble patches, there always exists a Hubble patch in which the field would stay on top of the hill longer than the quantum break-time (2.166). However, the de Sitter quantum breaking bound (2.174) demands that quantum breaking must not happen at all in a consistent theory, i.e. not in any Hubble patch. Therefore, eternal inflation violates the consistency condition (2.174). Avoidance of this violation implies the following bound:

$$V'' \lesssim -V/M_p^2. \quad (2.175)$$

In summary, it follows from the de Sitter quantum breaking bound that either the first derivative is sufficiently big (Eq. (2.173)) or that the second derivative is sufficiently negative:

$$\frac{M_p|V'|}{V} \gtrsim \sqrt{\alpha_{>}} \quad \vee \quad V'' \lesssim -V/M_p^2. \quad (2.176)$$

<sup>49</sup>In the presence of the maximal number of species,  $\mathcal{N}_{\text{sp}} \approx 10^{32}$ , the quantum break-time can be shortened to  $t_q \approx 10^{100}$  y but is still huge.

<sup>50</sup>Our study of extrema was motivated by the refined de Sitter swampland conjecture [160], which we shall discuss shortly.

We remark that this condition leaves enough room for inflationary model building. Whereas situations that necessarily lead to eternal inflation are excluded, as is e.g. the case for topological inflation [161, 162], other scenarios require closer scrutiny in order to make sure that they avoid quantum breaking. For example, hilltop inflation [163], in which inflation occurs near a maximum, is not necessarily incompatible with the de Sitter quantum breaking bound.

### Relationship to de Sitter Swampland Conjecture

It is also very interesting to study inflation in string theory because it has generically proven difficult to construct compactifications that contain such quasi-de Sitter states, as was already apparent since the early models of inflation driven by  $D$ -branes [164, 165]. Recently, the swampland program has spurred renewed interest in the consistency of de Sitter in string theory. The term swampland, which was coined in [166], refers to the space of consistent low-energy effective field theories that nevertheless cannot be completed into a string theory of quantum gravity in the ultraviolet.<sup>51</sup> Regarding quasi-de Sitter states, the conjecture has recently been put forward that an inflaton potential must satisfy the following conditions in order to avoid the swampland [156, 160]:<sup>52</sup>

$$\frac{M_p|V'|}{V} \gtrsim c_1 \quad \vee \quad V'' \lesssim -c_2 V/M_p^2, \quad (2.177)$$

where  $c_1$  and  $c_2$  are numbers of order 1.

This conjecture motivated us to express the de Sitter quantum breaking bound in the form (2.176). Our work is based on [157], where the relationship of quantum breaking and the constraint [156] on the first derivative of the inflation potential was already discussed. When we compare the conditions (2.176) and (2.177), we note that the constraint on the second derivative is identical. Thus, both exclude eternal inflation. In contrast, the bound on the first derivative due to quantum breaking is in general milder since  $\sqrt{\alpha_{>}}$  can be much smaller than 1. Therefore, quantum breaking does not generically exclude slow-roll inflation whereas the swampland conjecture (2.177) does, at least in the simplest scenarios.<sup>53</sup>

As an outlook, we can try to establish a more direct connection between the quantum breaking bound and the de Sitter swampland conjecture in string theory. If indeed quantum breaking leads to an inconsistency for de Sitter, then string

<sup>51</sup>A current review of the swampland program, including the de Sitter swampland conjecture on which we focus in the following, can be found in [167].

<sup>52</sup>First [156], only the part of the conjecture concerning the first derivative was proposed. Later [160], following the suggestions of [168] and [169], the conjecture was weakened by adding the condition concerning the second derivative. Some further exemplary discussions of the de Sitter swampland conjecture can be found in [170–180].

<sup>53</sup>A first discussion of this and other cosmological implications of the swampland conjecture can be found in [170].

theory as a consistent theory of quantum gravity must never allow for a state that experiences de Sitter quantum breaking. In this picture, the de Sitter swampland conjecture can be regarded as a consequence of the quantum breaking bound. String theory is obliged to escape a quasi-de Sitter state in order to avoid quantum breaking.

We can illustrate how string theory appears to respect the quantum breaking bound by considering a simple realization of an unstable extremum. Following the setup proposed in [164, 165], we study a  $D_3$ - and an anti- $D_3$ -brane in a 10-dimensional space on which 6 extra dimensions have been compactified. We choose their characteristic radii  $R$  to be much larger than the string length  $L_s$  and we shall assume that the  $D_3$ - and anti- $D_3$  brane are separated by a distance  $S$  that is much smaller than  $R$ . Moreover, the branes are aligned with 4 noncompact dimensions. In this situation, the branes fall towards each other due to a force that is mediated by the tree-level exchange of closed strings. In the regime  $S \gg L_s$ , this process was considered in [164, 165] with the goal of constructing slow-roll inflation.

For the present discussion, however, we will only be interested in the situation  $S \approx L_s$ . As soon as the branes are that close to each other, an open string mode becomes tachyonic. A complete form of its potential is unknown, but it suffices for our considerations that the mass of the tachyon is given as  $m^2 \approx -L_s^{-2}$ . Since the energy density of the brane scales as  $L_s^{-4}/g_s$ , we arrive at the escape time  $t_{\text{esc}} \approx L_s \ln(g_s^{-1})$ . We can also estimate the quantum break-time of the system. Using the general relation (2.56) with  $t_{\text{cl}} \approx L_s$ , we obtain  $t_{\text{q}} \approx L_s/g_s^2$ . We conclude that in the regime in which the string theory is weakly coupled, the escape time is much shorter than the quantum break-time, i.e. the bound (2.174) is satisfied.

We can equivalently derive this result from a 4-dimensional point of view. There the Hubble scale is

$$H^2 \approx \frac{L_s^{-4}}{g_s M_p^2} = L_s^{-2} \frac{g_s}{(R/L_s)^6} = -V'' \frac{g_s}{(R/L_s)^6}, \quad (2.178)$$

where we expressed the 4-dimensional Planck mass in terms of its 10-dimensional counterpart,  $M_p^2 = M_{10}^8 R^6$ , and we moreover used that  $M_{10}^8 = L_s^{-8}/g_s^2$ . As  $g_s \ll 1$  and  $L_s \ll R$ , it immediately follows that the bound (2.175) is satisfied. This shows that de Sitter quantum breaking does not take place.

### 2.5.2 Exclusion of de Sitter Vacua

The most immediate consequence of the de Sitter quantum breaking bound (2.176) is that a consistent theory must not possess any stable or metastable vacuum with a positive energy density. This exclusion of de Sitter vacua is particularly interesting since the same requirement also follows from the swampland conjecture (2.177). Therefore, one can choose either the quantum breaking bound or the de Sitter swampland conjecture as starting point for the following arguments.

Thus, any theory that *in principle* allows for a de Sitter vacuum can be ruled out. It is important to stress that it is inessential if these vacua are actually populated, e.g. as a result of cosmological evolution. If vacua with a positive energy density lead to an inconsistency, the mere fact that the theory possesses such vacua rules it out. This leads to important constraints on model building.

### Necessity of the QCD Axion

First, we study the strong CP problem of QCD. Usually, it is posed as a *naturalness* question: Why, among all possible  $\theta$ -vacua, do we live in the one in which QCD is CP-conserving to an extraordinary accuracy? However, if de Sitter vacua are excluded, the strong CP problem turns into a matter of consistency. The reason is that, as we shall show shortly, most  $\theta$ -vacua possess a positive vacuum energy density and therefore correspond to de Sitter. The only way out is to render the  $\theta$ -angle unphysical. Consequently, the axion solution to the strong CP problem arises as a mandatory consistency requirement, independently of any naturalness considerations or even a fine-tuning.

We will prove this statement by contradiction, i.e. we will assume that there is no axion in QCD and show that this leads to an inconsistency. If no axion is present, QCD contains distinct vacua that can be labeled by the  $\theta$ -parameter [181, 182]. Those  $\theta$ -vacua possess different energies and it follows from the Vafa-Witten theorem [183] that a global minimum of the energy is achieved for  $\theta = 0$ . Although the exact energy dependence is not known for large values  $\theta \cong \pi$ , it is clear that the maximal energy density is set by the QCD scale  $\Lambda_{\text{QCD}}^4 \approx (100 \text{ MeV})^4$ , where we ignore a mild suppression by the quark masses.

Now we can combine this knowledge with two experimental facts. First, we know that the value of  $\theta$  in the vacuum that we live in is close to zero,  $\theta \lesssim 10^{-10}$ . Secondly, we use the observation that the density of dark energy is very small,  $\varepsilon \lesssim (10^{-3} \text{ eV})^4$ , and in particular negligible as compared to the QCD scale  $\Lambda_{\text{QCD}}$ .<sup>54</sup> Notice that our present argument is independent of the cosmological constant problem. It is inessential for us why the vacuum energy is as small as it is, but we simply use the fact that whatever the reason is, it leads to the observed value.

The above findings imply that we live very close to the  $\theta$ -vacuum with the smallest energy. Therefore, other vacua exist that have a larger value of  $\theta$  and correspondingly a higher energy density of up to  $(100 \text{ MeV})^4$ . Whatever the mechanism is that relaxes the small vacuum energy in the present Universe to zero, its effect on vacua with energy densities of  $(100 \text{ MeV})^4$  is negligible. Consequently, we can safely conclude that the vacua with higher values of  $\theta$  correspond to de Sitter. However, such states are inconsistent by the quantum breaking bound. By contradiction, this proves that an axion must exist that renders  $\theta$  unphysical.<sup>55</sup>

<sup>54</sup>As explained in the beginning of section 2.5, the quantum breaking bound implies that the present vacuum energy cannot be constant but must slowly relax to zero.

<sup>55</sup>Note that any degree of freedom that relaxes  $\theta$  is effectively an axion, regardless of whether

Of course, each  $\theta$ -vacuum belongs to a different superselection-sector, i.e. no transitions among them are possible. As explained above, however, this is inessential for our argument. According to the de Sitter breaking bound, a consistent theory must not *possess* a de Sitter vacuum, even if this state is not realized in our Universe. The mere fact that the theory *in principle* allows for de Sitter states rules it out. Moreover, it is crucial to note that the role of  $\theta$  is special in the sense that unlike other parameters of the Standard Model, it specifies the choice of a vacuum in one and the same theory, rather than a choice of a theory. Therefore, if the Standard Model develops de Sitter vacua for some values of its parameters, this only rules out those values but not the whole theory.<sup>56</sup>

Finally, it is important to study whether de Sitter quantum breaking can still happen once the axion is introduced. In this case, the points  $\theta \neq 0$  are no longer vacua but relax to the state  $\theta = 0$ . The corresponding relaxation time is set by the inverse axion mass,  $t_{\text{esc}} \approx m_a^{-1} \approx f_a/\Lambda_{\text{QCD}}^2$ . Now we consider the state with energy density  $\varepsilon \approx \Lambda_{\text{QCD}}^4$  because it would have the shortest quantum break-time given by  $t_q \approx M_p^5/\Lambda_{\text{QCD}}^6$ . Representing it as  $t_q \approx t_{\text{esc}} M_p^5/(\Lambda_{\text{QCD}}^4 f_a)$ , we obtain  $t_q \approx 10^{76} t_{\text{esc}}$  even for  $f_a \approx M_p$ . Therefore, de Sitter quantum breaking cannot happen and the bound (2.174) is fulfilled.

After relaxation, the axion field continues to perform damped oscillations. We have studied quantum breaking for this model in section 2.3 and concluded that the classical approximation is extremely accurate. But even if quantum breaking were to happen for cosmic axions, this would not lead to an inconsistency. Instead, it would merely mark the point when quantum effects have to be taken into account.

### Exclusion of Spontaneously-Broken Discrete Symmetries

Next, we shall show that if de Sitter vacua are inconsistent, this rules out any extension of the Standard Model with a spontaneously-broken discrete symmetry, provided the phase transition happens after inflation.<sup>57</sup> This conclusion holds both for exact and for approximate symmetries. In short, the argument is the following: If the symmetry is exact, the scenario is ruled out because of the well-known domain wall problem [186]. However, if the symmetry is only approximate so that domain walls can be avoided, this leads to de Sitter vacua, which are also excluded. Thus, the domain wall problem and the de Sitter quantum breaking problem complement each other in theories with low-scale spontaneously-broken discrete symmetries. This rules out many well-motivated extensions of the Standard Model.

---

it is elementary or composite.

<sup>56</sup>Of course, extensions of the Standard Model exist in which other parameters, e.g. the Higgs mass, can be promoted to parameters of vacuum superselection and be relaxed dynamically (see e.g. [184, 185]). Our de Sitter bound then would become applicable to such models.

<sup>57</sup>Discrete symmetries with a very small scale below about 1 MeV are not excluded, as we shall discuss shortly.

First, we review the well-known *cosmological domain wall problem* [186], which occurs in the presence of spontaneously-broken discrete symmetries. Its key point is that the domain walls, which are formed during the phase transition of spontaneous symmetry breaking, possess an energy density that redshifts as  $\varepsilon \sim 1/\mathbf{a}$ , where  $\mathbf{a}$  is the scale factor. This means that their energy dilutes more slowly than that of matter or radiation. If domain walls existed, they would therefore quickly come to dominate the Universe, in contradiction with observations. One way to avoid this conclusion is to consider a case in which the domain walls are formed sufficiently late due to a very small scale  $v$  of symmetry breaking. From CMB-measurements, one can deduce the bound  $v \lesssim 0.9$  MeV [187, 188].

If the scale of symmetry breaking is bigger than this bound, there are essentially two ways to avoid the cosmological domain wall problem. The first one is to assume that the phase transition took place before inflation since in this case the exponential expansion stretches domain walls to superhorizon sizes. However, this solution is only viable if the symmetry breaking scale is sufficiently high. The second approach to tackle the domain wall problem is to introduce a soft explicit breaking of the discrete symmetry, thereby making the domain walls unstable. If this bias is strong enough, the domain walls decay before they start to dominate the Universe.<sup>58</sup>

Our goal is to show that the quantum breaking bound rules out the second solution since it would necessarily imply the existence of a metastable de Sitter vacuum. We begin by estimating how strong the explicit breaking has to be in order to avoid the domain wall problem. Although generalizations to higher discrete symmetries are straightforward, we consider the case of  $Z_2$  for concreteness. We assume that a scalar field  $\hat{\psi}$  spontaneously breaks the symmetry by its vacuum expectation value (VEV),  $\langle \hat{\psi} \rangle = \pm v$ . During the phase transition, domain walls that separate the two vacua  $\pm v$  are formed by the Kibble mechanism [190, 191]. Unless very small couplings are involved, the tension of the domain walls is of order  $\sigma \approx v^3$ . This corresponds to the force  $F_{\text{tension}} \approx \sigma R_H$  that stabilizes the domain wall, where  $R_H$  is the Hubble radius. Now we introduce a small split  $\beta$  of the energy densities of the vacua. It leads to a pressure force  $F_{\text{press}} \approx \beta R_H^2$  that destabilizes the domain walls. If  $F_{\text{press}} \gtrsim F_{\text{tension}}$ , the pressure takes over and forces the domain walls to disappear [192]. This leads to the bound  $\beta > \sigma/R_H$ , where  $R_H$  is the Hubble radius at the latest during nucleosynthesis.

Now we can proceed as in the case of axions. Thus, we assume that a discrete symmetry with a bias of  $\beta$  exists and then show that this leads to a contradiction. The key point is that after the decay of domain walls induced by the bias  $\beta$ , only the lowest-lying vacuum persists. In particular, this would be the vacuum that we live in. Since we know from experiments that the energy density in the present Universe is nonnegative, this means that another vacuum would exist with an

---

<sup>58</sup>For instance, an explicit breaking of sufficient strength can come from Planck-scale suppressed operators [189].

energy density of at least  $\beta$ . This vacuum corresponds to de Sitter and would thereby contradict the quantum breaking bound. Consequently, the soft breaking of the discrete symmetry is excluded.

Of course, the inconsistent de Sitter vacuum would not be populated as a result of a realistic cosmological evolution. But as for the case of axions, this is inessential for our argument.<sup>59</sup> The mere fact that theory in principle possesses an inconsistent de Sitter state rules it out.

Moreover, we remark that we cannot exclude that it is possible to evade the quantum breaking bound by making the bias  $\beta$  time-dependent in such a way that it goes to zero after the domain walls have decayed. We will not consider this possibility for two reasons. First, it appears that a model that can realize this idea would be rather involved. Secondly, the explicit breaking terms are expected to generate an energy splitting through quantum corrections. In order to avoid this, severe fine-tuning would be required.

In summary, the quantum breaking bound rules out a large class of phenomenologically-viable extensions of the Standard Model in which a discrete symmetry is spontaneously broken after inflation. An incomplete list of such models includes:

**NMSSM.** This is an extension of a Minimal Supersymmetric Standard Model by a gauge singlet superfield. The VEV of this superfield spontaneously breaks a discrete  $Z_3$  symmetry and generates a  $\mu$ -term in the superpotential. The VEV is around the weak scale and unless inflation happens at very low scales, the domain wall problem follows. The standard solution is to assume a small explicit breaking of the  $Z_3$  symmetry (see e.g. [193] and references therein). However, our analysis shows that such a solution implies the existence of a local de Sitter minimum and is therefore excluded by the quantum breaking bound.

**Spontaneous CP Breaking.** Another important example is a theory with spontaneous breaking of CP symmetry. This is achieved by an extension of the Standard Model either by a second doublet [194] or a singlet [195]. In both cases, there is a spontaneously-broken discrete symmetry around the weak scale and domain walls result. Again, an attempt to eliminate them by an explicit breaking leads to the creation of a local de Sitter minimum and is excluded.

**Constraints on Peccei-Quinn Models.** Exactly by the same reason as above, we exclude the versions of the Peccei-Quinn model with post-inflationary phase transitions and with a nontrivial discrete symmetry. Of course, there are versions of the theory free of domain walls that are fully compatible with the quantum breaking bound.

**Gaugino Condensate in Super-Yang-Mills.** It is known that the gaugino condensate in  $SU(N)$  gives rise to domain walls due to spontaneous breaking of a discrete  $Z_N$  symmetry [196]. This is important because the gaugino condensate

---

<sup>59</sup>In fact, the argument is even stronger for the case of discrete symmetries. Whereas  $\theta$ -vacua correspond to superselection sectors, a very small but nonzero probability exists that all Hubble patches that lead to the currently observed Universe happen to be in the false vacuum.

is a commonly accepted source for hidden sector supersymmetry breaking in supergravity theories [197]. If the phase transition with gaugino condensation takes place after inflation, the walls must be eliminated by an explicit breaking of the  $Z_N$ -symmetry. As we have explained, this results in the existence of unacceptable de Sitter minima, which are excluded by our criterion. Hence, we obtain the cosmological requirement that gauginos must condense before the end of inflation. In the simplest version (in which the gaugino sector is not directly coupled to the inflaton) this would translate as a lower bound on the scale of gaugino condensation, i.e. it must be above the reheating temperature.

As a final remark, we point out that an alternative solution to the domain wall problem exists for some scenarios [198, 199]. It is based on the idea of symmetry nonrestoration [200–202]. This mechanism is compatible with a discrete symmetry that is not explicitly broken but exact. The reason is that the symmetry is not restored at high temperature and therefore the domain walls never form. As shown in [198, 199], however, such a nonrestoration requires a very special choice of parameters. Whereas it can work in some models, such as the ones with spontaneously-broken  $CP$  and Peccei-Quinn symmetries, it is incompatible with renormalizable supersymmetric theories [203]. Therefore, it cannot eliminate domain walls in NMSSM.



# Chapter 3

## Storage of Quantum Information

One conclusion of the previous chapter is that the classical description of de Sitter and black holes can cease to be valid on macroscopically big scales. An immediate question that follows is how these systems can be described on the quantum level. The goal of the present chapter is to show that quantum information can play a crucial role.

First, we are more general and study generic, i.e. potentially nongravitational, bosonic systems in section 3.1. Building on the models and concepts of [204, 205], we work out a general mechanism by which nearly-gapless modes and correspondingly states of enhanced memory capacity can emerge. This phenomenon, which we shall call *assisted gaplessness*, can occur in any bosonic system, provided it possesses weak and attractive interactions. Moreover, we develop an analytic procedure for finding such nearly-gapless modes. We refer to it as *c-number method* and it is a generalization of the approach that was used in [51] to study a specific model. The fact that assisted gaplessness occurs in generic bosonic systems naturally leads to the idea that it could also be operative in black holes and de Sitter and be responsible for their large entropies. This approach, the essence of which was first suggested in [36], leads to the exciting possibility of using table-top experiments to simulate the storage and processing of information in gravitational systems. Similarly, such studies could contribute to understanding other systems of enhanced memory capacity, such as neural networks [204, 205].

In section 3.2, we turn to a concrete prototype system that we obtain as truncation of an attractive Bose gas in a one-dimensional box with Dirichlet boundary conditions. We first employ the *c-number method* to find states of enhanced memory capacity and then confirm their existence by numerical analysis.

In section 3.3, we study the phenomenon of *memory burden*, which was first described in [206]. Its essence is that a large amount of information tends to backreact on the system and thereby ties it to its initial state. After studying a prototype system, we discuss implications for black holes and de Sitter.

This chapter is based on the paper [5], which is joint work with Gia Dvali and

Marco Michel, as well as the paper [10], which is joint work with Gia Dvali, Lukas Eisemann and Marco Michel. To a large extent, this chapter is an ad verbatim reproduction of these publications. Sections 3.1 and 3.2 as well as appendix A.2, which pertains to the present chapter, follow [5]. Parts of [5], in particular the aspects presented in section 3.2, were reported independently by Marco Michel in his master's thesis [207]. Figs. 3.2, 3.3, 3.4, 3.5 and 3.6 are based on earlier versions presented in [207]. Section 3.3 follows [10].

## 3.1 Enhanced Memory Capacity in Attractive Cold Bosons

### 3.1.1 Storage of Information in Gapless Modes

We shall consider a completely generic quantum system. We can fully characterize it by its degrees of freedom and by the rules of the interactions among them. Each degree of freedom corresponds to a particular oscillatory mode of the system. In quantum field theory, such modes are described as quantum oscillators that can exist in various excited states. The level of excitation of a mode  $k$  in a given state  $|n_k\rangle$  can be conveniently described by an occupation number  $n_k$  of the corresponding quantum oscillator, with the usual creation/annihilation operators  $\hat{b}_k^\dagger$ ,  $\hat{b}_k$  and the number operator  $\hat{n}_k = \hat{b}_k^\dagger \hat{b}_k$  (where  $k = 0, 1, \dots, K$ ). At this point,  $k$  is a generic label. In the concrete models that we study in the following, it will denote the dimensionless wave number. We shall limit ourselves to bosonic degrees of freedom, which satisfy the standard canonical commutation relations:

$$[\hat{b}_j, \hat{b}_k^\dagger] = \delta_{jk}, \quad [\hat{b}_j, \hat{b}_k] = [\hat{b}_j^\dagger, \hat{b}_k^\dagger] = 0. \quad (3.1)$$

One of the most important characteristics of a system is the energy level-spacing between states of different occupation numbers, i.e.  $|n_k\rangle$  and  $|n_k \pm 1\rangle$ , which we shall denote by  $\mathcal{E}_k$ .

We will view quantum states from a perspective of quantum information theory. When a degree of freedom can choose among  $d$  different possible states  $|n_k\rangle$  with  $n_k = 0, 1, \dots, d-1$ , it represents a qudit. Then information can be stored in the set of  $d^{K+1}$  basic states  $|n_0, n_1, \dots\rangle$  and each basic state corresponds to a distinct pattern. In this setting, the energy cost of information storage and read-out is set by  $\mathcal{E}_k$ , i.e. for a pattern  $|n_0, n_1, \dots\rangle$ , it is given as  $E_{n_0, n_1, \dots} = \sum_k \mathcal{E}_k n_k$ . This means that the transition between patterns in which the occupation numbers differ significantly is in general expected to be costly.

This situation changes in systems that possess nearly-gapless modes. The latter term requires some quantification. Under a nearly-gapless mode we mean a mode for which the minimal excitation energy  $\mathcal{E}_k$  is much smaller than the typical energy gap  $E_{\text{typical}}$ , expected for the system of a given size. For instance, for a

nonrelativistic particle of mass  $m$  trapped in a box of size  $L$ , one would expect the energy gap between the ground state and the first excited state to be set by the inverse size of the box,  $E_{\text{typical}} \approx \hbar^2/(2mL^2)$ . The goal of this chapter is to show that systems with nearly-gapless modes have a greatly enhanced capability of information storage. Namely, based on the characteristics described in [204, 205], we can identify the following three key properties, on which we will elaborate in the following:

1. The density of patterns that can be stored within a given energy gap is exponentially enhanced.
2. The decoherence time of recorded information increases significantly.
3. The stored patterns can be rearranged under the influence of very soft external stimuli.

### Enhanced Entropy

Clearly, two states that only differ in the occupation numbers of nearly-gapless modes are almost degenerate in energy. Thus, if we imagine that a subset of  $N$  modes is nearly-gapless and that the maximal occupation number of each of those modes is  $d$ , then  $d^N$  patterns fit within a small energy gap. This constitutes the first property of enhanced information storage, namely the fact that a large number of patterns almost possess the same energy. Correspondingly, we can define an entropy as the logarithm of the number of such nearly-degenerate states:

$$\text{Entropy} = N \ln(d). \quad (3.2)$$

We note that this formula matches our discussion of the entropy of black holes and de Sitter in section 1.4. As stated in Eq. (1.28), on the order of  $N$  nearly-gapless modes are required in order to give a microscopic explanation of an entropy  $N$ .

### Long Decoherence Time

Apart from a low energy cost, systems that feature gapless modes possess a second property that makes them ideal information storers. Namely, gaplessness of a given mode  $\hat{b}_k$  implies that the disturbance from other modes is small since otherwise the gaplessness would be destroyed. This suppression of interaction is either due to a relatively high energy gap of the other modes or due to a very weak coupling to them (or both). In both cases, the time evolution into the other modes is small. Therefore, gaplessness implies a long information storage time.<sup>1</sup>

This point can be illustrated in very general terms on an example with one additional mode  $\hat{c}$  that can correspond to another mode of the system or to an

---

<sup>1</sup>For a particular model, this property was already discussed in [51].

environment. We assume that in the absence of the mode  $\hat{c}$ , the nearly-gapless mode  $\hat{b}_k$  would be close to an eigenmode of the Hamiltonian, i.e. it corresponds to a degree of freedom obtained after an approximate diagonalization procedure. How this can be achieved will become apparent in section 3.1.4. In this situation, the relevant part of the Hamiltonian can be written in the following  $2 \times 2$  form:

$$\hat{H} = \begin{pmatrix} \hat{b}_k^\dagger & \hat{c}^\dagger \end{pmatrix} \begin{pmatrix} \mathcal{E}_k & \frac{g}{2} \\ \frac{g}{2} & E_c \end{pmatrix} \begin{pmatrix} \hat{b}_k \\ \hat{c} \end{pmatrix}, \quad (3.3)$$

where  $E_c$  is the gap of the other mode and  $g$  is the coupling constant. In order not to disturb the nearly-vanishing gap  $\mathcal{E}_k$ ,  $g$  must satisfy  $g \ll \sqrt{\mathcal{E}_k E_c}$ , i.e.  $g$  must be sufficiently small in order to maintain the level-splitting. This implies that either the time evolution will be strongly suppressed due to the large level-splitting (in the regime of  $E_c \gg \mathcal{E}_k$ ) or the evolution timescale will be set by

$$t_{\text{coh}} \approx \hbar/\mathcal{E}_k \quad (3.4)$$

and thus will be long (in the regime of  $E_c \approx \mathcal{E}_k$ ). In both cases, we have an effective protection of the stored information. In other words, the information contained in a gapless mode  $\hat{b}_k$  is maintained either due to the suppression of the amplitude of oscillations or due to a very long timescale of this transition.

### Soft External Stimuli

Finally, the third property that makes systems with nearly-gapless modes ideal storers of information is the fact that information contained in those modes can be recorded and read out using soft external stimuli. This point, which was already discussed in [204], is of particular interest with regard to the experimental realization of such systems. As before, we will focus on a single nearly-gapless mode  $\hat{b}_k$ . Following [53], the essential features of the coupling to an external field can be captured by the Hamiltonian (3.3), where now  $\hat{c}$  could correspond to a mode of the photon field in an experimental setup.

We can start with no excitations in the nearly-gapless mode and a coherent state of the external field:

$$|\Phi(t=0)\rangle = |0\rangle_{b_k} \otimes |\gamma\rangle_c, \quad (3.5)$$

where  $\gamma$  parametrizes the occupation of the external coherent state. Straightforward calculation gives [53]:

$$\langle \Phi(t) | \hat{c}^\dagger \hat{c} | \Phi(t) \rangle = \gamma^2 \left( 1 - \frac{g^2}{\delta_g^2} \sin^2 \left( \frac{\delta_g t}{2} \right) \right), \quad (3.6)$$

where we defined

$$\delta_g = \sqrt{(E_c - \mathcal{E}_k)^2 + g^2}. \quad (3.7)$$

Thus, the coupling to the nearly-gapless mode leads to a fluctuating occupation of the external field. The amplitude becomes appreciable for  $E_c \approx \mathcal{E}_k$ , i.e. when the external mode is as soft as the nearly-gapless mode. As already discussed, this implies that the coupling has to be small,  $g \lesssim \mathcal{E}_k$ , in order not to disturb the gaplessness of the mode  $\hat{b}_k$ .

In this situation, the occupation number of the nearly-gapless mode evolves in time as,

$$\langle \Phi(t) | \hat{b}_k^\dagger \hat{b}_k | \Phi(t) \rangle = \gamma^2 \frac{g^2}{\delta_g^2} \sin^2 \left( \frac{\delta_g t}{2} \right). \quad (3.8)$$

This means that we can use soft excitations of an external field to bring the nearly-gapless mode to a desired state. Correspondingly, information can be read out from soft  $\hat{c}$ -quanta that are emitted due to the deexcitement of the  $\hat{b}_k$ -mode. In this way, soft radiation could be used to store and retrieve quantum information.

Furthermore, we remark that Eqs. (3.6) and (3.8) also show why soft external radiation is sensitive to the existence of nearly-gapless modes. If none are present, the lightest mode has a much bigger gap, i.e.  $\mathcal{E}_k \gg E_c$ . In that case, the amplitude of fluctuations gets suppressed as  $(g/\mathcal{E}_k)^2$ . This means that soft radiation stops interacting with the system. Thus, nearly-gapless modes exist whenever soft radiation, the energy  $E_\gamma$  of which is much smaller than the typical energy of the system, i.e.  $E_\gamma \ll E_{\text{typical}}$ , experiences a significant interaction.

The energy efficiency of the information storage within the gapless mode goes hand in hand with the difficulty of the read-out of information. Since the gap is small, the different information patterns are barely discriminable and the read-out time is correspondingly very long. Thus, if we would like to design a device that could read out the information on a timescale shorter than the inverse gap, such a reader must necessarily disturb the gap. In such a case, the reading device can be included in an effective Hamiltonian in form of a time-dependent interaction term that is switched on externally when needed. With regard to black holes, however, this challenge in reading out the recorded information turns out to be good news as such a delay would naturally explain why the quantum information stored in them cannot be resolved for a very long time. We will elaborate on this point in section 3.1.3.

### 3.1.2 Assisted Gaplessness

In view of the importance of nearly-gapless modes for information storage, we need to understand what physical mechanisms can allow a finite size system to deliver such modes. We shall focus on a mechanism schematized in [204, 205], which can be referred to as the phenomenon of *assisted gaplessness*. It represents a generalization of the original idea [36] of information storage in gapless modes that emerge in certain quantum critical states of attractive bosons. The key principle of the assisted gaplessness mechanism is easy to summarize. If the interaction energy

among the degrees of freedom of a system is negative, a high excitation of some of those modes lowers the excitation energy thresholds for the others. In this way, these highly excited degrees of freedom play the role of *master* modes that *assist* others in becoming easily-excitable. When the occupation numbers of the master modes reach certain critical levels, the assisted modes become nearly-gapless. At this point, a state of enhanced memory storage capacity is attained.

In order to understand the essence of the phenomenon, following [204, 205], we consider an exemplary situation in which a mode  $\hat{n}_0$ , which is typically the one with the smallest kinetic energy  $E_0$ , can be highly occupied and has the following negative-energy coupling with a set of  $K$  modes:

$$\hat{H} = \sum_{k=1}^K \epsilon_k (1 - \alpha \hat{n}_0) \hat{n}_k + \epsilon_0 \hat{n}_0 + \dots \quad (3.9)$$

In this way,  $\hat{n}_0$  becomes the *master* mode. Its interaction energy with each mode  $\hat{n}_k$  is proportional to the threshold energy  $\epsilon_k$  of the latter modes via an universal proportionality constant  $\alpha$ . Due to the negative sign, such a connection is *excitatory*, i.e. it is energetically favorable to simultaneously excite the inter-coupled modes.

Thus, on states in which the occupation number of the master mode is  $\langle \hat{n}_0 \rangle = N_0$ , the effective gap for other modes is lowered as,

$$\mathcal{E}_k = \epsilon_k (1 - \lambda), \quad (3.10)$$

where we introduced the collective coupling

$$\lambda := \alpha N_0. \quad (3.11)$$

We note that this formula is in full accordance with Eq. (2.1), which was important for our study of quantum breaking. Thus, we see that the master mode  $\hat{n}_0$  assists the rest of the modes in becoming more easily excitable. Accordingly, once the occupation number of the master mode reaches a critical value  $N_0 = \alpha^{-1}$  corresponding to  $\lambda = 1$ , the assisted modes  $\hat{n}_k$  become gapless. The corresponding excitation energy as a function of  $\lambda$  is plotted in Fig. 3.1a. Note that small deviations  $\delta N_0 \sim 1$  of the occupation number  $N_0$  from the critical value result in the generation of an effective gap of order  $\mathcal{E}_k \sim \epsilon_k \alpha$ . Correspondingly, the smaller  $\alpha$  is, the less sensitive the gap becomes to small fluctuations of the occupation number  $N_0$  around its critical value. Therefore, we will focus on cases with small  $\alpha$  and large  $N_0$ .

In the model (3.9), all states of the form  $|N_0, n_1, \dots, n_K\rangle$ , where  $n_{k \neq 0}$  can take different possible values from 0 to  $d - 1$ , possess the same energy. In accordance with our previous discussion in section 3.1.1, we see that gapless modes lead to an exponential number of information patterns that are degenerate in energy. The resulting density of states as function of the collective coupling  $\lambda$  is plotted in Fig.

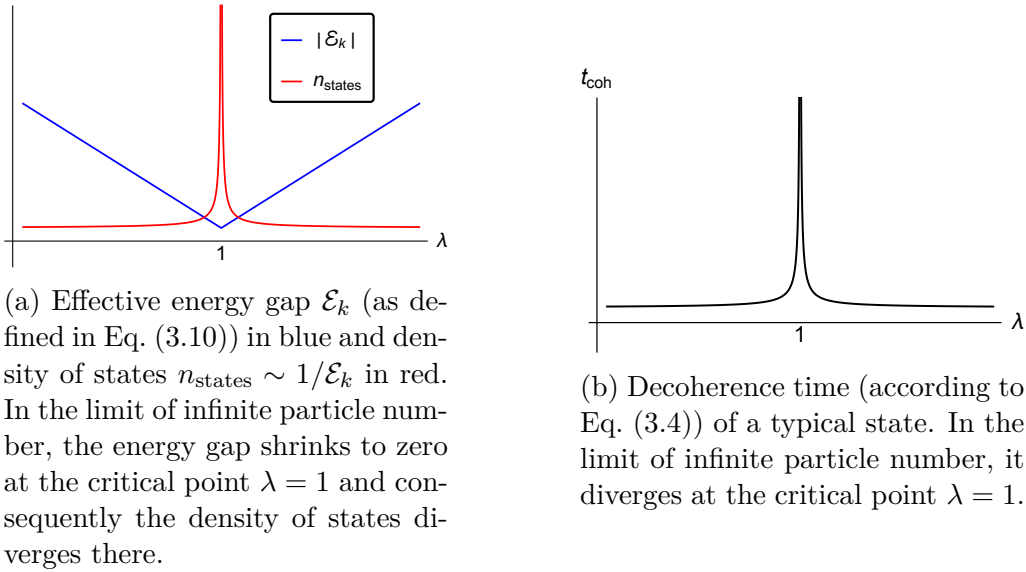


Figure 3.1: Schematic plots of the behavior of a system of attractive bosons such as (3.9) in the vicinity of a critical point with nearly-gapless modes that arise due to assisted gaplessness.

3.1a. Since the neighborhood in the Fock space with a large number of states that fit within a narrow energy gap is characterized by the same macroscopic parameter, i.e. a macroscopically large occupation number  $N_0$  of the  $\hat{n}_0$ -mode, we can say for sufficiently small  $d$  that the states  $|N_0, n_1, \dots, n_K\rangle$  for all possible values of  $n_{k \neq 0}$  are macroscopically-indistinguishable. Hence, they form a set of microstates belonging to the same macrostate. In this sense, Eq. (3.2) acquires the meaning of a microstate entropy, i.e. it is the logarithm of the number of such nearly-degenerate microstates, where  $K = N$  in this case.

An important point of our analysis is that we do not introduce a gapless mode by hand but discover that such modes emerge even if the system is confined within a box of finite size. This is a highly nontrivial phenomenon that requires a critical balance between the coupling and the occupation number. In this way, the decoherence time of quantum information stored in a gapless mode can be made arbitrarily long, even for fixed values of the size of the box and  $\hbar$  (see Fig. 3.1b).

Already the study of the prototype system suggests that the phenomenon of assisted gaplessness is generic. It will become evident in section 3.1.4 that this is indeed the case: The only requirements for assisted gaplessness to take place in a bosonic system are a weak attractive interaction and a high occupation number of some of the modes. Therefore, as explained in [204], we expect that gapless modes, which lead to states of high memory storage capacity, are a generic phenomenon in these systems. Only the details, such as the exact number of the emergent gapless modes and the corresponding microstate entropy, depend on the symmetry

structure and other details of the Hamiltonian.

However, we must stress that among all the states of a system, the subset in which gapless modes occur is small. Whereas some states of enhanced memory capacity exist in bosonic systems with weak and attractive interactions, those states are very rare as compared to the total number of states in the Hilbert space. Therefore, it can be a hard task to identify those states.

Lastly, we can compare our effect of assisted gaplessness to the well-known phenomenon of appearance of gapless excitations in the form of Goldstone bosons. The latter modes emerge as a result of a phase transition with the spontaneous breaking of a global symmetry. The crucial difference is that Goldstone modes consistently exist in a domain past the critical phase. This is not the case for assisted gaplessness. Our gapless modes only exist at the critical point and they appear due to a cancellation between the positive kinetic energy and the negative collective interaction energy with a certain highly-occupied master mode. In general, it is therefore hard to interpret the appearance of our gapless modes in terms of a Goldstone phenomenon of spontaneous breaking of any global symmetry.<sup>2</sup> This difference is what in particular makes the phenomenon of assisted gaplessness interesting since there is no *a priori* symmetry reason for the emergence of any gapless modes. This said, however, once assisted gaplessness takes place, the number of such modes can be highly enhanced by *unbroken* symmetries of the critical state, such as spherical symmetry [208].

### 3.1.3 Simulating Black Holes and Others in the Laboratory

#### Assisted Gaplessness in Black Holes

As we have seen, the phenomenon of assisted gaplessness appears to be generic in bosonic systems with weak and attractive interactions. Since gravity exhibits precisely these properties, the important question arises if the same mechanism could also be operative in black holes and thereby represent the key to a microscopic explanation of the Bekenstein-Hawking entropy (1.2). In this picture, assisted gaplessness would deliver the required  $S$  nearly-gapless modes (see Eq. (1.28)). If this is true, one can shed light on black holes, for which the lack of nonperturbative techniques prevents computations beyond the semiclassical limit, by looking for analogous properties in systems that are much easier to solve.

We note that this point of view is *a priori* independent of the quantum N-portrait of black holes, which we reviewed in section 1.3.1. Namely, as explained in section 1.4, any quantum description of a black hole must provide a microscopic explanation of the entropy and therefore contain on the order of  $S$  nearly-gapless modes. However, the idea that assisted gapless takes place in a black hole becomes

---

<sup>2</sup>We note, however, that for the model (2.42), to which we will turn in appendix A.2.1, the critical mode due to assisted gaplessness was mapped on a pseudo-Goldstone mode of a sigma model [51].

particularly plausible in the quantum N-portrait. The reason is that in this picture, the black hole is composed of a large number of soft gravitons. The corresponding highly-occupied mode represents a prime candidate for the master mode which is required for assisted gaplessness. We will make this point more explicit in section 3.3.3.

The question if a universal phenomenon, which also takes place in simpler nongravitational systems, could be operative in black holes was first investigated in [34, 36], where a system of attractive bosons in a box of dimensionality  $D \geq 1$  with periodic boundary conditions was studied.<sup>3</sup> It was noticed that the critical state of enhanced memory capacity in this simple system exhibits some similarities to certain universal scaling properties satisfied by analogous parameters for black holes. Therefore, it was hypothesized in [34, 36] that the emergence of gapless qudits responsible for nearly-degenerate microstates of a black hole in its bare essence is the same phenomenon as the appearance of gapless qudits around the quantum critical point in the system of attractive bosons.

This point of view is strengthened by the fact that it is difficult to read out information that is stored in nearly-gapless modes. As discussed in section 3.1.1, the read-out time is set by the inverse of the small gap (see also Eq. (3.4)). Therefore, as long as the gap is not disturbed by turning on additional couplings to an environment, it takes a very long time to resolve the information stored in the nearly-gapless modes. This could contribute to answering the long-standing question why the quantum information stored in black hole modes cannot be resolved for a very long time. The answer would be that information is unreadable because it is stored in nearly-gapless modes (see e.g. [53]).

Finally, the idea that assisted gaplessness takes place in black holes receives further support from the model of [208] (see [205] for its neural network realization), which describes a nonrelativistic bosonic quantum field living on a  $D$ -dimensional sphere and experiencing a momentum-dependent attractive self-interaction. This model comes closest to imitating the black hole information properties. Namely, it exhibits a one parameter family of critical states labeled by the occupation number  $N$  of the lowest momentum mode. In each state, a set of gapless modes emerges. The remarkable thing is that the number of these gapless modes scales as the area of a  $D - 1$ -dimensional sphere. This means that the resulting microstate entropy obeys an area law, similar to Bekenstein entropy of a black hole. Therefore, the emergent gapless modes represent holographic degrees of freedom and the model gives an explicit microscopic realization of the idea of holography, which is usually considered to be an exclusive property of gravitational systems, such as black holes [209, 210] or AdS-spaces [211, 212]. These findings give a strong motivation for further studying the proposed mechanism of emergence of gapless modes at criticality in systems of bosons with “gravity-like” attractive interactions.

---

<sup>3</sup>A simple example of this sort, which has been explicitly solved, is given by the system (2.42). It is the model that we use in appendix A.2.1 to demonstrate our  $c$ -number method.

### Mapping on Neural Networks

On top of its connection to black holes, we shall show that the phenomenon of assisted gaplessness has a direct application to quantum neural networks along the lines of [204, 205]. The key ingredients of any neural network are on the one hand the neurons and on the other hand the synaptic connections among them. Following [204, 205], it is possible to describe them by an effective Hamiltonian in which the neural excitations are the degrees of freedom. The threshold excitations correspond to kinetic energies and the synaptic connections translate as interaction terms. In this description, the time evolution of the excitations is generated by the effective Hamiltonian. In particular, this framework enables us to study the energetics of information storage. This is the aspect we shall focus on. So we will not study any specific algorithm, but our goal is to investigate the energy cost of recording and reading out information.

The synaptic connections can be either excitatory or inhibitory, i.e. an excitation of a given neuron  $k$  can either decrease or increase the probability of the excitation of another neuron  $j$ . In the effective Hamiltonian description of the network, the excitatory and inhibitory nature of the connections can be given an energetic meaning. This meaning is defined by the sign of the interaction energy of two or more simultaneously excited neurons. The negative and the positive signs of the interaction energy respectively translate as excitatory and inhibitory connections in an *energetic sense*. Below, we shall denote the parameter that sets the characteristic strength of these interactions by the same constant  $\alpha$  as we have used for the system of bosons.

As noticed in [204, 205], a neural network defined in this way in the case of negative (i.e. attractive and therefore “gravity-like”) synaptic connections exhibits the phenomenon of assisted gaplessness with sharply enhanced memory storage capacity. For describing the idea, it suffices to consider the simple Hamiltonian (3.9) and to think of it as representing a quantum neural network. Thus, we consider a network for which the synaptic connection energy of a set of interconnected neurons is negative. This means that the excitation of a given neuron lowers the threshold for the excitation of all the other neurons from this set, i.e. for the ones that are connected to the former neuron by negative energy couplings. If we normalize the characteristic step of the excitation to unity, then exciting a neuron to a level  $N$ , in general, lowers the threshold for the others by the amount  $\sim \alpha N$ . Thus, at the critical point  $\alpha N = 1$ , gapless modes emerge and we can store a large number of patterns within a very narrow energy gap.

More concretely, it was shown in [205] that such a neural network is isomorphic to the physical system of a bosonic quantum field. In this correspondence, the neural degrees of freedom are identified with the momentum modes of the field, whereas the synaptic connections correspond to the couplings among the different momentum modes. This mapping allows to give a unified description of the phenomena of enhanced memory storage capacity in neural networks and in systems

with cold bosons. Thus, the connection to neural networks also contributes to the relevance of investigating assisted gaplessness.

### Experimental Realization

The facts that the phenomenon of assisted gaplessness is generic in bosonic systems with weak attractive interactions and that it already takes place in simple systems such as (3.9) give a natural hope that it could be experimentally studied under laboratory conditions. For example, such an observation of emerging gapless modes could be achieved in systems with cold atoms (see e.g. [213, 214]). Such experiments, which have never been performed previously, could serve two purposes.

First, as already suggested in [36, 51–53], they promise to be relevant for the practical storage of quantum information. Namely, assisted gaplessness could enable the construction of devices that can store quantum information at a low energy cost and over an extended period of time. Such an application would have manifold importance, e.g. in the context of quantum computing.

The second purpose of the experimental observation of assisted gaplessness is that it could provide a framework to understand and simulate other systems of enhanced memory storage capacity. This gives an interesting prospect of studying in table-top quantum experiments the key mechanism of information storage in such seemingly-remote systems as black holes and quantum brain neural networks. Such simulations could both verify the proposed phenomenon of assisted gaplessness and check how far the similarity with black hole information processing goes.

For the case of black holes, a very concrete effect that one could check would be how the timescale of information storage near criticality scales with  $N_0$ , which plays the role of a macroscopic parameter analogous to the black hole mass. Another interesting question concerns the scrambling and release of information: When an excitation is added to a system of enhanced memory capacity, how fast does it get entangled with the rest of the system and how long does it take to read it out afterwards? Obviously, the main focus is on understanding generic features of enhanced information storage and by no means on imitating intrinsically geometrical properties of black holes.

#### 3.1.4 The $C$ -Number Method

So far, we have highlighted the relevance of nearly-gapless modes that arise due to the phenomenon of assisted gaplessness. In this light, a very important task is to find a method that enables the search for states with gapless modes in a systematic way in a theory of bosonic modes with a generic interaction Hamiltonian. We will do so in the following. Our method relies on the Bogoliubov approximation, in which mode operators are replaced by their expectation values [79]. In this way,

we transform the Hamiltonian in its Bogoliubov counterpart, which only depends on  $c$ -numbers. We will show that it suffices to look for flat directions in this Bogoliubov Hamiltonian to conclude that gapless modes exist in the spectrum of the full quantum system. This allows us to replace the difficult problem of diagonalization of the Hamiltonian by a much simpler task of extremizing a  $c$ -number function.

This approach, which we shall call *c-number method*, is a generalization of the one used in [51], where it was shown for a specific model that the appearance of a gapless mode at the critical point can be deduced from the minimization of a nonlinear sigma-model obtained by replacing the Hamiltonian by a  $c$ -number function. Apart from its practical application, the  $c$ -number method also serves a second purpose. The fact that any flat direction in the Bogoliubov Hamiltonian already implies a gapless mode supports the reasoning of [204] that the emergence of gapless modes, which leads to states of high memory storage capacity, is rather generic, provided the interacting degrees of freedom of a system are bosonic and that some of the interaction energies are negative.

### Procedure

We consider a set of  $K + 1$  bosonic quantum modes described by the creation and annihilation operators  $\hat{a}_k^\dagger, \hat{a}_k$  (where  $k = 0, 1, \dots, K$ ), which satisfy the standard canonical commutation relations

$$[\hat{a}_j, \hat{a}_k^\dagger] = \delta_{jk}, \quad [\hat{a}_j, \hat{a}_k] = [\hat{a}_j^\dagger, \hat{a}_k^\dagger] = 0. \quad (3.12)$$

We call the modes  $\hat{a}_k$  instead of  $\hat{b}_k$  since unlike before, the Hamiltonian is not required to be approximately diagonal in the  $\hat{a}_k$ -modes. For later convenience, we introduce the notation

$$\hat{\vec{a}} = (\hat{a}_1, \dots, \hat{a}_K), \quad \hat{\vec{a}}^\dagger = (\hat{a}_1^\dagger, \dots, \hat{a}_K^\dagger), \quad (3.13)$$

where no distinction will be made between a vector and its transpose. The reason for singling out one of the modes, in our notation  $\hat{a}_0$ , will become apparent shortly. We assume that the dynamics of the system is governed by a generic Hamiltonian,

$$\hat{H} = \hat{H}(\hat{\vec{a}}^\dagger, \hat{\vec{a}}, \hat{a}_0^\dagger, \hat{a}_0). \quad (3.14)$$

A priori, we do not have to put any restriction on it, i.e. we expect our method to work when (3.14) depends on all possible normal-ordered interactions of the modes. But the concrete application of the  $c$ -number method will be sensitive to the symmetries of the Hamiltonian. The reason is that any symmetry also leads to a gapless transformation.<sup>4</sup> However, we do not want to consider those but solely focus on the ones that arise due to a collective attractive interaction.

<sup>4</sup>The simplest example is the Hamiltonian of a noninteracting mode,

$$\hat{H} = \hat{a}^\dagger \hat{a}, \quad (3.15)$$

For the sake of simplicity, we will not consider the case of generic symmetries, but focus on a special case of particular physical importance. We assume that the Hamiltonian only possesses one symmetry, namely a global  $U(1)$ -symmetry due to particle number conservation. So the generic Hamiltonian reads

$$\begin{aligned} \hat{H} &= \sum_{k=0}^K \epsilon_k \hat{a}_k^\dagger \hat{a}_k + \sum_{k,j,m,n=0}^K \alpha_{kjmn}^{(4)} \hat{a}_k^\dagger \hat{a}_j^\dagger \hat{a}_m \hat{a}_n \\ &+ \sum_{k,j,m,n,o,p=0}^K \alpha_{kjmnop}^{(6)} \hat{a}_k^\dagger \hat{a}_j^\dagger \hat{a}_m^\dagger \hat{a}_n \hat{a}_o \hat{a}_p \\ &+ \sum_{k,j,m,n,o,p,q,r=0}^K \alpha_{kjmnopqr}^{(8)} \hat{a}_k^\dagger \hat{a}_j^\dagger \hat{a}_m^\dagger \hat{a}_n^\dagger \hat{a}_o \hat{a}_p \hat{a}_q \hat{a}_r + \dots, \end{aligned} \quad (3.16)$$

where  $\epsilon_k$ ,  $\alpha_{kjmn}^{(4)}$ ,  $\alpha_{kjmnop}^{(6)}$ ,  $\alpha_{kjmnopqr}^{(8)}$ , ... are some parameters. We shall assume that the full Hamiltonian is bounded from below, but some interaction terms can be negative so that the energy landscape is nontrivial. We are interested in the phenomenon of assisted gaplessness, i.e. we would like to identify states around which a high occupation of some modes assists other in becoming gapless. As explained, the nearly-gapless modes will lead to a neighborhood in the Fock space where a large number of states fits within a narrow energy gap. This causes the enhanced memory capacity in which we are interested.

Finding such critical states requires a diagonalization of the Hamiltonian, which in general is computationally a very hard task. Our goal is to show that under certain conditions, the diagonalization procedure can be substituted by a much simpler approach of finding an extremum of a  $c$ -number function. To this end, we perform the Bogoliubov approximation [79], i.e. we replace the creation and annihilation operators by  $c$ -numbers,

$$\hat{a} \rightarrow \vec{a}, \quad \hat{a}^\dagger \rightarrow \vec{a}^*, \quad (3.17a)$$

$$\hat{a}_0 \rightarrow \sqrt{N - \sum_{k=1}^K |a_k|^2}, \quad \hat{a}_0^\dagger \rightarrow \sqrt{N - \sum_{k=1}^K |a_k|^2}, \quad (3.17b)$$

where  $a_k$  are complex numbers and we introduced the abbreviation

$$\vec{a} = (a_1, \dots, a_K), \quad \vec{a}^* = (a_1^*, \dots, a_K^*). \quad (3.18)$$

Note that we have replaced  $K + 1$  quantum modes by only  $K$  complex variables. The reason is particle number conservation, as will become apparent in the proof of our method. Because of it, the sum of the moduli are fixed and moreover we

---

which possesses a global  $U(1)$ -symmetry,  $\hat{a} \rightarrow e^{i\varphi} \hat{a}$ , due to particle number conservation. So the states  $|\Psi(\hat{a})\rangle$  and  $|\Psi(e^{i\varphi} \hat{a})\rangle$  have the same expectation values of the energy, but this is not connected to attractive interaction.

have to fix a global phase. Furthermore, note that particle number conservation as in (3.17b) shows that the complex numbers scale as  $a_i \sim \sqrt{N}$ . In summary, we obtain the replacement

$$\hat{H}(\hat{a}^\dagger, \hat{a}, \hat{a}_0^\dagger, \hat{a}_0) \rightarrow H_{\text{bog}}(\vec{a}, \vec{a}^*), \quad (3.19)$$

where  $H_{\text{bog}}(\vec{a}, \vec{a}^*)$  is an algebraic  $c$ -number function, which depends on  $K$  complex variables.

We expect that the error in the Bogoliubov approximation scales as  $1/N$ . Thus, we can make it arbitrarily small if the particle number is large enough. Since we want to keep the collective coupling fixed, the relevant limit is

$$N \rightarrow \infty, \quad \alpha^{(i)} \rightarrow 0, \quad \text{with } \lambda^{(i)} \equiv \alpha^{(i)} N^{i/2-1} = \text{const.}, \quad (3.20)$$

where we suppressed the indices of the coupling constants. We note that we obtain the collective coupling  $\lambda = \alpha N$  for the special case of 4-point interaction, in accordance with Eq. (3.11). Moreover, it is important to emphasize the the double-scaling limit (3.20) is identical to the (semi)classical limit as discussed in Eq. (2.32). In this limit, the  $c$ -number method for finding gapless modes will be exact. For finite  $N$ , corrections appear that scale as a power of  $1/N$ . Thus, as already mentioned before, we will throughout be interested in the regime of large  $N$  and correspondingly small  $\alpha$ .

Before we can come to the main statement of this section, we introduce the notion of a *critical point* of the Bogoliubov Hamiltonian  $H_{\text{bog}}$ . It is defined as a value  $\vec{a}_o$  such that the first derivative vanishes,

$$\left. \frac{\partial H_{\text{bog}}}{\partial \vec{a}} \right|_{\vec{a}=\vec{a}_o} = 0, \quad (3.21)$$

and moreover the determinant of the second derivative matrix is zero,

$$\det \mathcal{M} \Big|_{\vec{a}=\vec{a}_o} = 0, \quad \text{where } \mathcal{M} \equiv \begin{pmatrix} \mathcal{B}^* & \mathcal{A} \\ \mathcal{A}^T & \mathcal{B} \end{pmatrix}. \quad (3.22)$$

Here the matrices  $\mathcal{A}$  and  $\mathcal{B}$  denote  $\mathcal{A}_{kj} \equiv \frac{\partial^2 H_{\text{bog}}}{\partial a_k^* \partial a_j}$  and  $\mathcal{B}_{kj} \equiv \frac{\partial^2 H_{\text{bog}}}{\partial a_k \partial a_j}$ , which implies  $B^T = B$  and  $A^\dagger = A$ . So we deal with a *stationary inflection* point of the function  $H_{\text{bog}}(\vec{a}, \vec{a}^*)$ , i.e. a point at which the curvature vanishes in some directions. Our goal is to prove the following implication.

**Theorem:** If the  $c$ -number function  $H_{\text{bog}}$  possesses a critical point (in the above sense), this implies – in the full quantum theory – the existence of a state with emergent gapless modes, and correspondingly, with an enhanced microstate entropy.<sup>5</sup> To put it shortly, any critical point is a point of an enhanced memory storage capacity.

<sup>5</sup>Note that example (3.9) is a special case in which all  $K$  modes become gapless. In general, conditions (3.21) and (3.22) only imply at least one gapless mode.

**Proof**

In order to prove this, we will follow the known procedure for determining the spectrum of quantum fluctuations around a given state. Namely we consider the expectation value of the Hamiltonian in an arbitrary state, for which only the expectation value of the particle number is fixed:

$$N = \sum_{k=0}^K \langle \hat{a}_k^\dagger \hat{a}_k \rangle. \quad (3.23)$$

In the following, expectation values will always refer to such a state. As explained, we moreover want to fix a global phase to exclude the gapless direction that arises due to the corresponding symmetry. Up to  $1/N$ -corrections, we therefore obtain

$$\langle \hat{a}_0 \rangle \approx \langle \hat{a}_0^\dagger \rangle \approx \sqrt{N - \sum_{k=1}^K \langle \hat{a}_k^\dagger \hat{a}_k \rangle}. \quad (3.24)$$

In this way, we can make particle number conservation manifest and obtain a Hamiltonian that only depends on  $K$  modes.

Next, we shift the remaining  $K$  mode operators by the constants corresponding to the above-discussed stationary inflection point of the  $c$ -number function  $H_{\text{bog}}$ ,

$$\hat{a} \rightarrow \vec{a}_o + \hat{\alpha}, \quad \hat{a}^\dagger \rightarrow \vec{a}_o^* + \hat{\alpha}^\dagger. \quad (3.25)$$

Obviously, the operators  $\hat{\alpha}_k^\dagger, \hat{\alpha}_k$  satisfy commutation relations analogous to (3.12). So the replacement (3.25) is always possible and exact, not only as an equation for the expectation values. But of course, the Hamiltonian is not diagonal in the new modes  $\hat{\alpha}_k^\dagger, \hat{\alpha}_k$ .

Now we want to expand the theory around a state in which the expectation values of the original  $\hat{a}_k$ -modes are given as  $\langle \hat{a}_k^\dagger \hat{a}_k \rangle = |a_{o,k}|^2$ . Thus, we write down the effective Hamiltonian in which we keep terms up to second order in the  $\hat{\alpha}_k$ -modes. Since  $\vec{a}_o$  extremizes the  $c$ -number function  $H_{\text{bog}}$ , terms linear in  $\hat{\alpha}_k$ -modes are absent from the Hamiltonian. Moreover, the  $c$ -numbers scale as  $a_k \sim \sqrt{N}$  whereas the  $\hat{\alpha}_k$  are independent of  $N$ . Thus, each additional factor of  $\hat{\alpha}_k$  leads to a suppression by  $1/\sqrt{N}$ . So in the limit (3.20) of large  $N$ , the second-order term dominates and the effective Hamiltonian takes the following form:

$$\langle \hat{\mathcal{H}} \rangle = H_0 + \langle \hat{\alpha}^\dagger \mathcal{A} \hat{\alpha} \rangle + \frac{1}{2} \left( \langle \hat{\alpha} \mathcal{B} \hat{\alpha} \rangle + \langle \hat{\alpha}^\dagger \mathcal{B}^* \hat{\alpha}^\dagger \rangle \right), \quad (3.26)$$

where the constant  $H_0 \equiv H_{\text{bog}}(\vec{a}_o, \vec{a}_o^*)$  denotes the value of the  $c$ -number function at the extremal point. Up to this irrelevant constant, we can rewrite the Hamiltonian in block-matrix form:

$$\langle \hat{\mathcal{H}} \rangle = \frac{1}{2} \left\langle \begin{pmatrix} \hat{\alpha}^\dagger & \hat{\alpha} \end{pmatrix} \begin{pmatrix} \mathcal{B}^* & \mathcal{A} \\ \mathcal{A}^T & \mathcal{B} \end{pmatrix} \begin{pmatrix} \hat{\alpha}^\dagger \\ \hat{\alpha} \end{pmatrix} \right\rangle + \text{const.} \quad (3.27)$$

Now we can bring the Hamiltonian into a canonical diagonal form by performing the following Bogoliubov transformation:

$$\begin{pmatrix} \hat{\alpha}^\dagger \\ \hat{\alpha} \end{pmatrix} = \mathcal{T} \begin{pmatrix} \hat{b}^\dagger \\ \hat{b} \end{pmatrix}, \quad \text{with } \mathcal{T} = \begin{pmatrix} V^* & U \\ U^* & V \end{pmatrix}, \quad (3.28)$$

or equivalently,

$$\hat{\alpha}_k = U_{kj}^* \hat{b}_j^\dagger + V_{kj} \hat{b}_j, \quad (3.29)$$

where  $U$  and  $V$  are the transformation matrices and  $\hat{b}_j^\dagger, \hat{b}_j$  are the new modes that form a diagonal canonical basis. The canonical commutation relations imply the conditions:

$$VV^\dagger - U^*U^T = \mathbb{1}, \quad VU^\dagger - U^*V^T = 0. \quad (3.30)$$

As always, we choose the matrices  $U$  and  $V$  such that off-diagonal terms, of the type  $\hat{b}_j \hat{b}_k$  and  $\hat{b}_j^\dagger \hat{b}_k^\dagger$ , are absent from the Hamiltonian. This implies that  $U, V$  satisfy

$$U^\dagger \mathcal{A}^T V^* + V^\dagger \mathcal{A} U^* + V^\dagger \mathcal{B}^* V^* + U^\dagger \mathcal{B} U^* = 0. \quad (3.31)$$

In this way, we bring the Hamiltonian to the form

$$\langle \hat{\mathcal{H}} \rangle = \langle \hat{b}_k^\dagger \mathcal{E}_{kj} \hat{b}_j \rangle + \text{const.}, \quad (3.32)$$

where the matrix  $\mathcal{E}$  is given by

$$\mathcal{E} \equiv U^\dagger \mathcal{A}^T U + V^\dagger \mathcal{A} V + V^\dagger \mathcal{B}^* U + U^\dagger \mathcal{B} V. \quad (3.33)$$

Note that the conditions (3.30) and (3.31) allow the multiplication of  $U$  and  $V$  by an arbitrary unitary matrix. Therefore, without loss of generality, we can set the Hermitian matrix  $\mathcal{E}$  to be diagonal.

Now, due to the fact that the modulus of the determinant of the matrix  $\mathcal{T}$  is 1, the condition  $\det \mathcal{M} = 0$  is equivalent to the condition  $\det \mathcal{E} = 0$ .<sup>6</sup> Thus, among the degrees of freedom described by the operators  $\hat{b}_k^\dagger, \hat{b}_k$ , there exist gapless modes. Moreover, the number of zero eigenvalues of the two matrices is the same since multiplication by regular matrices does not change the dimension of the kernel of a matrix. So the number of gapless modes is given by the number of zero eigenvalues of the matrix  $\mathcal{M}$ , i.e. by the number of independent flat directions at the critical point of the  $c$ -number function  $H_{\text{bog}}$ .

This conclusion is exact in the limit (3.20) of infinite  $N$ . In this case, the gap collapses to zero and the different quantum states that correspond to the

<sup>6</sup>Following [215], we can infer the determinant of the matrix  $\mathcal{T}$  from the relation

$$\mathcal{T} \mathcal{J} \mathcal{T}^\dagger = \mathcal{J}, \quad (3.34)$$

where  $\mathcal{J} = \text{diag}(\mathbb{1}, -\mathbb{1})$  and  $\mathbb{1}$  is a unit matrix of dimension  $K$ . The equality (3.34) in turn is a consequence of the Bogoliubov conditions (3.30).

different occupation numbers of the gapless modes become exactly degenerate. So the system can store an unlimited amount of information within an arbitrarily small energy gap. Note that the fact that we only make a statement about the expectation value of the Bogoliubov Hamiltonian in (3.32) is not a restriction since it suffices for us to find states with degenerate expectation values of the energy.

For finite  $N$ , corrections appear which scale as a power of  $1/N$ . They come from higher-order terms in the effective Hamiltonian (3.26) and from corrections to relation (3.24). So in this case, the modes will only be nearly-gapless, with a gap that scales as a power of  $1/N$ . Also the critical value  $\vec{a}_o$  will receive  $1/N$ -corrections. However, one can make all these corrections arbitrarily small if one chooses  $N$  large enough. So also for finite  $N$ , the information stored in the various states of the  $\hat{b}$ -modes is energy cost-efficient. In summary, we conclude that the critical point of the  $c$ -number function  $H_{\text{bog}}$  corresponds to the appearance of nearly-gapless modes in the full quantum theory. Each nearly-gapless mode corresponds to a zero eigenvalue of the second derivative matrix  $\mathcal{M}$ .

We remark that our  $c$ -number method is conceptually similar to the study of the Gross-Pitaevskii equation [77, 78], which we employed in section 2.2.4. The latter corresponds to working in position space and expanding the field operator  $\hat{\psi}$  around its classical value:  $\hat{\psi} = \psi_{\text{cl}} + \delta\hat{\psi}$ . In this approach, one can identify gapless modes by studying the spectrum of quantum fluctuations  $\delta\hat{\psi}$ . Our  $c$ -number method can be viewed as momentum space analogue of this technique. Namely, we first go to momentum space by expanding  $\hat{\psi}$  in mode operators  $\hat{a}$ . Then we proceed analogously to the Gross-Pitaevskii method by expanding mode operators around their classical values:  $\vec{\hat{a}} = \vec{a}_o + \vec{\hat{\alpha}}$ .

### Coherent State Basis

Finally, we note that an alternative proof of the enhanced memory capacity around the stationary inflection point of  $H_{\text{bog}}$  consists of moving to the basis of coherent states, as opposed to number eigenstates. We recall that coherent states  $|\vec{a}\rangle$  are the eigenstates of the destruction operators, i.e. for all modes we have  $\hat{a}_k |\vec{a}\rangle = a_k |\vec{a}\rangle$ , where  $a_k$  are complex eigenvalues. Obviously, coherent states satisfy  $|a_k|^2 = \langle \vec{a} | \hat{n}_k | \vec{a} \rangle$ . It is clear that taking an expectation value of the Hamiltonian (3.16) over a coherent state  $|\vec{a}\rangle$  simply amounts to the Bogoliubov approximation (3.17), i.e. to replacing the operators by  $c$ -numbers,  $\hat{a}_k \rightarrow a_k$ . Therefore, we have the relation

$$\langle \vec{a} | \hat{H} | \vec{a} \rangle = H_{\text{bog}}. \quad (3.35)$$

This means that coherent states explicitly realize the replacement (3.19). Since this procedure is exact also for finite  $N$ , it gives immediate meaning to the Bogoliubov Hamiltonian from the perspective of the full quantum system.

In particular, this construction is relevant when the Bogoliubov Hamiltonian possesses a stationary inflection point  $\vec{a}_o$ . If in this case the eigenvector with

vanishing eigenvalue is given by  $\vec{\delta a}$ , then we can consider the state  $|\vec{a}_\circ + \epsilon\vec{\delta a}\rangle$ . For small values of  $\epsilon$ , it fulfills

$$\langle \vec{a}_\circ + \epsilon\vec{\delta a} | \hat{H} | \vec{a}_\circ + \epsilon\vec{\delta a} \rangle = \langle \vec{a}_\circ | \hat{H} | \vec{a}_\circ \rangle . \quad (3.36)$$

Thus, we have obtained a family  $|\vec{a}_\circ + \epsilon\vec{\delta a}\rangle$  of quantum states with nearly degenerate expectation value of the energy. Information stored in them therefore occupies a narrow gap.

For quantifying the information storage capacity, we must take into account that coherent states do not form an orthonormal basis and that only coherent states with large enough differences in  $a_k$  are nearly orthogonal. Indeed, the scalar product of two coherent states  $|\vec{a}\rangle$  and  $|\vec{a}'\rangle$  is

$$|\langle \vec{a} | \vec{a}' \rangle|^2 = e^{-\sum_k |a_k - a'_k|^2} . \quad (3.37)$$

Because of this, although the coherent state parameter can take continuous values, only sufficiently distant states, which satisfy

$$\sum_k |a_k - a'_k|^2 \gg 1 , \quad (3.38)$$

contribute into the memory-capacity count. Therefore, the information storage capacity in the coherent state basis is the same as in the basis of number eigenstates of the Bogoliubov modes.<sup>7</sup> However, the usefulness of the coherent state basis lies in the ability of taking a smooth classical limit. This is convenient for the generalization of the enhanced memory storage phenomenon to classical systems, such as e.g. classical neural networks [204].

For an exemplary step-by-step application of the  $c$ -number method, we refer the reader to appendix A.2.1. There we use it to study the system (2.42), which we have already reviewed in section 2.2.4 from the perspective of quantum breaking. For this system, a complete analytic treatment is possible. This means that on the one hand, all equations resulting from the  $c$ -number method can be solved easily and on the other hand, the Bogoliubov transformation can be carried out explicitly. It is therefore a good starting point to both familiarize oneself with the method and to check its validity on a concrete example.

---

<sup>7</sup>Relation (3.38) implies that coherent states can be counted as different as soon as  $|n_k - n'_k| \gg \sqrt{n_k}$ , where  $n_k = |a_k|^2$  and  $n'_k = |a'_k|^2$ . So there are on the order of  $\sqrt{n_k}$  different possible expectation values of the particle number. In addition, however, there is the freedom of choosing a phase  $\varphi_k$ . Taking into account the uncertainty,  $\Delta n_k \Delta \varphi_k \gtrsim 1$ , this gives  $\sqrt{n_k}$  different phases for each modulus  $n_k$ . In sum, this gives  $n_k$  different states, the same result as in the basis of number eigenstates.

## 3.2 Prototype Model: 3-Mode System

### 3.2.1 Introduction of Bose Gas with Dirichlet Boundary Conditions

#### Choice of System

In order to demonstrate the  $c$ -number for finding critical states of enhanced memory, we apply it to a concrete prototype system. We consider a gas of cold bosons that experience a simple attractive contact interaction and are placed in a one-dimensional box with Dirichlet boundary conditions. Therefore, it is similar to the system studied previously in [36, 76], some aspects of which we have already discussed in section 2.2.4. The only difference is that in the latter model periodic boundary conditions were used. In the present system with Dirichlet boundary conditions, we moreover truncate the tower of momentum modes to three and thus end up with three interacting bosonic quantum modes with a specific Hamiltonian. Despite the expected simplicity of this 3-mode system, we shall discover that it exhibits a rich variety of quantum phases. The nature of quantum phase transitions is qualitatively different from the analogous system with periodic boundary conditions.

Since the three modes are bosonic, each of them can be in many different states labeled by its occupation number. Thus, from a quantum information point of view, they represent three qudits. The attractive interaction translates as negative interaction energy between different modes. Correspondingly, the system satisfies the conditions discussed above for the emergence of a nearly-gapless mode and for reaching the critical states of enhanced memory capacity. Our goal is to show that there is indeed a critical value of the coupling at which such a mode emerges. We will first identify it with our analytic method and then confirm its existence by numerical analysis.

In the light of models of the type [208], which are easy to access analytically and which have a much closer connection with black hole entropy, the reader may wonder why we do not focus on those as opposed to the one-dimensional case with nonperiodic boundary conditions. There are two reasons for this. The first one is presumed experimental simplicity. It should be easier to realize a simple contact interaction, as opposed to the momentum-dependent one considered in [208]. Moreover, the prototype models studied so far only used periodic boundary conditions. For an experimental realization, however, it is important to determine how sensitive the phenomenon of emergence of gapless modes is to boundary conditions. In particular, nonperiodic boundary conditions may also be easier to attain in an experimental setting. Needless to say, we are aware of the extraordinary difficulties in performing such experiments. Therefore, what we present is not a concrete experimental proposal. In particular, we do not discuss any of the prob-

lems that arise due to an imperfect isolation from the environment.<sup>8</sup> Nevertheless, we hope that the study of our prototype model can contribute to the experimental realization of a system that shares the key properties of our prototype model, in particular the emergence of gapless modes.

The second reason for the choice of our prototype model is that the nonperiodic and nonderivative case is harder to analyze analytically, and therefore it represents a better test of the  $c$ -number method. To put it shortly, we trade a simpler-solvable model with a higher entropy for a harder-analyzable one with a smaller entropy due to the idea that the latter model promises more experimental simplicity and a tougher theoretical test of our method. The price we pay for this choice is that our system only produces a single gapless mode at the critical point. Nevertheless, it suffices to illustrate the key qualitative point of assisted gaplessness in a simple setup with potential experimental prospects.

### Truncated Hamiltonian

The Hamiltonian of our prototype model, the one-dimensional Bose gas in a box, is given by

$$\hat{H} = \int_0^L dz \left[ \frac{\hbar^2}{2m} \partial_z \hat{\psi}^\dagger \partial_z \hat{\psi} - \frac{\hbar^2}{2m} \frac{\pi^2 \alpha}{L} \hat{\psi}^\dagger \hat{\psi}^\dagger \hat{\psi} \hat{\psi} \right]. \quad (3.39)$$

Here  $\alpha$  is a dimensionless, positive coupling constant describing the attractive four-point interaction of the atoms and  $L$  is the size of the system. Up to the choice of boundary conditions, the system (3.39) is identical to the periodic model (2.42) studied in the context of quantum breaking, where we identify  $L = 2\pi R$ . Unlike before, we impose Dirichlet boundary conditions so that the free eigenfunctions now read

$$\hat{\psi} = \sqrt{\frac{2}{L}} \sum_{k=1}^{\infty} \hat{a}_k \sin\left(\frac{k\pi z}{L}\right). \quad (3.40)$$

Going to momentum space, we then obtain

$$\begin{aligned} \hat{H}^{\text{full}} = & \frac{4\pi^2 \hbar^2}{2mL^2} \left[ \sum_{k=1}^{\infty} \frac{k^2}{4} \hat{a}_k^\dagger \hat{a}_k - \frac{\alpha}{8} \sum_{k,l,m=1}^{\infty} \left[ (\hat{a}_k^\dagger \hat{a}_l^\dagger \hat{a}_m \hat{a}_{k+l-m} + 2\hat{a}_k^\dagger \hat{a}_l^\dagger \hat{a}_m \hat{a}_{k-l+m}) \right. \right. \\ & \left. \left. - 2(\hat{a}_{l+m+k}^\dagger \hat{a}_l^\dagger \hat{a}_m \hat{a}_k + \hat{a}_k^\dagger \hat{a}_l^\dagger \hat{a}_m \hat{a}_{k+l+m}) \right] \right]. \quad (3.41) \end{aligned}$$

Both analytically and numerically, however, it is difficult to obtain explicit solutions of the full Hamiltonian (3.41). Therefore, we will truncate the system to

---

<sup>8</sup>We could try to understand the disturbance effects due to the environment as a fluctuation  $\delta N$  of the particle number. Since we expect it to grow slowly with the total number  $N$  of bosons, it is clear that the relative disturbance  $\delta N/N$  shrinks when we increase  $N$ . This suggests that choosing a large number of bosons, which is required in any case for decreasing the gap of the light modes, could also help to suppress disturbance effects from the environment.

the lowest three modes,  $k \leq 3$ . This is the smallest number of modes for which the nonperiodic system behaves qualitatively differently from its analogue with periodic boundary conditions. Explicitly, we obtain after truncation:

$$\begin{aligned} \hat{H} = & \frac{1}{4} \sum_{k=1}^3 k^2 \hat{a}_k^\dagger \hat{a}_k - \frac{\alpha}{8} \left[ 3\hat{a}_1^{\dagger 2} \hat{a}_1^2 + 8\hat{a}_1^\dagger \hat{a}_2^\dagger \hat{a}_1 \hat{a}_2 + 2\hat{a}_1^{\dagger 2} \hat{a}_2^2 + 2\hat{a}_2^{\dagger 2} \hat{a}_1^2 \right. \\ & + 8\hat{a}_1^\dagger \hat{a}_3^\dagger \hat{a}_1 \hat{a}_3 + 2\hat{a}_1^{\dagger 2} \hat{a}_3^2 + 2\hat{a}_3^{\dagger 2} \hat{a}_1^2 - 2\hat{a}_1^{\dagger 2} \hat{a}_1 \hat{a}_3 - 2\hat{a}_1^\dagger \hat{a}_3^\dagger \hat{a}_1^2 \\ & + 4\hat{a}_1^\dagger \hat{a}_2^\dagger \hat{a}_2 \hat{a}_3 + 4\hat{a}_2^\dagger \hat{a}_3^\dagger \hat{a}_1 \hat{a}_2 + 2\hat{a}_1^\dagger \hat{a}_3^\dagger \hat{a}_2^2 + 2\hat{a}_2^{\dagger 2} \hat{a}_1 \hat{a}_3 \\ & \left. + 3\hat{a}_2^{\dagger 2} \hat{a}_2^2 + 8\hat{a}_2^\dagger \hat{a}_3^\dagger \hat{a}_2 \hat{a}_3 + 2\hat{a}_2^{\dagger 2} \hat{a}_3^2 + 2\hat{a}_3^{\dagger 2} \hat{a}_2^2 + 3\hat{a}_3^{\dagger 2} \hat{a}_3^2 \right]. \end{aligned} \quad (3.42)$$

This Hamiltonian defines the prototype system that we shall study in the following. For convenience, we set  $L = 2\pi$  and  $\hbar = 2m = 1$  from now on. Our subsequent task is to understand the phase portrait of the Hamiltonian (3.42) with the aim of identifying an emergent gapless mode that leads to enhanced entropy states with long decoherence time and large information storage capacity.

To prepare the application of our analytic method, we now perform the Bogoliubov approximation. Clearly, since the conditions (3.21) and (3.22), which define critical points of the Bogoliubov Hamiltonian, allow for a reparametrization of the complex variables contained in  $\vec{a}$  and  $\vec{a}^*$ , we can use a different parametrization defined by<sup>9</sup>

$$\hat{a}_1 \rightarrow \sqrt{N(1-x)} \cos(\theta), \quad \hat{a}_2 \rightarrow \sqrt{Nx} e^{i\Delta_2}, \quad \hat{a}_3 \rightarrow \sqrt{N(1-x)} \sin(\theta) e^{i\Delta_3}. \quad (3.43)$$

As it should be, this substitution already incorporates particle number conservation, i.e. we replace three modes by only two complex numbers, or equivalently two moduli and two phases. Here  $0 \leq x \leq 1$  is the relative occupation of the 2-mode and  $0 \leq \theta \leq \pi/2$  characterizes how the remaining atoms are distributed among the 1- and 3-mode. Moreover,  $\Delta_2$  and  $\Delta_3$  are relative phases. The Bogoliubov Hamiltonian, which we obtain after plugging in the replacements (3.43) in the Hamiltonian (3.42), reads:

$$\begin{aligned} \frac{H_{\text{bog}}}{N} = & \frac{1}{4} \left( 1 + 3x + 8(1-x) \sin^2(\theta) \right) - \frac{\lambda}{8} \left[ \sin^2(2\theta) (1-x)^2 \left( \frac{1}{2} + \cos(2\Delta_3) \right) \right. \\ & + 3 + 2x - 2x^2 + 4x(1-x) \left( \cos(2\Delta_2) \cos^2(\theta) + \cos(2\Delta_2 - 2\Delta_3) \sin^2(\theta) \right) \\ & \left. + 2 \sin(2\theta) (1-x) \left( x \cos(2\Delta_2 - \Delta_3) + \cos(\Delta_3) \left( 2x - (1-x) \cos^2(\theta) \right) \right) \right]. \end{aligned} \quad (3.44)$$

<sup>9</sup>The equivalence of the vanishing of the second derivatives in  $\vec{a}$  and  $x$  is nontrivial and only holds if there are no unoccupied modes,  $a_k \neq 0$ . Schematically, the reason is that  $\frac{\partial H_{\text{bog}}}{\partial a} = a \frac{\partial H_{\text{bog}}}{\partial x}$  and therefore  $\frac{\partial^2 H_{\text{bog}}}{\partial^2 a} = a^2 \frac{\partial^2 H_{\text{bog}}}{\partial^2 x} + \frac{\partial H_{\text{bog}}}{\partial x}$ .

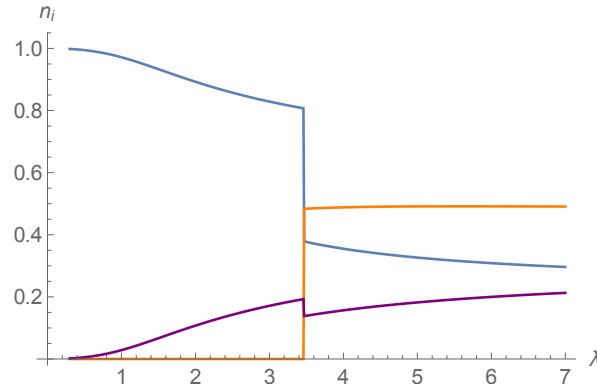


Figure 3.2: Relative occupation numbers of the ground state of the Bogoliubov Hamiltonian as functions of  $\lambda$ . The 1-mode is displayed in blue, the 2-mode in orange and the 3-mode in purple. There is a discontinuous change in the occupation numbers at  $\lambda_{gs} \approx 3.5$ .

### Analysis of the Ground State

As a preparatory exercise, we analyze the ground state of the Hamiltonian (3.42). We can do so by finding the global minimum of the Bogoliubov Hamiltonian (3.44). It is evident that the choices  $\Delta_2 = 0$  as well as  $\Delta_3 = 0$  or  $\Delta_3 = \pi$  are preferred since they minimize each term separately.<sup>10</sup> It is straightforward to minimize the energy with respect to  $\Delta_3$  and the remaining two continuous parameters  $x$  and  $\theta$  numerically.<sup>11</sup> The resulting occupation numbers of the ground state as functions of the collective coupling  $\lambda$  are displayed in Fig. 3.2. We observe that the occupation numbers change discontinuously at the critical point  $\lambda_{gs} \cong 3.5$ , where the subscript *gs* stands for ground state.

In order to understand this behavior better, we plot the Bogoliubov Hamiltonian as a function of  $x$  and  $\theta$  for the critical value  $\lambda = 3.5$  in Fig. 3.3. Since we observe two disconnected, degenerate minima, we can explain the discontinuous change of the occupation numbers as transition between the two minima. To analyze how the second minimum develops, we marginalize over  $\theta$  and  $\Delta_3$ , i.e. we only fix  $x$  and minimize the energy with respect to the remaining parameters  $\theta$  and  $\Delta_3$ . Fig. 3.4 shows the result for different values of  $\lambda$ . We conclude that a local minimum exists at  $x = 0$  for all values of  $\lambda$  and that another local minimum at  $x = x_{\min}(\lambda) \neq 0$  starts to exist for  $\lambda > \lambda_{lm}$ , where

$$\lambda_{lm} \cong 1.8. \quad (3.45)$$

Here the subscript *lm* stands for light mode since we observe that the critical point

<sup>10</sup>This follows from the last line of the Hamiltonian (3.44). For  $3n_2 > n_1$ ,  $\Delta_3 = 0$  is preferred and otherwise  $\Delta_3 = \pi$ .

<sup>11</sup>All numerical computations in this work are performed with the help of Mathematica [216].

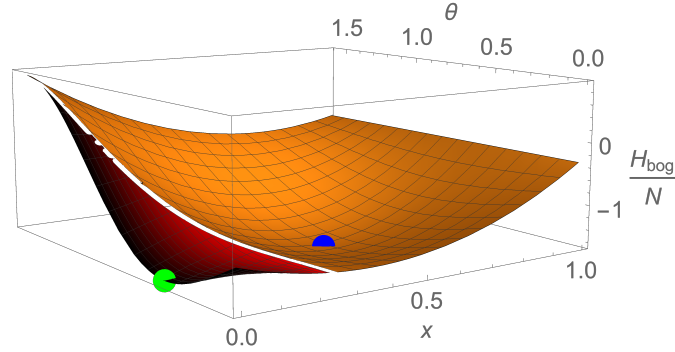


Figure 3.3: Bogoliubov energy (rescaled by the inverse particle number) for  $\lambda = 3.5$  as a function of  $x$  and  $\theta$ . The red surface is the region where  $\Delta_3 = \pi$  minimizes the energy and in the orange surface,  $\Delta_3 = 0$  is preferred. We observe two disconnected, degenerate minima, one for  $x = 0$  (green point) and one for  $x \neq 0$  (blue point).

$\lambda_{lm}$  corresponds to a stationary inflection point and will therefore be crucial for our discussion of the gapless mode in the next section. With regard to the ground state, we can conclude for now that  $\lambda_{gs}$  corresponds to the point where the second minimum becomes energetically favorable.

Thus, we expect from the analytic analysis that the ground state changes discontinuously at the critical point  $\lambda_{gs} \cong 3.5$ , i.e. that there is a first-order phase transition. We can check that this indeed happens in the quantum Hamiltonian for finite  $N$ . To this end, we diagonalize it numerically to find the true ground state. When we plot the expectation values of the occupation numbers of the ground state as functions of  $\lambda$ , the result is indistinguishable from Fig. 3.2 above already for  $N \gtrsim 100$ . We therefore confirm that there is a critical point at  $\lambda_{gs}$ , at which the ground state of the system changes discontinuously.

This represents a marked difference to the periodic system, where the ground state changes continuously, i.e. a second-order phase transition takes place [36, 76]. Because of the continuity of the transition, higher modes only get occupied slowly in that case so that one can describe the full system solely in terms of the lowest three modes. This makes it easy to obtain numerical results for the periodic system. As we have seen, however, the occupation numbers change discontinuously for Dirichlet boundary conditions. Therefore, the truncation to three modes is no longer justified already near the critical point. For this reason, the full system (3.41) does not necessarily need to exhibit the behavior which we observe for the

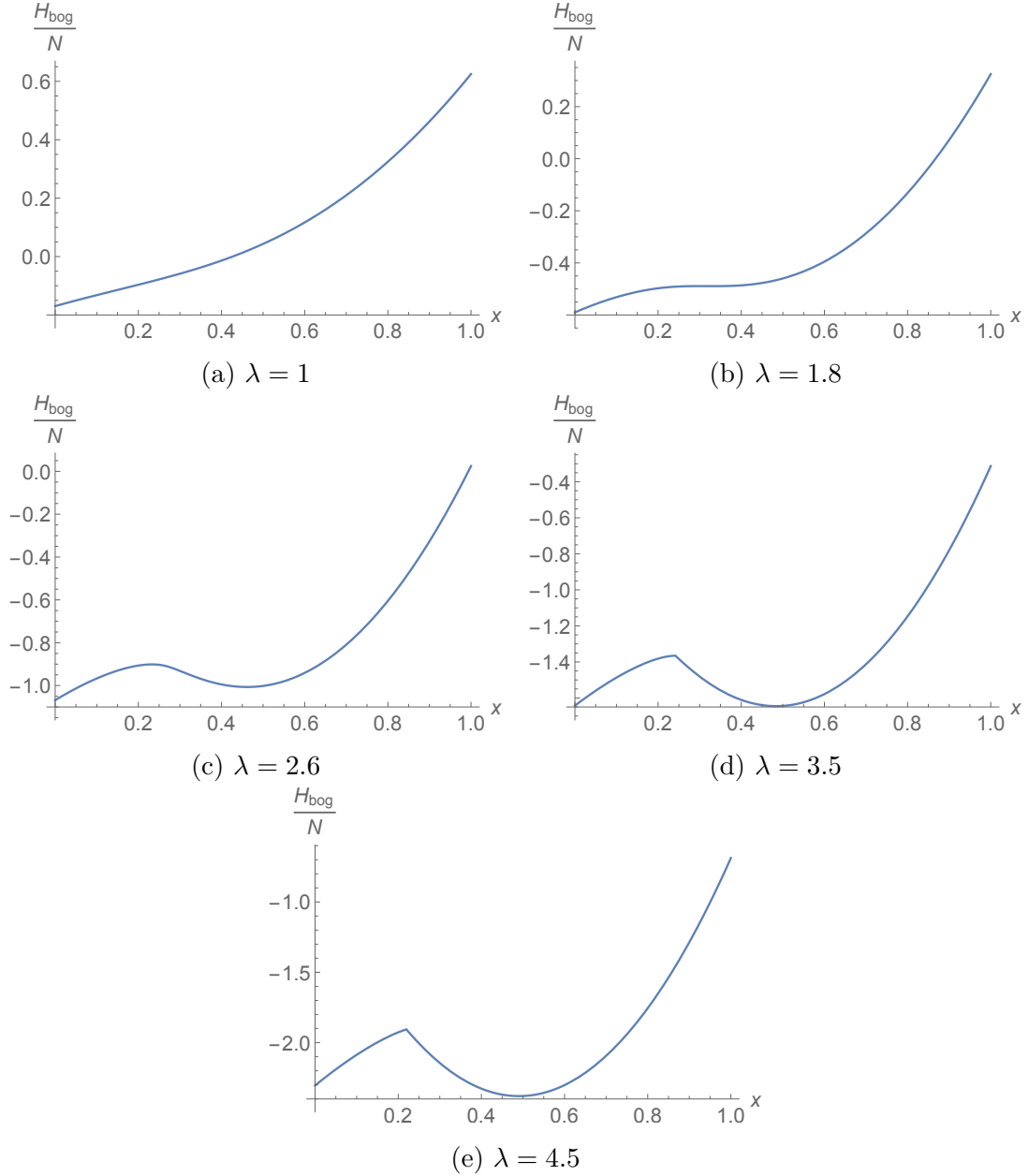


Figure 3.4: Minimal value of the Bogoliubov Hamiltonian (rescaled by the inverse particle number) subject to the constraint that the relative occupation of the 2-mode is  $x$ . At  $\lambda_{lm} \cong 1.8$ , a stationary inflection point signals the appearance of a second minimum and at  $\lambda_{gs} \cong 3.5$ , this second minimum becomes energetically favorable.

truncated Hamiltonian (3.42).

### 3.2.2 Critical Point with Gapless Mode

#### Application of $C$ -Number Method

We proceed to perform a detailed analysis of the point  $\lambda = \lambda_{lm}$ . Our goal is to show that it features a light mode and correspondingly an increased density of states, i.e. that the phenomenon of assisted gaplessness takes place at this point. First, we will do so using the analytic  $c$ -number method developed in section 3.1.4. As explained there, it allows us to forgo the involved analysis of the full spectrum. Instead, we are only faced with the much simpler task of showing that the Bogoliubov Hamiltonian, which solely depends on two complex variables, possesses a stationary inflection point.

Since we already expect from Fig. 3.4 that a stationary inflection point appears at  $\lambda = \lambda_{lm}$ , it remains to confirm that this is the case. To this end, we first study the first derivative of the Bogoliubov Hamiltonian. Setting it to zero yields four equations, which we can solve for the four Bogoliubov parameters  $x$ ,  $\theta$ ,  $\Delta_2$  and  $\Delta_3$ . We observe that the latter two parameters behave as in the second minimum,  $\Delta_2 = \Delta_3 = 0$ . Only the derivatives with respect to  $x$  and  $\theta$ , which are displayed in equation (A.7) in appendix A.2.2, yield nontrivial conditions. As we expect from the previous analysis, solutions, i.e. local extrema, only exist for  $\lambda > \lambda_{lm}$ , which we determine as  $\lambda_{lm} = 1.792$ . Next, we compute the matrix  $\mathcal{M}$  of second derivatives, which is displayed in equation (A.8). At the local minima, we plug in the above determined values of the Bogoliubov parameters and then compute its determinant. We display the result in Fig. 3.5a as a function of  $\lambda$ . We confirm that it vanishes as  $\lambda$  approaches  $\lambda_{lm}$  from above. Therefore,  $\lambda = \lambda_{lm}$  corresponds to a stationary inflection point in the Bogoliubov Hamiltonian and it follows from our  $c$ -number method that a nearly-gapless mode and consequently an increased degeneracy of states exists in the full spectrum.

In order to confirm this finding, and also to make a more quantitative statement, we explicitly perform the Bogoliubov transformation to obtain the full quantum spectrum in the limit  $N \rightarrow \infty$ . As explained in section 3.1.4, the first step is to replace  $\hat{a}_1/\hat{a}_1^\dagger \rightarrow \sqrt{N - \hat{a}_2^\dagger\hat{a}_2 - \hat{a}_3^\dagger\hat{a}_3}$  in the full Hamiltonian (3.42) to ensure that we only consider fluctuations that respect particle number conservation. Then we expand to second order around the point defined by the Bogoliubov approximation (3.43). We display the result in appendix A.2.2 in equations (A.10) and (A.11). As before, we subsequently look for pairs  $(x, \theta)$  where the linear term (A.10) vanishes and stable fluctuations exist. We obtain the same values as above. At those points, we calculate numerically the Bogoliubov transformation for the corresponding quadratic Hamiltonian using the method described in [215, 217]. The so obtained diagonal matrix contains the excitation energies associated to the Bogoliubov modes. The smallest energy gap as a function of  $\lambda$  is shown in Fig.

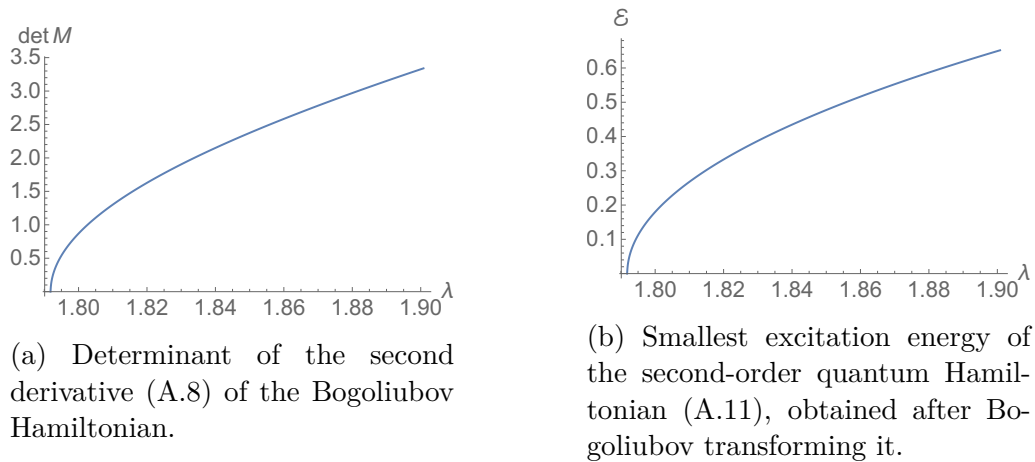


Figure 3.5: Excitation energy as a function of  $\lambda$  for  $N \rightarrow \infty$  derived in two different methods. In both cases, we observe a gapless excitation at  $\lambda_{lm} \cong 1.792$ . Stable excitations only exist for  $\lambda \geq \lambda_{lm}$ . As is clear from the Hamiltonian (3.41), the energy unit is  $\frac{4\pi^2\hbar^2}{2mL^2}$ .

3.5b. As expected, the result is in accordance with the previous one displayed in Fig. 3.5a. Thus, this analysis confirms that a gapless mode exists at  $\lambda_{lm}$  in the limit  $N \rightarrow \infty$ . For finite  $N$ , we therefore expect that a nearly-gapless mode, whose energy is suppressed as a power of  $1/N$ , appears close to  $\lambda_{lm}$ .

The critical state, around which the gapless modes emerge, is not the ground-state of the system. Nevertheless, the present analysis also shows that it is stable. This follows from the fact that the gaps of all modes are positive and large in the relevant regime  $\lambda \geq \lambda_{lm}$ , except for one almost flat direction (see Fig. 3.5b). This conclusion will be corroborated by the numerical analysis since it will not show any sign of decay, either. Of course, in order to perform any experimental analysis of the system, it has to be coupled to additional external modes. Such a coupling could destabilize the system, provided it is strong enough. But as we have discussed in section 3.1.1, any interaction to an external field has to be weak anyhow in order not to disturb the gaplessness of the Bogoliubov mode. We expect that the weakness of the external influence also ensures a sufficient stability of the critical state, although the matter has to be studied on a case by case basis for potential experimental setups.

### Slow Mode in Full Spectrum

Our goal is to confirm the existence of a light mode in the spectrum of the quantum system for finite  $N$ . To this end, we will use the fact that modes with a small energy gap  $\mathcal{E}$  evolve on the long timescale  $\hbar/\mathcal{E}$  (see Eq. (3.4)). When we consider a state close to a critical point of enhanced memory storage, we therefore expect the appearance of large timescales in its time evolution. So we will prove the

existence of a light mode by showing that quantum states with a drastically slower time evolution exist there.<sup>12</sup> As discussed in section 3.1.1, we expect such states to have an experimental signature in the form of absorption lines of low frequency.<sup>13</sup>

The timescale of evolution also determines how long a state can store information. We can imagine that we experimentally prepare a state in such a way that we can choose its components in a certain basis. Then it is possible to encode information in these components. If we measure the state before it has evolved significantly, we can directly read out the components and therefore the stored information. In contrast, if the state has already evolved, it is practically impossible to retrieve the information since this would require precise knowledge of the dynamics of the systems, in particular of its energy levels. In a narrow sense, the timescale of evolution therefore determines a decoherence time. It is the time after which the subset of nearly-gapless modes has been decohered by the rest of the system.

Practically, we need to come up with a procedure to single out a quantum state, for which we then analyze its time evolution. For  $\lambda = \lambda_{lm}$ , this quantum state should correspond to the stationary inflection point of the Bogoliubov Hamiltonian. In order to make a comparative statement, we moreover need to determine analogous quantum states at different values of  $\lambda$ . We will achieve this by constructing a method to associate a quantum state  $|\Phi_{\text{inf}}\rangle$  to the inflection point of the Bogoliubov Hamiltonian. This inflection point exists for all  $\lambda \gtrsim 1$  but is stationary only for  $\lambda = \lambda_{lm}$ .

Our approach to determine  $|\Phi_{\text{inf}}\rangle$  is to define a subspace of states close to the inflection point and then to select among those the state of minimal energy. On the one hand, this subspace should not be too big in order to be sensitive to properties of the stationary inflection point at  $\lambda = \lambda_{lm}$ . On the other hand, the subspace cannot be too small since otherwise the energy of the state that we obtain by minimization is too high. Of course, there is no unique way to determine this subspace and therefore no unique quantum state  $|\Phi_{\text{inf}}\rangle$ , but it suffices for us to come up with a method to find some quantum state with drastically slower time evolution. In particular, we expect that there are many different such quantum states corresponding to different occupation numbers of the light mode.

Concretely, we will construct the subspace using two conditions, which we derive from properties of the inflection point  $x_{\text{inf}}(\lambda)$  of the Bogoliubov Hamiltonian. First, we only consider quantum states  $|\Phi_{\text{inf}}\rangle$  for which the expectation value of the relative occupation of the 2-mode,  $n_2(t) := \langle \Phi_{\text{inf}} | \hat{a}_2^\dagger(t) \hat{a}_2(t) | \Phi_{\text{inf}} \rangle / N$ , is equal to

<sup>12</sup>For the periodic system, it was shown explicitly that the time evolution is significantly slower at the critical point [51].

<sup>13</sup>We remark that it does not suffice to look for eigenstates in the spectrum whose energies only differ by a small value  $\Delta E$ . The reason is that even when eigenstates have a similar energy, the transition between them can nevertheless be a suppressed higher-order process, i.e. it can be very hard to transit from one to the other. In this case, no light mode exists and a soft external stimulus cannot induce the transition.

$x_{\text{inf}}(\lambda)$ . Secondly, we restrict the basis used to form the quantum state  $|\Phi_{\text{inf}}\rangle$ , where – as in all numerical computations – we use number eigenstates of total occupation number  $N$  as basis. Namely, we determine from the Bogoliubov Hamiltonian all relative occupation numbers at the inflection point. Then we choose upper bounds  $\delta n_i$  on the spread of the different modes, i.e, we only consider basis elements for which the relative occupation numbers deviate by at most  $\delta n_i$  from the values determined from the Bogoliubov Hamiltonian. With the guideline that modes with bigger relative occupation should have a bigger spread, we empirically determine  $\delta n_1 = 0.4$ ,  $\delta n_2 = 0.375$  and  $\delta n_3 = 0.225$  to be a good choice.<sup>14</sup>

Once we have determined the state  $|\Phi_{\text{inf}}\rangle$ , we study its time evolution. In doing so, we use the full quantum Hamiltonian and therefore also the full basis. We show the result for  $N = 60$  for exemplary values of  $\lambda$  in Fig. 3.6, where we plotted  $n_2(t)$ . Clearly, drastically lower frequencies dominate around  $\lambda = \lambda_{lm}$ . In order to make a quantitative estimate about the coherence time as a function of the collective coupling  $\lambda$ , we extract a typical frequency from the time evolution of  $|\Phi_{\text{inf}}\rangle$ . To this end, we use a discrete Fourier transformation with respect to the  $n_{\text{max}}$  frequencies  $f_1, 2f_1, \dots, n_{\text{max}}f_1$  to obtain the Fourier coefficients  $c_1, c_2, \dots, c_{n_{\text{max}}}$ . With their help, we can define the mean frequency as

$$\bar{f} := f_1 \frac{\sum_{i=1}^{n_{\text{max}}} i |c_i|^2}{\sum_{i=1}^{n_{\text{max}}} |c_i|^2}. \quad (3.46)$$

As explained, the timescale of evolution can be interpreted as decoherence time, namely as the timescale after which the subset of nearly-gapless modes has been decohered by the other modes. In this sense, we get:

$$t_{\text{coh}} = \frac{1}{\bar{f}}. \quad (3.47)$$

For  $f_1 = 1/3000$  and  $n_{\text{max}} = 12000$ , we show  $t_{\text{coh}}$  as a function of  $\lambda$  in Fig. 3.7.<sup>15</sup> We observe that it increases distinctly around  $\lambda \cong 2.083$ .

The fact that for  $N = 60$  a state with drastically slower time evolution appears at  $\lambda_{lm}^{(60)} \cong 2.083$  is consistent with  $\lambda_{lm} \cong 1.792$  since we expect that as in the periodic system, the critical value  $\lambda_{lm}^{(N)}$  of the collective coupling at finite  $N$  receives  $1/N$ -corrections:<sup>16</sup>

$$\lambda_{lm}^{(N)} = \lambda_{lm} + a \cdot N^{-b}, \quad (3.48)$$

<sup>14</sup>We compared the results obtained in this truncation with the ones derived using the full basis. For  $N \leq 50$ , we observed that their qualitative behavior, which we shall discuss in a moment, is identical whereas this no longer seems to be the case for higher  $N$ . However, the only important point for us is to come up with some recipe to find the slowly evolving states.

<sup>15</sup>We checked that different choices of  $f_1$  and  $n_{\text{max}}$  lead to the same result. Therefore, cutting off low and high frequencies, which is required in a numerical treatment, has no influence on our findings.

<sup>16</sup>In contrast, note that we do not expect  $t_{\text{coh}}$  to diverge for infinite  $N$  because  $|\Phi_{\text{inf}}\rangle$  generically contains an admixture of nongapless modes.

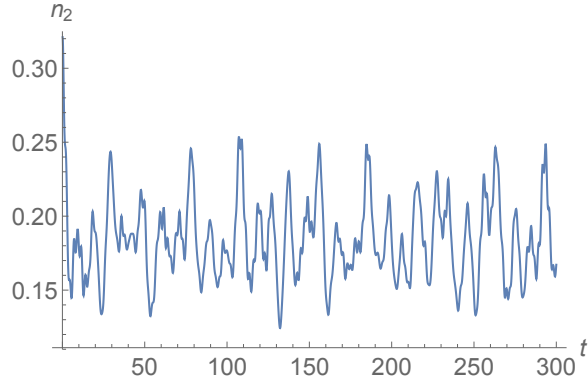
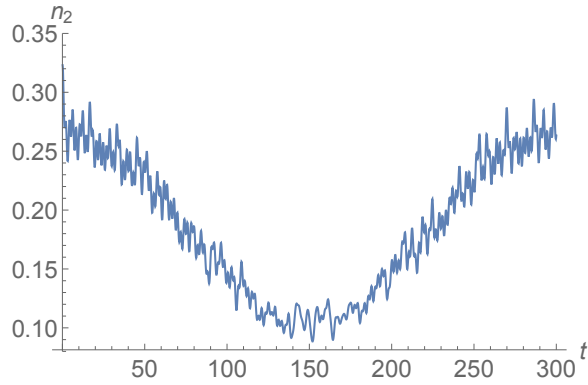
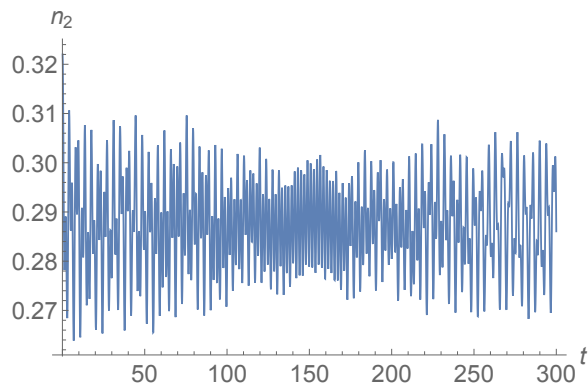
(a)  $\lambda = 1.9$ (b)  $\lambda = 2.083$ (c)  $\lambda = 2.2$ 

Figure 3.6: Time evolution of the quantum state  $|\Phi_{\text{inf}}\rangle$ , which corresponds to the inflection point of the Bogoliubov Hamiltonian. The value of  $n_2(t)$  is plotted for  $N = 60$ . We observe that lower frequencies dominate around  $\lambda \cong 2.083$ .

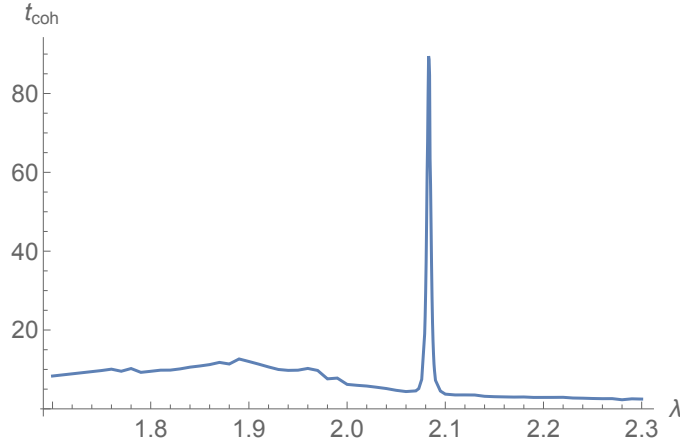


Figure 3.7: Estimate of the decoherence time  $t_{\text{coh}}$  associated to  $|\Phi_{\text{inf}}\rangle$  as a function of  $\lambda$  for  $N = 60$ . We observe that it increases distinctly around  $\lambda \cong 2.083$ .

where  $a > 0$  and  $b > 0$  are two undetermined parameters. To confirm that this is the case, we repeated the above analysis of the decoherence time as a function of  $\lambda$  for  $N$  between 40 and 90. This determines critical values  $\lambda_{lm}^{(N)}$  as the values of  $\lambda$  for which time evolution is the slowest at a given  $N$ . Subsequently, we fit the function (3.48) to the result and thereby determine  $a = 3.56$  and  $b = 0.61$ . We note that  $b$  is close to  $2/3$ , which was the result in the periodic system [76]. As is evident from Fig. 3.8, the numerically determined values  $\lambda_{lm}^{(N)}$  are well described by the fitted function (3.48). This is a clear indication that the slowed time evolution we found is due to the nearly-gapless Bogoliubov mode that we predict from the analytic treatment. So in summary, we observe the appearance of a nearly-gapless mode around  $\lambda = \lambda_{lm}$  also for finite  $N$ .

As a final remark, we discuss the critical state  $|\Phi_{\text{inf}}\rangle$  for  $N = 60$  and  $\lambda = 2.083$  in position space. Its particle density is given by

$$\rho(z) \equiv \langle \Phi_{\text{inf}} | |\hat{\psi}|^2 | \Phi_{\text{inf}} \rangle = \frac{1}{\pi} \sum_{k,l=1}^3 \langle \Phi_{\text{inf}} | \hat{a}_k^\dagger \hat{a}_l | \Phi_{\text{inf}} \rangle \sin\left(\frac{kz}{2}\right) \sin\left(\frac{lz}{2}\right). \quad (3.49)$$

We display it in Fig. 3.9, where we also illustrate what the gapless mode looks like in position space. To this end, we fix the critical value of the collective coupling,  $\lambda = 2.083$ , but slightly vary the value of  $x$  used in the minimization procedure that determines the quantum state:  $x_i = x_{\text{inf}}(\lambda) + \delta x_i$ . This determines a family of quantum states  $|\Phi_{\text{inf}, i}\rangle$ , where  $|\Phi_{\text{inf}, i}\rangle$  is a state of minimal energy subject to the constraint that its relative occupation of the 2-mode is  $x_i$ . Their particle densities are also shown in Fig. 3.9.

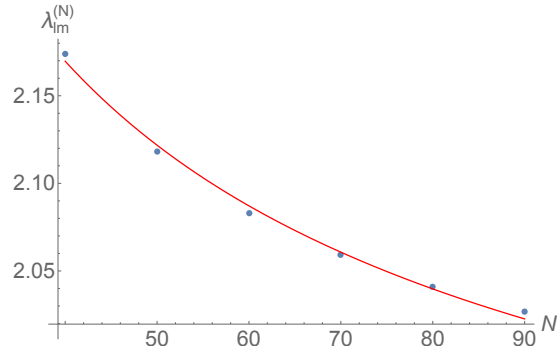


Figure 3.8: Critical value  $\lambda_{lm}^{(N)}$  as a function of particle number  $N$ . The positions obtained from numerical simulations are plotted in blue. The fitted function (3.48) is shown in red.

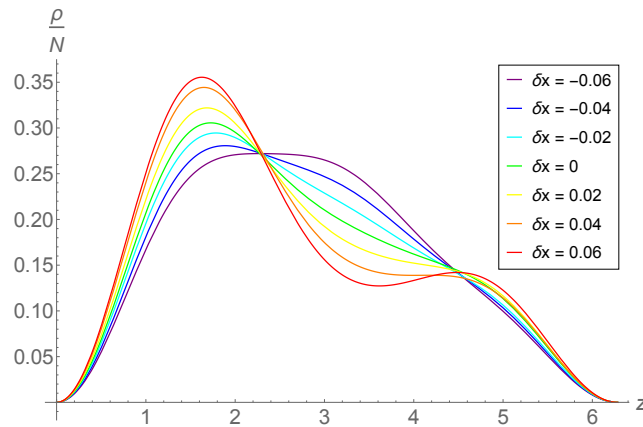


Figure 3.9: Variations of the critical state at  $\lambda = 2.083$  for  $N = 60$  in position space. The relative particle density  $\rho/N$  is plotted. The green line corresponds to the critical state  $|\Phi_{\text{inf}}\rangle$  itself and the adjacent lines are variations of it, which we obtained by slightly changing the value of  $x$  used in the minimization procedure that determines the quantum state:  $x_i = x_{\text{inf}}(\lambda) + \delta x_i$ . The values of  $\delta x_i$  are indicated in the plot.

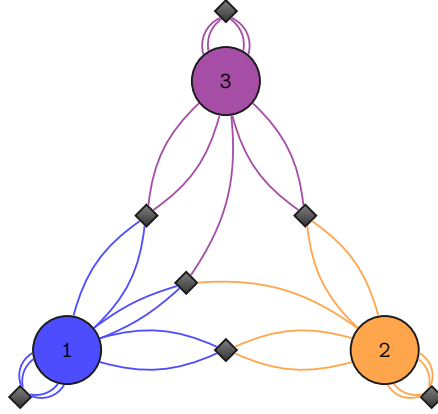


Figure 3.10: Representation of the Hamiltonian (3.42) as neural network. The three neurons are displayed as circles and diamonds represent interaction terms. The number of lines to a diamond indicates how many mode operators of the corresponding neuron participate in the interaction.

### 3.2.3 Neural Network Analogue

#### Mapping

Using the dictionary developed in section 3.1.3, we shall represent the system (3.42) as a neural network. Namely, it is fully isomorphic to a quantum neural network with three neurons in which the excitations of neurons are described by the momentum modes  $\hat{a}_k^\dagger, \hat{a}_k$  and the synaptic connections between the neurons are described by the interaction terms in (3.42).<sup>17</sup> Fig. 3.10 shows the representation of Hamiltonian (3.42) as neural network.

To make a closer contact with the neural network language, it is useful to rewrite the Hamiltonian as

$$\hat{H} = \sum_{k=1}^3 \epsilon_k \hat{a}_k^\dagger \hat{a}_k - \sum_{k,j=1}^3 \hat{a}_k^\dagger \hat{\mathcal{W}}_{kj} \hat{a}_j, \quad (3.50)$$

where  $\epsilon_k = \frac{1}{4}k^2$  are the threshold excitation energies of the neurons and  $\hat{\mathcal{W}}_{kj}$  is a

<sup>17</sup>We remark that this system only represents a part of a neural network that can be used for actual memory storage. In a realistic situation, one needs a first device to input information, a second one to store it and a third one to retrieve it. However, our system solely realizes the second part. So we only study situations in which no input or output operations take place.

Hermitian  $3 \times 3$  matrix operator of synaptic connections. Its elements are:

$$\hat{\mathcal{W}}_{11} = \frac{3\alpha}{8} \hat{a}_1^\dagger \hat{a}_1, \quad (3.51a)$$

$$\hat{\mathcal{W}}_{22} = \frac{3\alpha}{8} \hat{a}_2^\dagger \hat{a}_2, \quad (3.51b)$$

$$\hat{\mathcal{W}}_{33} = \frac{3\alpha}{8} \hat{a}_3^\dagger \hat{a}_3, \quad (3.51c)$$

$$\hat{\mathcal{W}}_{12} = \frac{\alpha}{8} \left( 4\hat{a}_2^\dagger \hat{a}_1 + 2\hat{a}_1^\dagger \hat{a}_2 + \frac{4}{3} \hat{a}_2^\dagger \hat{a}_3 + \hat{a}_3^\dagger \hat{a}_2 \right), \quad (3.51d)$$

$$\hat{\mathcal{W}}_{13} = \frac{\alpha}{8} \left( 4\hat{a}_3^\dagger \hat{a}_1 + 2\hat{a}_1^\dagger \hat{a}_3 + \frac{4}{3} \hat{a}_2^\dagger \hat{a}_2 - 2\hat{a}_1^\dagger \hat{a}_1 \right), \quad (3.51e)$$

$$\hat{\mathcal{W}}_{23} = \frac{\alpha}{8} \left( 4\hat{a}_3^\dagger \hat{a}_2 + 2\hat{a}_2^\dagger \hat{a}_3 + \frac{4}{3} \hat{a}_1^\dagger \hat{a}_2 + \hat{a}_2^\dagger \hat{a}_1 \right). \quad (3.51f)$$

Now we can directly apply all our results to the above neural network. We shall all the time assume the regime of very weak synaptic connections, i.e. we assume  $\alpha \ll 1$ . In this situation, we study the memory storage capacity of the network for various values of the total excitation level  $N$ .

First, we examine the memory storage capacity of the neural network around a state in which the total excitation level is well below the critical level,  $N \ll 1/\alpha$ . In such a regime, the negative energy of synaptic connections is negligible and does not contribute to lowering the energy gap. Note that the ability of the synaptic connection energy to lower the gap of neurons is parameterized by the strength of the collective coupling  $\lambda = \alpha N$ , which is very weak in the considered regime,  $N \ll 1/\alpha$ .

Correspondingly, in such a regime the energy difference between different number eigenstates  $|N - n_2 - n_3, n_2, n_3\rangle$  and  $|N - n'_2 - n'_3, n'_2, n'_3\rangle$  mostly comes from the first threshold energy term in the network Hamiltonian (3.50) and is very large

$$\mathcal{E}_{\lambda \ll 1} = \frac{1}{4} (3(n'_2 - n_2) + 8(n'_3 - n_3)) + \mathcal{O}(\lambda). \quad (3.52)$$

Hence, the patterns stored in such states occupy a very large energy gap. For example, in order to read a pattern stored in the state  $|N, 0, 0\rangle$  into the state  $|N - 1, 1, 0\rangle$ , we need to overcome an energy gap  $\mathcal{E} \simeq 3/4$ , i.e. an external stimulus that is needed for the read of information  $|N, 0, 0\rangle \rightarrow |N - 1, 1, 0\rangle$  has to have an energy of order  $\sim 3/4$ .

Now we increase the total excitation level  $N$ . With this increase, the contribution of the negative synaptic connection energy gradually lowers the gap between some neighboring states. The gap attains the smallest value when the total excitation level  $N$  reaches the critical point. As discussed above, this happens when  $\alpha N = \lambda_{tm}$ . At this point, a state becomes available around which a gapless excitation emerges. This means that for a certain relative distribution of excitation

levels, the gap between the set of patterns collapses to

$$\mathcal{E}_{\lambda=\lambda_{tm}} \approx \frac{1}{N^\beta}, \quad (3.53)$$

where  $\beta$  is a positive constant. By taking the double scaling limit (3.20), we can make the gap arbitrarily narrow. In this situation, the storage of patterns in such states becomes energetically cheap.

So far, we have described a quantum neural network. We can move to a classical neural network by using the coherent state basis and replacing the Hamiltonian operator by its expectation value over the coherent states. In this way, we obtain a classical neural network described by the  $c$ -number energy function  $H_{\text{bog}}(\vec{a}, \vec{a}^*)$ .

### Enhanced Pattern Storage

When discussing the storage of patterns in a neural network, we must introduce the notion of the pattern vector. In general, this vector is different from the quantum state vector of the system and may contain less information. This is determined by those characteristics of the state to which an external reading device is sensitive. Indeed, when the underlying quantum state characterizing the system is given by a coherent state, which is labeled by three complex numbers  $|a_1, a_2, a_3\rangle$ , the storage of a pattern and therefore the pattern vector is determined by the combinations of these numbers to which the reader is sensitive. If the reader is sensitive to the full quantum information, i.e. to the phases as well as to the absolute values of  $a_j$ , then the pattern vector can be identical to the quantum-state vector. If instead the reader is only sensitive to the absolute values, the pattern vector can be correspondingly chosen in the form  $(|a_1|, |a_2|, |a_3|)$ . Since we do not specify any external reading device, we shall keep the definition of the pattern vector flexible.

We can explicitly write down the pattern vector for our concrete system (3.50). First, we discuss the case in which the reader is sensitive to the full quantum information. Using the notations (3.43), the pattern vector can then be parameterized as

$$\begin{pmatrix} a_1 \\ a_2 \\ a_3 \end{pmatrix} = \sqrt{N} \begin{pmatrix} \sqrt{1-x} \cos(\theta) \\ \sqrt{x} e^{i\Delta_2} \\ \sqrt{1-x} \sin(\theta) e^{i\Delta_3} \end{pmatrix}, \quad (3.54)$$

where as before  $0 \leq x \leq 1$ . If in contrast the reader is only sensitive to the absolute values, we can effectively describe this situation by neglecting the phases in (3.54),  $\Delta_2 = \Delta_3 = 0$

As before, we can discuss states of enhanced memory capacity. Thereby, the role of the negative synaptic connection energy in creating such a state is the same since, up to  $1/N$ -corrections, the energy expectation value is identical in a number eigenstate and in a coherent state. So for  $\lambda \ll 1$ , when the synaptic connection term is negligible and the energy of the network is given by the threshold excitation energy, we obtain the energy gap (3.52). When we remember that due to the

properties of coherent states only patterns with large parameter differences that satisfy (3.38) count as distinct patterns, we conclude that the energy difference for distinguishable patterns is given by the threshold excitation energy and therefore necessarily large,  $\mathcal{E} \gtrsim 1$ . This situation changes dramatically in the critical state, where a stationary inflection point appears in the energy function  $H_{\text{bog}}(\vec{a}, \vec{a}^*)$ . Because of the corresponding flat direction, the energy difference between distinct patterns collapses to zero, as is evident from (3.53). Hence the system can store different patterns within an arbitrarily narrow energy gap.

In order to attain such a critical state of enhanced memory storage, one has to proceed as follows when one is given the system (3.50) with some small coupling  $\alpha \ll 1$ . First, one needs to go to a total excitation level of  $N = \lambda_{lm}/\alpha \cong 1.8/\alpha$ . Then one has to distribute those excitations so that the expectation values in the three neurons approximately match the stationary inflection point of the Bogoliubov Hamiltonian. This means one has to choose  $\langle \hat{a}_2^\dagger \hat{a}_2 \rangle = x_{\text{inf}} N \cong 0.32N$  as well as  $\langle \hat{a}_1^\dagger \hat{a}_1 \rangle = (1 - x_{\text{inf}}) \cos^2(\theta_{\text{inf}}) N \cong 0.67N$  and  $\langle \hat{a}_3^\dagger \hat{a}_3 \rangle = (1 - x_{\text{inf}}) \sin^2(\theta_{\text{inf}}) N \cong 0.01N$ . Around such a state, an increased number of patterns exists in a small energy gap, provided  $N$  is big enough.

One can also repeat this procedure for different, i.e. noncritical, values of  $\lambda$ . Then one finds that the energy gap is not small,  $\mathcal{E} \gtrsim 1$ . Determining in this way the minimal energy for pattern storage as a function of  $\lambda$ , one reproduces Fig. 3.5b. Of course, it is important to note that this plot is only valid in the limit of infinite  $N$ . For finite  $N$ , corrections appear that scale as a power of  $1/N$ . In particular, the critical value of  $\lambda$ , at which the enhanced memory storage takes place, deviates slightly from  $\lambda_{lm}$ . In Fig. 3.8, this critical value of  $\lambda$  is shown for some exemplary finite excitation levels  $N$ .

A small energy gap has a direct implication on the longevity of states, i.e. on the timescale  $t_{\text{coh}}$  on which excitation levels of the neurons start to change. As is exemplified in Fig. 3.6, this timescale is short,  $t_{\text{coh}} \approx 1$ , for states away from the critical point (Fig. 3.6a and 3.6c). In contrast, it is long,  $t_{\text{coh}} \gg 1$ , for critical states (Fig. 3.6b). If one investigates this timescale of evolution for different values of  $\lambda$ , this leads to Fig. 3.7. We observe that states that evolve significantly more slowly appear at the critical point.

The mechanism for memory storage, which is based on assisted gaplessness, can be summarized as follows. In the presence of excitatory synaptic connections, we increase the total excitation level to a point at which a flat direction appears in the energy landscape. On this plateau, there exists a large number of distinct states within a small energy gap. Those states are, however, very close, so typically one would expect that they mix very quickly and information gets washed out. But the key point is that we can distinguish them because they evolve very slowly. Thus, if we read out a state on a timescale smaller than its timescale of evolution, we will encounter it precisely as we have put it in the system.

To conclude this section, we have seen that a simple system of cold bosons

truncated only to three modes effectively describes a neural network of remarkable complexity. Most importantly, once excited to a critical level, it forms states of sharply enhanced memory capacity in which a large number of patterns can be stored within an arbitrarily very narrow energy gap. This behavior also persists when taking the classical limit of the neural network. The above connection opens up the possibility of simulating enhanced memory capacity neural networks in laboratory experiments with cold bosons.

### 3.3 Memory Burden

#### 3.3.1 General Mechanism

We have shown how assisted gaplessness leads to states with great capabilities of quantum information storage. In this section, we shall discuss that such systems of sharply enhanced memory storage capacity are subjected to a universal phenomenon of *memory burden* [206]. Its essence is that stored information generically backreacts on the systems and ties it to its initial state. In order to demonstrate how this comes about, we will again turn to the prototype model (3.9):

$$\hat{H} = \left(1 - \frac{\hat{n}_0}{N}\right) \sum_{k=1}^K \epsilon_k \hat{n}_k + \epsilon_0 \hat{n}_0 + \dots, \quad (3.55)$$

where we expressed the small attractive coupling  $\alpha$  in terms of a large parameter  $N$ , i.e.  $\alpha = 1/N$ . We recall that  $\hat{n}_0$  is the master mode and that the quantities  $\epsilon_k$  represent the threshold excitation energies in the absence of interactions. Although the precise form of the spectrum is unimportant, it is usual for quantum field theoretic systems that the number of modes increases with  $\epsilon_k$ . We have ignored the interactions among the  $\hat{n}_k$ -modes, but their addition is trivial and changes nothing in the essence of the phenomenon (see [204–206, 208]).

As is clear from Eq. (3.10), the effective energy gap functions for the model (3.55) read

$$\mathcal{E}_k = \epsilon_k \left(1 - \frac{n_0}{N}\right). \quad (3.56)$$

In the following, we shall denote expectation values by the same symbols as operators but without hats, i.e. in this case  $n_0 = \langle \hat{n}_0 \rangle$ . In accordance with our previous analysis of the model (3.9), the energy gaps are large and therefore the memory storage capacity is poor around the vacuum,  $n_0 = 0$ . However, a nonzero expectation value of the master mode  $n_0$  lowers the effective energy thresholds and they collapse to zero for a critical value  $n_0 = N$ . At this point, the modes  $\hat{n}_k$  can therefore be excited at zero or very little energy cost. Thus, an exponentially large number of information patterns can be stored in the orthogonal microstates that represent different number eigenstates of the  $\hat{n}_k$ -modes,

$$|pattern\rangle_n \equiv |n_1, n_2, \dots, n_K\rangle. \quad (3.57)$$

Following [206], we shall call the corresponding Fock space the *memory space*. Its dimensionality scales exponentially with  $K$  and leads to the entropy (3.2). Moreover, we will refer to the  $\hat{n}_k$ -s as *memory modes*.

We can discover the memory burden effect when we introduce a second type of degrees of freedom, to which the  $\hat{n}_k$ -modes can decay. We denote their creation and annihilation operators by  $\hat{c}_k^\dagger, \hat{c}_k$ , where  $k = 0, 1, 2, \dots, K$ , and correspondingly the new number operator is  $\hat{m}_k = \hat{c}_k^\dagger \hat{c}_k$ . The  $\hat{b}$ - and  $\hat{c}$ -sectors commute with each other and also the  $\hat{c}$ -sector satisfies the usual algebra,  $[\hat{c}_j, \hat{c}_k^\dagger] = \delta_{jk}$  and  $[\hat{c}_j, \hat{c}_k] = [\hat{c}_j^\dagger, \hat{c}_k^\dagger] = 0$ . We shall introduce the simplest possible interaction that allows the particle number transfer between the two sectors, but other choices do not affect the outcome. Thus, we consider the following Hamiltonian:

$$\hat{H} = \left(1 - \frac{\hat{n}_0}{N}\right) \sum_{k=1}^K \epsilon_k \hat{n}_k + \epsilon_0 \hat{n}_0 + \sum_{k=0}^K \epsilon_k \hat{m}_k + \frac{1}{2N} \sum_{k=0}^K \epsilon_k (\hat{b}_k^\dagger \hat{c}_k + \hat{c}_k^\dagger \hat{b}_k). \quad (3.58)$$

As will become evident, the choice of the last coefficient is motivated by the analogy to de Sitter and black holes.

Our goal is to study how the memory pattern influences the decay of the  $\hat{n}_0$ -mode into  $\hat{m}_0$ . Namely, although the states  $|n_1, \dots, n_K\rangle$  are nearly-degenerate in energy, they exert different backreactions on the master mode  $\hat{n}_0$  for different values  $n_{k \neq 0}$ . This backreaction is measured by a quantity to that we shall refer as memory burden [206]. A general definition of it is:

$$\mu \equiv \sum_{k=1}^K n_k \frac{\partial \mathcal{E}_k}{\partial n_0}. \quad (3.59)$$

For the particular case of (3.56), this gives

$$\mu \equiv -\frac{\epsilon_{pat}}{N}, \quad (3.60)$$

where  $\epsilon_{pat} = \sum_{k=1}^K \epsilon_k n_k$  represents the would-be cost of the pattern in the state  $n_0 = 0$ , i.e.  $\epsilon_{pat}$  is an unactualized energy cost. It is important not to confuse this quantity with an actual energy cost of the pattern  $E_{pat} = \langle \hat{H} \rangle$ .

Now we study the time evolution of the system, where we use the initial state

$$|\text{in}\rangle = |N, n_1, \dots, n_K\rangle_n \otimes |0, 0, \dots, 0\rangle_m. \quad (3.61)$$

The resulting occupation numbers as functions of time are given by [206]

$$\begin{aligned} m_0(t) &= NA \sin^2\left(\frac{t}{\tau}\right), \\ n_0(t) &= N - m_0(t), \end{aligned} \quad (3.62)$$

where  $A \equiv 1/(1 + (\frac{N\mu}{\epsilon_0})^2)$  and  $\tau \equiv \frac{2N}{\epsilon_0} \sqrt{A}$ . These findings already suffice to capture the essence of the memory burden effect since the time evolutions for small and large values of  $\mu$  are very different. The critical value is set by  $|\mu| \approx \epsilon_0/N$ .

First, we investigate the case  $|\mu| \ll \epsilon_0/N$ . Then we have  $A \simeq 1$ , i.e.

$$n_0(t) \simeq N \left( 1 - \sin^2 \left( \frac{t\epsilon_0}{2N} \right) \right). \quad (3.63)$$

Thus, the occupation number of the master mode almost fully diminishes after the time  $t \simeq \pi N/\epsilon_0$ . As both the  $\hat{n}_{k \neq 0}$ - and  $\hat{m}_{k \neq 0}$ -modes are unoccupied, the system behaves as if they did not exist and effectively reduces to the two modes  $\hat{n}_0$  and  $\hat{m}_0$ . In contrast, in the case  $|\mu| \gg \epsilon_0/N$ , the master mode only loses the following small fraction of its initial occupation number:

$$\frac{\delta n_0}{n_0} = \frac{\epsilon_0^2}{N^2 \mu^2} = \left( \frac{\epsilon_0}{\epsilon_{\text{pat}}} \right)^2. \quad (3.64)$$

We conclude that the system is stabilized against the decay by the burden of its own memory.

The physics behind this phenomenon is very transparent. Any decay process that changes the value of  $n_0$  takes the system away from the critical state of enhanced memory capacity. As a result, the  $\hat{n}_{k \neq 0}$ -modes are no longer gapless and the stored memory pattern becomes very expensive. Indeed, a decrease of the master mode by  $\delta n_0 = N - n_0$  increases the actual energy cost of the pattern by  $\delta E_{\text{pat}} = \delta n_0 |\mu|$ . Thus, the fact that the stored quantum information becomes very expensive if  $n_0$  changes creates a memory burden that backreacts on the decay process and tries to shut it down.

One could wonder whether it is possible to avoid memory burden by offloading the expensive pattern into the  $\hat{m}_{k \neq 0}$ -sector together with the emitted  $\hat{m}_0$ -particles. However, this does not work due to an enormous energy splitting between the  $\hat{n}_k$ -modes and their  $\hat{m}_k$ -partners. We recall that the later modes are “normal”. This is clear from the explicit form of time evolutions, which for initial times takes the form,

$$\begin{aligned} m_k(t) &\simeq \frac{n_k}{N^2} \sin^2 \left( \frac{t\epsilon_k}{2} \right), \\ n_k(t) &= n_k - m_k(t). \end{aligned} \quad (3.65)$$

This shows that the pattern stored in  $\hat{n}_k$ -modes gets imprinted into the corresponding  $\hat{m}_k$ -modes with  $1/N^2$ -suppressed coefficients:

$$|\text{pattern}\rangle_m = \left| \frac{n_1}{N^2}, \dots, \frac{n_K}{N^2} \right\rangle_m. \quad (3.66)$$

We note that we deal with an intrinsically quantum effect due to finite  $N$ .

Having explained the essence of the memory burden phenomenon, it is important to study if a system can delay or even avoid the effect. Above all, this depends on two aspects. The first one is the form of the functional dependence of  $\mu$  on the

control parameter  $n_0$  in the vicinity of a given enhanced memory state  $n_0 = N$ . The second one is whether the memory enhancement takes place for some other values  $n_0 = N'$ .

In the model (3.55), we assumed a simple linear dependence of  $\mathcal{E}_k$  on  $n_0$ . However, the dependence may be nonlinear. For example, we can take

$$\hat{H} = \left(1 - \frac{\hat{n}_0}{N}\right)^p \sum_{k=1}^K \epsilon_k \hat{n}_k + \dots, \quad (3.67)$$

with  $p > 1$ . According to (3.59), the memory burden correspondingly depends on the departure  $\delta n_0$  from the critical state as

$$\mu = -p \left(\frac{\delta n_0}{N}\right)^{p-1} \frac{\epsilon_{\text{pat}}}{N}. \quad (3.68)$$

We see that for a nonlinear dependence of  $\mathcal{E}_k$  on  $n_0$ , the memory burden becomes a higher order effect in  $\delta n_0/N$  and the backreaction is delayed. Equating the burden (3.68) to the critical value  $\mu = -\epsilon_0/N$ , we get an upper bound on  $\delta n_0$  above which the backreaction from the memory burden cannot be ignored:

$$\delta n_0 = \left(\frac{\epsilon_0}{p\epsilon_{\text{pat}}}\right)^{1/(p-1)} N. \quad (3.69)$$

Since any nontrivial pattern satisfies  $\epsilon_{\text{pat}} > \epsilon_0$ , the absolute upper bound is  $\delta n_0 \approx N$ . Thus, at the latest after its *naive* half-decay time,

$$t_M \approx N\epsilon_0^{-1}, \quad (3.70)$$

the memory burden stabilizes the system, unless the memory pattern is offloaded beforehand.

As already discussed at length in [206], such offloading is possible if the system possesses another state of enhanced memory capacity, i.e. if for a different value  $n_0 = N'$ , a different set of modes  $\hat{n}'_{k'}$  becomes gapless. This can be modeled by the following Hamiltonian:

$$\hat{H} = \left(1 - \frac{\hat{n}_0}{N}\right)^p \sum_{k=1}^K \epsilon_k \hat{n}_k + \left(1 - \frac{\hat{n}_0}{N'}\right)^p \sum_{k'=1}^{K'} \epsilon'_{k'} \hat{n}'_{k'} + \dots, \quad (3.71)$$

where  $N' < N$  and “...” includes mixing with the  $\hat{c}$ -sector analogous to the terms in (3.58). In the theory (3.71), a new set of memory modes  $\hat{n}'_{k'}$  becomes gapless after changing  $n_0$  by  $\delta n_0 = N - N'$ . At the same time, the old ones  $\hat{n}_k$  acquire nonzero gaps given by  $\mathcal{E}_k = \epsilon_k \left(1 - N'/N\right)^p$ .

As soon as other sets of gapless modes exist, the system can avoid the memory burden by offloading the pattern from  $\hat{n}_k$ -modes into  $\hat{n}'_{k'}$ -ones. For the efficiency

of such a process, the mixing between  $\hat{b}_0$ - and  $\hat{c}_0$ -modes should be larger than  $1/N$ . Whether or not a full rewriting of a pattern from  $\hat{n}_k$ -modes into  $\hat{n}'_k$ -ones can be realized in a concrete system constitutes an interesting subject of future research. If such an offloading is possible, we remark that during this process the pattern becomes scrambled, i.e. the modes  $\hat{n}'_k$  become entangled with each other in the new state [206].

But even if such a continuous rewriting from one set of nearly-gapless modes to another one is possible, there are indications that the system will stabilize after a certain time. The reason is that generically the occupation of the initial pattern is  $\sum_{k=1}^K n_k \cong Kd/2$ , where  $d$  is the maximal occupation per  $\hat{n}_k$ -mode and we assumed an equal probability for all quantum states. Therefore, if there are less  $\hat{n}'_k$ -modes than  $\hat{n}_k$ -ones, which is usually the case since the system becomes less energetic, then offloading will stop as soon as the number of modes in the next level is too small. Therefore, the memory burden will stabilize the system at the latest when the number of nearly-gapless modes has reached

$$K_M \approx K, \quad (3.72)$$

i.e. when the entropy has decreased by a sizable fraction, e.g. by half.

In summary, a system can handle memory burden in two ways.

1. If  $p$  is sufficiently large, the memory burden can be postponed until  $\delta n_0$  becomes large. During this time, the pattern can stay encoded in the  $\hat{n}_k$ -modes.
2. Another option is that the memory burden gets eased by a continuous offloading of the pattern into other sets of modes, which become nearly-gapless for a smaller occupation number  $N'$  of the master mode  $\hat{n}_0$ . But also in this case, the system will stabilize at the latest when the number of accessible nearly-gapless modes has decreased by a significant fraction.

Finally, it is important to understand that the memory burden effect does not reduce to a statement that a system likes to be in a state of high entropy, although the two effects are related. The entropy is a property of a macrostate whereas memory burden is a property of a particular microstate from a given macro-ensemble, *a priori* unrelated to the number of fellow members in the ensemble. However, by simple combinatorics it is clear that for a system of microstate entropy  $S$ , the number of empty patterns is exponentially suppressed [206].

### 3.3.2 Application to de Sitter

We have described a universal phenomenon of memory burden, which appears to be generic in systems of enhanced memory storage capacity. As explained in section 1.4, de Sitter must be a prominent member of the above category because

of its Gibbons-Hawking entropy [32]. Since the modes that carry this information possess a gap that is much smaller than the smallest gap of any free mode (see Eq. (1.30)), it seems unavoidable that the nearly-gapless modes arise due to an interaction, i.e. that assisted gaplessness is at work. Just as in the case of a black hole, this resonates with the fact that gravity is bosonic and features attractive interactions.

If assisted gaplessness is operative in de Sitter, this means that the Gibbons-Hawking  $S$  entropy is attained because a certain control parameter  $n_0$  assumes a critical value  $N$ . Whatever the precise origin of  $n_0$  is, we know that classically the value of this control parameter is set by  $\Lambda$ , which is a fixed parameter of the theory. However, the quantum evolution caused by Gibbons-Hawking evaporation must lead to a change of  $n_0$  and thus to a subsequent departure from the enhanced memory state. This results in a memory burden effect which becomes strong after a certain critical time. It is important to note that for this conclusion, we do not need to know the precise origin of the degrees of freedom that are responsible for the Gibbons-Hawking entropy. The mere fact that they exist suffices.

First, we will consider the case in which no offloading of information to other levels takes place. We will explain shortly why rewriting can play no significant role for de Sitter. Then it is reasonable to assume that the critical time after which memory burden sets in must be bounded from above by the time during which the total energy radiated away via Gibbons-Hawking quanta becomes comparable to the energy of the entire Hubble patch. As is evident from Eq. (1.15), the latter is given by  $E_{dS} \approx SH$ , where  $H$  is the Hubble scale. Because each Hawking quantum carries an energy of order  $H$ , the effect gets strong at the latest after the total number of emitted quanta becomes on the order of  $S$ :

$$t_M^{\text{dS}} \approx SH^{-1}, \quad (3.73)$$

in agreement with Eq. (3.70). We set  $\hbar = 1$  from now. The timescale (3.73), after which memory burden has to set in at the latest, is the same as the quantum break-time of de Sitter (2.164) derived before. We will comment on the connection to quantum breaking shortly. We emphasize that at this point, we have not made any extra assumption that ties the control parameter  $n_0$  to the energy of the system. Our statement merely is that when a memory-storing device loses half of its mass, then typically also the control parameter  $n_0$  changes significantly. Therefore, it is pushed out of the original state of enhanced memory capacity. For this reason, we expect that the above qualitative picture is rather insensitive to the details of the microscopic theory.

Next, we will make the description of memory storage in de Sitter more quantitative by mapping it onto the model (3.55). In doing so, we will assume that the mode  $\hat{n}_0$  carries a significant part of the de Sitter energy. On the one hand, we make this assumption for simplicity. On the other hand, it is motivated by the connection to the corpuscular picture [44] of de Sitter, which we reviewed in

section 1.3.2 and further developed in section 2.4. Namely, it is very natural to identify the master mode  $\hat{n}_0$  with the soft graviton mode of wavelength  $R_H$  and occupation number  $N \approx S$  (see Eq. (2.124)). Still, the following discussion will be largely insensitive to this identification.

In the mapping onto the model (3.55), the first step is to set  $\epsilon_0 = H$  in order to match the energy of the emitted Gibbons-Hawking quanta. To obtain the correct rate, we must moreover choose  $N = S$  for the critical occupation number of the control mode. In this way, the state loses its total energy  $E_{dS} \approx SH$  after on the order of  $S$  quanta have been emitted. Finally, we need to reproduce the Gibbons-Hawking entropy. This determines the number of nearly-gapless modes  $\hat{n}_k$  as  $K = S$ . Having expressed all relevant quantities in terms of the Hubble scale  $H$  and the Gibbons-Hawking entropy  $S$ , we conclude that Eq. (3.70) reproduces the timescale (3.73), after which Gibbons-Hawking decay has to get stabilized because of memory burden. We emphasize that so far, our conclusions still do not rely on any assumption about the microscopic structure of de Sitter other than the requirement that it can describe the Gibbons-Hawking entropy.

Even without speculating where the critical modes  $\hat{n}_k$  come from, we can still gain some more valuable information. For example, these modes can be labeled by quantum numbers that are symmetries of the de Sitter space in the classical limit. In order to have a level degeneracy  $S$ , these modes must belong to very high angular harmonics, which leads to the estimate  $\epsilon_k \sim \sqrt{S} \epsilon_0$ . Of course, this scaling also fully matches the holographic counting [209, 210] naively applied to de Sitter, which implies the existence of  $S$  Planck wavelength qubits. We can thus estimate that the typical *unactualized* energy of a memory pattern carried by a de Sitter patch is equal to  $\epsilon_{\text{pat}} \sim S^{3/2} \epsilon_0 \approx E_{dS} \sqrt{S}$ . This scaling reveals how incredibly efficient de Sitter's memory storage is. A pattern that with naive counting would exceed the energy of the entire de Sitter patch by a factor of  $\sqrt{S}$  is stored at the same cost as the empty pattern. Of course, this is nothing more than restating the fact that an enormous microstate degeneracy must underlie the Gibbons-Hawking entropy.

Next, we turn to the question why rewriting cannot efficiently ease the memory burden in de Sitter. The reason is that the critical number  $N$  is set by the cosmological constant  $\Lambda$ . Consequently, it represents a *fixed parameter* of the theory. So even if de Sitter possesses information storing minima for other values of  $n_0 = N' \neq N$ , their energy must be an increasing function of  $|N - N'|$ . We can illustrate this with the help of the following Hamiltonian:

$$\hat{H} = \left(1 - \frac{\hat{n}_0}{N}\right)^p \sum_{k=1}^K \epsilon_k \hat{n}_k + \left( \left(1 - \frac{\hat{n}_0}{N'}\right)^p + \left(1 - \frac{\hat{n}_0}{N}\right)^q \right) \sum_{k'=1}^{K'} \epsilon'_{k'} \hat{n}'_{k'} + \dots, \quad (3.74)$$

where  $q > 0$ . The resulting energy landscape is plotted in Fig. 3.11.

Even if two sets of modes  $\hat{n}'_{k'}$  and  $\hat{n}_k$  could carry an identical pattern,  $n'_{k'} = n_k$ , its energy costs in the state  $n_0 = N'$  exceeds the one in the state  $n_0 = N$  by the

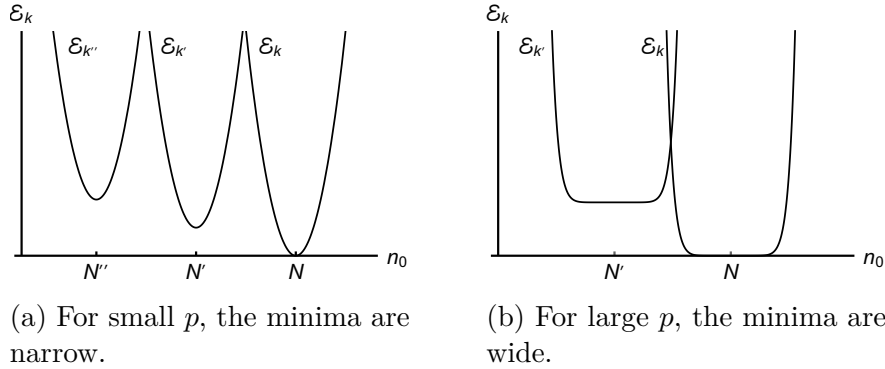


Figure 3.11: Highly schematic plots (for even values of  $p$ ) of the energy thresholds of the memory modes in a theory with cosmological constant. Only around a single value of  $n_0$ , gapless modes emerge.

amount  $E_{\text{pat}} = (1 - n_0/N)^q \epsilon_{\text{pat}}$ . So even if de Sitter keeps copying the pattern from one set of modes into another one, the memory burden increases steadily. Since we do not fully specify the microscopic theory of de Sitter, we cannot say what  $p$  and  $q$  are. However, a universal constraint on the parameters is that in the limit  $N \rightarrow \infty$ , only a single macrostate of enhanced memory capacity must exist. This is necessary for matching the semiclassical description of de Sitter. Under these circumstances, it is clear that the memory burden should set in at the latest for  $\delta n_0 \approx N$ , again reproducing Eq. (3.73). After this point, it strongly backreacts on the decay process.

It is important to note that the phenomenon of memory burden in de Sitter is purely quantum. In the (semi)classical limit (1.24), which implies  $N \rightarrow \infty$ , the information-carrying modes become exactly gapless and therefore the time it takes to resolve them diverges. Accordingly, the timescale (3.73) after which memory burden starts to backreact becomes infinite. Since memory burden is inaccessible in the (semi)classical limit, any classical metric description of de Sitter has to break down once the backreaction due to memory burden becomes significant. Therefore, we have rediscovered the phenomenon of de Sitter quantum breaking, which we have discussed in section 2.4, in the language of quantum information.

Finally, we turn to implications for inflation, where the information stored in the nearly-gapless modes – we shall call it *M-pattern* – can have crucial phenomenological implications. Since the *M-pattern* is purely quantum, the (semi)classical evolution cannot affect it. Therefore, it cannot be erased by slow-roll inflation so that it represents a cumulative quantum effect that is sensitive to the whole history of the Universe and not only the last 60 e-foldings. Therefore, the M-pattern is fully analogous to the  $1/N$ -effects discussed in section 2.4.6.

Both effects are easier to observe if inflation lasted longer. In particular, the M-pattern has the strongest influence if the end of inflation is maximally close to

quantum breaking.<sup>18</sup> The reason is that the M-pattern represents quantum hair stored in degrees of freedom that initially are essentially gapless. Therefore, it is not surprising that due to quantum uncertainty, a very long time is required for decoding a pattern of such a narrow energy gap. This means that the situation with the M-pattern is exactly opposite to other forms of preexisting information which are readily eliminated by a de Sitter phase. This creates the exciting prospect to search for imprints of the primordial M-pattern in observational data. Answering the question how to detect it requires a separate investigation.

### 3.3.3 Application to Black Holes

In great analogy to de Sitter, black holes possess an enhanced information storage capacity due to their Bekenstein-Hawking entropy (1.2). Therefore, they are also subjected to the phenomenon of memory burden. As for de Sitter, we can make the generic argument that at the latest after a black hole has lost half of its mass, the backreaction due to memory burden becomes strong:

$$t_M^{\text{bh}} \approx S r_g, \quad (3.75)$$

where we recall that  $r_g = M/M_p^2$  corresponds to the Schwarzschild radius and  $M$  is the black hole mass. Note that this formula holds irrespective of whether or not rewriting takes place in a black hole. If it does not, it is due to Eq. (3.70). If it does, it follows from Eq. (3.72) and the fact that after losing half its mass, the black hole has lost more than half its entropy. So as for de Sitter, the backreaction due to memory burden sets in at the latest after its naive half lifetime.

We can make this argument without assuming that the control parameter  $n_0$  represents the black hole mass. When we add this assumption, it is straightforward to map a black hole on the model (3.55), which leads to the identifications  $\epsilon_0 = r_g^{-1}$ ,  $N = S$  as well as  $K = S$ . Clearly, both Eq. (3.70) and (3.72) support the bound (3.75). Moreover, the resulting microscopic picture of the black hole fully resonates with the quantum N-portrait, which we outlined in section 1.3.1. In this picture, the black hole consists of  $N \approx S$  soft gravitons of wavelength  $r_g$ .

Additionally, the relationship to quantum breaking is full analogous to the de Sitter case. Since memory burden is a fully quantum phenomenon, this means that any (semi)classical description has to break down once it sets in. Therefore, it is not surprising that the quantum break-time (1.13) of a black hole is given by the timescale (3.75). At this point, the black hole either gets stabilized or it has to start releasing information, in accordance with Page's argument [42].

---

<sup>18</sup>This is independent of the question if quantum breaking in de Sitter leads to an inconsistency. As explained in section 2.4.6, any inflationary scenario that experiences quantum breaking is highly disfavored since the semiclassical description of the late inflationary epoch shows no conflict with observations.

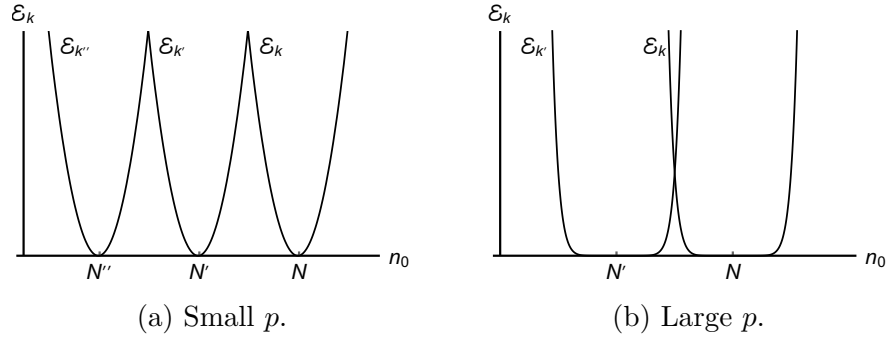


Figure 3.12: Highly schematic plots (for even values of  $p$ ) of the energy thresholds of the memory modes for the case of black holes. Multiple minima exist, corresponding to different possible black hole masses.

However, there is one crucial difference between black holes and de Sitter. Whereas a theory with cosmological constant only allows for a single de Sitter state, one and the same theory features a multitude of different black hole solutions. Correspondingly, numerous sets of modes  $\hat{n}_k, \hat{n}'_k, \dots$ , which become gapless at different points, must exist. In this energy landscape, which is plotted in Fig. 3.12, rewriting of a pattern between different sets of modes can play a crucial role for black hole evolution, as was suggested in [206]. In particular, it can lead to the scrambling of information.



# Chapter 4

## Infrared Physics and Information

In the previous chapter, we concluded that nearly-gapless modes play a crucial role for the storage of information. For a long time, it has also been known that understanding the behavior of soft modes is important for the study of scattering processes in gapless theories.<sup>1</sup> Therefore, we will investigate in this chapter if there is a connection between these two subject areas.

We begin in section 4.1 by reviewing known results in infrared physics. The starting point is the long-known finding that in gapless theories, soft loops lead to vanishing amplitudes for any nontrivial scattering process [57]. There are two procedures to deal with these so-called infrared divergences and to obtain nonzero rates: the inclusive formalism [57–59], in which the emission of soft modes is taken into account, and the dressed formalism [60–65], in which all charged asymptotic states are dressed with soft modes. During the review of these approaches, we also comment on the relationship of the soft photon/graviton theorem and charge conservation [218], which has recently received renewed attention in a different context [219].

In section 4.2, we propose a physical criterion to distinguish between soft emission and soft dressing. It enables us to develop a new approach to deal with infrared divergences, which is able to simultaneously describe both the emission of soft radiation and the dressing by soft modes. In this *combined formalism*, we obtain the same finite rates that the two preexisting procedures yield.

In section 4.3, we go one step further by studying the density matrix of the final state. Its diagonal contains the known rates but the off-diagonal elements encode information about the coherence of the final state. Our study is motivated by the recent finding that the inclusive and dressed formalisms can only lead to full coherence or full decoherence [66, 67]. In contrast, an important strength of the combined formalism is that it leads to a small but nonzero amount of decoherence, as we expect it to occur due to the emission of unobserved soft radiation.

---

<sup>1</sup>In this context, any mode with an energy that is much smaller than the characteristic energy of the process is soft.

In section 4.4, we come to implications of infrared physics for black holes. First, we examine the recent suggestion that the emission of infrared radiation could account for the whole information of a black hole [56]. However, our findings imply that this is not the case, but that it only leads to a subleading correction. Secondly, we study the relationship of asymptotic symmetries of gravity at null infinity, namely the BMS group [68–70], and black holes. We are motivated by the recently discussed connection of the soft graviton theorem and BMS transformations [220] and in particular by the suggestion that asymptotic symmetries could assume the role of classical black hole hair [221–224]. In contrast, we show that they cannot lead to observable features, but that they only represent a bookkeeping tool.

This chapter is based on the paper [2], which is joint work with Cesar Gomez, as well as the papers [4, 6], which are joint work with Cesar Gomez and Raoul Letschka. To a large extent, this chapter is an ad verbatim reproduction of these publications. Sections 4.1, 4.2 and 4.3 follow [6], where section 4.3 additionally uses material from [4]. Section 4.4 and appendix A.3, which pertains to the present chapter, follow [2].

## 4.1 Review of Infrared Physics

### 4.1.1 Tree Level Processes: Soft Theorem

We will begin by studying tree level processes, which are free of infrared divergences. As a first step, we review the derivation of the soft photon/graviton theorem [58, 59, 218]. Since the situation is fully analogous in gravity and in QED, we will confine ourselves to QED for calculations and only comment on gravity. We consider an arbitrary scattering process  $\alpha \rightarrow \beta$ , where initial and final states may contain both charged particles and photons. Our goal is to investigate what happens when we add a soft photon in the final state:  $\alpha \rightarrow \beta + \gamma_1$ . The additional soft photon can be emitted from any electron line. It turns out, however, that only the emission from external legs is relevant since only such a process leads to a divergent contribution. We will call such photons *IR-modes*.

In contrast, soft photons that are emitted from internal lines are *non-IR-modes*. The comparison between IR-modes and non-IR-modes is displayed in Fig. 4.1. Throughout we will not consider non-IR-modes. So the term soft will always refer to soft IR-modes.

As a first step, we study the emission of a soft photon from a fixed external leg with momentum  $p$ . For concreteness, we take it to be ingoing. We assume that the process  $\alpha \rightarrow \beta$  is described by the amplitude  $S_{\alpha, \beta} = \dots \Gamma(p; q) u_p$ , where  $u_p$  is the spinor of the ingoing electron on which we focus and  $\Gamma(p; q)$  is an arbitrary vertex function. The rest of the diagram, indicated by the dots, is not essential for our considerations. Then the amplitude  $S_{\alpha, \beta \vec{k}}^{(l), p}$  that includes the emission of the soft photon of momentum  $\vec{k}$  and polarization  $l$  from the electron with momentum

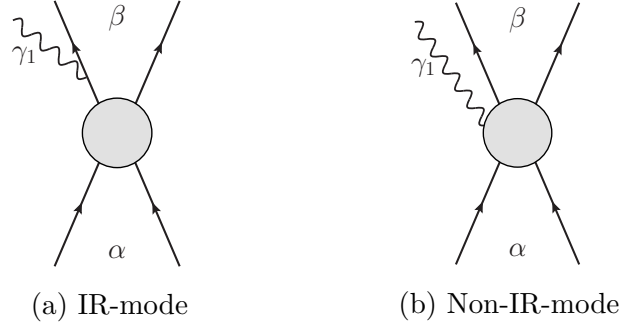


Figure 4.1: Comparison of IR-radiation and non-IR radiation. A mode  $\gamma_1$  is IR if it is emitted from an external line.

$p$  is

$$S_{\alpha, \beta \vec{k}}^{(l), p} = \dots \Gamma(p - k; q) \frac{\not{p} - \not{k} + m}{(p - k)^2 - m^2 + i\epsilon} e^{-\frac{\not{\epsilon}_{\vec{k}, l}^*}{\sqrt{2(2\pi)^3 |\vec{k}|}} u_p}. \quad (4.1)$$

Apart from the additional electron propagator and an additional vertex, this amplitude also contains the polarization vector  $\epsilon_{\vec{k}, l}^\mu$  of the photon as well as the normalization  $1/\sqrt{2(2\pi)^3 |\vec{k}|}$  of the final photon. The star denotes complex conjugation. Since the momentum of the photon is small, the electron propagator is almost on-shell. We can extract the leading singularity,

$$\frac{\not{p} - \not{k} + m}{(p - k)^2 - m^2 + i\epsilon} \not{\epsilon}_{\vec{k}, l}^* u_p = \frac{2p \cdot \epsilon_{\vec{k}, l}^* - \not{k} \not{\epsilon}_{\vec{k}, l}^*}{(p - k)^2 - m^2 + i\epsilon} u_p \cong \frac{p \cdot \epsilon_{\vec{k}, l}^*}{-p \cdot k} u_p, \quad (4.2)$$

where we used the Dirac equation in the first equality and focused on the leading singularity for small  $|\vec{k}|$  in the second step. Then the diagram gives

$$S_{\alpha, \beta \vec{k}}^{(l), p} = \frac{p \cdot \epsilon_{\vec{k}, l}^*}{-p \cdot k} \frac{e}{\sqrt{2(2\pi)^3 |\vec{k}|}} S_{\alpha, \beta}, \quad (4.3)$$

where we used that  $\Gamma(p - k; q) \cong \Gamma(p; q)$  to leading order for small  $|\vec{k}|$ . The important observation at this point is that the contribution of the soft photon factorizes from the rest of the diagram. Additionally, it only depends on properties of the external electron but not on any other details of the process.

We can repeat the same procedure for all external legs so that we obtain the amplitude  $S_{\alpha, \beta \vec{k}}^{(l)}$  for the emission of a soft photon:

$$S_{\alpha, \beta \vec{k}}^{(l)} \stackrel{|\vec{k}| \rightarrow 0}{\cong} \frac{\mathcal{F}_{\alpha, \beta}^{(l)}(\vec{k})}{|\vec{k}|^{1/2}} S_{\alpha, \beta}, \quad (4.4)$$

where we introduced the notation

$$\mathcal{F}_{\alpha,\beta}^{(l)}(\vec{k}) = \sum_{n \in \alpha,\beta} \frac{e_n \eta_n}{\sqrt{2(2\pi)^3}} \frac{p_n \cdot \varepsilon_{l,\vec{k}}^*}{p_n \cdot k}. \quad (4.5)$$

Here  $e_n$  is the charge of the  $n^{\text{th}}$  particle and  $p_n$  is its momentum. The sum includes all incoming and outgoing charged particles. Moreover,  $\eta_n = +1$  or  $-1$  for an outgoing or incoming charged particle, respectively. The reason for the sign difference is that emission from an incoming particle takes away momentum from the electron propagator whereas emission from an outgoing one adds momentum. Analogously, one can consider the absorption of a soft photon. The same argument as above yields

$$S_{\alpha\vec{k},\beta} \stackrel{|\vec{k}| \rightarrow 0}{\simeq} \frac{-\mathcal{F}_{\alpha,\beta}^{(l)*}(\vec{k})}{|\vec{k}|^{1/2}} S_{\alpha,\beta}, \quad (4.6)$$

i.e. up to a sign and complex conjugation, absorption and emission give the same contribution.

In gravity, a fully analogous argument gives the same relation (4.4), but now the soft factor is

$$\mathcal{F}_{\alpha,\beta}^{(l)}(\vec{k}) = \sum_{n \in \alpha,\beta} \frac{\sqrt{8\pi G_N} \eta_n p_n^\mu p_n^\nu \varepsilon_{l,\vec{k} \mu\nu}^*}{\sqrt{2(2\pi)^3} p_n \cdot k}, \quad (4.7)$$

where  $\varepsilon_{l,\vec{k} \mu\nu}$  corresponds to the polarization tensor of a graviton.

### 4.1.2 Charge Conservation

The meaning of the soft photon/graviton theorem is manifold. A very interesting early application [218] was to derive charge conservation from it. To this end, only one additional ingredient is needed, namely Lorentz invariance. In a pure  $S$ -matrix formulation, one can show that Lorentz invariance implies that any amplitude must be invariant under the shift [218],

$$\varepsilon_{l,\vec{k}}^\mu \rightarrow \varepsilon_{l,\vec{k}}^\mu + \lambda_l(\vec{k}) k^\mu, \quad (4.8)$$

where  $\lambda_l(\vec{k})$  is an arbitrary function. We will not repeat the argument of [218], but simply note that invariance under (4.8) can also be derived as a straightforward consequence of gauge invariance, i.e. the decoupling of longitudinal photons. Of course, the latter argument is less powerful since it requires a Lagrangian description of the system. Now we can plug the shift (4.8) into the soft factor (4.5). Invariance then implies that

$$\lambda_l^*(\vec{k}) \sum_{n \in \alpha,\beta} e_n \eta_n = 0, \quad (4.9)$$

i.e. that the total incoming charge must be equal to the total outgoing charge. In this way, one can derive charge conservation in a pure  $S$ -matrix formulation. In gravity, the same argument yields the equality of inertial and gravitational mass [218].

### Comment on New Conservation Laws

Recently, it has been proposed that previously unknown symmetries exist in QED and gravity [219,225–231]. These arguments were based on considerations of asymptotic symmetries, in particular the BMS-group [68–70] in gravity. We will further discuss aspects of these asymptotic symmetries in section 4.4.2. Already now, however, we want to point out that the proposed symmetries do not contain more information than the soft theorems themselves. Since absorption and emission of soft photons give analogous contributions, we can rewrite the soft theorem as

$$\lim_{|\vec{k}| \rightarrow 0} \langle \beta | \hat{a}_k \hat{S} - \hat{S} \hat{a}_k^\dagger | \alpha \rangle = \frac{\mathcal{F}_{\alpha,\beta}^{(l)}(\vec{k}) + \mathcal{F}_{\alpha,\beta}^{(l)*}(\vec{k})}{|\vec{k}|^{1/2}} \langle \beta | \hat{S} | \alpha \rangle. \quad (4.10)$$

Moreover, we can define the operator  $\hat{Q}$  as

$$\hat{Q} = \int d^3 \vec{k} f(\vec{k}) \sum_l \left( \hat{a}_{l,\vec{k}}^\dagger - \int d^3 \vec{p} \hat{\rho}(\vec{p}) \left( \frac{p \cdot (\varepsilon_{l,\vec{k}} + \varepsilon_{l,\vec{k}}^*)}{\sqrt{2(2\pi)^3 |\vec{k}| p \cdot k}} \right) \right), \quad (4.11)$$

where an arbitrary function  $f(\vec{k})$  parametrizes the integration over different possible momenta  $\vec{k}$  of the soft photon, and

$$\hat{\rho}(\vec{p}) = e \sum_s \left( \hat{b}_{s,\vec{p}}^\dagger \hat{b}_{s,\vec{p}} - \hat{d}_{s,\vec{p}}^\dagger \hat{d}_{s,\vec{p}} \right) \quad (4.12)$$

is the charge density operator for electrons and positrons, with  $\hat{b}_{s,\vec{p}}^\dagger / \hat{d}_{s,\vec{p}}^\dagger$  the creation operators for an electron/positron of spin  $s$  and momentum  $\vec{p}$ . Up to a derivative with respect to angles and transformation into position space, this operator appears to be equivalent to the charges considered in [219,225–231]. There, the first term is dubbed soft charge and the second one hard charge. Now we can write (4.10) as

$$\langle \beta | \hat{Q}^\dagger \hat{S} - \hat{S} \hat{Q} | \alpha \rangle = 0. \quad (4.13)$$

In this way, we reproduce the Ward identities of [219,225–231]. However, this is simply a formal rewriting of the soft theorem. It does not contain more information than the fact that soft photons decouple, i.e. that the amplitude for emission or absorption of a soft photon only depends on initial and final charged states but not on any other properties of the process.

One might be tempted to promote equation (4.13) to an operator identity since in that case,  $\hat{Q}$  would correspond to a nontrivial conserved charge, i.e. imply a new conservation law. However, it is easy to show that in general

$$\hat{Q}^\dagger \hat{S} - \hat{S} \hat{Q} \neq 0. \quad (4.14)$$

We can verify the former equation by contradiction. Assuming  $\hat{Q}^\dagger \hat{S} - \hat{S} \hat{Q} = 0$ , it would follow that  $\langle \beta | \hat{Q} | \beta \rangle = \langle \alpha | \hat{S}^\dagger \hat{Q} \hat{S} | \alpha \rangle = \langle \alpha | \hat{Q}^\dagger | \alpha \rangle$ . Plugging in the definition (4.11) and using the fact that the asymptotic states  $|\alpha\rangle$  and  $|\beta\rangle$  do not contain soft photons, we would deduce for arbitrary  $\vec{k}$  and arbitrary polarization that

$$\mathcal{F}_{\alpha,\beta}^{(l)}(\vec{k}) + \mathcal{F}_{\alpha,\beta}^{(l)*}(\vec{k}) = 0. \quad (4.15)$$

However, this equality is only fulfilled when  $\mathcal{F}_{\alpha,\beta}^{(l)}(\vec{k}) = 0$ . Since this condition will be of further importance, we will briefly stop to analyze it. Using the integral (4.23), which we shall discuss shortly, it is easy to show that it holds if and only if the charge of the initial state  $|\alpha\rangle$  and the charge of the final state  $|\beta\rangle$  match at each angle [66]. When the latter condition is fulfilled, we shall call the two states equivalent,  $|\alpha\rangle \approx |\beta\rangle$ . This condition is slightly weaker than the equality of two states since, for example, a positron and an electron at exactly the same angle are equivalent but not equal to a state without charged particles. However, such states form a set of measure zero of all possible states. Therefore, we can call a scattering process with equivalent initial and final states trivial. In summary, we conclude that  $\mathcal{F}_{\alpha,\beta}^{(l)}(\vec{k}) = 0$  only holds when  $|\alpha\rangle \approx |\beta\rangle$ . As this is not true in any nontrivial scattering process, it follows by contradiction that in general we have (4.14). In particular, we have that

$$\hat{Q}^\dagger \hat{S} - \hat{S} \hat{Q} = 0 \quad \Leftrightarrow \quad \alpha \approx \beta. \quad (4.16)$$

The operator  $\hat{Q}$  only corresponds to a conserved charge for processes of trivial forward scattering.

Finally, we want to remark that the well-known decoupling of soft photons and gravitons can be interpreted as a symmetry. We refer the reader to [232–236] for the argument, the physical upshot of which can be summarized as follows: We consider an arbitrary scattering process with initial state  $|\alpha\rangle$  and final state  $|\beta\rangle$ . Now we add a soft mode of momentum  $\vec{k}$  to the initial state:  $\hat{a}_{\vec{k}}^\dagger |\alpha\rangle$ . In this situation, there always exists a finite energy scale – which depends on the process in question – below which the soft excitation decouples. Thus, if we choose the energy of the soft mode below this energy scale, it cannot interact with the other particles and the final state simply is  $\hat{a}_{\vec{k}}^\dagger |\beta\rangle$ . In this sense, the well-known decoupling of soft gravitons and photons can be interpreted as symmetry of a scattering process. However, this symmetry bears no relevance beyond the decoupling of soft modes. In particular, this phenomenon cannot account for the information of a black hole (see section 4.4.1).

### 4.1.3 Loop Corrections: Infrared Divergences

So far, we have discussed the soft theorem for tree level processes. Its real power, however, only comes into play once we include loop corrections, for they lead to infrared divergences. Therefore, we will again consider the arbitrary process  $\alpha \rightarrow \beta$  but now study loop corrections in order to review the results of [57–59]. As before, we are solely interested in divergent contributions. It turns out that they only come from loops among external legs. Moreover, only the soft part of the integration over the loop momentum matters, i.e. we only integrate loops up to a cut-off scale  $\Lambda$  that cannot exceed the typical energy scale of the process, e.g. the center-of-mass energy.

As a first step, we compute the contribution of one soft loop. Initially, we consider the loop between two fixed external legs with momenta  $p_1$  and  $p_2$ . We get

$$\begin{aligned}
S_{\alpha,\beta}^{1\text{loop}pp'} &= \int_{\lambda}^{\Lambda} d^4k \dots \Gamma_1(p_1 - \eta_1 k; q_1) \frac{\not{p}_1 - \eta_1 \not{k} + m}{(p_1 - \eta_1 k)^2 - m^2 + i\epsilon} e_1 \gamma^{\mu} u_{p_1} \\
&\cdot \Gamma_2(p_2 + \eta_2 k; q_2) \frac{\not{p}_2 + \eta_2 \not{k} + m}{(p_2 + \eta_2 k)^2 - m^2 + i\epsilon} e_2 \gamma^{\nu} u_{p_2} \\
&\cdot \frac{-i\eta_{\mu\nu}}{(2\pi)^4(k^2 - i\epsilon)}, \tag{4.17}
\end{aligned}$$

where we introduced an IR-regulator  $\lambda$  that will be set to zero in the end. Moreover,  $\eta_1$  and  $\eta_2$  account for the fact that the electrons may be outgoing or ingoing. Approximating the two electron propagators in the soft limit as in (4.2), this gives

$$S_{\alpha,\beta}^{1\text{loop}pp'} = S_{\alpha,\beta} e_1 e_2 \int_{\lambda}^{\Lambda} d^4k \frac{p_1^{\mu}}{-\eta_1 p_1 \cdot k + i\epsilon} \frac{p_2^{\nu}}{\eta_2 p_2 \cdot k + i\epsilon} \frac{-i\eta_{\mu\nu}}{(2\pi)^4(k^2 - i\epsilon)}. \tag{4.18}$$

As for the case of emission, the important point is that the contribution of the soft part of the loop integral factorizes. Since only the first term in  $1/(k^2 - i\epsilon) = i\pi\delta(k^2) + \text{PV}1/k^2$  gives a divergent contribution,<sup>2</sup> we arrive at

$$S_{\alpha,\beta}^{1\text{loop}pp'} = S_{\alpha,\beta} \frac{-e_1 e_2}{2(2\pi)^3} \int_{\lambda}^{\Lambda} \frac{d^3\vec{k}}{|\vec{k}|} \frac{\eta_1 \eta_2 p_1 \cdot p_2}{p_1 \cdot k p_2 \cdot k}. \tag{4.19}$$

Next we sum over all possible soft loops between external legs,

$$S_{\alpha,\beta}^{1\text{loop}} = S_{\alpha,\beta} \frac{1}{2} \int_{\lambda}^{\Lambda} \frac{d^3\vec{k}}{|\vec{k}|} \frac{-1}{2(2\pi)^3} \sum_{n,m \in \alpha,\beta} \frac{\eta_n \eta_m e_n e_m p_n \cdot p_m}{p_n \cdot k p_m \cdot k}, \tag{4.20}$$

where the additional factor of  $1/2$  accounts for the fact that each loop is counted twice in the sum. Since  $\sum_l \varepsilon_{\vec{k},l}^{\mu} \varepsilon_{\vec{k},l}^{\nu} = \eta^{\mu\nu}$ , we observe that we can write the result

<sup>2</sup>Here PV denotes the principal value.

in terms of the soft factor (4.5), which we encountered in the soft photon theorem:

$$S_{\alpha,\beta}^{1\text{loop}} = S_{\alpha,\beta} \frac{-1}{2} \int_{\lambda}^{\Lambda} \frac{d^3 \vec{k}}{|\vec{k}|} \sum_l |\mathcal{F}_{\alpha,\beta}^{(l)}(\vec{k})|^2. \quad (4.21)$$

The radial integral is straightforward,

$$\int_{\lambda}^{\Lambda} \frac{d^3 \vec{k}}{|\vec{k}|} \sum_l |\mathcal{F}_{\alpha,\beta}^{(l)}(\vec{k})|^2 = B_{\alpha,\beta} \ln \frac{\Lambda}{\lambda}, \quad (4.22)$$

and the angular part gives

$$\begin{aligned} B_{\alpha,\beta} &= \frac{1}{2(2\pi)^3} \sum_{n,m \in \alpha,\beta} \int d^2 \Omega \frac{\eta_n \eta_m e_n e_m p_n \cdot p_m}{p_n \cdot \hat{k} p_m \cdot \hat{k}} \\ &= -\frac{1}{8\pi^2} \sum_{n,m \in \alpha,\beta} \eta_n \eta_m e_n e_m \beta_{nm}^{-1} \ln \left( \frac{1 + \beta_{nm}}{1 - \beta_{nm}} \right), \end{aligned} \quad (4.23)$$

where  $\hat{k}$  indicates the normalized photon vector and  $\beta_{nm}$  is the relative velocity:

$$\beta_{nm} = \left( 1 - \frac{m_n^2 m_m^2}{(p_n \cdot p_m)^2} \right)^{1/2}. \quad (4.24)$$

Clearly,  $B_{\alpha,\beta}$  is nonnegative. Moreover, as already discussed at the end of section 4.1.2, it is zero only if initial and final state are equivalent, i.e. when their charge matches at each angle. Finally, we obtain:

$$S_{\alpha,\beta}^{1\text{loop}} = S_{\alpha,\beta} \frac{-1}{2} B_{\alpha,\beta} \ln \frac{\Lambda}{\lambda}. \quad (4.25)$$

In the limit when the regulator vanishes,  $\lambda \rightarrow 0$ , we get  $S_{\alpha,\beta}^{1\text{loop}} \rightarrow -\infty$  for any nontrivial scattering process. This means that perturbation theory breaks down and we have to resum all orders in the coupling.

Whereas this task is not doable in general, it turns out that the resummation can be performed for soft loops. The reason is that in the soft limit, the factorization of soft loops persists to higher orders. For example, for two loops with soft momenta  $\vec{k}_1$  and  $\vec{k}_2$ , one observes [59]:

$$\begin{aligned} &\frac{1}{\eta_1 p_1 \cdot k_1 + i\epsilon} \cdot \frac{1}{\eta_1 p_1 \cdot (k_1 + k_2) + i\epsilon} + \frac{1}{\eta_1 p_1 \cdot k_2 + i\epsilon} \cdot \frac{1}{\eta_1 p_1 \cdot (k_2 + k_1) + i\epsilon} \\ &= \frac{1}{\eta_1 p_1 \cdot k_1 + i\epsilon} \cdot \frac{1}{\eta_1 p_1 \cdot k_2 + i\epsilon}. \end{aligned} \quad (4.26)$$

Generalizing this formula inductively to higher orders, we conclude that the contribution of exactly  $n$  soft loops is

$$S_{\alpha,\beta}^{n\text{loop}} = S_{\alpha,\beta} \frac{\left( -\frac{1}{2} B_{\alpha,\beta} \ln \frac{\Lambda}{\lambda} \right)^n}{n!}, \quad (4.27)$$

where the factor  $1/n!$  accounts for the overcounting of permutations of the soft loops. Therefore, we can resum the contribution of soft loops to all orders:

$$S_{\alpha,\beta}^{\text{loop}} = S_{\alpha,\beta} \left( \frac{\lambda}{\Lambda} \right)^{B_{\alpha,\beta}/2}. \quad (4.28)$$

When we send  $\lambda \rightarrow 0$ , we observe that the amplitude for any nontrivial scattering process, in which  $\alpha \not\approx \beta$ , vanishes. This is the famous infrared divergence.<sup>3</sup> However, it is important to point out that this does not hint towards a problem of the theory. Rather, it is a physical result. It states that no nontrivial scattering process can take place without the emission of soft photons.

In gravity, we obtain a formula analogous to (4.28), but now the exponent is given by

$$B_{\alpha,\beta} = \frac{G_N}{2\pi} \sum_{n,m \in \alpha,\beta} \eta_n \eta_m m_n m_m \frac{1 + \beta_{nm}^2}{\beta_{nm} (1 - \beta_{nm}^2)^{1/2}} \ln \left( \frac{1 + \beta_{nm}}{1 - \beta_{nm}} \right), \quad (4.29)$$

where  $m_n$  is the mass of the  $n^{\text{th}}$  particle.

#### 4.1.4 Taking Emission into Account: Inclusive Formalism

The most straightforward way to interpret the missing photons is in terms of soft bremsstrahlung [57–59]. Then – as just said – the vanishing of any nontrivial amplitude due to soft loops indicates that no momentum transfer can happen without the emission of soft photons. Therefore, it is natural to include the emission of any photon state whose total energy is below some small scale  $\epsilon$ , which we can identify as resolution scale of a detector in an experimental setup. Since this yields an inclusive rate, we can call this approach *inclusive formalism*. We compute:

$$\Gamma_{\alpha,\beta}^{\text{emission}} = \sum_n \frac{1}{n!} \left( \prod_{i=1}^n \int_{\lambda}^{\epsilon} d^3 \vec{k}_i \sum_{l_i} \right) \theta(\epsilon - \sum_{j=1}^n |\vec{k}_j|) \left| \langle 0 | \hat{a}_{l_1, \vec{k}_1} \dots \hat{a}_{l_n, \vec{k}_n} \otimes \langle \beta | \right) \hat{S} | \alpha \rangle \right|^2, \quad (4.30)$$

where  $n$  sums over the number of emitted soft photons. Using the soft theorem (4.4), it is straightforward to conclude that

$$\Gamma_{\alpha,\beta}^{\text{emission}} = \sum_n \frac{1}{n!} \left( \prod_{i=1}^n \int_{\lambda}^{\epsilon} \frac{d^3 \vec{k}_i}{|\vec{k}_i|} \sum_{l_i} |\mathcal{F}_{\alpha,\beta}^{(l_i)}(\vec{k}_i)|^2 \right) \theta(\epsilon - \sum_{j=1}^n |\vec{k}_j|) |S_{\alpha,\beta}|^2. \quad (4.31)$$

The same integral appears as in the computation of soft loops. Using the result (4.22), we obtain

$$\Gamma_{\alpha,\beta}^{\text{emission}} = \left( \frac{\epsilon}{\lambda} \right)^{B_{\alpha,\beta}} f(B_{\alpha,\beta}) |S_{\alpha,\beta}|^2. \quad (4.32)$$

<sup>3</sup>Since the amplitude vanishes, one may wonder why the terminology “divergence” is used. The reason probably is that before resummation, each order of perturbation theory diverges.

The additional function  $f(B_{\alpha,\beta})$  is due to energy conservation, which is encoded in the  $\theta$ -function [58, 59]:

$$f(x) = \frac{e^{-\gamma x}}{\Gamma(1+x)}. \quad (4.33)$$

Here  $\gamma$  is Euler's constant and  $\Gamma$  is the gamma function. For small  $x$ , it can be approximated as

$$f(x) = 1 - \frac{\pi^2}{12}x^2. \quad (4.34)$$

Therefore, its effect is subleading in this regime. For large  $x$ , it scales as

$$f(x) \sim \frac{1}{x!}. \quad (4.35)$$

In this parameter range, it leads to a sizable suppression but no definite statement about the rate can be made due to lack of knowledge about  $|S_{\alpha,\beta}|^2$  [58].

Now we can combine the contributions (4.28) due to soft loops and (4.32) from soft emission to obtain

$$\Gamma_{\alpha,\beta}^{\text{inclusive, tot}} = \left(\frac{\epsilon}{\Lambda}\right)^{B_{\alpha,\beta}} f(B_{\alpha,\beta}) |S_{\alpha,\beta}|^2. \quad (4.36)$$

The IR-regulator  $\lambda$  has dropped out so  $\Gamma_{\alpha,\beta}^{\text{inclusive}}$  is IR-finite. This is the well-known central result of IR-physics [57–59]: Taking into account soft emission leads to an IR-finite rate. Moreover, the dependence of the rate (4.36) on the resolution scale is sensible. It vanishes in the limit of zero resolution,  $\epsilon \rightarrow 0$ , because then no bremsstrahlung can be emitted. Moreover, it can reproduce the spectrum of classical bremsstrahlung. To first order in  $\alpha$ , the differential rate scales as  $d\Gamma_{\alpha,\beta}^{\text{inclusive, tot}}/d\epsilon \propto B/\epsilon$ . Consequently, the emitted energy per frequency is constant, as we expect it from the classical calculation.

#### 4.1.5 Modifying Asymptotic States: Dressed Formalism

Soon after Weinberg finished his seminal work on the inclusive formalism, a different take on infrared divergences was proposed by Chung [60]. His goal was to avoid the inclusion of radiation but to modify the asymptotic charged states by dressing them with soft photons in such a way that IR-finite amplitudes can be obtained. In what follows, we call this approach *dressed formalism*. We will first focus on the computation, i.e. simply assume an appropriate dressing of the asymptotic states but not motivate it. Afterwards, we will derive the modification of the asymptotic states from first principles.

In order to determine an appropriate dressing of charged states, we start from the observation that we can split the soft factor  $\mathcal{F}_{\alpha,\beta}^{(l)}(\vec{k})$  in a part that depends only on the initial state and in another one that depends only on the final state:

$$\mathcal{F}_{\alpha,\beta}^{(l)}(\vec{k}) = \mathcal{F}_{\beta}^{(l)}(\vec{k}) - \mathcal{F}_{\alpha}^{(l)}(\vec{k}), \quad (4.37)$$

where accordingly

$$\mathcal{F}_\alpha^{(l)}(\vec{k}) = \sum_{n \in \alpha} \frac{e_n}{\sqrt{2(2\pi)^3}} \frac{p_n \cdot \varepsilon_{l, \vec{k}}^*}{p_n \cdot \vec{k}}, \quad (4.38)$$

and  $\mathcal{F}_\beta^{(l)}(\vec{k})$  is defined analogously. Using these functions, we introduce the coherent state

$$|D(\alpha)\rangle_\lambda^r := \exp\left\{-\frac{1}{2}B_\alpha \ln \frac{r}{\lambda}\right\} \exp\left\{\int_\lambda^r \frac{d^3\vec{k}}{\sqrt{|\vec{k}|}} \sum_l \mathcal{F}_\alpha^{(l)}(\vec{k}) \hat{a}_{l, \vec{k}}^\dagger\right\} |0\rangle. \quad (4.39)$$

Here  $r$  is a nonzero regulator needed for the definition of the coherent state. Investigating its physical meaning will be crucial in the following discussions. Therefore, we explicitly indicated the borders of integration in  $|D(\alpha)\rangle_\lambda^r$ . The state (4.39) is normalized, i.e.  $\int_\lambda^r \frac{d^3\vec{k}}{|\vec{k}|} \sum_l |\mathcal{F}_\alpha^{(l)}(\vec{k})|^2 = B_\alpha \ln \frac{r}{\lambda}$ , which leads to

$$B_\alpha = \frac{1}{2(2\pi)^3} \sum_{n, m \in \alpha} \int d^2\Omega \frac{e_n e_m p_n \cdot p_m}{p_n \cdot \hat{k} p_m \cdot \hat{k}}. \quad (4.40)$$

Already at this point, it becomes apparent that the factor  $B_\alpha \ln \frac{r}{\lambda}$  in the normalization of the coherent state, and equivalently the expectation value of the particle number, diverge for  $\lambda \rightarrow 0$ . We will postpone the discussion of how the state can nevertheless be well-defined to section 4.1.6.

As explained, our goal is to show that including the dressing (4.39) leads to an IR-finite amplitude [60]. The starting point is to modify the asymptotic charged states by replacing

$$|\alpha\rangle \rightarrow |\alpha\rangle_\lambda^r := |\alpha\rangle \otimes |D(\alpha)\rangle_\lambda^r, \quad (4.41)$$

i.e. to add to an asymptotic state  $|\alpha\rangle$  a specific cloud of soft photons – defined by the factor  $\mathcal{F}_\alpha^{(l)}(\vec{k})$  connected to emission or absorption. To leading order in the coupling, the additional soft photons in the asymptotic states give three divergent contributions to a generic amplitude  $S_{\alpha, \beta}$ . The first one arises when the final dressing states absorb photons that were emitted from external lines. It gives

$$S_{\alpha, \beta}^{\text{1em}} = \langle \beta | \left( \int_\lambda^r \frac{d^3\vec{k}}{\sqrt{|\vec{k}|}} \sum_l \mathcal{F}_\alpha^{(l)\star}(\vec{k}) \hat{a}_{l, \vec{k}} \right) \hat{S} | \alpha \rangle = \int_\lambda^r \frac{d^3\vec{k}}{|\vec{k}|} \mathcal{F}_\alpha^{(l)\star}(\vec{k}) \mathcal{F}_{\alpha, \beta}^{(l)}(\vec{k}) S_{\alpha, \beta}, \quad (4.42)$$

where we used the soft theorem in the last step. Analogously, the absorption of a photon from the dressing of the initial state yields

$$S_{\alpha, \beta}^{\text{1abs}} = - \int_\lambda^r \frac{d^3\vec{k}}{|\vec{k}|} \mathcal{F}_\beta^{(l)}(\vec{k}) \mathcal{F}_{\alpha, \beta}^{(l)\star}(\vec{k}) S_{\alpha, \beta}. \quad (4.43)$$

When we sum these two contributions, the factors  $\mathcal{F}_\alpha^{(l)}(\vec{k})$  and  $\mathcal{F}_\beta^{(l)\star}(\vec{k})$  combine to form  $\mathcal{F}_{\alpha,\beta}^{(l)}(\vec{k})$  and we obtain<sup>4</sup>

$$S_{\alpha,\beta}^{\text{1em}} + S_{\alpha,\beta}^{\text{1abs}} = \int_\lambda^r \frac{d^3\vec{k}}{|\vec{k}|} \left| \mathcal{F}_{\alpha,\beta}^{(l)}(\vec{k}) \right|^2 S_{\alpha,\beta} = B_{\alpha,\beta} \ln \frac{r}{\lambda} S_{\alpha,\beta}, \quad (4.44)$$

where we used Eq. (4.22) in the last step. We get an analogous contribution as from emission (see Eq. (4.32)), up to an additional factor of 2 after squaring in the rate.

Fortunately, there is a third contribution due to the overlap of coherent states. Since we will need the corresponding computation shortly, we will calculate it to all orders and only specialize to the first order in the end. We get

$$\begin{aligned} \frac{r}{\lambda} \langle D(\alpha) | D(\beta) \rangle_\lambda^r &= e^{-\frac{1}{2} \int_\lambda^r \frac{d^3\vec{k}}{|\vec{k}|} \sum_l \left( |\mathcal{F}_\alpha^{(l)}(\vec{k})|^2 + |\mathcal{F}_\beta^{(l)}(\vec{k})|^2 \right)} \\ &\quad \cdot \langle 0 | e^{\int_\lambda^r \frac{d^3\vec{k}}{\sqrt{|\vec{k}|}} \sum_l \mathcal{F}_\alpha^{(l)\star}(\vec{k}) \hat{a}_{l,\vec{k}}} e^{\int_\lambda^r \frac{d^3\vec{k}}{\sqrt{|\vec{k}|}} \sum_l \mathcal{F}_\beta^{(l)}(\vec{k}) \hat{a}_{l,\vec{k}}^\dagger} | 0 \rangle \\ &= e^{-\frac{1}{2} \int_\lambda^r \frac{d^3\vec{k}}{|\vec{k}|} \sum_l \left| \mathcal{F}_{\alpha,\beta}^{(l)}(\vec{k}) \right|^2} \\ &= \left( \frac{\lambda}{r} \right)^{B_{\alpha,\beta}/2}. \end{aligned} \quad (4.45)$$

To first order, this gives

$$S_{\alpha,\beta}^{\text{1overlap}} = -\frac{1}{2} B_{\alpha,\beta} \ln \frac{r}{\lambda} S_{\alpha,\beta}. \quad (4.46)$$

Summing all three contributions, we end up with

$$S_{\alpha,\beta}^{\text{1dressed}} = S_{\alpha,\beta}^{\text{1em}} + S_{\alpha,\beta}^{\text{1abs}} + S_{\alpha,\beta}^{\text{1overlap}} = \frac{1}{2} B_{\alpha,\beta} \ln \frac{r}{\lambda} S_{\alpha,\beta}. \quad (4.47)$$

As before, this argument persists to all orders in the coupling and we get [60]

$$S_{\alpha,\beta}^{\text{dressed}} = \left( \frac{r}{\lambda} \right)^{B_{\alpha,\beta}/2} S_{\alpha,\beta}. \quad (4.48)$$

Combining with the loop contribution (4.28), we arrive at the final result

$$S_{\alpha,\beta}^{\text{dressed, tot}} = \left( \frac{r}{\Lambda} \right)^{B_{\alpha,\beta}/2} S_{\alpha,\beta}. \quad (4.49)$$

Thus, we get an IR-finite amplitude.

---

<sup>4</sup>Note that  $\sum_l \mathcal{F}_\alpha^{(l)\star}(\vec{k}) \mathcal{F}_\beta^{(l)}(\vec{k})$  is real.

Moreover, if we identify  $r = \epsilon$ , we also obtain the same IR-finite rate (4.36) that we obtained in the inclusive formalism, up to a subleading deviation due to the absence of the  $f(B_{\alpha,\beta})$ -function, which encodes energy conservation. It is natural to expect that the dressed formalism does not incorporate energy conservation since it is symmetric by construction: Initial and final states are dressed in an analogous manner. Unlike the inclusive formalism, the dressed formalism therefore cannot describe how charged particles lose energy due to soft radiation.

The present result is puzzling mainly for two reasons. First, it remains to be justified why charged particles should be dressed as in (4.41). Secondly, it is not clear why these different procedures, i.e. inclusion of soft emission and dressing of asymptotic states, can both cancel IR-divergences. In particular, there is no reason why the soft photon dressing should be sensitive to the resolution scale, i.e. why one would identify  $r = \epsilon$ . In the remainder of this section, we will answer the first question by showing how the long-range dynamics of a gapless theory such as QED imply that asymptotic states should be dressed as in (4.41). In section 4.2, we will come to the second question. It will turn out that generically both dressing and radiation should be present in a scattering process and that indeed  $r$  should not be identified with  $\epsilon$ .

### 4.1.6 Introduction to von Neumann Spaces

Before we can study dressed states in more detail, we have to give a brief review of how the Fock space can be constructed and what complications arise in a gapless theory. In particular, we want to understand how states with an infinite particle number, such as the coherent state (4.39), can be defined. Our starting point are the Hilbert spaces in each momentum mode  $\vec{k}$ . We are given well-defined Hilbert spaces  $\mathcal{H}_{\vec{k}}$ , which feature inner products  $\langle \cdot, \cdot \rangle_{\vec{k}}$  and creation and annihilation operators  $\hat{a}_{l,\vec{k}}^\dagger, \hat{a}_{l,\vec{k}}$  that fulfill canonical commutation relations:

$$[\hat{a}_{l,\vec{k}}, \hat{a}_{l',\vec{k}}^\dagger] \sim \delta_{ll'}, \quad [\hat{a}_{l,\vec{k}}, \hat{a}_{l',\vec{k}}] = [\hat{a}_{l,\vec{k}}^\dagger, \hat{a}_{l',\vec{k}}^\dagger] = 0. \quad (4.50)$$

We already included the polarization  $l$  since we will later be interested in photons. The problem lies in defining the tensor product  $\otimes_{\vec{k}} \mathcal{H}_{\vec{k}}$  of the infinitely many Hilbert spaces corresponding to all possible momenta  $\vec{k}$ .

For this task we can rely on the seminal work by von Neumann [237], who defined the space  $\mathcal{H}_{\text{VN}} \subset \otimes_{\vec{k}} \mathcal{H}_{\vec{k}}$ . It consists of elements for which a scalar product can be defined. For  $|\varphi\rangle, |\Psi\rangle \in \mathcal{H}_{\text{VN}}$ , i.e.  $|\varphi\rangle = \otimes_{\vec{k}} |\varphi_{\vec{k}}\rangle_{\vec{k}}$  and  $|\Psi\rangle = \otimes_{\vec{k}} |\Psi_{\vec{k}}\rangle_{\vec{k}}$ , it is given as

$$\langle \varphi | \Psi \rangle := \prod_{\vec{k}} \langle \varphi_{\vec{k}} | \Psi_{\vec{k}} \rangle_{\vec{k}}. \quad (4.51)$$

It is clear from this definition that the von Neumann space is very big. In particular, it contains any product of states that are normalizable in the individual  $\mathcal{H}_{\vec{k}}$ ,

i.e.  $|\varphi\rangle = \otimes_{\vec{k}} |\varphi\rangle_{\vec{k}}$  such that  $\langle \varphi_{\vec{k}} | \varphi_{\vec{k}} \rangle_{\vec{k}} = 1$  for all  $\vec{k}$ . W.l.o.g. we will assume normalized states from now on.

This scalar product defines an equivalence relation in the von Neumann space given by

$$|\varphi\rangle \sim |\Psi\rangle \Leftrightarrow \sum_{\vec{k}} \left| \langle \varphi_{\vec{k}} | \Psi_{\vec{k}} \rangle_{\vec{k}} - 1 \right| \text{ convergent.} \quad (4.52)$$

The significance of this equivalence relation lies in the fact that elements from different equivalence classes are orthogonal,

$$|\varphi\rangle \approx |\Psi\rangle \Rightarrow \langle \varphi | \Psi \rangle = 0. \quad (4.53)$$

Therefore, the equivalence classes constitute mutually disjoint subspaces in the von Neumann space. The physical implications of this construction were derived in [238]. First of all, a special role is played by the equivalence class of  $|0\rangle := \otimes_{\vec{k}} |0\rangle_{\vec{k}}$ , which we denote by  $[0]$ . In it, one has the standard representation of canonical commutation relations:

$$\left[ \hat{a}_{l,\vec{k}}, \hat{a}_{l',\vec{k}'}^\dagger \right] = \delta^{(3)}(\vec{k} - \vec{k}') \delta_{ll'}, \quad \left[ \hat{a}_{l,\vec{k}}, \hat{a}_{l',\vec{k}'} \right] = \left[ \hat{a}_{l,\vec{k}}^\dagger, \hat{a}_{l',\vec{k}'}^\dagger \right] = 0. \quad (4.54)$$

Then we can define the particle number operator as

$$\hat{N} := \sum_{\vec{k},l} \hat{a}_{\vec{k},l}^\dagger \hat{a}_{\vec{k},l}, \quad (4.55)$$

i.e.  $\langle \varphi | \hat{N} | \varphi \rangle$  is finite for each  $\varphi \in [0]$ . Therefore, this equivalence class alone represents the whole Fock space.

One can also understand the other equivalence classes in terms of particle number [238]. Two states are in the same equivalence class if and only if their difference in particle number is finite,

$$|\varphi\rangle \sim |\Psi\rangle \Leftrightarrow \langle \varphi | \hat{N} | \varphi \rangle - \langle \Psi | \hat{N} | \Psi \rangle < \infty, \quad (4.56)$$

where it is understood that the subtraction is performed before the sum over the momentum modes. Since one can moreover show that each equivalence class is isomorphic to the Fock space, it follows that the von Neumann space can be thought of as infinite product of Fock spaces with unitarily inequivalent representations of the commutation relations in each subspace. So in each equivalence class  $[\alpha]$ , we have:

$$\left[ \hat{a}_{l,\vec{k}}^{[\alpha]}, \hat{a}_{l',\vec{k}'}^{[\alpha]\dagger} \right] = \delta^{(3)}(\vec{k} - \vec{k}') \delta_{ll'}, \quad \left[ \hat{a}_{l,\vec{k}}^{[\alpha]}, \hat{a}_{l',\vec{k}'}^{[\alpha]} \right] = \left[ \hat{a}_{l,\vec{k}}^{[\alpha]\dagger}, \hat{a}_{l',\vec{k}'}^{[\alpha]\dagger} \right] = 0. \quad (4.57)$$

This immediately raises the question which subspace of  $\mathcal{H}_{\text{VN}}$  is physically relevant. A reasonable requirement for any state to be physical is that it has finite energy. Whenever a theory has a mass gap, the Fock space – defined by the requirement of

finite particle number – is the only equivalence class with finite energy and therefore contains all physically relevant states. So it makes sense to restrict oneself to the Fock space.

However, the situation is drastically different in a gapless theory. Then there can be states that contain an infinite amount of zero modes but nevertheless carry finite energy. Therefore, there are distinct equivalence classes with finite energy and there is no reason to restrict oneself to only one of them. In a gapless theory, states of different equivalence classes are therefore physically sensible. In fact, as we shall discuss, the  $S$ -matrix generically enforces the transition between different equivalence classes so that it is impossible to restrict oneself to a single equivalence class in an interacting system. The fact that states in different equivalence classes are – by definition – orthogonal will be important in the following.

### 4.1.7 Dressing from Asymptotic Dynamics

With the tools of von Neumann spaces at our disposal, our next goal is to sketch the derivation [61–65] of why asymptotic states should be dressed as in (4.41). This gives the justification of Chung’s calculation [60]. In an  $S$ -matrix calculation, asymptotic states must be approximate eigenstates of the Hamiltonian in the limit of large separation. In a theory without long-range forces, in which interaction falls off fast with separation, this leads to eigenstates of the free Hamiltonian. However, the crucial observation is that in a gapless theory, asymptotic dynamics cannot be approximated by the free Hamiltonian, but the leading order of the interaction term has to be taken into account as well [65]. It is given by<sup>5</sup>

$$\hat{W}(t)_\lambda^r = \exp \left\{ \frac{1}{\sqrt{2(2\pi)^3}} \int_\lambda^r \frac{d^3 \vec{k}}{\sqrt{|\vec{k}|}} \sum_l \int d^3 \vec{p} \hat{\rho}(\vec{p}) \left( \frac{p \cdot \varepsilon_{l, \vec{k}}^*}{p \cdot k} \hat{a}_{l, \vec{k}}^\dagger e^{i \frac{p \cdot k}{p_0} t} - \text{h.c.} \right) \right\}, \quad (4.58)$$

where  $\hat{\rho}(\vec{p})$  is the charge density operator (4.12) of electrons and positrons. We can define asymptotic states by applying  $\hat{W}(t)_\lambda^r$  to a bare state  $|\alpha\rangle$  of electrons and positrons [65],

$$|\alpha\rangle_\lambda^r := \hat{W}(t_{\text{obs}})_\lambda^r |\alpha\rangle, \quad (4.59)$$

where  $t_{\text{obs}}$  is a so far arbitrary reference time. We keep it finite for now, but following [60, 65], we will set it to zero for the computation. The reason we can do so is that the final result only depends on the divergent zero-mode part of the dressing state whereas the phase controlled by  $t_{\text{obs}}$  only changes the finite part of nonzero modes.<sup>6</sup>

<sup>5</sup>We omit the Coulomb phase both in the definition of the asymptotic state and in the  $S$ -matrix since it will not matter for our discussion.

<sup>6</sup>Strictly speaking, one can even be more general and choose an arbitrary state in the equivalence class  $[\alpha]$  [65]. But since only the zero-mode part of dressing matters, we can adopt the choice (4.59) of [60, 65]. We will further comment on this freedom in choosing a dressing state in section 4.2.3.

Clearly, definition (4.59) also depends on  $r$  and is nontrivial only for  $r$  nonzero. However, there is little discussion of its physical meaning in the standard literature on infrared physics. Typically, the identification  $r = \epsilon$  is assumed for the simple reason that in such a case the rates in the inclusive and in the dressed formalism match approximately. In contrast, we will argue that the two scales are in general different. While we will discuss this point in more detail when we turn to the density matrix of the final state in section 4.3, we briefly comment on the interpretation of  $r$  already now. If one wants to interpret  $|\alpha\rangle\rangle_\lambda^r$  as initial or final state of scattering, it is most natural to think of  $t_{\text{obs}}$  as the timescale after which the state will be measured. Once  $t_{\text{obs}}$  is fixed,  $r$  is no longer independent. The reason is the fact, noted in [65], that the phases wash out if  $kt_{\text{obs}}$  is sufficiently big, i.e.  $\lim_{t \gg k^{-1}} \exp(ikpt/p_0)/pk \approx 0$ . Therefore, all modes with  $k > t_{\text{obs}}^{-1}$  effectively disappear and do not contribute to the asymptotic dynamics any more:

$$\hat{W}(t_{\text{obs}})_\lambda^r \approx \hat{W}(t_{\text{obs}})_\lambda^{t_{\text{obs}}^{-1}}. \quad (4.60)$$

Thus, if we only want to consider the physical modes, we have to set

$$r = t_{\text{obs}}^{-1}, \quad (4.61)$$

i.e. we can identify  $r$  with the timescale  $t_{\text{obs}}$  after which the final state is measured. The choice (4.61) can also be justified from a more physical point of view. Namely it is crucial for the photons in the dressing state that they decouple. Since a photon of energy  $r$  needs a timescale of  $r^{-1}$  to interact, it only makes sense to consider  $r < t_{\text{obs}}^{-1}$ .

Before we investigate the dressed states more closely, we want to mention that the  $S$ -matrix is not modified in the dressed formalism [65]. The reason is that in the limit of infinite time, relation (4.60) becomes

$$\lim_{t \rightarrow \infty} \hat{W}(t) = \mathbb{1}, \quad (4.62)$$

which follows from  $\lim_{t \rightarrow \pm\infty} \exp(ikpt/p_0)/pk = \pm i\pi\delta(kp)$ . For this reason, asymptotic dynamics do not contribute to the  $S$ -matrix but only modify the asymptotic states. Setting  $t_{\text{obs}} = 0$ , we get the asymptotic state (4.59):

$$|\alpha\rangle\rangle_\lambda^r = |\alpha\rangle \otimes |D(\alpha)\rangle_\lambda^r, \quad (4.63)$$

where we plugged in Eq. (4.58). In this way, we recover the dressing state  $|D(\alpha)\rangle_\lambda^r$ , which we already introduced in Eq. (4.39). So the justification for considering dressed asymptotic states lies in taking into account the long-range interaction of asymptotic dynamics. Once this is properly done, Chung's computation shows that we obtain IR-finite amplitudes.

When we investigate the particle number of the dressing state,

$${}_\lambda^r \langle D(\alpha) | \hat{N} | D(\alpha) \rangle_\lambda^r = B_\alpha \ln \frac{r}{\lambda}, \quad (4.64)$$

it becomes evident that it contains an infinite number of zero-energy photons in the limit  $\lambda \rightarrow 0$ . Thus, although the states possess the finite energy  $B_\alpha r$ , they are not in the equivalence class  $[0]$ , i.e. in the Fock space. This is the reason why they can only be defined in the bigger von Neumann space. Note that varying  $r$  does not change the equivalence class but only alters the energy of the dressing state. So the equivalence class only depends on the zero-momentum part of  $\mathcal{F}_\alpha^{(l)}(\vec{k})$ . In order to decide whether different dressing states are in different equivalence classes, we recall Eq. (4.45):

$${}^r_\lambda \langle D(\alpha) | D(\beta) \rangle_\lambda^r = \left( \frac{\lambda}{r} \right)^{B_{\alpha,\beta}/2}. \quad (4.65)$$

As we have discussed at the end of section 4.1.2,  $B_{\alpha,\beta} = 0$  only if  $|\alpha\rangle \approx |\beta\rangle$ , i.e. if their charges match anglewise. If this is not the case,  $|D(\alpha)\rangle_\lambda^r$  and  $|D(\beta)\rangle_\lambda^r$  have vanishing overlap for  $\lambda \rightarrow 0$  and therefore are in different equivalence classes. Thus, there is a different equivalence class for each charge distribution on the sphere. We can parametrize the equivalence classes as  $[\alpha]$  in terms of the charged states  $|\alpha\rangle$ .

### 4.1.8 Collinear Divergences

As a side remark, we note that an interesting question is what happens when one sends the mass of some of the hard particles to zero. In gravity, this situation is not special, i.e. the kinematical factor  $B_{\alpha,\beta}$  (Eq. (4.29)) stays finite.<sup>7</sup> This is related to the fact that gravitational radiation is quadrupolar. In QED, however, the situation is drastically different. In the limit of a small electron mass  $m$ , it follows from (4.23) that the exponent  $B_{\alpha,\beta}$  scales as

$$B_{\alpha,\beta} \sim -\ln m, \quad (4.66)$$

i.e. it becomes infinite for massless electrons. The only exception are processes of trivial scattering, in which initial and final state are equivalent. Thus, it is clear from (4.36) that the rate of any nontrivial scattering process vanishes.

As a consequence, one could try to consider a wider class of processes such that a nonvanishing total rate can be obtained. This was achieved in [241], where – on top of all soft emission processes – a special class of emission *and absorption* processes was considered, namely the emission and absorption of *collinear* photons of arbitrary energy. Taking into account both emission and absorption is moreover required for Lorentz covariance: Unlike in the soft theorem (4.4), a single amplitude of a particular emission process violates Lorentz invariance in the collinear limit. However, it is doubtful whether it makes sense to consider absorption processes since the origin of the absorbed photons of arbitrary energy is unclear.

<sup>7</sup>The explicit expression for  $B_{\alpha,\beta}$  in the massless limit was derived in [49, 239, 240].

## 4.2 Combined Formalism

As we have explained, one can obtain IR-finite rates by either employing the dressed or the inclusive formalism. In the inclusive formalism, one leaves the initial state unchanged but adds soft radiation to the final state. In contrast, the dressed formalism corresponds to modifying initial and final states in an analogous manner by dressing them with a cloud of soft photons. Those soft photons are inseparably tied to the charged states, so they do not correspond to radiation but to a redefinition of asymptotic electrons and positrons. We shall make this statement explicit shortly.

Since both formalisms yield – up to subleading corrections – the same rate, the question arises if they are equivalent. This would come as a big surprise since the requirements of the two formalisms – emission of bremsstrahlung versus well-defined asymptotic states – are very different. Both requirements are, however, very reasonable and should be fulfilled. Therefore, we shall argue that both dressing and soft radiation should be present in a generic process. Thus, the goal of this section is to present a concrete formalism that interpolates between the inclusive and the dressed formalism and makes the distinction between radiation and dressing explicit. We shall call it *combined formalism* and we derive it from first principles by applying the  $S$ -matrix, as operator in  $\mathcal{H}_{\text{VN}}$ , to the dressed initial state  $|\alpha\rangle\rangle_\lambda^r$ . This will lead to a final state that consists both of dressed charged particles  $|\beta\rangle\rangle_\lambda^r$  and of additional soft bremsstrahlung radiation.

Not surprisingly, it will turn out that also in the combined formalism, one obtains the same IR-finite rate as in the two known formalisms. This finding immediately raises the question about the relevance of our construction. However, one can go one step further than the rate and investigate the density matrix of the final state. Obviously, its diagonal contains the known IR-finite rates. So the task consists in determining the IR-limit of the off-diagonal pieces of the density matrix. These elements encode the information about the quantum coherence of the final state. We will show that only in the combined formalism, physically reasonable off-diagonal elements can be obtained. We will study this question in section 4.3.

### 4.2.1 Equivalence Classes as Radiative Vacua

In gapless theories, we have seen that nontrivial asymptotic dynamics lead to dressing states (4.39), which – in the limit  $\lambda \rightarrow 0$  – no longer belong to the Fock space because of an infinite number of zero-energy photons. However, as explained in section 4.1.6, each equivalence class of the von Neumann space is isomorphic to the Fock space. In particular, there is a representation of the commutation relations (4.57) in each of them [238]. We can formally relate those to the Fock

space operators (4.54) via:

$$\hat{a}_{l,\vec{k}}^{[\alpha]} = \hat{W}(0)\hat{a}_{l,\vec{k}}\hat{W}^\dagger(0). \quad (4.67)$$

For finite  $\lambda$ , this representation is unitarily equivalent whereas it is not for  $\lambda \rightarrow 0$ . From the perspective of the operators  $\hat{a}_{l,\vec{k}}^{[\alpha]}$ , the corresponding dressing state is a vacuum:

$$\hat{a}_{l,\vec{k}}^{[\alpha]}|\alpha\rangle_\lambda^r = 0. \quad (4.68)$$

Thus,  $\hat{a}_{l,\vec{k}}^{[\alpha]\dagger}$  represents excitations on top of the vacuum of the equivalence class  $[\alpha]$ , i.e.  $\hat{a}_{l,\vec{k}}^{[\alpha]\dagger}$  corresponds to radiation on top of the dressing state defined by  $|D(\alpha)\rangle$ . This shows explicitly that there is no radiation in the dressed formalism.

For  $|\vec{k}| > r$ , we have

$$\hat{a}_{l,\vec{k}}^{[\alpha]} = \hat{a}_{l,\vec{k}}, \quad (4.69)$$

i.e. photons of energy above  $r$  are insensitive to the dressing and can be treated as if they were defined in the Fock space. As the subsequent calculations will confirm, only those photons constitute physical radiation. In contrast, photons of smaller energy solely occur in the dressing states but do not exhibit dynamics of their own. This is in line with the well-known decoupling of soft photons [232–236, 242, 243]. We remark that this is also consistent with the identification  $r = t_{\text{obs}}^{-1}$  (see Eq. (4.61)). Namely we expect that on the timescale  $t_{\text{obs}}$ , the softest radiation photons that can be produced have an energy  $t_{\text{obs}}^{-1}$ , so all photons of smaller energy are decoupled.<sup>8</sup>

For our argument, however, the precise identification of the scale  $r$  is inessential. The only important point is that  $r$  splits the Hilbert space of photons in two parts. Photons below  $r$  are part of the dressing. Those are symmetric, i.e. initial and final states are analogously dressed. Moreover, the dressing of the initial state is only sensitive to the initial state, but not to the final states and likewise for the final state. Since the dressing states contain an infinite amount of photons, they are not in the Fock space, but can only be defined in the larger von Neumann space. In contrast, photons above  $r$  are part of radiation. They are asymmetric since we can prepare an initial state without radiation, i.e. radiation only occurs in the final state but not in the initial state. In turn, it will become clear that it is sensitive to both the initial and the final state. In particular, it depends on the difference of initial and final state, i.e. on the transfer momentum. The radiation state contains a finite number of photons and is well-defined in the Fock space. Thus, physical radiation is completely independent of the problems arising due to an infinite number of photons.

<sup>8</sup>That  $t_{\text{obs}}^{-1}$  should correspond to an effective IR-cutoff for physical radiation was also proposed in [244–246].

Radiation is characterized by a second scale  $\epsilon$ , which we can identify with the detector resolution. It is crucial to note that the scales  $r$  and  $\epsilon$  are in general independent since they contain different physical information. The energy  $r$  describes the timescale after which the state is observed. In contrast, the scale  $\epsilon$  corresponds to the resolution scale of the particular device used to measure the final state. As explained, the only requirement is that  $r < \epsilon$ . In fact, it will turn out that  $r \ll \epsilon$  is needed for a well-defined separation of dressing and radiation. In this limit, the energy carried by the dressing states is negligible. So all energy is carried by the radiation state whereas the only significant contribution to the number of photons comes from the dressing. In total, we obtain the following hierarchy of scales:

$$\lambda < r < \epsilon < \Lambda, \quad (4.70)$$

where  $\Lambda$  is the energy scale of the whole process, e.g. the center-of-mass energy. In the existing literature, the scales  $\lambda$ ,  $\epsilon$  and  $\Lambda$  are well-known. However, there is no additional scale  $r$ . The reason is that – as we will show – all rates are independent of  $r$ . So the introduction of the scale  $r$ , which separates dressing from radiation, is unnecessary if one is solely interested in rates. In contrast, it will turn out that the final density matrix does depend on  $r$ . The reason is that unlike the rate, the density matrix is sensitive to the timescale after which it is measured. Therefore, we have to keep the scale  $r$  in order to derive an IR-finite density matrix.

Introducing the new scale  $r$  amounts to interpolating between the well-known dressed and inclusive formalisms. We can consider the two limiting cases. For  $r = \epsilon$ , there is no radiation, but all photons are attributed to dressing. This leads to Chung's calculation [60], but corresponds to the unsatisfactory situation that there is no soft emission and that the resolution scale  $\epsilon$  appears in the dressing of the initial state. The opposite limiting case is to set  $r = \lambda$ . Then there is no dressing, in particular the initial state is bare, but the final state contains photons of arbitrarily low energies. This leads to the calculations by Yennie, Frautschi and Suura [58] as well as Weinberg [59]. However, this construction lacks well-defined asymptotic states. For these reasons, we will work in the combined formalism that realizes the general hierarchy (4.70). We will demonstrate that doing so leads to the well-known IR-finite rates, but additionally it will allow us to obtain a well-defined density matrix of the final state.

### 4.2.2 Calculation of Final State

We consider a generic scattering process. In order to determine the final state, we need two ingredients: a well-defined initial state and the  $S$ -matrix of QED. Having defined the initial state (4.63), it remains to apply the  $S$ -matrix to it:  $\hat{S} |\alpha\rangle_\lambda^r$ . The first step is to insert an identity that is decomposed as a tensor product of three factors. The first one, which we shall denote by  $D$  and which will correspond to dressing, consists of all possible photon states composed of quanta with an

energy below  $r$ . Analogously, the second one, which we shall call  $\gamma$  and which will represent soft radiation, contains all possible photon states in which each photon has an energy above  $r$  but below  $\epsilon$ . Finally, the third factor  $\beta$  is composed of all remaining states, i.e. photons with energy above  $\epsilon$  and all other excitations, in particular charged particles. We obtain:

$$\hat{S}|\alpha\rangle_\lambda^r = \sum_{\substack{D \\ (\lambda < E_D < r)}} \sum_{\substack{\gamma \\ (r < E_\gamma < \epsilon)}} \sum_{\substack{\beta \\ (\epsilon < E_\beta)}} \left( |\beta\rangle \otimes |\gamma\rangle \otimes |D\rangle \right) \left( \langle D| \otimes \langle \gamma| \otimes \langle \beta| \right) \hat{S}|\alpha\rangle_\lambda^r. \quad (4.71)$$

We will first turn to the sum over  $D$ . From Chung's computation [60] we know that  $\left( \langle D(\beta)| \otimes \langle \gamma| \otimes \langle \beta| \right) \hat{S}|\alpha\rangle_\lambda^r \neq 0$ , i.e. when we take the appropriate dressing  $|D(\beta)\rangle$  of the final state  $|\beta\rangle$ , we obtain an IR-finite amplitude. (From the point of view of this computation,  $|\gamma\rangle$  is a hard state.) This implies that any state  $|D\rangle$  that belongs to a different equivalence class than  $|D(\beta)\rangle$  has zero overlap with  $\hat{S}|\alpha\rangle_\lambda^r$ . In other words, the state in the mode  $\vec{k} = 0$ , in which the number of photons is infinite, is fixed. In the identity, one would nevertheless have to perform independent sums over photons in the modes  $0 < |\vec{k}| < r$ .<sup>9</sup> However, if we take  $r$  small enough, those modes do not change the result of  $\hat{S}|\alpha\rangle_\lambda^r$  and we can proceed as for Eq. (4.59) and fix them by the state  $|D(\beta)\rangle$ . For  $r \ll \epsilon$ , we therefore obtain

$$\sum_{\substack{D \\ (\lambda < E_D < r)}} |D\rangle \langle D| \simeq |D(\beta)\rangle \langle D(\beta)|. \quad (4.72)$$

This means that the dressing is not independent but fixed by the hard state  $|\beta\rangle$ . In [60], the same approximation is used, i.e. the modes  $0 < |\vec{k}| < r$  are not treated as independent.

In contrast, we will not neglect any states in the sum over radiation. As explained, the definition of a radiation photon generically depends on the radiative vacuum on top of which it is defined. However, it follows from (4.67) that this distinction is inessential for photons of energy greater than  $r$  and we can treat them as if they were defined in the usual Fock space. Writing out the sum over radiation explicitly gives

$$\sum_{\substack{\gamma \\ (r < E_\gamma < \epsilon)}} |\gamma\rangle \langle \gamma| = \sum_n \frac{1}{n!} \left( \prod_{i=1}^n \int_r^\epsilon d^3 \vec{k}_i \sum_{l_i} \right) \left( \hat{a}_{l_1, \vec{k}_1}^\dagger \dots \hat{a}_{l_n, \vec{k}_n}^\dagger |0\rangle \right) \left( \langle 0| \hat{a}_{l_1, \vec{k}_1} \dots \hat{a}_{l_n, \vec{k}_n} \right), \quad (4.73)$$

<sup>9</sup>In other words, as is discussed in [65], one can replace  $\mathcal{F}_\alpha^{(l)}(\vec{k})$  by  $\mathcal{F}_\alpha^{(l)}(\vec{k})\varphi(\vec{k})$ , where  $\varphi(\vec{k})$  is an arbitrary function that fulfills  $\varphi(\vec{k}) = 1$  in a neighborhood of  $\vec{k} = 0$ . Then neglecting the sum over modes  $0 < |\vec{k}| < r$  corresponds to setting  $\varphi(\vec{k}) = 1$  everywhere.

where  $1/n!$  comes from the normalization of the photon states. We will not resolve the third sum over hard modes  $\beta$ . In total, we obtain

$$\hat{S}|\alpha\rangle\rangle_\lambda^r = \sum_\beta \sum_n \frac{1}{n!} \left( \prod_{i=1}^n \int_r^\epsilon d^3 \vec{k}_i \sum_{l_i} \right) \left( |\beta\rangle\rangle_\lambda^r \otimes |\gamma_n\rangle \right) \left( \langle \gamma_n | \otimes \langle \langle \beta | \rangle \rangle_\lambda^r \right) \hat{S}|\alpha\rangle\rangle_\lambda^r, \quad (4.74)$$

where we introduced the notation  $|\gamma_n\rangle = \hat{a}_{l_1, \vec{k}_1}^\dagger \dots \hat{a}_{l_n, \vec{k}_n}^\dagger |0\rangle$ .

Now we can use the fact that the soft photon theorem (4.4) holds in an arbitrary process to obtain  $\left( \langle \gamma_n | \otimes \langle \langle \beta | \rangle \rangle_\lambda^r \right) \hat{S}|\alpha\rangle\rangle_\lambda^r = \langle \langle \beta | \rangle \rangle_\lambda^r \hat{S}|\alpha\rangle\rangle_\lambda^r \prod_{i=1}^n \mathcal{F}_{\alpha, \beta}^{(l_i)}(\vec{k}_i) / \sqrt{|\vec{k}_i|}$ , where the soft factor  $\mathcal{F}_{\alpha, \beta}^{(l_i)}(\vec{k}_i)$  is displayed in Eq. (4.5). Moreover, it follows from Chung's result (4.49), which arises from combing the contributions of soft loops and of the dressing states, that

$$\langle \langle \beta | \rangle \rangle_\lambda^r \hat{S}|\alpha\rangle\rangle_\lambda^r = \left( \frac{r}{\lambda} \right)^{B_{\alpha, \beta/2}} S_{\alpha, \beta}. \quad (4.75)$$

So we obtain

$$\hat{S}|\alpha\rangle\rangle_\lambda^r = \sum_\beta \left( \frac{r}{\Lambda} \right)^{B_{\alpha, \beta/2}} S_{\alpha, \beta} |\beta\rangle\rangle_\lambda^r \otimes \sum_n \frac{1}{n!} \left( \prod_{i=1}^n \int_r^\epsilon \frac{d^3 \vec{k}_i}{\sqrt{|\vec{k}_i|}} \sum_{l_i} \mathcal{F}_{\alpha, \beta}^{(l_i)}(\vec{k}_i) \hat{a}_{l_i, \vec{k}_i}^\dagger \right) |0\rangle. \quad (4.76)$$

We can resum this final photon state:

$$\hat{S}|\alpha\rangle\rangle_\lambda^r = \sum_\beta \left( \frac{\epsilon}{\Lambda} \right)^{B_{\alpha, \beta/2}} S_{\alpha, \beta} (|\beta\rangle\rangle_\lambda^r \otimes |\gamma(\alpha, \beta)\rangle_r^\epsilon), \quad (4.77)$$

where

$$|\gamma(\alpha, \beta)\rangle_r^\epsilon = \left( \frac{r}{\epsilon} \right)^{B_{\alpha, \beta/2}} e^{\int_r^\epsilon \frac{d\vec{k}}{\sqrt{|\vec{k}|}} \sum_l \mathcal{F}_{\alpha, \beta}^{(l)}(\vec{k}) \hat{a}_{l, \vec{k}}^\dagger} |0\rangle \quad (4.78)$$

is a normalized coherent radiation state and we used the integral (4.22) to compute the norm.

Formula (4.77) makes the physics of the process very transparent. Both in the initial and in the final state, charged particles are dressed, as is required for well-defined asymptotic states. The dressings consist of photons of energy below  $r$  and only depend on their respective state. This means that the dressing  $|D(\alpha)\rangle\rangle_\lambda^r$  of the initial state only depends on  $|\alpha\rangle$  and the dressing  $|D(\beta)\rangle\rangle_\lambda^r$  of the final state only depends on  $|\beta\rangle$ . On top of the dressing, the final state (but not the initial state) also contains radiation. The radiation  $|\gamma(\alpha, \beta)\rangle_r^\epsilon$  is made up of photons of energy above  $r$  and depends both on the initial and on the final state of the hard electrons, and in particular on the momentum transfer between them.

As we have explained, a difficulty that arises from IR-physics – which also seemingly leads to full decoherence – comes from the fact that the dressing states

are no longer in the Fock space due to the infinite number of zero-energy photons. For this reason, those states can only be defined in the much larger von Neumann space, which is isomorphic to an infinite product of Fock spaces. In our approach, we manage to separate this difficulty from the physical radiation. Namely only the dressing states  $|D(\alpha)\rangle_\lambda^r$  and  $|D(\beta)\rangle_\lambda^r$  contain an infinite number of photons, but these state do not correspond to physical radiation. Instead, they are part of the definition of asymptotic states. On top of the radiative vacuum defined by  $|D(\beta)\rangle_\lambda^r$ , the radiation state  $|\gamma(\alpha, \beta)\rangle_r^\epsilon$  exists. Since it only contains a finite number of photons of energies above  $r$ , it can be treated as if they were part of the usual Fock space. Solely the radiation is measurable and for  $r \ll \epsilon$ , only it carries a significant energy.

We can check that the amplitude (4.77) indeed gives the correct rate. To this end, we need to sum over all possible soft radiation in the final state, i.e. over all radiation states in which the sum of all photon energies is below  $\epsilon$ . For  $r \ll \epsilon$ , we get

$$\begin{aligned} \Gamma_{\alpha, \beta} &= \sum_n \frac{1}{n!} \left( \prod_{i=1}^n \int_r^\epsilon d^3 \vec{k}_i \sum_{l_i} \right) \theta(\epsilon - \sum_{j=1}^n |\vec{k}_j|) \left| \langle 0 | \hat{a}_{l_1, \vec{k}_1} \dots \hat{a}_{l_n, \vec{k}_n} \otimes_\lambda^r \langle \beta | \right) \hat{S} |\alpha\rangle_\lambda^r \right|^2 \\ &= \left( \frac{r}{\Lambda} \right)^{B_{\alpha, \beta}} \sum_n \frac{1}{n!} \left( \prod_{i=1}^n \int_r^\epsilon \frac{d^3 \vec{k}_i}{|\vec{k}_i|} \sum_{l_i} |\mathcal{F}_{\alpha, \beta}^{(l_i)}(\vec{k}_i)|^2 \right) \theta(\epsilon - \sum_{j=1}^n |\vec{k}_j|) |S_{\alpha, \beta}|^2 \\ &= \left( \frac{\epsilon}{\Lambda} \right)^{B_{\alpha, \beta}} f(B_{\alpha, \beta}) |S_{\alpha, \beta}|^2, \end{aligned} \quad (4.79)$$

where  $f(B_{\alpha, \beta})$  was defined in Eq. (4.33). This is the well-known result (4.36) in the inclusive formalism [58, 59]. If we neglect the function  $f(B_{\alpha, \beta})$ , which is possible for weak coupling, the rate (4.79) is also identical to the result (4.49) in the dressed formalism [60]. In particular, it is clear that the answer that we obtain is IR-finite since the regulator  $\lambda$  has dropped out. It is important to note that we never required IR-finiteness. It simply arises as a consequence of applying the  $S$ -matrix to a well-defined initial state.

Moreover, we observe that the rate (4.79) is also independent of the scale  $r$ . As we have discussed, our approach interpolates between the dressed formalism, which corresponds to  $r = \epsilon$ , and the inclusive formalism, which we obtain for  $r = \lambda$ .<sup>10</sup> The fact that our result is independent of  $r$  implies that not only dressed and inclusive formalism yield – except for  $f(B_{\alpha, \beta})$  – the same rate, but that this is also true for the interpolation between them.

As a side remark, we will for a moment take the limit  $r = \lambda$ , in which the dressings vanish and we obtain the inclusive formalism. Then formula (4.77) becomes

<sup>10</sup>Sending  $\epsilon \rightarrow r$  for fixed  $r$  corresponds to a situation in which no soft emission takes place. When we work with well-defined, i.e. dressed states, the rate of such a process is suppressed by the possibly small factor  $(r/\Lambda)^{B_{\alpha, \beta}}$  but nonvanishing.

$$\hat{S}|\alpha\rangle = \sum_{\beta} \left(\frac{\epsilon}{\Lambda}\right)^{B_{\alpha,\beta}/2} S_{\alpha,\beta} (|\beta\rangle \otimes |\gamma(\alpha,\beta)\rangle_{\lambda}^{\epsilon}), \quad (4.80)$$

where the electron states are not dressed. This leads to the IR-finite amplitude:

$$\langle \lambda | \langle \gamma(\alpha,\beta) | \otimes \langle \beta | \hat{S} | \alpha \rangle = \left(\frac{\epsilon}{\Lambda}\right)^{B_{\alpha,\beta}/2} S_{\alpha,\beta}. \quad (4.81)$$

So if we use as final state the correct state of radiation  $|\gamma(\alpha,\beta)\rangle_{\lambda}^{\epsilon}$ , which depends both on initial and final electrons, we get an IR-finite amplitude in the inclusive formalism. However, the price to pay is that on the one hand, we are not able to obtain the factor  $f(B_{\alpha,\beta})$  that encodes energy conservation and that on the other hand the radiation state  $|\gamma(\alpha,\beta)\rangle_{\lambda}^{\epsilon}$  contains an infinite number of zero-energy photons and is no longer part of the Fock space. Nevertheless, it is a physically sensible state since it only contains a finite energy.

### 4.2.3 Large Gauge Transformations and Dressing

Another interesting question is how gauge transformations  $\varepsilon_{l,\vec{k}}^{\mu} \rightarrow \varepsilon_{l,\vec{k}}^{\mu} + \lambda_l(\vec{k})k^{\mu}$ , which were already introduced in (4.8), act on dressed states. Since dressing is determined by photons with  $|\vec{k}| < r$ , only large gauge transformations, for which  $\lambda_l(\vec{k})$  has support for  $|\vec{k}| < r$ , act nontrivially. With the definition  $\tilde{\lambda}_l(\vec{k}) = \lambda_l(\vec{k}) \sum_{n \in \alpha} e_n / \sqrt{2(2\pi)^3}$ , those lead to the transformed dressed state

$$\begin{aligned} |\tilde{\alpha}\rangle_{\lambda}^r &= \exp \left\{ -\frac{1}{2} \int_{\lambda}^r \frac{d^3 \vec{k}}{|\vec{k}|} \sum_l |\mathcal{F}_{\alpha}^{(l)}(\vec{k}) + \tilde{\lambda}_l^*(\vec{k})|^2 \right\} \\ &\exp \left\{ \int_{\lambda}^r \frac{d^3 \vec{k}}{\sqrt{|\vec{k}|}} \sum_l (\mathcal{F}_{\alpha}^{(l)}(\vec{k}) + \tilde{\lambda}_l^*(\vec{k})) \hat{a}_{l,\vec{k}}^{\dagger} \right\} |\alpha\rangle. \end{aligned} \quad (4.82)$$

Thus, dressing states are not invariant under gauge transformations [61–65].<sup>11</sup>

Since the number of photons only changes by a finite amount, the equivalence class to which the dressing state belongs and consequently also the cancellation of IR-divergences are left invariant. Instead, gauge transformations merely correspond to choosing a different representative of the equivalence class, i.e. to modifying the choice (4.59). However, the amplitude is not invariant under this transformation,

$${}^r_{\lambda} \langle \langle \beta | \hat{S} | \tilde{\alpha} \rangle \rangle_{\lambda}^r = {}^r_{\lambda} \langle \langle \beta | \hat{S} | \alpha \rangle \rangle_{\lambda}^r \left( 1 - \frac{1}{2} \int_{\lambda}^r \frac{d^3 \vec{k}}{|\vec{k}|} \sum_l |\tilde{\lambda}_l(\vec{k})|^2 \right), \quad (4.83)$$

<sup>11</sup>In contrast, the radiation state (4.78) is manifestly gauge-invariant.

where we restricted ourselves to the leading order in  $\tilde{\lambda}_l(\vec{k})$ . This effect is weak for sufficiently small  $r \tilde{\lambda}_l(\vec{k})$  but generically nonzero. In order to restore full invariance, one has to apply the same shift (4.8) to both initial and final states:<sup>12</sup>  ${}^r_\lambda \langle \langle \tilde{\beta} | \hat{S} | \tilde{\alpha} \rangle \rangle_\lambda^r = {}^r_\lambda \langle \langle \beta | \hat{S} | \alpha \rangle \rangle_\lambda^r$ . This shows that dressing states do not exhibit dynamics of their own, but that – in line with our previous discussion – the physical meaning of dressing is to decouple photons of energy below  $r$ .

In our combined formalism, which includes both dressing and radiation, there is an interesting interpretation of the gauge transformed dressing state (4.82). Up to an inessential phase factor, it can be written as

$$|\tilde{\alpha}\rangle_\lambda^r \sim \exp \left\{ -\frac{1}{2} \int_\lambda^r \frac{d^3 \vec{k}}{|\vec{k}|} \sum_l |\tilde{\lambda}_l(\vec{k})|^2 \right\} \exp \left\{ \int_\lambda^r \frac{d^3 \vec{k}}{\sqrt{|\vec{k}|}} \sum_l \tilde{\lambda}_l^*(\vec{k}) \hat{a}_{l,\vec{k}}^{[\alpha]\dagger} \right\} |\alpha\rangle_\lambda^r, \quad (4.84)$$

where  $\hat{a}_{l,\vec{k}}^{[\alpha]\dagger}$  is defined in Eq. (4.67). It becomes evident that large gauge transformations correspond to adding photons that are not defined in the Fock space, but according to the representation of the commutation relations in the equivalence class  $[\alpha]$ .

## 4.3 Reduced Density Matrix

### 4.3.1 Well-Defined Tracing

So far, we have proposed a combined formalism, which can simultaneously describe dressing and radiation. In doing so, we have introduced a new energy scale  $r$  which separates dressing from radiation. We have shown that the rates are independent of  $r$ , i.e. we obtain the same IR-finite results as in the two known formalisms. In this section, we want to go one step further and investigate the density matrix of the final state. This is particularly interesting since it turns out to be sensitive to  $r$ . For a particular simplified setup, the density matrix in the presence of soft bremsstrahlung was already studied some time ago. In a framework of real time evolution [244–246], which goes beyond the  $S$ -matrix description, the result was that tracing over unresolvable soft radiation leads to some loss of coherence. But for realistic timescales, the decoherence is generically small. As it should be, it does not spoil the interference properties that we observe in Nature.

However, it was also derived in [244–246] how coherence depends on the timescale  $t_{\text{obs}}$ , after which the final state is observed: Albeit slowly, it decreases as the timescale increases. In the limit of infinite time, one obtains full decoherence.

<sup>12</sup>This is evident in the computations because all results solely depend on the difference  $\mathcal{F}_{\alpha,\beta}^{(l)}(\vec{k})$ . Therefore, it is possible to describe the same physical process with dressings that are shifted by a common function,  $\mathcal{F}_\alpha^{(l)}(\vec{k}) \rightarrow \mathcal{F}_\alpha^{(l)}(\vec{k}) + C(\vec{k})$  and  $\mathcal{F}_\beta^{(l)}(\vec{k}) \rightarrow \mathcal{F}_\beta^{(l)}(\vec{k}) + C(\vec{k})$ . Such modifications of the dressing states have recently been considered in [247, 248].

Since this is precisely the limit on which the definition of the  $S$ -matrix is based, it is immediately evident that it might be difficult to derive the density matrix in the  $S$ -matrix formalism. In the inclusive formalism, this expectation turns out to be fulfilled. Tracing over soft radiation, which is required for IR-finiteness, leads to full decoherence [245, 246]. In an independent line of research, this finding has recently received renewed interest in the context of a generic scattering process [66]. However, if it were not possible to improve this result, this would mean that the  $S$ -matrix is *in principle* unable to describe any interference phenomena in QED. This finding is a clear indication that the inclusive formalism is insufficient for describing the density matrix of the final scattering state.

In the dressed formalism, the opposite situation is realized. The reason is that the dressing photons are part of the definition of the asymptotic states and are independent of the scattering process. Therefore, there is no reason to trace over them. In fact, it is not even clear how to define the trace in the von Neumann space since it would amount to squeezing the infinite von Neumann subspaces into a single Fock space. This means that there is no tracing and no decoherence in the dressed formalism.<sup>13</sup> Also this finding is unsatisfactory since one expects some decoherence due to the emission of unresolvable soft bremsstrahlung.

Our goal is to show that the situation improves in the combined formalism that we propose. Since in this case the final state consists both of dressing (defined by the scale  $r$ ) and of soft radiation (defined by the scale  $\epsilon$ ), we have at our disposal a well-defined notion of trace: We have to trace over radiation but not over dressing. In this way, we avoid full decoherence. Moreover, comparison with the results of [244–246] allows us to confirm that the scale  $r$  is set by the timescale after which the final state is observed,  $r = t_{\text{obs}}^{-1}$ .

Before tracing, the density matrix of the final state (4.77) reads

$$\begin{aligned} \hat{\rho}^{\text{full}} &= \hat{S} |\alpha\rangle\rangle_{\lambda}^r \langle\langle\alpha| \hat{S} \\ &= \sum_{\beta, \beta'} \left(\frac{\epsilon}{\Lambda}\right)^{\frac{B_{\alpha, \beta} + B_{\alpha, \beta'}}{2}} S_{\alpha, \beta} S_{\alpha, \beta'}^* (|\beta\rangle\rangle_{\lambda}^r \otimes |\gamma(\alpha, \beta)\rangle_r^{\epsilon}) \left(\langle\langle\gamma(\alpha, \beta')| \otimes \langle\langle\beta'| \right). \end{aligned} \quad (4.85)$$

Using an arbitrary basis  $\{|\gamma\rangle\}_{\gamma}$  of radiation, i.e. in the space of photons with

---

<sup>13</sup>The density matrix of the final state has also recently been studied in [67, 249], where the scales of radiation and dressing were identified,  $r = \epsilon$ , and a tracing over dressing states was performed. Since states in different equivalence classes are orthogonal, a similar result as in the inclusive formalism, i.e. a fully decohered density matrix of the final state, was obtained. As explained, however, both the mathematical soundness and the physical meaning of tracing over dressing states are unclear to us.

energies above  $r$  but below  $\epsilon$ , the trace is

$$\hat{\rho}^{\text{red}} = \sum_{\gamma} \theta(E_{\gamma} - \epsilon) \sum_{\beta, \beta'} \left( \frac{\epsilon}{\Lambda} \right)^{\frac{B_{\alpha, \beta} + B_{\alpha, \beta'}}{2}} S_{\alpha, \beta} S_{\alpha, \beta'}^* \langle \beta | \rangle_{\lambda}^r \langle \langle \beta | \rangle_{\lambda}^r \langle \gamma | \gamma(\alpha, \beta) \rangle_r^{\epsilon} \langle \gamma(\alpha, \beta') | \gamma \rangle, \quad (4.86)$$

where as in the computation of the rate, we imposed that the total energy  $E_{\gamma}$  in radiation is at most  $\epsilon$ . If we neglect energy conservation for a moment, the computation becomes particularly transparent:

$$\hat{\rho}^{\text{red}} \cong \sum_{\beta, \beta'} \left( \frac{\epsilon}{\Lambda} \right)^{\frac{B_{\alpha, \beta} + B_{\alpha, \beta'}}{2}} S_{\alpha, \beta} S_{\alpha, \beta'}^* \langle \gamma(\alpha, \beta') | \gamma(\alpha, \beta) \rangle_r^{\epsilon} \langle \beta | \rangle_{\lambda}^r \langle \langle \beta | \rangle_{\lambda}^r. \quad (4.87)$$

Thus, we only have to compute the overlap of coherent radiation states:

$$\begin{aligned} \langle \gamma(\alpha, \beta') | \gamma(\alpha, \beta) \rangle_r^{\epsilon} &= e^{-\frac{1}{2} \int_r^{\epsilon} \frac{d^3 \vec{k}}{|\vec{k}|} \sum_l |\mathcal{F}_{\alpha, \beta}^{(l)}(\vec{k})|^2 + |\mathcal{F}_{\alpha, \beta'}^{(l)}(\vec{k})|^2} \\ &\quad \cdot \langle 0 | e^{\int_r^{\epsilon} \frac{d^3 \vec{k}}{\sqrt{|\vec{k}|}} \sum_l \mathcal{F}_{\alpha, \beta'}^{(l)*}(\vec{k}) \hat{a}_{l, \vec{k}}} e^{\int_r^{\epsilon} \frac{d^3 \vec{k}}{\sqrt{|\vec{k}|}} \sum_l \mathcal{F}_{\alpha, \beta}^{(l)}(\vec{k}) \hat{a}_{l, \vec{k}}^{\dagger}} | 0 \rangle \\ &= e^{-\frac{1}{2} \int_r^{\epsilon} \frac{d^3 \vec{k}}{|\vec{k}|} \sum_l \left| \mathcal{F}_{\alpha, \beta}^{(l)}(\vec{k}) - \mathcal{F}_{\alpha, \beta'}^{(l)}(\vec{k}) \right|^2} \\ &= e^{-\frac{1}{2} \int_r^{\epsilon} \frac{d^3 \vec{k}}{|\vec{k}|} \sum_l \left| \mathcal{F}_{\beta, \beta'}^{(l)}(\vec{k}) \right|^2} \\ &= \left( \frac{r}{\epsilon} \right)^{B_{\beta, \beta'} / 2}, \end{aligned} \quad (4.88)$$

where the kinematical factor for a hypothetical process  $\beta \rightarrow \beta'$  appeared. In total, we obtain the element of the reduced density matrix,

$$\rho_{\beta\beta'}^{\text{red}} = \left( \frac{\epsilon}{\Lambda} \right)^{\frac{B_{\alpha, \beta} + B_{\alpha, \beta'}}{2}} \left( \frac{r}{\epsilon} \right)^{\frac{B_{\beta, \beta'}}{2}} S_{\alpha, \beta} S_{\alpha, \beta'}^*, \quad (4.89)$$

where it is understood that indices refer to dressed states. Clearly, this result is IR-finite. Had we taken into account energy conservation, we would have gotten the result (which is a generalization of the computation in [66]):

$$\rho_{\beta\beta'}^{\text{red}} = \left( \frac{\epsilon}{\Lambda} \right)^{\frac{B_{\alpha, \beta} + B_{\alpha, \beta'}}{2}} \left( \frac{r}{\epsilon} \right)^{\frac{B_{\beta, \beta'}}{2}} f \left( \frac{B_{\alpha, \beta} + B_{\alpha, \beta'} - B_{\beta, \beta'}}{2} \right) S_{\alpha, \beta} S_{\alpha, \beta'}^*. \quad (4.90)$$

As it should be, we observe that the diagonal terms reproduce the well-known rates (4.79), i.e.  $\rho_{\beta\beta}^{\text{red}} = \Gamma_{\alpha, \beta}$ .

Finally, we can use the matrix element (4.90) to further justify our choice (4.61) of  $r$ . In a framework of real time evolution, it was derived in [244–246] for

a particular simplified setup that the off-diagonal elements of the density matrix scale as  $(1/t_{\text{obs}})^{B_{\beta, \beta'}/2}$ , where  $t_{\text{obs}}$  is the timescale after which the final state is measured. Comparing this with (4.90), we conclude that the identification  $r \sim t_{\text{obs}}^{-1}$  was indeed justified. In this way, we obtain the same behavior as in [244–246]: The longer we wait before we measure the final state, the smaller we have to choose  $r$  and the more the off-diagonal elements of the density matrix get suppressed. We note, however, that our combined formalism does not rely on the identification (4.61) and holds for general  $r$ .

### 4.3.2 Generalization to Superposition as Initial State

As suggested in [249], it is interesting to study a situation in which the initial state  $|\psi\rangle$  is not a momentum eigenstate,

$$|\psi\rangle\rangle_{\lambda}^r = \sum_{\alpha} f_{\alpha}^{(\psi)} |\alpha\rangle\rangle_{\lambda}^r, \quad (4.91)$$

where  $\sum_{\alpha} |f_{\alpha}^{(\psi)}|^2 = 1$  and we used the linearity of the definition (4.59) of dressing. Generalizing the above calculations, we get

$$\begin{aligned} \rho_{\beta, \beta'}^{\text{red}} &= \sum_{\alpha, \alpha'} f_{\alpha}^{(\psi)} f_{\alpha'}^{(\psi)*} \left(\frac{\epsilon}{\Lambda}\right)^{\frac{B_{\alpha, \beta} + B_{\alpha', \beta'}}{2}} \left(\frac{r}{\epsilon}\right)^{\frac{B_{\alpha, \beta} + B_{\alpha', \beta'} - B_{\alpha, \beta, \alpha', \beta'}}{2}} \\ &\cdot f(B_{\alpha, \beta, \alpha', \beta'}) S_{\alpha, \beta} S_{\alpha', \beta'}^*, \end{aligned} \quad (4.92)$$

where

$$B_{\alpha, \beta, \alpha', \beta'} = \frac{1}{2(2\pi)^3} \sum_{\substack{n \in \alpha, \beta \\ m \in \alpha', \beta'}} \int d^2\Omega \frac{\eta_n \eta_m \epsilon_n \epsilon_m \mathbf{p}_n \cdot \mathbf{p}_m}{\mathbf{p}_n \cdot \hat{\mathbf{k}} \mathbf{p}_m \cdot \hat{\mathbf{k}}}. \quad (4.93)$$

The density matrix (4.92) applies to the most general case and thereby constitutes the main result of this section.

Clearly, this density matrix avoids full decoherence. In order to further analyze our result, we can decompose the sums:

$$B_{\alpha, \beta, \alpha', \beta'} = \frac{B_{\alpha, \beta'} + B_{\alpha', \beta} - B_{\alpha, \alpha'} - B_{\beta, \beta'}}{2}. \quad (4.94)$$

This shows that if there is only one momentum eigenstate in the initial state,  $f_{\alpha}^{(\psi)} = \delta_{\alpha}^{\alpha_0}$ , the general density matrix (4.92) reduces to the result (4.90) obtained before. It is moreover interesting to analyze the rates that we obtain:

$$\rho_{\beta, \beta}^{\text{red}} = \sum_{\alpha, \alpha'} f_{\alpha}^{(\psi)} f_{\alpha'}^{(\psi)*} \left(\frac{\epsilon}{\Lambda}\right)^{\frac{B_{\alpha, \beta} + B_{\alpha', \beta}}{2}} \left(\frac{r}{\epsilon}\right)^{\frac{B_{\alpha, \alpha'}}{2}} f\left(\frac{B_{\alpha, \beta} + B_{\alpha', \beta} - B_{\alpha, \alpha'}}{2}\right) S_{\alpha, \beta} S_{\alpha', \beta}^*. \quad (4.95)$$

The  $f(B)$ -function is subleading since it we can approximate it as  $f(B) \sim 1 - B^2$  for small  $B$  (see Eq. (4.34)) and additionally it is insensitive to the ratio  $r/\epsilon$ . Therefore, we can focus on the other two IR-factors,  $(\epsilon/\Lambda)^{(B_{\alpha,\beta}+B_{\alpha',\beta})/2}$  and  $(r/\epsilon)^{B_{\alpha,\alpha'}/2}$ . Clearly, both are always smaller than 1. In the case of constructive interference, they therefore always lead to a suppression of the rate. For destructive interference, however, they can work in both directions, i.e. they can also serve to diminish suppressing contributions and thereby increase the rate. The  $r$ -dependent contribution  $(r/\epsilon)^{B_{\alpha,\alpha'}/2}$  is particularly interesting since it does not factorize, i.e. it cannot be absorbed in a redefinition of  $S_{\alpha,\beta}$ . These findings also hold for the off-diagonal elements. It is straightforward to show that the exponent of the  $r$ -dependent term in Eq. (4.92) is positive [249], so it also leads to a factor smaller than 1. As before, this means that it leads to a suppression of off-diagonal elements if there is constructive interference. In particular, this is always the case when the initial state is only a single momentum eigenstate. In contrast, it can cause both suppression and enhancement for destructive interference.

### 4.3.3 Estimate of Amount of Decoherence

At this point, it is important to estimate the amount of decoherence and the corresponding loss of information that arises due to tracing over soft modes. To this end, we compute the entanglement entropy of hard and soft modes. It is defined as the von Neumann entropy of the density matrix  $\rho^{\text{red}}$  obtained after tracing over soft radiation. For giving an upper bound, it turns out that it is useful to investigate what off-diagonal elements would be needed to obtain a pure density matrix. Thus, we assume that we are given a density matrix  $|\Psi\rangle\rangle_{\lambda}^r \langle\langle\Psi|$  defined by a state

$$|\Psi\rangle\rangle_{\lambda}^r = \sum_{\beta} a_{\beta} |\beta\rangle\rangle_{\lambda}^r, \quad (4.96)$$

which fulfills  $|a_{\beta}|^2 = \rho_{\beta,\beta}^{\text{red}}$  but can have arbitrary phases. This means that  $\rho^{\text{pure}}$  and  $\rho^{\text{red}}$  have the same diagonal and therefore describe the same rates. Now we can parameterize the deviation from purity as the quotient of the actual element of the reduced density matrix (4.92) and the element required for purity:

$$c_{\beta,\beta'}^{(\Psi)} = \frac{\rho_{\beta,\beta'}^{\text{red}}}{a_{\beta} a_{\beta'}^*}. \quad (4.97)$$

So the deviations of the  $c_{\beta,\beta'}^{(\Psi)}$  from 1 determine the decoherence and full coherence corresponds to  $c_{\beta,\beta'}^{(\Psi)} = 1$ .

In the following, our goal is to give an upper bound on the von Neumann entropy  $S_{\text{soft}} = -\text{Tr} \rho^{(\alpha),\text{red}} \ln \rho^{(\alpha),\text{red}}$  in terms of  $c_{\beta,\beta'}^{(\Psi)}$ . To this end, we use the following argument: If all off-diagonal element were zero, the maximal entropy would be given by  $S_{\text{max}} = \ln d_H$ , where  $d_H$  is the dimension of the hard Hilbert

space. This maximal entropy would be reached if all final hard states were equally probable, i.e. all diagonal elements were equal. For our estimate, we will therefore restrict ourselves to a density matrix in which all diagonal elements are equal. Such a density matrix is pure if all elements, i.e. also the off-diagonal ones, are equal. In order to derive the upper bound on the entropy, we can consequently define  $\Delta_{\max} := \max_{\beta, \beta'} |1 - c_{\beta, \beta'}^{(\Psi)}|$  and then multiply the off-diagonal elements of the pure density matrix, in which all entries are equal, by the function  $c := 1 - \Delta_{\max}$ .<sup>14</sup> In this setup, the eigenvalues of the density matrix are<sup>15</sup>

$$e_1 = \frac{1 + (d_H - 1)c}{d_H} \quad \text{and} \quad e_i = \frac{1 - c}{d_H} \quad \text{for } i \in [2, d_H]. \quad (4.98)$$

To leading order in  $\Delta_{\max}$ , this gives the bound

$$S_{\text{soft}} < \Delta_{\max} \ln \left( \frac{d_H}{\Delta_{\max}} \right). \quad (4.99)$$

As expected, we obtain  $S_{\text{soft}} = 0$ , i.e. purity, for  $\Delta_{\max} = 0$ . Full decoherence can only be obtained in the limit  $\Delta_{\max} = 1$ . For small  $\Delta_{\max}$ , we obtain the simple bound on the relative entropy

$$\frac{S_{\text{soft}}}{S_{\max}} \lesssim \max_{\beta, \beta'} |1 - c_{\beta, \beta'}^{(\Psi)}|. \quad (4.100)$$

As expected, deviations of the  $c_{\beta, \beta'}^{(\Psi)}$  from 1 determine decoherence.

To derive a concrete bound on the entanglement entropy, we have to choose  $a_\beta$ . As said, the absolute value is fixed by the requirement  $|a_\beta|^2 = \rho_{\beta, \beta}^{\text{red}}$ . To obtain a bound that is maximally sharp, we therefore have to set the phases such that  $c_{\beta, \beta'}^{(\Psi)}$  is minimal. In the explicit computation of  $c_{\beta, \beta'}^{(\Psi)}$ , it turns out that a good choice is<sup>16</sup>

$$a_\beta = \left( \sum_{\alpha, \alpha'} f_\alpha^{(\psi)} f_{\alpha'}^{(\psi)*} \left( \frac{\epsilon}{\Lambda} \right)^{\frac{B_{\alpha, \beta} + B_{\alpha', \beta}}{2}} \left( \frac{r}{\epsilon} \right)^{\frac{B_{\alpha, \alpha'}}{2}} f \left( \frac{B_{\alpha, \beta} + B_{\alpha', \beta} - B_{\alpha, \alpha'}}{2} \right) S_{\alpha, \beta} S_{\alpha', \beta}^* \right)^{1/2} \\ \cdot \exp \left[ i \arg \sum_{\alpha} f_\alpha^{(\psi)} \left( \frac{\epsilon}{\Lambda} \right)^{\frac{B_{\alpha, \beta}}{2}} S_{\alpha, \beta} \right]. \quad (4.101)$$

<sup>14</sup>At this point, one can wonder why we could not use  $c := 1 + \Delta_{\max}$  instead. The reason is that any  $c > 1$  would lead to an unphysical density matrix with negative eigenvalues. Note that it is nonetheless not excluded that some  $c_{\beta, \beta'}^{(\Psi)}$  are bigger than 1.

<sup>15</sup>These are the eigenvalues of a quadratic matrix of dimension  $d_H$  that has  $1/d_H$  on the diagonal and  $c/d_H$  on all off-diagonal elements. A linearly independent set of eigenvectors  $v_i$  is given by the entries  $(v_1)_k = 1$  and  $(v_i)_k = \delta_{k1} - \delta_{ki}$  for  $i \in [2, d_H]$ .

<sup>16</sup>The absolute value is fixed by rate (4.95). The phase is chosen such that it reproduces the density matrix (4.92) in the limit  $r \rightarrow \epsilon$  and  $f(B) \rightarrow 1$ .

Now we evaluate (4.100) in the regime of weak coupling where all kinematical factors become small,  $B \ll 1$ . Then we can expand the exponential and the  $f(B)$ -functions. In the regime  $r \ll \epsilon$ , in which we work throughout, the contribution of the  $f(B)$ -functions is, as already explained, subleading and we will ignore it. Then we obtain to leading order

$$\begin{aligned} \frac{S_{\text{soft}}}{S_{\text{max}}} &\lesssim \ln \frac{\epsilon}{r} \max_{\beta, \beta'} \frac{1}{2} \\ &\cdot \left| \frac{\sum_{\alpha, \alpha'} f_{\alpha}^{(\psi)} f_{\alpha'}^{(\psi)*} \left(\frac{\epsilon}{\Lambda}\right)^{\frac{B_{\alpha, \beta} + B_{\alpha', \beta'}}{2}} S_{\alpha, \beta} S_{\alpha', \beta'}^* (B_{\alpha, \beta} + B_{\alpha', \beta'} - 2B_{\alpha, \beta, \alpha', \beta'})}{\left(\sum_{\alpha} f_{\alpha}^{(\psi)} \left(\frac{\epsilon}{\Lambda}\right)^{\frac{B_{\alpha, \beta}}{2}} S_{\alpha, \beta}\right) \left(\sum_{\alpha} f_{\alpha}^{(\psi)*} \left(\frac{\epsilon}{\Lambda}\right)^{\frac{B_{\alpha, \beta'}}{2}} S_{\alpha, \beta'}^*\right)} \right. \\ &- \frac{\sum_{\alpha, \alpha'} f_{\alpha}^{(\psi)} f_{\alpha'}^{(\psi)*} \left(\frac{\epsilon}{\Lambda}\right)^{\frac{B_{\alpha, \beta} + B_{\alpha', \beta}}{2}} S_{\alpha, \beta} S_{\alpha', \beta}^* B_{\alpha, \alpha'}}{2 \left| \sum_{\alpha} f_{\alpha}^{(\psi)} \left(\frac{\epsilon}{\Lambda}\right)^{\frac{B_{\alpha, \beta}}{2}} S_{\alpha, \beta} \right|^2} \\ &\left. - \frac{\sum_{\alpha, \alpha'} f_{\alpha}^{(\psi)} f_{\alpha'}^{(\psi)*} \left(\frac{\epsilon}{\Lambda}\right)^{\frac{B_{\alpha, \beta'} + B_{\alpha', \beta'}}{2}} S_{\alpha, \beta'} S_{\alpha', \beta'}^* B_{\alpha, \alpha'}}{2 \left| \sum_{\alpha} f_{\alpha}^{(\psi)} \left(\frac{\epsilon}{\Lambda}\right)^{\frac{B_{\alpha, \beta'}}{2}} S_{\alpha, \beta'} \right|^2} \right|. \end{aligned} \quad (4.102)$$

Already at this point, the physical properties of this result become evident. First, decoherence depends logarithmically on the ratio  $\epsilon/r$ . This means that it gets big if the resolution gets worse, i.e.  $\epsilon$  increases, or if one waits longer before measuring the final state, i.e.  $r$  decreases. In the limit of the best achievable resolution,  $\epsilon = r$ , there is no decoherence.<sup>17</sup> Moreover, we observe that the bound on the entanglement entropy scales with the kinematical factors  $B$ , i.e. becomes small for small  $B$ -factors.<sup>18</sup> Since they are proportional to  $e^2$  and the momentum transfer, we conclude that decoherence scales with the coupling. Finally, it also depends on the kinematics of the scattering process. In the case in which the initial state is a single momentum eigenstates, this dependence becomes particularly transparent:

$$\frac{S_{\text{soft}}}{S_{\text{max}}} \lesssim \ln \frac{\epsilon}{r} \max_{\beta, \beta'} \frac{B_{\beta, \beta'}}{2}. \quad (4.103)$$

<sup>17</sup>Our derivation of the density matrix (4.92) relies on  $r \ll \epsilon$  and is no longer valid in the limit  $r = \epsilon$ , which corresponds to the dressed formalism. However, it is easy to rederive the density matrix in this case and one obtains (4.92) but without the  $r$ -dependent factor and without the  $f(B)$ -function. Therefore, the bound (4.102) also holds for  $r = \epsilon$  and shows that there is no decoherence in this limit.

<sup>18</sup>An exception could occur in the case of fully destructive interference, i.e. when one of the denominators in Eq. (4.102) vanishes. However, as long as only a small fraction of the entries of the density matrix goes to zero, it is clear that the amount of decoherence is still small. In that case, one would have to employ a more sophisticated bound than the one that we use here.

Since the kinematical factor  $B_{\beta, \beta'}$  depends on the angle between the electrons in  $\beta$  and  $\beta'$ , we conclude that decoherence scales with the angle between different final states, i.e. it gets bigger for bigger angles. This means that decoherence increases for final states whose bremsstrahlung is macroscopically different.

#### 4.3.4 Implications for Optical Theorem

In this section, we briefly discuss how infrared divergences in the optical theorem and infrared divergences in the density matrix are related. To this end, we show that the off-diagonal elements of the optical theorem are generically related to the off-diagonal elements of a density matrix. Therefore, infrared divergences can lead to a vanishing off-diagonal element in the optical theorem if and only if the off-diagonal element of the density matrix vanishes as well.

In general, the optical theorem – as a straightforward consequence of unitarity – relates the imaginary part of the amplitude for the process  $\beta \rightarrow \beta'$  to the sum of the product of two amplitudes with arbitrary intermediate state,

$$\begin{aligned} & -i \left( {}^r_{\lambda} \langle \langle \beta | \hat{S}_{\text{nt}} | \beta' \rangle \rangle_{\lambda}^r - \left( {}^r_{\lambda} \langle \langle \beta' | \hat{S}_{\text{nt}} | \beta \rangle \rangle_{\lambda}^r \right)^{\star} \right) \\ & = \sum_{\substack{\gamma \\ (r < E_{\gamma} < \epsilon)}} \sum_{\substack{\alpha \\ (\epsilon < E_{\alpha})}} {}^r_{\lambda} \langle \langle \beta | \hat{S}_{\text{nt}} (|\alpha\rangle_{\lambda}^r \otimes |\gamma\rangle) \left( {}^r_{\lambda} \langle \langle \beta' | \hat{S}_{\text{nt}} (|\alpha\rangle_{\lambda}^r \otimes |\gamma\rangle) \right)^{\star}, \end{aligned} \quad (4.104)$$

where we have decomposed a complete set of states as a tensor product of hard states  $|\alpha\rangle_{\lambda}^r$  and radiation  $|\gamma\rangle$ .<sup>19</sup> Here  $\hat{S}_{\text{nt}}$  denotes the nontrivial part of the  $S$ -matrix:  $\hat{S} = 1 + i\hat{S}_{\text{nt}}$ . We will drop the subscript since the distinction between  $\hat{S}_{\text{nt}}$  and  $\hat{S}$  will be inessential for our consideration.

Now we can use that the absorption and the emission of soft photons lead to analogous contributions (see Eq. (4.6)). Since we have  $B_{\alpha, \beta} = B_{\beta, \alpha}$  and moreover all soft correction factors are real, we conclude that we can write the r.h.s. of the optical theorem in terms of the matrix elements  $\rho_{\beta, \beta'}^{\text{red}, (\alpha)}$  of the reduced density matrix defined in Eq. (4.86):

$$-i \left( {}^r_{\lambda} \langle \langle \beta | \hat{S}_{\text{nt}} | \beta' \rangle \rangle_{\lambda}^r - \left( {}^r_{\lambda} \langle \langle \beta' | \hat{S}_{\text{nt}} | \beta \rangle \rangle_{\lambda}^r \right)^{\star} \right) = \sum_{\alpha} \rho_{\beta, \beta'}^{\text{red}, (\alpha)}. \quad (4.105)$$

While from the perspective of the optical theorem,  $|\alpha\rangle_{\lambda}^r$  is an intermediate state, it takes the role of the initial state for the density matrix. For this reason, we explicitly indicated the initial state in the notation  $\rho_{\beta, \beta'}^{\text{red}, (\alpha)}$ . In summary, the (off-)diagonal elements of the optical theorem are related to the (off-)diagonal elements of the density matrix.

This enables us to check if the IR-behavior of the two sides of the equation match. First, we consider the limit  $r \rightarrow 0$ , which corresponds to the inclusive

<sup>19</sup>According to the decomposition (4.74), we do not independently sum over photons of energy smaller than  $r$  since they are already contained in the dressing of the hard states.

formalism. In this case, we know that the off-diagonal elements of the density matrix vanish whereas only the diagonal entries are finite. Indeed, this matches the behavior of the l.h.s. of the optical theorem. Namely, it is important to notice that we did not include radiation in the states  $|\beta\rangle\rangle_\lambda^r$  and  $|\beta'\rangle\rangle_\lambda^r$ . Therefore, in the limit of the inclusive formalism, off-diagonal element with  $|\beta\rangle\rangle_\lambda^r \not\approx |\beta'\rangle\rangle_\lambda^r$  vanish because of soft loops. Only diagonal entries are finite.

In this opposite limit  $r \rightarrow \epsilon$  of the dressed formalism, the off-diagonal entries of the density matrix are maximal. Again, this matches the behavior of the l.h.s. of the optical theorem since individual amplitudes without radiation are maximized by taking  $r \rightarrow \epsilon$ .

Finally, we remark that one can obtain nonvanishing off-diagonal elements of the optical theorem also in the inclusive formalism. As usual, one has to include radiation in the process  $\beta \rightarrow \beta'$ . The resulting IR-finite optical theorem can moreover be used to define an effective IR-finite density matrix in the inclusive formalism. We will, however, not reproduce this construction, which we have developed in [4], because the combined formalism provides us with a first-principle derivation of the density matrix.

## 4.4 Implications for Black Holes

### 4.4.1 Information in Soft Modes

Next, we come to a very interesting connection of infrared physics and black hole information. As is the case in any nontrivial process in gravity, the gravitons emitted during Hawking evaporation are expected to be accompanied by soft IR-modes. Since the energy of Hawking quanta is  $\hbar r_g^{-1}$ , a mode can be called soft in this context if its energy is much smaller than  $\hbar r_g^{-1}$ .

It is very interesting to investigate how much information the soft modes that accompany the Hawking quanta carry. In particular, the very interesting proposal was made [56] that those could carry all information of the black hole. In this picture, which we already briefly introduced in section 1.5, one would observe a completely mixed final state if one does not resolve the soft modes. However, once all soft modes are measured, a pure state would be obtained. Thus, soft modes alone would suffice to purify Hawking radiation.

The goal of this section is to critically examine the proposal [56] and to investigate how much information is contained in soft IR-modes. First, we will investigate the number of IR-modes that are produced in the process of Hawking evaporation. Those set the maximal amount of information that the soft sector can carry. Secondly, we will apply the results of section 4.3.3, in which we estimated the amount of entanglement between hard particles and soft modes. In both cases, the conclusion will be that soft modes only give a subleading contribution to the black hole entropy.

In order to make a quantitative statement about the contribution of soft modes to Hawking evaporation, we do not require an explicit  $S$ -matrix computation of this process. This may seem surprising at first, but this fact is due to the power of infrared physics. Namely, the corresponding contributions are only sensitive to the asymptotic states. Even if we do not know the diagram, the knowledge of initial and final states suffices to compute the contribution of infrared modes. We will first do so for the emission of a single Hawking quantum.

Thus, we consider as initial state a black hole at rest, i.e. its 4-momentum is  $p_{\text{bh}} = (M, \vec{0})$ . In the final state, we have a massless Hawking quantum with  $p_{\text{H}} = (r_g^{-1}, r_g^{-1} \vec{e})$ , where  $\vec{e}$  is an arbitrary unit vector and we have momentarily set  $\hbar = 1$ . Correspondingly, the final state of the black hole is  $p'_{\text{bh}} = (M - r_g^{-1}, -r_g^{-1} \vec{e})$ . This asymptotic data alone suffices to compute the infrared exponent  $B_{\alpha, \beta}$ . To leading order in  $r_g^{-1}/M_p$ , a straightforward calculation of Eq. (4.29) gives

$$B_{\alpha, \beta} \approx \frac{r_g^{-2}}{M_p^2}. \quad (4.106)$$

This is the coupling strength that we expect in a process with momentum transfer  $r_g^{-1}$ . In terms of  $N = M^2/M_p^2$ , we get

$$B_{\alpha, \beta} \approx \frac{1}{N}. \quad (4.107)$$

### Number of Soft Modes

First, we want to study the number of produced IR-modes. To this end, only physical radiation matters. We begin by determining its relevant energy scales. Since we deal with a process of black hole evaporation, the scale  $r$ , which separate dressing from radiation, is given by the lifetime  $t_{\text{b-h}} \approx Nr_g$  of the black hole. Thus we get

$$r \approx \frac{r_g^{-1}}{N}. \quad (4.108)$$

This implies that the best achievable resolution is

$$\epsilon_{\text{best}} \approx \frac{r_g^{-1}}{N}. \quad (4.109)$$

However, the resolution cannot be too bad, either. To be able to observe Hawking evaporation, we need at least

$$\epsilon_{\text{worst}} \approx r_g^{-1}. \quad (4.110)$$

Next, we recall the computation (4.31) of soft emission. The exponential  $e^{B_{\alpha, \beta} \ln \frac{\epsilon}{\lambda}}$  arises from a resummation of emission processes with different numbers of soft photons in the final state. Specifically, the  $n^{\text{th}}$  summand of the exponential series comes from the emission of  $n$  IR-modes. Therefore, we can estimate the

number of soft modes from the term which gives the biggest contribution in the series. We get<sup>20</sup>

$$n_{\text{soft}}^{\text{unres}} \sim B_{\alpha,\beta} \ln \frac{\epsilon}{\lambda}. \quad (4.111)$$

If no soft gravitons are measured, the number of unresolved soft modes scales logarithmically with the infrared resolution scale  $\epsilon$ .

Now we can investigate how many more soft gravitons we can resolve when we lower the energy scale of resolution from  $\epsilon_1$  to  $\epsilon_2$ :

$$n_{\text{soft}}^{\text{res}} \sim B_{\alpha,\beta} \ln \frac{\epsilon_1}{\epsilon_2}. \quad (4.112)$$

Plugging in the worst possible resolution (4.110) and the best achievable resolution (4.109) in the process of black hole evaporation as well as Eq. (4.107), we get

$$n_{\text{soft}}^{\text{res}} \lesssim \frac{1}{N} \ln N. \quad (4.113)$$

Thus, after the black hole has evaporated by emitting  $N$  Hawking quanta, the maximal entropy contained in the soft IR-modes is

$$S_{\text{soft}} \lesssim \ln N. \quad (4.114)$$

Independently of the question whether IR-modes are strongly entangled with the Hawking quanta, this shows that they cannot account for the whole entropy of the black hole but could only give a logarithmic correction. Of course, this leaves open the possibility that non-IR soft modes could account for the bulk of black hole information. However, since they are independent of IR-divergences and accompanying dressing tools, the results of infrared physics do not constrain them.

### Entanglement of Soft and Hard Modes

As a second independent argument, we can apply the entropy bound (4.103) derived previously. Plugging in as before  $\epsilon \approx r_g^{-1}$ ,  $r \approx r_g^{-1}/N$  and  $B_{\alpha,\beta} \approx 1/N$  as well as  $S_{\text{max}} = N$ , we get

$$S_{\text{soft}} \lesssim \ln N, \quad (4.115)$$

which is in full accordance with the previous argument based on the number of soft modes. We conclude that soft modes give at most a logarithmic correction to the black hole entropy.

---

<sup>20</sup>Strictly speaking, this formula is only valid in the inclusive formalism, i.e. the limit  $r \rightarrow \lambda$ . In the general case of the combined formalism, one would effectively have to replace  $\lambda$  by  $r$ . Since the final answer is independent of  $\lambda$ , however, this does not change our conclusions.

### 4.4.2 BMS Symmetries and Memory Effect

The asymptotic symmetry group of gravity at null infinity, the BMS group, has been known since the sixties [68–70]. It was discovered during the study of gravitational waves. When a gauge appropriate for this investigation was constructed, it was realized that a full gauge fixing is not possible. Instead, an infinite-dimensional group of residual gauge transformations remains. Together with the Lorentz group, those so-called supertranslations form the BMS group.

Recently, it was suggested that those symmetries can have important implications for the puzzle of black hole information. There are two related but distinct lines of argument. First, it is possible to establish an equivalence of BMS transformations and the soft graviton theorem [220].<sup>21</sup> From this starting point one can investigate what contribution soft gravitons give to the black hole entropy. This has been the subject of the previous section 4.4.1.

Secondly, however, one can try to exploit the relationship of BMS transformations and the gravitational memory effect. The latter is the well-known fact [250] that a gravitational wave that passes through results in a permanent displacement of test particles. The new discovery consists in the observation [221] that this memory effect directly corresponds to a supertranslation, i.e. the metrics before and after the wave passes through differ by a supertranslation.

This fact promises to be very interesting from the perspective of black hole physics. We can imagine the following gedankenexperiment. One starts with a black hole of mass  $M$  and injects radiation with a total energy  $\mu$  and with an angular distribution of energy  $\mathcal{F}_{\text{in}}$ . This results in a black hole of mass  $M + \mu$ . Moreover, as we have discussed in section 1.3.1, the black hole must be sensitive to other characteristics of the injected radiation, provided no classical or semiclassical limit is taken: In order to preserve unitarity, the final state of the black hole therefore also has to depend on  $\mathcal{F}_{\text{in}}$ . If a different angular distribution of energy  $\mathcal{F}_{\text{in},i}$  with the same total energy  $\mu$  is used, the final state of the black hole must also be different.

The question that we will investigate is if any traces of the characteristics of these black holes are still accessible in the (semi)classical limit. We know that the classical black hole metrics corresponding to different  $\mathcal{F}_{\text{in},i}$  must fulfill the no hair theorem. Thus, they are related by diffeomorphisms outside the horizon. Now the interesting connection to BMS symmetries is as follows: Because of the gravitational memory effect, we know that each angular distribution of energy  $\mathcal{F}_{\text{in},i}$  is related to a supertranslation, which we denote by  $T^i$ . The latter is a diffeomorphism, i.e. precisely corresponds to the only kind of classically allowed hair. This leads to the proposal [221–224] that supertranslations could be a candidate

---

<sup>21</sup>Additionally, it has also been discussed to what extent BMS transformations lead to new symmetries. We have briefly discussed this question in section 4.1.2. Partly based on [232–236], we have argued that they bear no physical relevance beyond the well-known decoupling of soft gravitons.

for classical black hole hair. The goal of the present section is to investigate this approach, which has received widespread attention (see e.g. [74, 251–262]). Our conclusion will be that supertranslations can act as a natural bookkeeping tool in the process of black hole formation and evaporation, but that they do not constitute physical hair which could be measured outside the horizon.

### Recap of BMS-Gauge and Memory Effect

We first recap some properties of BMS-gauge, which is defined by the four gauge conditions [68–70]

$$g_{11} = g_{1A} = 0, \quad \det g_{AB} = r^2 \sin^2 \theta, \quad (4.116)$$

where  $A, B, \dots = 2, 3$ . Typically, BMS-gauge is used to study a spacetime asymptotically, i.e. for  $r \rightarrow \infty$ , but it is possible to extend the metric to the bulk by imposing the conditions (4.116) to all orders in  $1/r$ . In a typical situation, however, a metric in BMS-gauge does not cover the whole spacetime.

Such a metric in BMS-gauge exists both in retarded time  $u$ , which is suited to describe outgoing radiation, and in advanced time  $v$ , which is suited to describe incoming radiation. The matching between these two metrics will be crucial for our treatment. Explicitly, an asymptotically flat metric in retarded time takes the form [68–70]:

$$ds^2 = \left( -1 + \frac{m_B^+}{r} + O(r^{-2}) \right) du^2 - \left( 2 + O(r^{-2}) \right) dudr \quad (4.117)$$

$$+ r^2 \left( \gamma_{AB} + C_{AB}^+ r^{-1} + O(r^{-2}) \right) dx^A dx^B + O(r^{-2}) dx^A du, \quad (4.118)$$

where the metric on the sphere has to fulfill the requirement  $\det g_{AB} = r^2 \sin^2 \theta$ . Here  $m_B^+$  is the Bondi mass,  $\gamma_{AB}$  the standard metric on the sphere and

$$C_{AB}^+ = \left( 2D_A D_B - \gamma_{AB} D^2 \right) C^+ \quad (4.119)$$

is determined by the supertranslation field  $C^+$ , where  $D_A$  is the covariant derivative on the sphere. It is helpful to expand the supertranslation field in spherical harmonics. Then the mode  $l = 0$  represents a time shift and the mode  $l = 1$  corresponds to spatial translations. Therefore, all modes with  $l \geq 2$  define proper supertranslations. Metrics with different values of  $C^+$  are connected via asymptotic diffeomorphisms, i.e. the choice of the supertranslation field constitutes a residual gauge freedom of BMS-gauge. These diffeomorphisms are the famous supertranslations. Therefore, we can define a supertranslation  $T^+$  in the group  $BMS_+$  at future null infinity by the change it induces in the supertranslation field:

$$T^+ := \Delta C^+. \quad (4.120)$$

In order to analyze the effect of supertranslations, we will need the constraint equation  $G_{00} = 8\pi G_N T_{00}$ , the leading order of which reads in BMS-gauge:

$$\partial_u m_B^+ = \frac{1}{4G_N} D^2 (D^2 + 2) \partial_u C^+ - \mathcal{F}_{\text{out}}, \quad (4.121)$$

where

$$\mathcal{F}_{\text{out}} = \frac{1}{8} (\partial_u C_{AB}^+) (\partial_u C^{+AB}) + 4\pi \lim_{r \rightarrow \infty} (r^2 T_{uu}) \quad (4.122)$$

is the total incoming null energy, composed of gravitational waves (first summand) and other forms of gravitating energy (second summand).

### Advanced Coordinates

The situation in advanced coordinates is very similar. The metric takes the form

$$ds^2 = \left( -1 + \frac{m_{\bar{B}}}{r} + O(r^{-2}) \right) dv^2 + \left( 2 + O(r^{-2}) \right) dv dr \quad (4.123)$$

$$+ r^2 \left( \gamma_{AB} + C_{AB}^- r^{-1} + O(r^{-2}) \right) dx^A dx^B + O(r^{-2}) dx^A dv, \quad (4.124)$$

where the supertranslation field in advanced coordinates and the supertranslations of the group  $BMS_-$  at past null infinity are defined as in (4.119) and (4.120). The constraint equation becomes

$$\partial_u m_{\bar{B}} = \frac{1}{4G_N} D^2 (D^2 + 2) \partial_u C^- + \mathcal{F}_{\text{in}}, \quad (4.125)$$

where  $\mathcal{F}_{\text{in}}$  is the incoming energy, in analogy to (4.122).

### Measurement of the Supertranslation Field: Memory Effect

As already discussed, one can change the value of the supertranslation field by a diffeomorphism. Therefore, it follows by general covariance that the absolute value of the supertranslation field cannot have any experimental relevance. However, since it corresponds to physical outgoing or ingoing radiation, the difference of the supertranslation field at different times does have experimental implications: It describes the memory effect caused by the radiation, i.e. a permanent displacement of test masses after the radiation has passed [221, 250, 263].

We will restrict ourselves to a simple situation in which we start with some stationary metric  $g_{\mu\nu}^1$  and we finish in a different stationary metric  $g_{\mu\nu}^2$ . In between, there is a radiation epoch, i.e.  $\mathcal{F}_{\text{in/out}}$  only has support during this time span. Asymptotically on  $\mathcal{J}^\pm$ , the process defines a nonstationary metric interpolating between  $g_{\mu\nu}^1$  and  $g_{\mu\nu}^2$ , which should be a solution to the Einstein equations.

Since Birkhoff's theorem implies that we can set  $\partial_A m_B^\pm = 0$  in a stationary metric, we can single out the zero-mode from (4.121) by integrating over the sphere:

$$\mu^+ = -\frac{\int du \int d^2\Omega \mathcal{F}_{\text{out}}}{4\pi}, \quad (4.126)$$

where we first consider retarded time and  $\mu^+ = m_{B,2}^+ - m_{B,1}^+$  is the total change of Bondi mass due to the radiation epoch. This formula shows explicitly that the Bondi mass  $m_B^+$  is monotonically decreasing, i.e. it measures the energy which has not yet left the bulk. Defining the emitted energy with nontrivial angular distribution as  $\Delta\tilde{\mathcal{F}}_{\text{out}} := \int du \mathcal{F}_{\text{out}} - \mu^+$ , the constraint (4.121) becomes

$$0 = \frac{1}{4G_N} D^2(D^2 + 2)T^+ - \Delta\tilde{\mathcal{F}}_{\text{out}}. \quad (4.127)$$

Thus, angular features in the outgoing radiation induces a supertranslation  $T^+ = \Delta C^+$ . Note that it is independent of the total emitted energy  $\mu^+$ .

In advanced coordinates, we get from the constraint (4.125):

$$\mu^- = \frac{\int dv \int d^2\Omega \mathcal{F}_{\text{in}}}{4\pi}. \quad (4.128)$$

The advanced Bondi mass  $m_B^-$  is monotonically increasing, i.e. it measures the energy which has already entered the bulk. Defining  $\Delta\tilde{\mathcal{F}}_{\text{in}} := \int dv \mathcal{F}_{\text{in}} - \mu^-$ , the constraint (4.125) becomes

$$0 = \frac{1}{4G_N} D^2(D^2 + 2)T^- + \Delta\tilde{\mathcal{F}}_{\text{in}}. \quad (4.129)$$

This formula implies that an advanced supertranslation  $T^-$  tracks angular features in the incoming radiation.

### Goldstone Supertranslations

Our goal is to investigate black hole hair, i.e. characteristics of a black hole beyond its mass and other ADM-conserved quantities. Therefore, we will be interested in systems that have the same energy. For this reason, we will consider the following two-step scattering process. First, we inject a wave with total energy  $\mu$  and an angular distribution  $\mathcal{F}_{\text{in}}$ . Then we wait till the system has returned the same amount of energy  $\mu$  and record its angular distribution  $\mathcal{F}_{\text{out}}$ .<sup>22</sup> While such systems are of course special, we will see that black holes can be one of them. This is a zero-energy process in the sense that the total energy of the system does not change. Thus, this process, which is depicted in figure 4.2, constitutes a transformation between degenerate systems and therefore defines hair.

<sup>22</sup>We restrict ourselves for now to pure gravitational radiation, which propagates along null geodesics. Therefore, all emitted energy is bound to reach future null infinity  $\mathcal{J}^+$ .

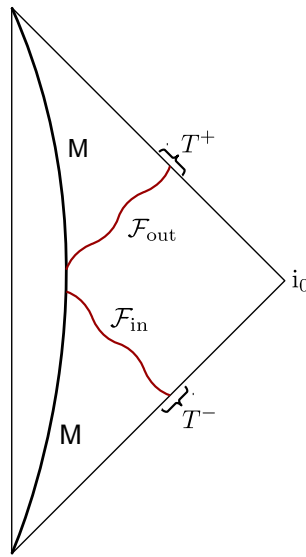


Figure 4.2: A Goldstone supertranslation on a generic system of mass  $M$ . Radiation with angular distribution  $\mathcal{F}_{\text{in}}$  is injected in such a way that radiation with angular distribution  $\mathcal{F}_{\text{out}}$  is returned. Since  $\int dv \int d^2\Omega \mathcal{F}_{\text{in}} = \int du \int d^2\Omega \mathcal{F}_{\text{out}}$ , the total energy of the system remains unchanged. Here  $\mathcal{F}_{\text{in}}$  can be described in terms of the supertranslation  $T^-$  and  $\mathcal{F}_{\text{out}}$  in terms of  $T^+$ .

As far as we reduce ourselves to gravitational radiation, we can generically describe this process in terms of two supertranslations: At  $\mathcal{J}^-$ ,  $T^-$  is determined by the angular distribution  $\Delta\tilde{\mathcal{F}}_{\text{in}}$  of incoming energy according to the constraint (4.129) and at  $\mathcal{J}^+$ ,  $T^+$  follows from the angular distribution  $\Delta\tilde{\mathcal{F}}_{\text{out}}$  of outgoing energy via the constraint (4.127). Thus, the whole process is associated to an element  $(T^-, T^+)$  in the product group  $BMS_- \otimes BMS_+$ . It describes a zero-energy transition which interpolates between two spacetimes of the same total energy.

It is crucial to note that for an asymptotic observer,  $T^-$  and  $T^+$  are independent. Whereas one is free to choose  $T^-$  by preparing an appropriate incoming radiation,  $T^+$  is sensitive to the properties of the system in the bulk. In other words,  $T^+$  is a response of the system which does not only depend on the ingoing radiation, parameterized by  $T^-$ , but also on the state of the system and its particular dynamics, which are not entirely visible asymptotically. In particular, there is no reason why  $(T^-, T^+)$  should be in *any* subgroup of  $BMS_- \otimes BMS_+$ .

### Coordinate Matching

In order to compare ingoing and outgoing radiation, i.e.  $T^-$  and  $T^+$ , we need to relate the supertranslation field  $C^-$  in advanced coordinates to the supertranslation

field  $C^+$  in retarded coordinates. Namely, we assume that we are given a classical spacetime whose asymptotic behavior is fully known to us. Then it is possible to describe this spacetime both in advanced and retarded BMS-gauge. Given an advanced coordinate system  $g_{\mu\nu}^v$ , we want to know if there is a unique retarded coordinate system  $g_{\mu\nu}^u$  we can associate to it. If we have such a mapping, it determines the relation of the advanced supertranslation field  $C^-$ , defined as the  $r^1$  part of  $g_{AB}^v$ , and the retarded supertranslation field  $C^+$ , defined as the  $r^1$  part of  $g_{AB}^u$ .

Given  $g_{\mu\nu}^v$ , we therefore have to find a diffeomorphism  $\mathcal{D}$  such that  $g_{\mu\nu}^u := \mathcal{D}(g_{\mu\nu}^v)$  is in retarded BMS-gauge. Then we can read off from  $g_{\mu\nu}^u$  the  $C^+$  associated to  $C^-$ . However, we could have instead considered the diffeomorphism  $\mathcal{D}' = T^+ \circ \mathcal{D}$ , where  $T^+$  is a supertranslation diffeomorphism in retarded coordinates. Also  $\mathcal{D}'$  transforms the metric in advanced BMS-gauge to a metric in retarded BMS-coordinates. Clearly, if  $T^+$  is a nontrivial supertranslation, the supertranslation field in the resulting metric differs from the one in  $g^u$ . From this consideration it is obvious that the matching between the advanced and the retarded supertranslation field is in general not unique.

The only hope we could have is that there is a natural way to identify  $C^-$  and  $C^+$ . In a static situation, a natural prescription is to require that the spatial part of the two metrics matches, i.e.

$$g_{AB}^u = g_{AB}^v. \quad (4.130)$$

As is shown explicitly in appendix A.3.1 for the example of the Schwarzschild metric, we can achieve this by identifying  $C^+(\theta, \varphi) = -C^-(\theta, \varphi)$ , as also proposed in [257]. Up to a sign, we match the supertranslation field anglewise. Consequently, the same matching holds for the supertranslations:

$$T^+(\theta, \varphi) = -T^-(\theta, \varphi). \quad (4.131)$$

There are several reasons why the coordinate matching (4.131) is natural. First of all, the prescription (4.130) comes from a simple intuition. For an observer in a static spacetime who lives on a sphere of fixed radius, the description of the sphere should be the same independently of the choice of time coordinate. More generically, it is possible to require that the action of advanced and retarded supertranslations is the same in the bulk. This was done in [257, 258] for the cases of Schwarzschild and Minkowski.

Moreover, we can consider a detector at big radius which is sensitive to gravitational memory. Then we investigate a process of back scattering, in which the angular distributions of incoming and outgoing energy are identical at each angle. This corresponds to a wall in the bulk which reflects the wave without further modifying it. In this case, the memory effect the ingoing wave causes, parameterized by  $T^-$ , is exactly canceled by the memory effect of the outgoing wave, parameterized by  $T^+$ , so that there is no overall memory effect after the process.

In that case, if we match  $T^-$  and  $T^+$  at each angle as in (4.131), it is possible to simply describe the overall memory effect as  $T^- + T^+$ .

However, it is crucial to stress that the coordinate matching (4.131) does not have any constraining power on the physical process. It does not predict outgoing from ingoing radiation, but only shows how one and the same setup can be described in different coordinates. This is also evident from figure 4.2. The matching condition at  $i^0$  only relates the absolute values of the supertranslation fields. In contrast, processes of nonzero energy solely determine a change of the supertranslation field, as is clear from equations (4.127) and (4.129). Thus, radiation of nonzero energy is independent of the coordinate matching.

### 4.4.3 Study of BMS Hair

#### Planetary Hair

In order to make the ideas presented above concrete, we first discuss an exemplary system without horizon, which we shall call planet for concreteness. We start from a spherically symmetric nongravitational source  $T_{\mu\nu}$ , which sources a spherically symmetric spacetime  $g_{\mu\nu}$  with ADM-mass  $M$ . In such a spacetime, we want to realize a Goldstone supertranslation, i.e. we send in a wave with total energy  $\mu$  and angular distribution  $\Delta\tilde{\mathcal{F}}_{\text{in}}$  in such a way that after some time, the planet emits a wave of the same energy  $\mu$  but with a possibly different angular distribution  $\Delta\tilde{\mathcal{F}}_{\text{out}}$ . Of course, only a special class of planets behaves in that way.

We explicitly construct such spacetimes in appendix A.3.2, to which we refer the reader for details of the calculation. First, we consider the incoming wave. As discussed, the angular distribution  $\Delta\tilde{\mathcal{F}}_{\text{in}}$  of injected energy determines an advanced supertranslation  $T^-$ . As derived in equation (A.25), we can use it to describe the change of the metric due to the injected radiation:

$$\delta g_{\mu\nu}^v = \tau_{v_0, v_1}(v) s^-(r) \left( \mathcal{L}_{\xi_v(T^-)} g_{\mu\nu}^v + \frac{2\mu G_N}{r} \delta_\mu^0 \delta_\nu^0 \right), \quad (4.132)$$

where  $\mathcal{L}_{\xi_v(T^-)} g_{\mu\nu}^v$  is an infinitesimal supertranslation which changes the supertranslation field by a small amount  $T^-$ . Whereas the asymptotic supertranslation  $T^-$  only depends on the leading part of the incoming energy, it is crucial to note that the transformation (4.132) is also sensitive to a careful choice of the subleading components of the incoming wave.<sup>23</sup> Only with a particular choice, the wave acts as a diffeomorphism not only asymptotically but also in the bulk outside the planet.

We observe that the effect of the wave is twofold. First, it adds the total mass  $\mu$  to the planet and secondly, it supertranslates the metric by  $T^-$ . However, these

<sup>23</sup>Subleading terms are the  $1/r^3$ -term in  $T_{00}$  and the whole  $T_{0A}$  in (A.26). If one does not insist that the wave acts as a supertranslation also in the bulk, one is free to choose the coefficient of one of the two terms. The other one is determined by energy conservation:  $T_{\mu\nu}{}^{;\mu} = 0$ .

effects are localized both in space and time. The function  $\tau_{v_0, v_1}(v)$  describes the smooth interpolation between  $g_{\mu\nu}^v$  and  $g_{\mu\nu}^v + \delta g_{\mu\nu}^v$ , i.e. we have  $\tau_{v_0, v_1}(v < v_0) = 0$  and  $\tau_{v_0, v_1}(v > v_1) = 1$ . The function  $s^-(r)$  describes the absorption of the wave, namely absorption takes place whenever  $s^-(r) < 0$ . There is no absorption outside the planet, i.e.  $s^-(r > R) = 1$ , where  $R$  is the radius of the planet, and the wave is fully absorbed before it reaches the center,  $s^-(r = 0) = 0$ . It will be crucial to note that the transformation  $s^-(r)\mathcal{L}_{\xi_v(T^-)}g_{\mu\nu}^v$  only acts as a diffeomorphism when  $s^{-\prime}(r) = 0$ .

Moreover, the transformation (4.132) shows that we focus on planets which have a second very special property aside from the fact that they emit as much energy as they receive: Namely there is no transport of energy between different angles. This means that the mass of the planet does not redistribute after absorption (the same will be true after emission). The fact that this assumption is unnatural and not true for generic systems will contribute to our conclusions.

As a second step, we consider the emission of a wave by the planet. Of course, the properties of the emitted wave depend on the internal dynamics of the source  $T_{\mu\nu}$ . It is crucial to note we cannot resolve them in our purely gravitational treatment, i.e. we cannot predict what wave will be emitted. From the point of view of gravity, any emission process is possible as long as it respects energy-momentum-conservation. However, we can study the effect of a given emitted wave. As derived in equation (A.31), it can be described in terms of the supertranslation  $T^+$  induced by the angular distribution  $\Delta\tilde{\mathcal{F}}_{\text{out}}$  of outgoing energy:

$$\delta g_{\mu\nu}^u = \tau_{u_0, u_1}(u)s^+(r) \left( \mathcal{L}_{\xi_u(T^+)}g_{\mu\nu}^u - \frac{2\mu G_N}{r}\delta_\mu^0\delta_\nu^0 \right). \quad (4.133)$$

As for the case of absorption, the emission has two effects: It decreases the total mass by  $\mu$  and it supertranslates the metric by  $T^+$ . Moreover, it is localized in space and time in an analogous manner.

We want to compare the planet before and after the Goldstone supertranslation, i.e. we are interested in the combined effect of the transformations (4.132) and (4.133). To this end, we have to specify a mapping between the advanced and retarded supertranslations. As explained in section 4.4.2, we employ the anglewise matching (4.131). Thus, we obtain the static final state of the planet:

$$\begin{aligned} \delta g_{\mu\nu}^{\text{tot}} &= \theta(r - R)\mathcal{L}_{\xi_u(T^+ - T^-)}g_{\mu\nu} \\ &+ \theta(R - r) \left( s^+(r)\mathcal{L}_{\xi_u(T^+)}g_{\mu\nu} - s^-(r)\mathcal{L}_{\xi_u(T^-)}g_{\mu\nu} \right). \end{aligned} \quad (4.134)$$

We get a planet which has the same ADM-mass but a different angular distribution of mass. This is clear from the fact that the transformation (4.134) acts as a diffeomorphism only outside the planet.

Since we used in our computation a planet with the special property that its angular distribution of energy is frozen, we can read off the distribution from the

difference of energy distributions of the injected and emitted wave. In this case,  $T^- - T^+$  encodes all information about the angular energy distribution of the planet in the bulk.<sup>24</sup> However, this is no longer true for generic systems which exhibit nontrivial dynamics after absorption and emission. In that case,  $T^-$  and  $T^+$  merely encode the initial state. Only with full knowledge of the theory which governs the internal dynamics of the planet, we can infer the state of the planet at a later time from the asymptotic data  $T^-$  and  $T^+$ .

### The Role of Supertranslations

In summary, we obtain the following key properties of a Goldstone supertranslation in the case of a planet: Outside the planet, it acts as a diffeomorphism. In particular, it does not change its ADM-mass. In contrast, it does not act as a diffeomorphism inside the planet where absorption takes place. Therefore, it is not a trivial global diffeomorphism but changes the spacetime physically. Thus, the Goldstone supertranslation encodes differences in the angular distribution among matter configurations degenerate with respect to the ADM-conserved quantities.

It is crucial to discuss the role of supertranslations in this process:

- For an asymptotic observer,  $(T^-, T^+)$  can be used as label for the angular features of ingoing and outgoing radiation.
- An asymptotic observer, however, cannot infer  $T^+$  from  $T^-$ . This is only possible with knowledge of internal dynamics of the planet.
- Thus,  $(T^-, T^+)$  is a bookkeeping tool but without detailed information about the interior, it does not have predictive power.

As we shall discuss in a moment, the same conclusions hold in the black hole case. The only difference is that the internal dynamics leading to emission are fully quantum mechanical for a black hole. This will mean that in any classical description, supertranslation cannot constrain or even predict black hole evaporation.

### Hidden Angular Features

Finally, we discuss the transformation (4.134) when we do not have access to  $(T^-, T^+)$ , i.e. when we do not record ingoing and outgoing radiation but only

---

<sup>24</sup>For the planet with frozen energy distribution, there is also a very literal way in which one can interpret the quantity  $T^- - T^+$ : One can imagine a gedankenexperiment where a source of light is located in the interior of the planet after the Goldstone supertranslation and we collect the light rays on the sky. The light sent from this common center point determines in this way a section at infinity described by the supertranslation field  $T^- - T^+$ . Thus, the different redshift effects due to the inhomogeneities of the planet matter distribution define a supertranslated section in the sky as the one for which light rays originate from a common spacetime point. This is reminiscent of Penrose's concept of "good sections" [264].

compare the initial and final state of the planet. In that case, the planet possesses an interesting property, namely a special kind of no-hair-theorem. Concretely, we take the perspective of an observer who has no access to the interior of the planet and discuss the difference between two planets which have the same mass but a different angular mass distribution. As we have observed, the transformation (4.134) acts as a diffeomorphism outside the planet. Therefore, an outside observer cannot distinguish the two following cases when he is given a supertranslated outside metric. First, it could be the result of the transformation (4.134), where the planet was physically changed due to a Goldstone supertranslation. Secondly, however, one can also obtain the supertranslated metric by acting on the initial planet with a global diffeomorphism. In this case, clearly, the planet does not change. Thus, also for a planet, an outside observer is not able to resolve angular features. In order to decide whether two asymptotic metrics differing by a supertranslation describe two different distributions of matter or the same distribution of matter in different coordinates, one needs access to the whole spacetime, i.e. the interior of the source.

We conclude that generic gravitational systems possess physical angular features which are inaccessible for an outside observer. This is an indication that the microstates of a black hole have a nontrivial projection on angular features. The only difference is that while the restriction to outside measurements was artificial in the case of the planet, an outside observer has *in principle* no access to the interior of a black hole. As we will discuss in the next section, he can therefore never decide whether a supertranslated metric corresponds to a physical change of the matter inside the black hole or to a global and therefore meaningless diffeomorphism. This is the reason for the classical no-hair theorem of a black hole and why we assign an entropy to the black hole and not to the planet.

#### 4.4.4 Black Hole Quantum Hair

##### Supertranslations as Bookkeeping Device

Now we are ready to discuss the system of our interest, namely black holes. Since absorption and emission are of different nature in that case, we will discuss them separately. For absorption, we can proceed in full analogy to the planet and inject a wave with total energy  $\mu$  and arbitrary angular distribution  $\Delta\tilde{\mathcal{F}}_{\text{in}}$ . By Birkhoff's theorem, the spacetime outside the black hole is the same as for the planet so that the wave behaves identically. As in the case of the planet, the wave cannot be absorbed outside the horizon and acts as a diffeomorphism everywhere outside the black hole and also on the horizon.

For the planet, we observed that the knowledge of injected energy alone does not suffice to predict what radiation the planet emits. Instead, this can only be done with knowledge of the interior dynamics of the planet. Those, however, can be described classically in the case of the planet. For the black hole, the situation

is even worse. Not only do we not have access to any interior dynamics, but these dynamics are also fully quantum. It is impossible to describe them even with full classical knowledge of the interior of the black hole.

Before we elaborate on this point, we first show how it is possible to use supertranslations as bookkeeping device for black hole evaporation. Unlike for the case of the planet, this is a nontrivial question since the evaporation products are generic quantum states. In order to define an associated supertranslation, we shall proceed as follows. We consider an ensemble of *quantum-mechanically* identical black holes of mass  $M$ .<sup>25</sup> For each black hole, we wait until it has emitted exactly one Hawking quantum. We only record their angular features, i.e. the deviation from an isotropic emission. This means that we assume that the microstates of the black hole have a nontrivial projection on angular features of the evaporation products. Thus, we record the Hawking quanta using a filter for angular features, where we use one for each spherical mode  $(l, m)$ . This defines a probability distribution for the angular features of the ensemble:

$$P(l, m). \quad (4.135)$$

Obviously, the probability distribution (4.135) only contains a part of the quantum-mechanically available information. However, we will only focus on it since it can be described in terms of classical supertranslations. At this point, it is crucial to point out that the probability distribution (4.135) does not originate from a mixed state but as a result of an ordinary quantum measurement. Thus, unlike in a description in terms of a mixed state, it is not associated to any fundamental loss of information.

Since we need to recover a featureless emission in the semiclassical limit, it follows that

$$P(0, 0) = 1 - \delta, \quad (4.136)$$

where  $\delta \rightarrow 0$  in the semiclassical limit. This means that only a fraction  $\delta$  of the emitted quanta carries features. For  $l \geq 2$ , we consequently get

$$P(l, m) = \delta A_{l,m}, \quad (4.137)$$

where  $\sum_{l=2}^{\infty} \sum_{m=-l}^{m=l} A_{l,m} = 1$ . The information contained in the  $P(l, m)$  is purely quantum mechanical. At the semiclassical level, we have that  $P(l, m) = \delta_{l0}$  and in the classical limit, we have no emission at all.

Using the quantum probability distribution (4.135), we can associate to every Hawking quantum an average energy flux:

$$\mathcal{F}_{\text{out}} = \hbar r_g^{-1} \sum_{l=0}^{\infty} \sum_{m=-l}^{m=l} P(l, m) Y_{l,m}, \quad (4.138)$$

---

<sup>25</sup>Experimentally, we can realize this by preparing identical quantum states in such a way that they collapse and form black holes.

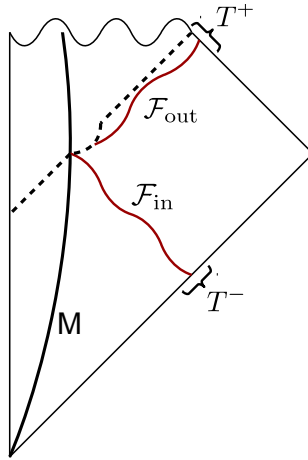


Figure 4.3: A Goldstone supertranslation on a black hole of mass  $M$ . First, it absorbs radiation with angular distribution  $\mathcal{F}_{\text{in}}$  and then it evaporates radiation with angular distribution  $\mathcal{F}_{\text{out}}$ . Since  $\int dv \int d^2\Omega \mathcal{F}_{\text{in}} = \int du d^2\Omega \mathcal{F}_{\text{out}}$ , the total energy of the black hole remains unchanged. Here  $\mathcal{F}_{\text{in}}$  can be described in terms of the supertranslation  $T^-$  and  $\mathcal{F}_{\text{out}}$  in terms of  $T^+$ .

where  $Y_{l,m}$  are the standard spherical harmonics. Just like for the case of the planet, where we considered a classical process of emission, we can use the flux (4.138) to define a *classical* supertranslation  $T^+$ . Of course, this is only possible as long as  $\hbar \neq 0$  since the energy flux is zero otherwise. When we record the quantum-mechanically emitted energy  $\mathcal{F}_{\text{out}}$ , we can proceed in analogy to the planet and use the supertranslation fields  $T^-$  and  $T^+$  to track the evolution of the black hole. Concretely, in order to perform a Goldstone supertranslation, we first inject an energy  $\mu$  and then we wait until  $n_H = \mu/(\hbar r_g^{-1})$  quanta have evaporated, as is depicted in figure 4.3. Then we end up with a black hole of the same mass as before the process. Of course, the sensitivity of the final state on the initial state is suppressed by  $\mu/M$ , but unitarity dictates that the dependence is never trivial.

### Insufficiency of Supertranslation Hair

However, it is impossible to predict  $T^+$  solely from the knowledge of  $T^-$ . The reason is that the wave that we inject acts as a diffeomorphism outside the horizon and also on the horizon. Therefore, the geometry outside the black hole is unaltered after the wave has passed. Since the semiclassical Hawking calculation is only sensitive to the geometry on the horizon and outside the black hole, its result cannot change as a result of a supertranslation diffeomorphism. Therefore, additional knowledge about the interior is required to predict  $T^+$ .

We can make this argument more concrete by taking the perspective of an

observer who lives in a Schwarzschild metric supertranslated by  $T^-$ . The observer has no record of how the black hole was formed and is only allowed to make experiments outside the horizon. Her goal is to determine the microstate of the black hole. More specifically, she wants to know if the black hole is in the bald microstate, whose evaporation products are featureless and in particular perfectly isotropic, or in a nontrivial microstate, whose evaporation products carry some angular features. By our definition of microstate, one way to do so is to wait till the black hole has evaporated and to determine the properties of the evaporation products.

The question we are asking is if there is another way to determine the microstate of a black hole. The answer is negative, for the following reason: When an outside observer finds herself in a black hole metric with supertranslation field  $T^-$ , this can happen because of two very distinct reasons. Firstly, it could be the result of injecting a wave with a nontrivial angular distribution of energy into a black hole. In that case, the black hole is in a nontrivial microstate and  $T^-$  indeed characterizes the microstate.

However, there is a second way in which we can obtain a supertranslated Schwarzschild metric. Namely, we can consider a featureless microstate, whose evaporation products are isotropic, and apply a supertranslation diffeomorphism to this setup. In this way, we do not change the physical state of the black hole but only describe it in a different metric. Thus,  $T^-$  can also correspond to a featureless microstate described in different coordinates.

Without access to the evaporation products, the only way to distinguish those two cases – injection of wave with angular features versus global diffeomorphism – is to enter the black hole. There, the wave acts nontrivially, i.e. not as a diffeomorphism, whereas the global diffeomorphism still does. Since the same exterior metric can correspond to both a trivial and a nontrivial microstate, the metric alone cannot suffice to predict the evaporation products. From the outside, it is therefore impossible to distinguish classical supertranslation hair and global diffeomorphisms.

In summary, as in the case of a planet, we can use  $(T^-, T^+)$  as a natural bookkeeping device for the black hole to track the angular features of ingoing and outgoing radiation. However, knowing  $T^-$  does not suffice to predict  $T^+$ , i.e. an observer outside the black hole cannot infer  $T^+$  from  $T^-$ . This is only possible with a microscopic model of the interior dynamics of the black hole, which is inaccessible in any (semi)classical limit.

### Generalization to Evaporation

Having discussed how we can implant hair on a black hole with a Goldstone supertranslation, it is trivially to consider the case of pure evaporation. We obtain it if we just leave out the first part of the Goldstone supertranslation, namely the injection of a wave. Therefore, it suffices to consider  $\mathcal{J}^+$  as screen, where the

constraint (4.127) determines the retarded supertranslation field  $T^+$  in terms of the angular distribution  $\Delta\tilde{\mathcal{F}}_{\text{out}}$ . In that case, the metric outside the black hole changes according to (4.133):

$$\delta g_{\mu\nu}^u = \tau_{u_0, u_1}(u) \left( \mathcal{L}_{\xi_u(T^+)} g_{\mu\nu}^u - \frac{2\mu G_N}{r} \delta_\mu^0 \delta_\nu^0 \right). \quad (4.139)$$

This equation shows that the backreaction splits in two parts. First, energy conservation dictates that the mass of the black hole is reduced by the total emitted energy  $\mu = \int du \int d^2\Omega \mathcal{F}_{\text{out}}$ . This part of the backreaction is undebatable but does not suffice to ensure unitarity of the process. Fortunately,  $\mathcal{F}_{\text{out}}$  contains more information than just the emitted energy, namely the supertranslation  $T^+$ . Consequently, we obtain the backreacted black hole not only by reducing its mass but by supertranslating it by  $T^+$ . In this way, supertranslations can be used as bookkeeping device for emission.

#### 4.4.5 Relationship to Black Hole N-Portrait

So far, we have not specified the magnitude of deviations from a thermal evaporation. We can estimate them by requiring that we reproduce Page's time [42] in our approach. In its most basic formulation, which we have already introduced in section 1.3.1, Page's time is a direct consequence of describing the black hole evaporation in a Hilbert space of fixed dimension. In brief, if we keep the dimension of the full Hilbert space, which describes at any time both the black hole and the emitted radiation, fixed and equal to  $2^N$ , then at  $t = t_P$ , which corresponds to the half lifetime, i.e. the evaporation of  $\sim N/2$  quanta, there is no place to continue increasing the entanglement between the radiation and the black hole internal degrees of freedom. At this time, entanglement starts to decrease and information starts to be delivered.

Since Page's time corresponds to the timescale for the emission of the order of  $N$  quanta, we first consider an ensemble of  $N$  identical quantum mechanical black holes and for each of them, we record the first emitted quantum. For a measurement on a single black hole, the standard deviation is

$$\sigma_1 \sim O(1) \quad (4.140)$$

since the quanta are distributed isotropically to leading order. However, when we average over  $N$  measurements, the standard deviation decreases as

$$\sigma_N \sim \frac{1}{\sqrt{N}}. \quad (4.141)$$

Features become visible as soon as their strength gets bigger than the uncertainty of the measurement. After Page's time we can therefore resolve features with the relative amplitude

$$\delta \sim \frac{1}{\sqrt{N}}. \quad (4.142)$$

In the formulation of the probability distribution (4.136), this means that after  $O(N)$  measurement, those features becomes visible which are only carried by a fraction  $1/\sqrt{N}$  of the quanta.

So far, we have only considered one emission for  $N$  identical black holes. If we consider instead  $O(N)$  emissions of a single black hole, the difference is that the probability distribution for each emission step is generically different. This is true because of the backreaction of the previously emitted quanta. However, the argument in terms of the resolution stays the same, i.e. after Page's time, we can still resolve those features which are only carried by a fraction  $\delta \sim 1/\sqrt{N}$  of quanta. Thus, unitarity requires that features must exist the relative strength of which is at least given by (4.142). This finding resonates with the black hole  $N$ -portrait [34] since it predicts the existence of deviations from thermality that scale as a power of  $1/N$ .

# Chapter 5

## Future Perspectives

### 5.1 Summary

We shall summarize our findings. First, we discuss each chapter separately and then we try to draw overall conclusions.

#### 5.1.1 Quantum Breaking

In the first chapter, we studied the question of quantum breaking. To begin with, we pointed out that it is useful to characterize a generic system in terms of two universal parameters, the (leading) quantum coupling, which scales as  $\alpha \sim \hbar$ , and the occupation number of the state, which scales as  $N \sim \hbar^{-1}$ . The product of those two determines a third important quantity, namely the collective coupling  $\lambda = \alpha N \sim \hbar^0$ . Already from their dependence on  $\hbar$ , it is evident that  $\alpha$  and  $\lambda$  describe fundamentally different phenomena. Whereas  $\alpha$  fixes the strength of quantum processes,  $\lambda$  determines the importance of classical nonlinearities. This distinction enables us to draw conclusions about quantum breaking by studying the classical limit  $\hbar \rightarrow 0$ . Since the quantum break-time has to become infinite in this limit, the corresponding timescale must scale as  $t_q \sim 1/\alpha$ . This observation culminates in the generic relation (2.56).

As a first concrete example, we studied a prototype model of a self-interacting scalar field. In an approximation which neglects classical nonlinearities, we computed the quantum break-time due to various scattering processes and concluded that its lower bound, Eq. (2.34), fully agrees with the generic dependence (2.56). Moreover, we showed how classical nonlinearities can be described in the  $S$ -matrix language. Namely, they correspond to processes in which the occupation numbers of both initial and final states are macroscopic, i.e. scale as  $N$ . Finally, we reviewed findings of [40], where it was shown that the self-interacting scalar also exhibits a special regime of fast quantum breaking,  $t_q \sim \ln(1/\alpha)$ . This can only happen, however, if the collective coupling is overcritical,  $\lambda \gtrsim 1$ , and the system

additionally possesses a classical instability.

A straightforward application of the results for the self-interacting scalar field is the study of quantum breaking in cosmic QCD axions. We concluded that their quantum break-time is larger than the age of the Universe by many orders of magnitude so that approximating them as classical is fully justified. Moreover, we commented on contrary claims made in [71, 101–103], in particular by emphasizing the distinction between classical and quantum timescales. The result that cosmic axions can be described accurately as classically-oscillating field is of particular importance for experimental axion searches.

Next, we turned to gravity by studying de Sitter. Following [44], the first step was to give a quantum resolution of the classical metric, i.e. to understand de Sitter as a multi-graviton state defined on Minkowski vacuum. A key motivation for adopting this picture instead of viewing de Sitter as a fundamental vacuum consists in the well-known problem that no  $S$ -matrix exists in the latter case. We showed that our corpuscular picture of de Sitter is able to reproduce all its known classical and semiclassical properties, such as redshift and Gibbons-Hawking particle production, as ordinary  $S$ -matrix processes of scattering and decay. Once a quantum resolution of the spacetime is given, a finite quantum break-time emerges. As displayed in Eq. (2.164), the result is that the description in terms of a classical metric breaks down at the latest after  $t_q \approx 1/(\hbar G_N \Lambda^{3/2})$ , in agreement with the findings of [44]. Since the gravitational coupling is  $\alpha = \hbar G_N \Lambda$ , we see that de Sitter obeys the general relation (2.56), which states that the quantum break-time scales as  $1/\alpha$ .

For both inflation and the present dark energy correspond to quasi-de Sitter states, the fact that we see no signs of deviations from the classical metric description in both cases has important consequences. For the present Universe, it implies that the cosmological constant could not have been too big since otherwise quantum breaking would have happened on a timescale shorter than the age of the Universe. Although this argument cannot explain why today's dark energy is as small as it is, it leads to a new perspective on the cosmological constant problem. For the early Universe, the requirement that no observable quantum breaking takes place leads to a model-dependent upper bound on the total duration of inflation.

Finally, we discussed if quantum breaking is a sign of a fundamental inconsistency of de Sitter. As explained in [44, 50], the reason that this could be an issue is that the cosmological constant  $\Lambda$ , which sources the spacetime, represents a fixed parameter of the theory. Whereas  $\Lambda$  is eternally tied to de Sitter, quantum effects cause a complete deviation from it after  $t_q$ . If this conflict indeed implies that quantum breaking leads to an inconsistency in the special case of de Sitter, this results in the *quantum breaking bound*. It requires that any consistent theory must exit a quasi-de Sitter state on a timescale that is shorter than the quantum break-time. This criterion bears similarities to the de Sitter swampland conjecture [156, 160] in string theory, but unlike the latter, it is not in conflict

with slow-roll inflation. Instead, it only rules out the regime of self-reproduction. Moreover, it implies that the present dark energy cannot be constant but must slowly evolve in time. Finally, an immediate consequence of the quantum breaking bound (or equivalently the de Sitter swampland conjecture) is that any metastable de Sitter vacuum is excluded. This has important implications for physics beyond the Standard Model. It rules out any model with a spontaneously-broken discrete symmetry and it makes the axion solution to the strong CP problem mandatory.

### 5.1.2 Storage of Quantum Information

In the second chapter, we turned again to a generic, nongravitational setup and studied the question of how a quantum system can achieve an efficient memory storage. Building on the results of [36,204,205], we pointed out that nearly-gapless modes play a crucial role, i.e. systems that contain those have great capabilities of information storage. First, nearly-gapless degrees of freedom lead to states that are almost degenerate in energy and therefore to a big microstate entropy. Secondly, they cause the decoherence time to be long and moreover they can be excited by soft external stimuli. Generalizing the models of [204,205], we subsequently showed that nearly-gapless modes can emerge due to a general mechanism which we call *assisted gaplessness*. The only prerequisites for it to occur are that the system is bosonic and that it features weak and attractive interactions. In this case, a high occupation number of one of the modes can lower the energy threshold for others and in this way assist them in becoming gapless.

Since gravity is bosonic and its interactions are attractive, the question immediately arises if assisted gaplessness could be operative in black holes and de Sitter and be responsible for their large entropies. As already emphasized in [36], such a picture would not only pave the way for a microscopic explanation of the Bekenstein-Hawking and Gibbons-Hawking entropy, but it also opens up the exciting prospect of simulating those gravitational systems. Since assisted gaplessness takes place in simpler nongravitational systems, which are much easier to control both experimentally and theoretically, one can use those to draw conclusions about information storage and processing in black holes and de Sitter. Similarly, such analogue models have the potential to facilitate the analysis of further systems of enhanced memory storage, such as neural networks. Finally, it is also very interesting to study nongravitational systems that exhibit assisted gaplessness in their own right since they could enable an efficient storage of quantum information under laboratory conditions.

If states of enhanced memory capacity exist, we generically expect that they are scarce among all states of a Hilbert space. Therefore, we proposed an analytic approach for finding them, which we call *c-number method* and which is a generalization of the procedure employed in [51]. Apart from greatly facilitating computations, it also serves to confirm our previous statement that bosonic systems

with weak and attractive interactions generically feature some states of enhanced memory capacity. We demonstrated the  $c$ -number method on a prototype model, which we obtained as truncation of a one-dimensional Bose gas with an attractive 4-point interaction and Dirichlet boundary conditions, and numerically confirmed our findings.

Finally, we discussed the phenomenon of *memory burden*, which was first analyzed in [206]. Its essence is that in systems of enhanced memory capacity, the stored information generically leads to a strong backreaction that tends to tie the system to its initial state. For both de Sitter and black holes, we concluded that memory burden describes the information-theoretic aspect of quantum breaking. In the case of inflation, the stored information moreover acts as an observable that is sensitive to the whole history of the Universe and not only the last 60 e-foldings. For black holes, it remains an open question whether memory burden leads to a slowdown of evaporation. If future studies show that this is true, it would contribute to the interest in considering small primordial black holes as dark matter candidates.

### 5.1.3 Infrared Physics and Information

Motivated by the importance of nearly-gapless modes for information storage, we turned to infrared physics in the last chapter. After a brief comment on the relationship of soft theorems and charge conservation, we reviewed key results on infrared divergences. The starting point is the observation that in gapless theories such as QED and perturbative gravity, the soft part of loop corrections leads to a vanishing amplitude for any nontrivial process [57]. This is not a problem, however, but a physical result. The probability that scattering takes place without the emission of any soft bremsstrahlung is zero.

Therefore, a very natural way to deal with infrared divergences is the inclusive formalism [57–59]. In this approach, one enlarges the final state by infrared radiation, which is defined as a state of arbitrary photon/graviton number but with a total energy below some resolution scale  $\epsilon$ . Doing so leads to a finite total rate. However, there exists an alternative approach, the dressed formalism [60–65], in which no infrared radiation is taken into account. Instead, both final and initial charged states are dressed with a coherent state of soft photons/gravitons that is characterized by an energy scale  $r$ . The justification for this modification of asymptotic states lies in the fact that gapless theories exhibit nontrivial asymptotic dynamics. If one sets  $r = \epsilon$ , the dressed formalism leads to the same finite rate as the inclusive formalism, up to subleading corrections.

This result is surprising for two reasons. First, it is unclear why two very different approaches should yield the same result. Secondly and more importantly, considering both infrared emission and soft dressing at the same time leads to unphysical infinite rates. For these reasons, we have developed a combined formalism

that is able to simultaneously describe both radiation and dressing. The key step is to give a physical interpretation of the scale  $r$ . Based on earlier work [244–246], we argued that it is set by the inverse timescale of the process in question and thereby determines the softest radiation that can be produced in the given setup. Thus, photons with energy above  $r$  (but below  $\epsilon$ ) represent physical infrared radiation whereas photons softer than  $r$  are effectively decoupled and therefore constitute dressing. We computed the total rate in the combined formalism and showed that it is independent of  $r$ , thereby explaining why the inclusive and dressed formalism yield the same result.

Subsequently, we went one step further and calculated the density matrix of the final state. Its diagonal is composed of the known rates, but its off-diagonal elements contain information about the coherence of the final state. Whereas the inclusive and the dressed formalism would respectively yield a fully decohered and a fully coherent density matrix [66, 67], a crucial strength of the combined formalism is that it leads to a small but nonzero amount of decoherence. This is what we physically expect because of tracing over unobserved infrared radiation.

The relationship of infrared divergences and quantum coherence has important implications for the puzzle of black hole information. Namely, we expect that like any process in gravity, the emission of a Hawking quantum is accompanied by infrared radiation. This leads to the question of how much information is lost if we do not observe the soft radiation. In particular, the proposal [56] was made that infrared gravitons could carry all information of a black hole. In this picture, the combined system of Hawking quanta and soft gravitons would be pure and a mixed state would only arise due to tracing over soft radiation. Our results show, however, that this is not the case. Because Hawking quanta become softer for bigger black holes, infrared radiation can at most account for a subleading logarithmic part of the black hole entropy.

Finally, the connection [220] of the soft graviton theorem and asymptotic symmetries at null infinity led us to study the proposal of [221–224] that BMS supertranslations could play a crucial role for black hole information. The starting point of this suggestion is the long-known fact [250] that physical radiation causes a memory effect, i.e. a permanent displacement of test masses. In turn, the memory effect can be mapped on a supertranslation diffeomorphism [221]. This fact that physical radiation, as it is absorbed or emitted by a black hole, can be described by a diffeomorphism raises the hope that one could define classical black hole hair that is nevertheless compatible with the no-hair theorem. Our results show, however, that such hair cannot be observable in the classical or semiclassical limit. Although supertranslations can be used as a natural bookkeeping device to describe absorption and emission, they have no constraining or predictive power on black hole evaporation.

### 5.1.4 Overall Conclusions

One conclusion that we can draw is that the limitations of classical physics tend to be more severe than naively expected. In particular, the description in terms of general relativity can break down for macroscopically large gravitational systems. As we have briefly discussed in the introductory section 1.3.1, this observation is crucial for understanding the puzzle of black hole information. For de Sitter, quantum breaking leads to a drastic change of perspective. Whereas the spacetime is eternal on the classical level, the description in terms of a metric develops a finite timescale of validity due to backreaction from quantum effects. This has particularly interesting implications for inflation. It enables the search for new observables in scenarios that are close to quantum breaking and it rules out models that last longer than their quantum-break time.

The breakdown of the classical description for black holes and de Sitter immediately highlights the needs for nonperturbative computation techniques beyond the semiclassical limit. In the absence of those, a viable strategy is to study simpler analogue systems that share important characteristics with gravity. Whereas the focus is traditionally placed on geometrical features, we have proposed to view their enhanced memory storage capacity as the key property of black holes and de Sitter. This makes it possible to learn about information storage and processing in those gravitational systems by studying much simpler models that are accessible in table-top experiments.

In many fields of particle physics, the problem is not to come up with some viable model to explain a certain phenomenon. On the contrary, there exist a plethora of proposed scenarios, e.g. for inflation, dark matter and dark energy. So the challenge consists in selecting from these manifolds models the one that is realized in Nature. Typically, the more parameters a model has, the harder it is to rule it out. For a long time, it was thought that quantum gravity has little to say about these mostly low-energy questions. This perspective changes, however, if de Sitter quantum breaking indeed leads to an inconsistency. In this case, a constant dark energy, inflationary self-reproduction and many well-motivated extensions of the Standard Model are ruled. It is particularly interesting that for more involved models, it is more likely that they are excluded because of quantum breaking. Additionally, an inconsistency of de Sitter states makes the existence of the QCD axion mandatory.

## 5.2 Outlook

There are many promising ways to continue the research summarized above. For example, we have seen that computational limitations often make it difficult to predict in what way the true quantum evolution deviates from the classical description, i.e. what the “broken” quantum state looks like. Apart from its generic

conceptual relevance, such a study can have important phenomenological implications. Namely, it would allow to draw conclusions about what imprints the  $1/N$ -effects, which are sensitive to the whole history of inflation, leave on inflationary perturbations. Similarly, it could be interesting to investigate if there is a regime in which quantum breaking can lead to observable signatures in the gravitational wave signals due to black hole mergers. Finally, an explicit study of the final state of quantum breaking in a simplified model promises to provide further insights into the question if it leads to an inconsistency in the special case of de Sitter.

Concerning the enhanced memory storage, an important task would be to study analogue models that match the information storage and processing properties of a black hole as closely as possible (see [206] for a concrete suggestion). If such systems can be found, it would show that the large entropy of black holes indeed arises due to a universal phenomenon that is not tied to gravity. Moreover, the analysis of explicit analogue models allows to investigate if rewriting of information between different critical levels plays a role in a black hole. On the one hand, this can show if memory burden leads to a slowdown of evaporation. On the other hand, one could draw conclusions about the question if fast scrambling [265, 266] is realized in black holes. While we have shown that critical states of enhanced memory capacity generically exist in bosonic systems with weak and attractive interactions, it would additionally be important to investigate to what extent a system dynamically evolves towards them.<sup>1</sup>

Although we have concluded that infrared physics alone cannot elucidate the puzzle of black hole information, it would nevertheless be very interesting to investigate if we can learn more from it about black hole evolution. Namely, the great strength of infrared physics is that it is only sensitive to initial and final states. Therefore, it allows to make statements about the corrections to scattering processes involving black holes even if we do not know how to actually compute the diagram itself. Due to collinear divergences that arise for a vanishing electron mass, such an approach could for example yield constraints on the Yukawa couplings from black hole physics.<sup>2</sup>

---

<sup>1</sup>In the language of neural networks, this question was already studied in [267].

<sup>2</sup>First results on this question were already obtained in [268].



# Appendix

## A.1 Concerning Chapter 2

### A.1.1 Calculation of the Rate of Particle Production

In order to obtain the correct prefactors for the normalizations which we use, we rederive how a general  $S$ -matrix element determines the differential decay rate. We consider an initial coherent state  $|N\rangle$ , in which a constituent quantum of energy  $m_g$  decays to two particles with 4-momenta  $p_1 = (p_{0,1}, \vec{p}_1)$  and  $p_2 = (p_{0,2}, \vec{p}_2)$ . This leads to the final state  $|N'\rangle \otimes |f_\Psi\rangle$ , where  $|N'\rangle$  is a possibly different coherent state and  $|f_\Psi\rangle = \hat{b}_{\vec{p}_1}^\dagger \hat{b}_{\vec{p}_2}^\dagger |0\rangle$  describes the two external particles. The differential transition probability is given by the square of the  $S$ -matrix element  $\mathcal{A}$ , divided by the norms of final and initial state and multiplied by the phase space factor:

$$dw_{\text{fi}} = \frac{|\mathcal{A}|^2}{\langle N|N\rangle \langle N'|N'\rangle \langle f_\Psi|f_\Psi\rangle} \frac{d^3\vec{p}_1 V}{(2\pi)^3} \frac{d^3\vec{p}_2 V}{(2\pi)^3} = |\mathcal{A}|^2 d^3\vec{p}_1 d^3\vec{p}_2,$$

where we used that coherent states are normalized,  $\langle N|N\rangle = \langle N'|N'\rangle = 1$ , and that  $\langle f_\Psi|f_\Psi\rangle = \left(\delta^{(3)}(\vec{0})\right)^2 = (V/(2\pi)^3)^2$ . Defining the Feynman amplitude  $\mathcal{M}$  via

$$\mathcal{A} = (2\pi)^4 \delta(m_g - p_{0,1} - p_{0,2}) \delta^{(3)}(\vec{p}_1 - \vec{p}_2) \mathcal{M},$$

we obtain the differential rate

$$d\Gamma = \frac{dw_{\text{fi}}}{T} = |\mathcal{M}|^2 (2\pi)^4 V \delta(m_g - p_{0,1} - p_{0,2}) |\vec{p}_1|^2 d|\vec{p}_1| d^2\Omega,$$

where we regularized the divergence of the one-dimensional  $\delta$ -distribution with the help of the time  $T$  during which the reaction happens,  $\delta(0) = \frac{T}{2\pi}$ . Evaluating the last  $\delta$ -distribution, we get

$$\frac{d\Gamma}{d\Omega} = \frac{|\vec{p}_1| V |\mathcal{M}|^2}{16\pi^2 m \zeta_\Psi(p_1)^2 \zeta_\Psi(p_2)^2},$$

with  $\zeta_\Psi(p) = ((2\pi)^3 2p_0)^{-1/2}$ .

For our application to particle production, the  $S$ -matrix element (2.151) yields the Feynman amplitude

$$\mathcal{M} = \frac{1}{\sqrt{2m_g}} \mathcal{K}(-p, p') \sqrt{\frac{N'}{V}} \left(1 - \frac{\Delta N^2}{8N}\right).$$

Thus, we get for the differential decay constant:

$$\frac{d\Gamma}{d\Omega} = \frac{\sqrt{\frac{m_g^2}{4} - m_\Psi^2} N'}{2\pi M_p^2 m_g^2} (p \cdot p' + 2m_\Psi^2)^2 \left(1 - \frac{\Delta N^2}{4N}\right),$$

where we plugged in (2.146). After integrating over the angles, we obtain the final decay constant to leading order in  $1/N$ :

$$\Gamma = \frac{2\sqrt{\frac{m_g^2}{4} - m_\Psi^2} N}{M_p^2 m_g^2} (p \cdot p' + 2m_\Psi^2)^2 \left(1 - \frac{\Delta N^2 - 4\Delta N}{4N}\right).$$

## A.2 Concerning Chapter 3

### A.2.1 Review of Periodic Bose Gas

In order to provide a detailed example, we apply the  $c$ -number method to the one-dimensional Bose gas with periodic boundary conditions and attractive four-point interaction, which we already studied in section 2.2.4 from the perspective of quantum breaking.<sup>1</sup> Based on the analysis of [76], quantum information features of this system have already been studied in a series of papers [36, 40, 51–53, 136, 271]. In particular, the replacement of the Hamiltonian by a  $c$ -number function has already been used to find its critical point in [51].

Our starting point is the Hamiltonian (2.49) in momentum space. As we shall justify later, we expect that for small coupling, momentum modes with  $|k| > 1$  are suppressed due to their higher kinetic energy. Therefore, we first truncate the system to the modes with  $|k| \leq 1$ :

$$\hat{H} = \sum_{l=\pm 1} \hat{a}_l^\dagger \hat{a}_l - \frac{\alpha}{4} \sum_{l,m,n=-1}^1 \hat{a}_l^\dagger \hat{a}_m^\dagger \hat{a}_{n+l} \hat{a}_{m-n}. \quad (\text{A.1})$$

For convenience, we have set  $\hbar = R = 2m = 1$ . Following the method introduced in section 3.1.4, we then replace the creation and annihilation operators by  $c$ -numbers. As explained, we have to take into account symmetries in this procedure. The first one is conservation of particle number, which is incorporated in the replacement rule of the 0-mode. An additional symmetry of the system consists in momentum

<sup>1</sup>The repulsive case, in which we are not interested, is the Lieb-Liniger model [269, 270].

conservation. In the superselection sector of zero momentum, it implies that the expectation values of the particle numbers in the 1- and  $-1$ -mode have to be the same:  $\langle a_1^\dagger a_1 \rangle = \langle a_{-1}^\dagger a_{-1} \rangle$ . Moreover, the Hamiltonian is invariant under an additional phase symmetry,  $\hat{a}_1 \rightarrow e^{i\phi} \hat{a}_1$  and  $\hat{a}_{-1} \rightarrow e^{-i\phi} \hat{a}_{-1}$ . So in total, we have to eliminate an absolute value and a phase. In addition to the replacement rule (3.17b) due to particle number conservation, we consequently get:  $a_{-1} \rightarrow a_1$ . Thus, the Bogoliubov replacement (3.17) reads

$$\hat{a} = \begin{pmatrix} \hat{a}_{-1} \\ \hat{a}_1 \end{pmatrix} \rightarrow \begin{pmatrix} a_1 \\ a_1 \end{pmatrix}, \quad \hat{a}^\dagger = \begin{pmatrix} \hat{a}_{-1}^\dagger \\ \hat{a}_1^\dagger \end{pmatrix} \rightarrow \begin{pmatrix} a_1^* \\ a_1^* \end{pmatrix}, \quad (\text{A.2})$$

and

$$\hat{a}_0 \rightarrow \sqrt{N - 2|a_1|^2}, \quad \hat{a}_0^\dagger \rightarrow \sqrt{N - 2|a_1|^2}. \quad (\text{A.3})$$

This gives the following Bogoliubov Hamiltonian:

$$H_{\text{bog}} = 2|a_1|^2 - \frac{\alpha}{4} \left( N^2 + 2N(a_1 + a_1^*)^2 - 2|a_1|^2(3|a_1|^2 + 2a_1^2 + 2a_1^{*2}) \right). \quad (\text{A.4})$$

For this so obtained complex-valued function, we want to find a flat direction. First we look for an extremal point by finding a solution to (3.21):

$$\frac{\partial H_{\text{bog}}}{\partial a_1} = 2a_1^* - \alpha \left( N(a_1 + a_1^*) - 3a_1^2 a_1^* - 3a_1 a_1^{*2} - a_1^{*3} \right) = 0. \quad (\text{A.5})$$

An obvious solution is  $a_1 = 0$ .<sup>2</sup> The second step is to evaluate the matrix  $\mathcal{M}$  of second derivatives at this point. We need to determine when it fulfills (3.22), i.e. when its determinant vanishes:

$$\det \mathcal{M} = -4 + 4\alpha N = 0. \quad (\text{A.6})$$

This is the case for a collective coupling  $\lambda = \alpha N = 1$ . Therefore, we expect a critical mode to appear for  $\lambda_{lm} = 1$  in a state where all particles are in the 0-mode.

This fully matches our previous finding in section 2.2.4. As is evident from Eq. (2.53), also the bilinear quantum Hamiltonian shows that a nearly-gapless mode emerges for  $\lambda = 1$ . Moreover, this finding has been confirmed by a numerical analysis of the full Hamiltonian for finite  $N$  [76, 136, 271]. As is expected, both the gap and the critical value of  $\lambda$  receive corrections that are suppressed as a power of  $1/N$ .

---

<sup>2</sup>There are two other solutions at  $a_1 \approx \pm 0.5345 \sqrt{\frac{\alpha N - 1}{\alpha}}$ . However, the determinant of the second derivative matrix  $\mathcal{M}$  never vanishes at these points, i.e. there is no flat direction.

### A.2.2 Formulas

- First and second derivative of Bogoliubov Hamiltonian (3.44) for  $\Delta_2 = \Delta_3 = 0$ :

$$\begin{aligned} \frac{1}{N} \frac{\partial H_{\text{bog}}}{\partial x} &= \frac{1}{16} \left[ -16\lambda \sin(2\theta) - 2\lambda \sin(4\theta) + 16 \cos(2\theta) - 9\lambda + 28\lambda x \sin(2\theta) \right. \\ &\quad \left. + 2\lambda x \sin(4\theta) + 3\lambda(x-1) \cos(4\theta) + 21\lambda x - 4 \right], \end{aligned} \quad (\text{A.7a})$$

$$\begin{aligned} \frac{1}{N} \frac{\partial H_{\text{bog}}}{\partial \theta} &= \frac{1}{4} (x-1) \left[ -8 \sin(2\theta) + \lambda(x-1) \cos(4\theta) \right. \\ &\quad \left. - \lambda \cos(2\theta) (3(x-1) \sin(2\theta) - 7x + 1) \right], \end{aligned} \quad (\text{A.7b})$$

$$\frac{1}{N} \frac{\partial^2 H_{\text{bog}}}{\partial x^2} = \frac{1}{16} \lambda (28 \sin(2\theta) + 2 \sin(4\theta) + 3 \cos(4\theta) + 21), \quad (\text{A.8a})$$

$$\begin{aligned} \frac{1}{N} \frac{\partial^2 H_{\text{bog}}}{\partial x \partial \theta} &= \frac{1}{4} \left( -8 \sin(2\theta) + 2\lambda(7x-4) \cos(2\theta) \right. \\ &\quad \left. + \lambda(x-1)(2 \cos(4\theta) - 3 \sin(4\theta)) \right), \end{aligned} \quad (\text{A.8b})$$

$$\begin{aligned} \frac{1}{N} \frac{\partial^2 H_{\text{bog}}}{\partial \theta^2} &= \frac{1}{2} (1-x) \left( 8 \cos(2\theta) + \lambda \left( (7x-1) \sin(2\theta) + 2(x-1) \sin(4\theta) \right. \right. \\ &\quad \left. \left. + 3(x-1) \cos(4\theta) \right) \right). \end{aligned} \quad (\text{A.8c})$$

- Second-order expansion of the full quantum Hamiltonian (3.42) around the point defined by the replacements (3.43) of macroscopic occupation for  $\Delta_2 = \Delta_3 = 0$ :

$$H_{\text{quad}} = H_{\text{quad}}^{(1)} + \frac{1}{2} H_{\text{quad}}^{(2)}, \quad (\text{A.9})$$

where we neglected the constant zeroth order. The first and second order are given by

$$\begin{aligned} \frac{H_{\text{quad}}^{(1)}}{\sqrt{N}} &= \frac{1}{8\sqrt{(1-x)\cos^2(\theta)}} \left[ \right. \\ &\quad + 6\hat{a}_2 \sqrt{x} \left( 3\lambda(1-x)^{3/2} \sin^3(\theta) + \lambda\sqrt{1-x}(4x-3) \sin(\theta) \right. \\ &\quad + (\lambda(2x-1)+1)\sqrt{-(x-1)\cos^2(\theta)} + \lambda \tan^2(\theta) \left( (1-x)\cos^2(\theta) \right)^{3/2} \Big) \\ &\quad + \hat{a}_3 \left( \lambda(x-1)^2 \cos(4\theta) + \lambda(7x-1)(x-1) \cos(2\theta) \right. \\ &\quad \left. + \sqrt{4-4x} \sin(\theta) \sqrt{-(x-1)\cos^2(\theta)} (3\lambda(x-1) \cos(2\theta) + 8) \right) \Big] \\ &\quad + \text{h.c.} \end{aligned} \quad (\text{A.10})$$

and

$$\begin{aligned}
H_{\text{quad}}^{(2)} = & \frac{1}{128 ((1-x) \cos^2(\theta))^{3/2}} \left[ \right. \\
& + 16\hat{a}_2\hat{a}_2\lambda \left( \sqrt{1-x}((23-16x)x-4) \sin(\theta) \right. \\
& + 4(4x-1) \left( (1-x) \cos^2(\theta) \right)^{3/2} \\
& \left. - (1-x)^{3/2} \sin^3(\theta)(2(x-1) \cos(2\theta) + 21x-6) \right) \\
& + 16\hat{a}_2^\dagger\hat{a}_2 \left( 2 \sec^2(\theta)(\lambda(10x-1) + 3) \left( (1-x) \cos^2(\theta) \right)^{3/2} \right. \\
& + \sin(\theta) \left( -14\lambda(1-x)^{5/2} \sin^4(\theta) - 7\lambda(1-x)^{3/2}(7x-4) \sin^2(\theta) \right. \\
& \left. - 6\lambda \tan^3(\theta) \sec(\theta) \left( -(x-1) \cos^2(\theta) \right)^{5/2} + \lambda\sqrt{1-x}((49-32x)x-14) \right. \\
& \left. \left. - 2 \tan(\theta) \sec(\theta)(\lambda(13x-4) + 3) \left( (1-x) \cos^2(\theta) \right)^{3/2} \right) \right) \\
& + 16\hat{a}_2\hat{a}_3\lambda\sqrt{x} \left( (1-x) \cos^2(\theta) \right) \left( 8(x-1) \cos(2\theta) + 3x \sec^2(\theta) \right. \\
& \left. + 10\sqrt{1-x} \sin(\theta) \sqrt{-(x-1) \cos^2(\theta)} - x + 1 \right) \\
& + 16\hat{a}_2\hat{a}_3^\dagger\lambda\sqrt{x} \left( (1-x) \cos^2(\theta) \right) \left( 10(x-1) \cos(2\theta) + 3x \sec^2(\theta) \right. \\
& \left. + 2\sqrt{1-x} \sin(\theta) \sqrt{-(x-1) \cos^2(\theta)} + x - 1 \right) \\
& + \hat{a}_3\hat{a}_3\lambda(x-1) \left( 32 \cos(2\theta) \sqrt{(1-x) \cos^2(\theta)} + 32x \sqrt{(1-x) \cos^2(\theta)} \right. \\
& + 32 \cos(4\theta) \sec^2(\theta) \left( (1-x) \cos^2(\theta) \right)^{3/2} \\
& \left. - 6\sqrt{1-x} \sin(\theta)(4(3x-2) \cos(2\theta) + 3(x-1) \cos(4\theta) + 17x-5) \right) \\
& + 16\hat{a}_3\hat{a}_3^\dagger \left( (1-x) \cos^2(\theta) \right) \sec^2(\theta) \left( 2(\lambda(3x-1) + 8) \sqrt{(1-x) \cos^2(\theta)} \right. \\
& + \sin(\theta) \left( \sin(\theta) \left( \lambda \sin(\theta) \left( 5(x-1) \sin(\theta) \left( 3\sqrt{1-x} \sin(\theta) \right. \right. \right. \right. \\
& \left. \left. \left. + 4\sqrt{(1-x) \cos^2(\theta)} \right) + 9\sqrt{1-x}(3-4x) \right) \right. \\
& \left. \left. - 2(\lambda(13x-11) + 8) \sqrt{(1-x) \cos^2(\theta)} \right) + 12\lambda\sqrt{1-x}(2x-1) \right) \right) \\
& \left. + \text{h.c.} \right] \tag{A.11}
\end{aligned}$$

## A.3 Concerning Chapter 4

### A.3.1 Matching in Schwarzschild Coordinates

In this section, we demonstrate explicitly how we can transform a Schwarzschild metric with nontrivial supertranslation field from advanced to retarded coordinates. In this way, we show how we can naturally identify the advanced supertranslation field  $C^-$  with the retarded one  $C^+$ . We start from the Schwarzschild metric  $g_{\mu\nu}^{v,0}$  in advanced coordinates without supertranslation field:

$$ds^2 = -\left(1 - \frac{2G_N M}{r}\right)dv^2 + 2dvdr + r^2 d\Omega^2. \quad (\text{A.12})$$

The corresponding generators of supertranslations are

$$\xi_v^v = f^-, \quad (\text{A.13a})$$

$$\xi_v^r = -\frac{1}{2}D^2 f^-, \quad (\text{A.13b})$$

$$\xi_v^A = \frac{f^{-,A}}{r}, \quad (\text{A.13c})$$

which are characterized by an arbitrary function  $f^-$  on the sphere. Thus, the supertranslated metric is

$$g_{\mu\nu}^v(f^-) = g_{\mu\nu}^{v,0} + \mathcal{L}_{\xi_v(f^-)} g_{\mu\nu}^{v,0}. \quad (\text{A.14})$$

In retarded coordinates, the Schwarzschild metric  $g_{\mu\nu}^{u,0}$  without supertranslation field is:

$$ds^2 = -\left(1 - \frac{2G_N M}{r}\right)du^2 - 2dudr + r^2 d\Omega^2. \quad (\text{A.15})$$

The corresponding generators of supertranslations are

$$\xi_u^v = f^+, \quad (\text{A.16a})$$

$$\xi_u^r = \frac{1}{2}D^2 f^+, \quad (\text{A.16b})$$

$$\xi_u^A = -\frac{f^{+,A}}{r}, \quad (\text{A.16c})$$

where it is important to note that the signs of  $\xi_u^r$  and  $\xi_u^A$  have changed with respect to (A.13). The supertranslated metric is:

$$g_{\mu\nu}^u(f^+) = g_{\mu\nu}^{u,0} + \mathcal{L}_{\xi_u(f^+)} g_{\mu\nu}^{u,0}. \quad (\text{A.17})$$

The task now is to transform  $g_{\mu\nu}^v$  to retarded coordinates. As explained in section 4.4.2, there can in general not be a unique way to match the advanced and

retarded supertranslation fields. However, a natural choice in a static metric is to require that the spherical metrics match:  $g_{AB}^v(f^-) = g_{AB}^u(f^+)$ . Therefore, we use the diffeomorphism  $\mathcal{D}_m$  defined by

$$v = u + 2 \int_{r_0}^r \frac{1}{1 - \frac{2G_{NM}}{r}} dr' - \frac{D^2 f^-}{1 - \frac{2G_{NM}}{r}} - 2f^-. \quad (\text{A.18})$$

Then it turns out that

$$\mathcal{D}_m \left( g_{\mu\nu}^v(f^-) \right) = g_{\mu\nu}^{u,0} - \mathcal{L}_{\xi_u(f^-)} g_{\mu\nu}^{u,0} = g_{\mu\nu}^u(-f^-). \quad (\text{A.19})$$

Thus, we identify

$$f^+ = -f^-. \quad (\text{A.20})$$

Up to a sign, the supertranslation field in advanced coordinates matches the retarded one anglewise. With this choice, not only the spherical metrics match but also the  $g_{00}$ -components, i.e. the Newtonian potentials.

### A.3.2 Explicit Solution for Goldstone Supertranslation of a Planet

#### Step 1: Absorption

The Goldstone supertranslation consists of two steps: First, an initially spherically symmetric planet absorbs a wave. As is well-known (see e.g. (9.3) in [272]), the metric of a static spherically symmetric spacetime can be cast in the general form

$$ds^2 = -A(r)dt^2 + B(r)dr^2 + r^2 d\Omega^2, \quad (\text{A.21})$$

where all physical information is contained in the  $tt$ - and  $rr$ -components. Since we want to describe a planet, there should neither be a surface of infinite redshift, i.e.  $A(r) > 0 \forall r$ , nor an event horizon, i.e.  $B(r) < \infty \forall r$ . Furthermore, asymptotic flatness implies that  $A(r) \xrightarrow{r \rightarrow \infty} 1$  and  $B(r) \xrightarrow{r \rightarrow \infty} 1$  sufficiently fast. Using the transformation

$$v = t + \int_{r_0}^r dr' \sqrt{\frac{B}{A}}, \quad (\text{A.22})$$

we obtain the metric  $g_{\mu\nu}^v$  in advanced BMS-gauge:

$$ds^2 = -Adv^2 + 2\sqrt{AB} dvdr + r^2 d\Omega^2, \quad (\text{A.23})$$

which is suited to describe incoming radiation. Note that this metric describes the whole spacetime and not only its asymptotic region, i.e.  $r \rightarrow \infty$ .

We will restrict ourselves to infinitesimal supertranslations. In advanced time, these are generated by

$$\xi_v^v = f^-, \quad (\text{A.24a})$$

$$\xi_v^r = -\frac{1}{2}r D_B \xi_v^B, \quad (\text{A.24b})$$

$$\xi_v^A = f^{-,A} \int_r^\infty dr' (\sqrt{AB} r'^{-2}), \quad (\text{A.24c})$$

where an arbitrary function  $f^-$  on the sphere determines the change of the supertranslation field. We denote it by  $f^-$  instead of  $T^-$  in this appendix to avoid confusion with the energy-momentum-tensor of the wave. The minus-superscript indicates that we deal with a supertranslation in advanced coordinates. Our goal is to realize the infinitesimal diffeomorphism defined by (A.24) in a physical process, i.e. outside the planet, we want to have the stationary metric  $g_{\mu\nu}^v$  before some time  $v_0$  and after some point of time  $v_1$ , we want to end up in the stationary metric  $g_{\mu\nu}^v + \mathcal{L}_{\xi_v(f^-)} g_{\mu\nu}^v$ . For  $v_0 < v < v_1$ , physical radiation interpolates between the two metrics. Inside the planet, the wave should be absorbed so that the transformation fades out and the metric around the origin remains unchanged. Adding as final ingredient a change of the Bondi mass  $\mu$ , which is necessary to ensure the positive energy condition, we obtain

$$\delta g_{\mu\nu}^v = \tau_{v_0, v_1}(v) s^-(r) \left( \mathcal{L}_{\xi_v(f^-)} g_{\mu\nu}^v + \frac{2\mu G_N}{r} \delta_\mu^0 \delta_\nu^0 \right), \quad (\text{A.25})$$

where  $0 \leq \tau_{v_0, v_1}(v) \leq 1$  parametrizes the interpolation, i.e.  $\tau_{v_0, v_1}(v < v_0) = 0$  and  $\tau_{v_0, v_1}(v > v_1) = 1$ . The function  $s^-(r)$  describes the absorption of the wave by the planet. It has the property that it is monotonically increasing with  $s^-(0) = 0$  and  $s^-(\infty) = 1$ , where  $s^-(0) = 0$  ensures that the wave is fully absorbed before the origin and no black hole forms. Moreover,  $s^{-\prime}(r) \neq 0$  is only permissible whenever the local energy density of the planet is nonzero. The magnitude of  $s^{-\prime}(r)$  determines how much absorption happens at  $r$ . It is crucial to note that the transformation  $s^-(r) \mathcal{L}_{\xi_v(f^-)} g_{\mu\nu}^v$  is a diffeomorphism only where  $s^-(r)$  is constant. Thus, the transformation (A.25) acts as a diffeomorphism only outside the planet but not inside. This reflects the fact that we want to obtain a physically different planet. A transformation which acts as a diffeomorphism everywhere could not achieve this.

Since we work with infinitesimal supertranslations, it is important that we stay within the regime of validity of this first-order approximation, i.e. that terms linear in  $f^-$  dominate. As it will turn out in the calculation, this is the case if  $\max_{(\theta, \varphi)} |f^-| \ll v_1 - v_0$ . This means that the timeshift induced by the supertranslation must be much smaller than the timescale of the process, i.e. the supertranslation must be performed slowly. We will choose  $v_1 - v_0$  such that this is the case and so that we can neglect all higher orders in  $f^-$  when we calculate the Einstein equations.

We have to show that the transformation (A.25) leads to a valid solution of the Einstein equations. Thus, if we calculate the Einstein  $G_{\mu\nu}$  and consequently the new energy-momentum-tensor  $T_{\mu\nu}$ , we have to demonstrate that this is a valid source. To this end, we have to perform two checks. First of all, it must be conserved,  $T_{\mu\nu}{}^{;\mu} = 0$ . This is trivially true in our construction because of the Bianchi identity,  $G_{\mu\nu}{}^{;\mu} = 0$ . Secondly, we have to show that  $T_{\mu\nu}$  fulfills an appropriate energy condition. For that purpose, we first note that this perturbation only depends on the local geometry, except for  $\xi_v^\mu$  and  $s^-(r)$ , which also depend on spacetime points at bigger radii. Thus, outside the planet, we have the same solution as in [224], except for the fact that we perform our supertranslation slowly:

$$T_{00} = \frac{1}{4\pi r^2} \left[ \mu - \frac{1}{4} D^2 (D^2 + 2) f^- + \frac{3M}{2r} D^2 f^- \right] \tau'_{v_0, v_1}(v), \quad (\text{A.26a})$$

$$T_{0A} = \frac{3M}{8\pi r^2} D_A f^- \tau'_{v_0, v_1}(v), \quad (\text{A.26b})$$

where we used that there is no absorption outside the planet:  $s^-(r > R) = 1$ . Obviously, the energy condition is fulfilled. At this point, we remark that leaving out all subleading parts, which are proportional to  $M$ , would also lead to a valid wave in the metric (A.23), i.e.  $T_{\mu\nu}{}^{;\mu}$  would also be true to all orders if one only considered the leading order of (A.26). This means that we add the subleading parts to (A.26) not because of energy conservation but since we want to realize the transition (A.25) not only to leading order in  $1/r$ , but to all orders.<sup>3</sup>

Fortunately, we do not either have to worry about the energy condition inside the planet. For a small enough perturbation, this is true since the energy condition inside a planet is not only marginally fulfilled. This means that  $s^-(r)$  can be nonzero inside the planet: This corresponds to absorption of the wave by the planet.

Lastly, we have to show that the wave is still a valid solution after it has been partly absorbed. For the purpose of illustration, we model the planet as a sequence of massive shells with vacuum in between,  $T_{\mu\nu} = 0$ . In that case, the only nontrivial question is whether (A.25) fulfills the energy condition after it passed some or all of the shells. Therefore, we calculate the energy-momentum-tensor in this region. By Birkhoff's theorem, the local geometry corresponds to a Schwarzschild solution with diminished mass  $\tilde{M}$  (where  $\tilde{M}$  can be zero). It only depends on the matter which it has passed via  $\xi_v^\mu$ . We parameterize the difference of  $\xi_v^\mu$  and the vector field one would get in a pure Schwarzschild geometry of mass  $\tilde{M}$  by

$$\sigma := \int_{R_{\min}}^{R_{\max}} dr' ((\sqrt{AB} - 1) r'^{-2}), \quad (\text{A.27})$$

<sup>3</sup>Of course, energy conservation relates the two subleading parts of  $T_{00}$  and  $T_{0A}$ . When we choose one, it determines the other.

where we have no matter for  $r > R_{\max}$  and between  $r$  and  $R_{\min}$ .<sup>4</sup> Explicitly, this means that we can write

$$\xi_v^A = f^{-,A} \left( \frac{1}{r} + \sigma \right),$$

where it is important that  $\sigma$  does not depend on  $r$  in our region of interest. Of course,  $\sigma = 0$  corresponds to the case when there is no matter outside.

With the help of Mathematica [216], we compute:

$$T_{00} = \frac{1}{4\pi r^2} \left[ \tilde{\mu} - (1 + \sigma r) \left( \frac{1}{4} D^2 (D^2 + 2) \tilde{f}^- - \frac{3\tilde{M}}{2r} D^2 \tilde{f}^- \right) \right] \tau'_{v_0, v_1}(v), \quad (\text{A.28a})$$

$$T_{0A} = \left[ \frac{3\tilde{M}}{8\pi r^2} D_A \tilde{f}^- + \frac{\sigma}{16\pi} D_A (D^2 + 2) \tilde{f}^- \right] \tau'_{v_0, v_1}(v), \quad (\text{A.28b})$$

$$T_{AB} = -\frac{\sigma r}{8\pi} \left[ (2D_A D_B - \gamma_{AB} D^2) \tilde{f}^- \right] \tau'_{v_0, v_1}(v), \quad (\text{A.28c})$$

where  $\tilde{f}^- = s^-(r) f^-$  is the supertranslation which is attenuated because of absorption in the outer shells. It is crucial to note that  $s^{-\prime}(r) = 0$  in this calculation since we are not inside one of the shells of the planet and likewise  $\tilde{\mu} = s^-(r) \mu$ . As we can estimate  $\sigma$  very crudely as  $\sigma < 1/R$ , we see that for sufficiently large  $\mu$ , the energy condition is fulfilled. With a more accurate estimate, we expect that the freedom of choosing  $\mu$  is not restricted when the wave passes a massive shell. In summary, we have shown that the metric (A.25), which describes the dynamical transition from a spherically symmetric planet to a counterpart with nontrivial angular distribution of mass, is a valid solution.

## Step 2: Emission

The second step is to describe the emission of the wave by the planet. Thus, our initial metric is the one after absorption, as determined by equation (A.25):

$$\delta g_{\mu\nu}^v = s^-(r) \left( \mathcal{L}_{\xi_v(f^-)} g_{\mu\nu}^v + \frac{2\mu G_N}{r} \delta_\mu^0 \delta_\nu^0 \right). \quad (\text{A.29})$$

As we want to consider emission, our first step is to transform it to retarded coordinates. Intuitively, it is clear that it should be possible to describe a slightly asymmetrical planet also in retarded coordinates. While it is generically hard to write down the corresponding diffeomorphism which connects the two metrics, we can use that the metric of a planet does not differ from Schwarzschild in the exterior region. Therefore, we can use the diffeomorphism (A.18) to obtain

$$g_{\mu\nu}^u = g_{\mu\nu}^{u,0} + s^-(r) \left( \mathcal{L}_{\xi_u(-f^-)} g_{\mu\nu}^{u,0} + \theta(R - r) \text{dev} \right), \quad (\text{A.30})$$

<sup>4</sup>We use that  $AB = 1$  in a Schwarzschild geometry of arbitrary mass.

where  $g_{\mu\nu}^{u,0}$  is the metric of the initial, spherically symmetric planet in retarded coordinates. This means that we apply a supertranslation in retarded coordinates which is defined by the function  $f^-$  used to defined the advanced supertranslation. The function  $\text{dev}$  accounts for the fact that we do not know the continuation of the matching diffeomorphism (A.18) to the interior of the planet. Therefore,  $g_{\mu\nu}^u$  might deviate slightly from BMS-gauge but only in the interior. We expect, however, that the matching diffeomorphism can be continued such that  $\text{dev} = 0$ . Finally, we want to point out that  $g_{\mu\nu}^u(r=0) = g_{\mu\nu}^{u,0}(r=0)$  since  $s^-(r=0) = 0$ , i.e. the wave does not reach the center and the mass distribution of the planet is still spherically symmetric around  $r=0$ .

The case of the planet provides us with another justification why the matching (A.20) is natural. With this identification, both the metric (A.29) in advanced coordinates and the metric (A.30) in retarded coordinates cover the whole manifold. Extrapolating the results of [257, 258], where finite supertranslations of Schwarzschild and Minkowski are discussed, we expect that for any other matching, i.e. for any other value of the supertranslation field, this is no longer the case. If this is true, the requirement that the BMS-coordinate system covers the whole manifold singles out a unique value of the advanced supertranslation field as well as a unique value of the retarded supertranslation field, and therefore a coordinate matching.

Next, we want to describe how the metric (A.30) emits a wave. This wave should realize a supertranslation described by  $f^+$ , which is generically different from  $f^-$ :

$$\delta g_{\mu\nu}^u = \tau_{u_0, u_1}(u) s^+(r) \left( \mathcal{L}_{\xi_u(f^+)} g_{\mu\nu}^{u,0} - \frac{2\mu G_N}{r} \delta_\mu^0 \delta_\nu^0 \right), \quad (\text{A.31})$$

where we used that  $\mathcal{L}_{\xi_u(f^+)} g_{\mu\nu}^u = \mathcal{L}_{\xi_u(f^+)} g_{\mu\nu}^{u,0}$  to first order in  $f^+$  and  $f^-$ . Thus, working only to first order simplifies our calculations significantly since we can simply use the calculations for the absorption. The wave (A.28) becomes:

$$T_{00} = \frac{1}{4\pi r^2} \left[ \tilde{\mu} - (1 + \sigma r) \left( \frac{1}{4} D^2 (D^2 + 2) \tilde{f}^+ - \frac{3\tilde{M}}{2r} D^2 \tilde{f}^+ \right) \right] \tau'_{u_0, u_1}(u), \quad (\text{A.32a})$$

$$T_{0A} = - \left[ \frac{3\tilde{M}}{8\pi r^2} D_A \tilde{f}^+ + \frac{\sigma}{16\pi} D_A (D^2 + 2) \tilde{f}^+ \right] \tau'_{u_0, u_1}(u), \quad (\text{A.32b})$$

$$T_{AB} = - \frac{\sigma r}{8\pi} \left[ (2D_A D_B - \gamma_{AB} D^2) \tilde{f}^+ \right] \tau'_{u_0, u_1}(u). \quad (\text{A.32c})$$

As for the absorption, we have shown that we can realize the transformation (A.31) with a physical wave.

Finally, we analyze the joint effect of absorption and emission. Combining the transformations (A.25) and (A.31), we get total total change of the metric:

$$\begin{aligned} \delta g_{\mu\nu}^{\text{tot}} &= \theta(r-R) \mathcal{L}_{\xi_u(f^+ - f^-)} g_{\mu\nu}^{u,0} \\ &+ \theta(R-r) \left( s^+(r) \mathcal{L}_{\xi_u(f^+)} g_{\mu\nu}^{u,0} - s^-(r) \mathcal{L}_{\xi_u(f^-)} g_{\mu\nu}^{u,0} + \text{dev} \right), \end{aligned} \quad (\text{A.33})$$

where we used retarded coordinates. As desired, the mass of the planet stays invariant. Moreover,  $\delta g_{\mu\nu}^{\text{tot}}$  acts as a diffeomorphism outside the planet, namely it is the difference of the advanced supertranslation, described by  $f^-$ , and the retarded supertranslation, described by  $f^+$ . If we furthermore assume that the term  $\text{dev}$ , which reflects our incomplete knowledge of the matching between advanced and retarded coordinates in the planet, is zero, we see that the metric does not change for  $f^- = f^+$ . We obtain a trivial transformation if the angular energy distribution of ingoing and outgoing radiation is anglewise the same.

# Bibliography

- [1] G. Dvali, C. Gomez, and S. Zell, “Quantum Break-Time of de Sitter,” *J. Cosmol. Astropart. Phys.* **1706** (2017) 028, [arXiv:1701.08776 \[hep-th\]](#).
- [2] C. Gomez and S. Zell, “Black Hole Evaporation, Quantum Hair and Supertranslations,” *Eur. Phys. J. C* **78** (2018) 320, [arXiv:1707.08580 \[hep-th\]](#).
- [3] G. Dvali and S. Zell, “Classicality and Quantum Break-Time for Cosmic Axions,” *J. Cosmol. Astropart. Phys.* **1807** (2018) 064, [arXiv:1710.00835 \[hep-ph\]](#).
- [4] C. Gomez, R. Letschka, and S. Zell, “Infrared Divergences and Quantum Coherence,” *Eur. Phys. J. C* **78** (2018) 610, [arXiv:1712.02355 \[hep-th\]](#).
- [5] G. Dvali, M. Michel, and S. Zell, “Finding Critical States of Enhanced Memory Capacity in Attractive Cold Bosons,” *Eur. Phys. J. Quantum Technology* **6** (2019) 1, [arXiv:1805.10292 \[quant-ph\]](#).
- [6] C. Gomez, R. Letschka, and S. Zell, “The Scales of the Infrared,” *J. High Energy Phys.* **1809** (2018) 115, [arXiv:1807.07079 \[hep-th\]](#).
- [7] G. Dvali, C. Gomez, and S. Zell, “Quantum Breaking Bound on de Sitter and Swampland,” *Fortsch. Phys.* **67** (2019) 1800094, [arXiv:1810.11002 \[hep-th\]](#).
- [8] G. Dvali, C. Gomez, and S. Zell, “Discrete Symmetries Excluded by Quantum Breaking,” [arXiv:1811.03077 \[hep-th\]](#), to be published.
- [9] G. Dvali, C. Gomez, and S. Zell, “A Proof of the Axion?,” [arXiv:1811.03079 \[hep-th\]](#), to be published.
- [10] G. Dvali, L. Eisemann, M. Michel, and S. Zell, “Universe’s Primordial Quantum Memories,” *J. Cosmol. Astropart. Phys.* **1903** (2019) 010, [arXiv:1812.08749 \[hep-th\]](#).

- [11] **LIGO Scientific Collaboration and Virgo Collaboration**, “Observation of Gravitational Waves from a Binary Black Hole Merger,” *Phys. Rev. Lett.* **116** (2016) 061102, arXiv:1602.03837 [gr-qc].
- [12] A. Einstein, “Naherungsweise Integration der Feldgleichungen der Gravitation,” *Sitzungsberichte der Koniglich Preufischen Akademie der Wissenschaften (Berlin)* (1916) 688.
- [13] **CMS Collaboration**, “Observation of a new boson at a mass of 125 GeV with the CMS experiment at the LHC,” *Phys. Lett. B* **716** (2012) 30, arXiv:1207.7235 [hep-ex].
- [14] **ATLAS Collaboration**, “Observation of a new particle in the search for the Standard Model Higgs boson with the ATLAS detector at the LHC,” *Phys. Lett. B* **716** (2012) 1, arXiv:1207.7214 [hep-ex].
- [15] F. Englert and R. Brout, “Broken Symmetry and the Mass of Gauge Vector Mesons,” *Phys. Rev. Lett.* **13** (1964) 321.
- [16] P. W. Higgs, “Broken symmetries, massless particles and gauge fields,” *Phys. Lett.* **12** (1964) 132.
- [17] P. W. Higgs, “Broken Symmetries and the Masses of Gauge Bosons,” *Phys. Rev. Lett.* **13** (1964) 508.
- [18] **Planck Collaboration**, “Planck 2015. XX. Constraints on inflation,” *Astron. Astrophys.* **594** (2015) A20, arXiv:1502.02114 [astro-ph.CO].
- [19] **Planck Collaboration**, “Planck 2018 results. X. Constraints on inflation,” arXiv:1807.06211 [astro-ph.CO].
- [20] A. H. Guth, “The Inflationary Universe: A Possible Solution to the Horizon and Flatness Problems,” *Phys. Rev. D* **23** (1981) 347.
- [21] F. Zwicky, “Die Rotverschiebung von extragalaktischen Nebeln,” *Helv. Phys. Acta* **6** (1933) 110.
- [22] **High-Z Supernova Search Team**, “Observational Evidence from Supernovae for an Accelerating Universe and a Cosmological Constant,” *Astron. J.* **116** (1998) 1009, arXiv:astro-ph/9805201.
- [23] **Supernova Cosmology Project**, “Measurements of  $\Omega$  and  $\Lambda$  from 42 high-redshift supernovae,” *Astrophys. J.* **517** (1999) 565, arXiv:1205.3494 [astro-ph.CO].
- [24] A. Spiezia, “Status and prospect of LHC BSM searches,” *PoS ALPS2018* (2018) 025.

- [25] S. W. Hawking, “Particle creation by black holes,” *Commun. Math. Phys.* **43** (1975) 199.
- [26] S. W. Hawking, “Breakdown of predictability in gravitational collapse,” *Phys. Rev. D* **14** (1976) 2460.
- [27] **The GAMBIT Collaboration**, “Status of the scalar singlet dark matter model,” *Eur. Phys. J. C* **77** (2017) 568.
- [28] T. Asaka, S. Blanchet, and M. Shaposhnikov, “The  $\nu$ MSM, dark matter and neutrino masses,” *Phys. Lett. B* **631** (2005) 151, [arXiv:hep-ph/0503065](#).
- [29] T. Asaka and M. Shaposhnikov, “The  $\nu$ MSM, dark matter and baryon asymmetry of the universe,” *Phys. Lett. B* **620** (2005) 17, [arXiv:hep-ph/0505013](#).
- [30] F. Bezrukov and M. Shaposhnikov, “The Standard Model Higgs boson as the inflaton,” *Phys. Lett. B* **659** (2008) 703, [arXiv:0904.1537 \[hep-ph\]](#).
- [31] J. D. Bekenstein, “Black holes and entropy,” *Phys. Rev. D* **7** (1973) 2333.
- [32] G. W. Gibbons and S. W. Hawking, “Cosmological event horizons, thermodynamics, and particle creation,” *Phys. Rev. D* **15** (1977) 2738.
- [33] B. Carr, F. Kühnel, and M. Sandstad, “Primordial Black Holes as Dark Matter,” *Phys. Rev. D* **94** (2016) 083504, [arXiv:1607.06077 \[astro-ph.CO\]](#).
- [34] G. Dvali and C. Gomez, “Black Hole’s Quantum N-Portrait,” *Fortschr. Phys.* **61** (2013) 742, [arXiv:1112.3359 \[hep-th\]](#).
- [35] G. Dvali and C. Gomez, “Black Hole’s 1/N Hair,” *Phys. Lett. B* **719** (2013) 419, [arXiv:1203.6575 \[hep-th\]](#).
- [36] G. Dvali and C. Gomez, “Black Holes as Critical Point of Quantum Phase Transition,” *Eur. Phys. J. C* **74** (2014) 2752, [arXiv:1207.4059 \[hep-th\]](#).
- [37] G. Dvali and C. Gomez, “Black Hole Macro-Quantumness,” [arXiv:1212.0765 \[hep-th\]](#).
- [38] P. T. Chrusciel, J. Lopes Costa, and M. Heusler, “Stationary Black Holes: Uniqueness and Beyond,” *Living Rev. Rel.* **15** (2012) 7, [arXiv:1205.6112 \[gr-qc\]](#).
- [39] G. Dvali, “Non-Thermal Corrections to Hawking Radiation Versus the Information Paradox,” *Fortsch. Phys.* **64** (2016) 106, [arXiv:1509.04645 \[hep-th\]](#).

- [40] G. Dvali, D. Flassig, C. Gomez, A. Pritzel, and N. Wintergerst, “Scrambling in the Black Hole Portrait,” *Phys. Rev. D* **88** (2013) 124041, [arXiv:1307.3458 \[hep-th\]](#).
- [41] D. N. Page, “Is Black-Hole Evaporation Predictable?,” *Phys. Rev. Lett.* **44** (1980) 301.
- [42] D. N. Page, “Information in black hole radiation,” *Phys. Rev. Lett.* **71** (1993) 3743, [arXiv:hep-th/9306083](#).
- [43] G. Dvali and C. Gomez, “Landau-Ginzburg limit of black hole’s quantum portrait: Self-similarity and critical exponent,” *Phys. Lett.* **B716** (2012) 240, [arXiv:1203.3372 \[hep-th\]](#).
- [44] G. Dvali and C. Gomez, “Quantum Compositeness of Gravity: Black Holes, AdS and Inflation,” *J. Cosmol. Astropart. Phys.* **1401** (2014) 023, [arXiv:1312.4795 \[hep-th\]](#).
- [45] G. Dvali, C. Gomez, R. Isermann, D. Lüster, and S. Stieberger, “Black hole formation and classicalization in ultra-Planckian  $2 \rightarrow N$  scattering,” *Nucl. Phys. B* **893** (2015) 187, [arXiv:1409.7405 \[hep-th\]](#).
- [46] G. Dvali and C. Gomez, “Self-Completeness of Einstein Gravity,” [arXiv:1005.3497 \[hep-th\]](#).
- [47] G. Dvali, G. F. Giudice, C. Gomez, and A. Kehagias, “UV-Completion by Classicalization,” *J. High Energy Phys.* **1108** (2011) 108, [arXiv:1010.1415 \[hep-ph\]](#).
- [48] G. Dvali, C. Gomez, and A. Kehagias, “Classicalization of Gravitons and Goldstones,” *J. High Energy Phys.* **1111** (2011) 070, [arXiv:1103.5963 \[hep-th\]](#).
- [49] A. Addazi, M. Bianchi, and G. Veneziano, “Glimpses of black hole formation/evaporation in highly inelastic, ultra-planckian string collisions,” *J. High Energy Phys.* **1702** (2017) 111, [arXiv:1611.03643 \[hep-th\]](#).
- [50] G. Dvali and C. Gomez, “Quantum Exclusion of Positive Cosmological Constant?,” *Ann. Phys.* **528** (2014) 68, [arXiv:1412.8077 \[hep-th\]](#).
- [51] G. Dvali, A. Franca, C. Gomez, and N. Wintergerst, “Nambu-Goldstone Effective Theory of Information at Quantum Criticality,” *Phys. Rev. D* **92** (2015) 125002, [arXiv:1507.02948 \[hep-th\]](#).
- [52] G. Dvali and M. Panchenko, “Black Hole Type Quantum Computing in Critical Bose-Einstein Systems,” [arXiv:1507.08952 \[hep-th\]](#).

- [53] G. Dvali and M. Panchenko, “Black Hole Based Quantum Computing in Labs and in the Sky,” *Fortschr. Phys.* **64** (2016) 569, arXiv:1601.01329 [hep-th].
- [54] J. D. Bekenstein, “Universal upper bound on the entropy-to-energy ratio for bounded systems,” *Phys. Rev. D* **23** (1981) 287.
- [55] H. J. Bremermann, “Quantum noise and information,” in *Proceedings of the Fifth Berkeley Symposium on Mathematical Statistics and Probability*, vol. 4, p. 15. 1967.
- [56] A. Strominger, “Black Hole Information Revisited,” arXiv:1706.07143 [hep-th].
- [57] F. Bloch and A. Nordsieck, “Note on the Radiation Field of the electron,” *Phys. Rev.* **52** (1937) 54.
- [58] D. R. Yennie, S. C. Frautschi, and H. Suura, “The infrared divergence phenomena and high-energy processes,” *Annals Phys.* **13** (1961) 379.
- [59] S. Weinberg, “Infrared photons and gravitons,” *Phys. Rev.* **140** (1965) B516.
- [60] V. Chung, “Infrared divergence in quantum electrodynamics,” *Phys. Rev.* **140** (1965) B1110.
- [61] T. W. B. Kibble, “Coherent soft-photon states and infrared divergences. I. classical currents,” *J. Math. Phys.* **9** (1968) 315.
- [62] T. W. B. Kibble, “Coherent soft-photon states and infrared divergences. II. mass-shell singularities of green’s functions,” *Phys. Rev.* **173** (1968) 1527.
- [63] T. W. B. Kibble, “Coherent soft-photon states and infrared divergences. III. asymptotic states and reduction formulas,” *Phys. Rev.* **174** (1968) 1882.
- [64] T. W. B. Kibble, “Coherent soft-photon states and infrared divergences. IV. the scattering operator,” *Phys. Rev.* **175** (1968) 1624.
- [65] P. P. Kulish and L. D. Faddeev, “Asymptotic conditions and infrared divergences in quantum electrodynamics,” *Theor. Math. Phys.* **4** (1970) 745.
- [66] D. Carney, L. Chaurette, D. Neuenfeld, and G. W. Semenoff, “Infrared quantum information,” *Phys. Rev. Lett.* **119** (2017) 180502, arXiv:1706.03782 [hep-th].

- [67] D. Carney, L. Chaurette, D. Neuenfeld, and G. W. Semenoff, “Dressed infrared quantum information,” *Phys. Rev. D* **97** (2018) 025007, [arXiv:1710.02531 \[hep-th\]](#).
- [68] H. Bondi, M. Van der Burg, and A. Metzner, “Gravitational waves in general relativity. VII. Waves from axi-symmetric isolated systems,” *Proc. R. Soc. London, Ser. A* **269** (1962) 21.
- [69] R. K. Sachs, “Gravitational waves in general relativity. VIII. Waves in asymptotically flat space-time,” *Proc. R. Soc. London, Ser. A* **270** (1962) 103.
- [70] R. Sachs, “Asymptotic symmetries in gravitational theory,” *Phys. Rev.* **128** (1962) 2851.
- [71] P. Sikivie and Q. Yang, “Bose-Einstein Condensation of Dark Matter Axions,” *Phys. Rev. Lett.* **103** (2009) 111301, [arXiv:0901.1106 \[hep-ph\]](#).
- [72] G. Dvali, C. Gomez, and S. Zell, “On the substructure of the cosmological constant,” *PoS CORFU2016* (2017) 094.
- [73] S. Zell, “A corpuscular picture of gravitational scattering,” Master’s thesis, Ludwig-Maximilians-Universität Munich, 2015.
- [74] G. Dvali, C. Gomez, and D. Lüst, “Classical Limit of Black Hole Quantum N-Portrait and BMS Symmetry,” *Phys. Lett. B* **753** (2016) 173, [arXiv:1509.02114 \[hep-th\]](#).
- [75] D. V. Semikoz and I. I. Tkachev, “Condensation of bosons in kinetic regime,” *Phys. Rev.* **D55** (1997) 489, [arXiv:hep-ph/9507306](#).
- [76] R. Kanamoto, H. Saito, and M. Ueda, “Quantum phase transition in one-dimensional Bose-Einstein condensates with attractive interactions,” *Phys. Rev. A* **67** (2003) 013608, [arXiv:cond-mat/0210229](#).
- [77] E. P. Gross, “Structure of a quantized vortex in boson systems,” *Il Nuovo Cimento* **20** (1961) 454.
- [78] L. Pitaevskii, “Vortex lines in an imperfect bose gas,” *J. Exptl. Theoret. Phys.* **40** (1961) 646.
- [79] N. Bogoliubov, “On the theory of superfluidity,” *J. Phys.* **11** (1947) 23.
- [80] S. Weinberg, “A new light boson?,” *Phys. Rev. Lett.* **40** (1978) 223.
- [81] F. Wilczek, “Problem of Strong  $P$  and  $T$  Invariance in the Presence of Instantons,” *Phys. Rev. Lett.* **40** (1978) 279.

- [82] R. D. Peccei and H. R. Quinn, "CP conservation in the presence of pseudoparticles," *Phys. Rev. Lett.* **38** (1977) 1440.
- [83] J. E. Kim, "Light pseudoscalars, particle physics and cosmology," *Phys. Rep.* **150** (1987) 1.
- [84] M. S. Turner, "Windows on the axion," *Phys. Rep.* **197** (1990) 67.
- [85] G. G. Raffelt, "Astrophysical methods to constrain axions and other novel particle phenomena," *Phys. Rep.* **198** (1990) 1.
- [86] J. E. Kim, "Weak-interaction singlet and strong CP invariance," *Phys. Rev. Lett.* **43** (1979) 103.
- [87] M. A. Shifman, A. Vainshtein, and V. I. Zakharov, "Can confinement ensure natural CP invariance of strong interactions?," *Nucl. Phys. B* **166** (1980) 493.
- [88] A. R. Zhitnitsky, "On Possible Suppression of the Axion Hadron Interactions. (In Russian)," *Sov. J. Nucl. Phys.* **31** (1980) 260.
- [89] M. Dine, W. Fischler, and M. Srednicki, "A simple solution to the strong CP problem with a harmless axion," *Phys. Lett. B* **104** (1981) 199.
- [90] J. Preskill, M. B. Wise, and F. Wilczek, "Cosmology of the invisible axion," *Phys. Lett. B* **120** (1983) 127.
- [91] L. F. Abbott and P. Sikivie, "A cosmological bound on the invisible axion," *Phys. Lett. B* **120** (1983) 133.
- [92] M. Dine and W. Fischler, "The not-so-harmless axion," *Phys. Lett. B* **120** (1983) 137.
- [93] G. R. Dvali, "Removing the cosmological bound on the axion scale," arXiv:hep-ph/9505253 [hep-ph].
- [94] **The ALPS Collaboration**, "Resonant laser power build-up in ALPS – a "light-shining-through-walls" experiment," *Nucl. Instr. Meth. Phys. Res. A* **612** (2009) 83, arXiv:0905.4159 [physics.ins-det].
- [95] **The ADMX Collaboration**, "A SQUID-based microwave cavity search for dark-matter axions," *Phys. Rev. Lett.* **104** (2010) 041301, arXiv:0910.5914 [astro-ph.CO].
- [96] **The CAST Collaboration**, "CAST search for sub-eV mass solar axions with 3He buffer gas," *Phys. Rev. Lett.* **107** (2011) 261302, arXiv:1106.3919 [hep-ex].

- [97] D. Budker, P. W. Graham, M. Ledbetter, S. Rajendran, and A. O. Sushkov, “Proposal for a cosmic axion spin precession experiment (CASPEr),” *Phys. Rev. X* **4** (2014) 021030, arXiv:1306.6089 [hep-ph].
- [98] **The IAXO Collaboration**, “Conceptual design of the international axion observatory (IA XO),” *J. Instrum.* **9** (2014) T05002, arXiv:1401.3233 [physics.ins-det].
- [99] **The MADMAX Working Group**, “Dielectric haloscopes: A new way to detect axion dark matter,” *Phys. Rev. Lett.* **118** (2017) 091801, arXiv:1611.05865 [physics.ins-det].
- [100] **nEDM Collaboration**, “Search for axion-like dark matter through nuclear spin precession in electric and magnetic fields,” *Phys. Rev. X* **7** (2017) 041034, arXiv:1708.06367 [hep-ph].
- [101] O. Erken, P. Sikivie, H. Tam, and Q. Yang, “Cosmic axion thermalization,” *Phys. Rev. D* **85** (2012) 063520, arXiv:1111.1157 [astro-ph.CO].
- [102] P. Sikivie, “The case for axion dark matter,” *Phys. Lett. B* **695** (2011) 22, arXiv:1003.2426 [astro-ph.GA].
- [103] N. Banik and P. Sikivie, “Axions and the galactic angular momentum distribution,” *Phys. Rev. D* **88** (2013) 123517, arXiv:1307.3547 [astro-ph.GA].
- [104] C. Cheng and P. Fung, “The evolution operator technique in solving the Schrodinger equation, and its application to disentangling exponential operators and solving the problem of a mass-varying harmonic oscillator,” *J. Phys. A: Math. Gen.* **21** (1988) 4115.
- [105] N. W. McLachlan, *Theory and application of Mathieu functions*. Clarendon Press, 1951.
- [106] A. H. Guth, M. P. Hertzberg, and C. Prescod-Weinstein, “Do dark matter axions form a condensate with long-range correlation?,” *Phys. Rev. D* **92** (2015) 103513, arXiv:1412.5930 [astro-ph.CO].
- [107] P. Sikivie and E. M. Todarello, “Duration of classicality in highly degenerate interacting bosonic systems,” *Phys. Lett. B* **770** (2017) 331, arXiv:1607.00949 [hep-ph].
- [108] M. P. Hertzberg, “Quantum and classical behavior in interacting bosonic systems,” *J. Cosmol. Astropart. Phys.* **1611** (2016) 037, arXiv:1609.01342 [hep-ph].

- [109] F. Kühnel, “Thoughts on the Vacuum Energy in the Quantum N-Portrait,” *Mod. Phys. Lett. A* **30** (2015) 1550197, [arXiv:1408.5897 \[gr-qc\]](#).
- [110] F. Kühnel and M. Sandstad, “Corpuscular Consideration of Eternal Inflation,” *Eur. Phys. J. C* **75** (2015) 505, [arXiv:1504.02377 \[gr-qc\]](#).
- [111] L. Berezhiani, “On corpuscular theory of inflation,” *Eur. Phys. J C* **77** (2017) 106, [arXiv:1610.08433 \[hep-th\]](#).
- [112] G. Dvali, S. Hofmann, and J. Khoury, “Degravitation of the Cosmological Constant and Graviton Width,” *Phys. Rev. D* **76** (2007) 084006, [arXiv:hep-th/0703027](#).
- [113] M. Fierz and W. Pauli, “On relativistic wave equations for particles of arbitrary spin in an electromagnetic field,” *Proc. Roy. Soc. Lond.* **A173** (1939) 211.
- [114] G. Dvali, “Predictive power of strong coupling in theories with large distance modified gravity,” *New J. Phys.* **8** (2006) 326, [arXiv:hep-th/0610013](#).
- [115] C. Deffayet, G. R. Dvali, and G. Gabadadze, “Accelerated Universe from Gravity Leaking to Extra Dimensions,” *Phys. Rev. D* **65** (2002) 044023, [arXiv:astro-ph/0105068](#).
- [116] C. de Rham, G. Gabadadze, L. Heisenberg, and D. Pirtskhalava, “Cosmic Acceleration and the Helicity-0 Graviton,” *Phys. Rev. D* **83** (2011) 103516, [arXiv:1010.1780 \[hep-th\]](#).
- [117] K. Koyama, G. Niz, and G. Tasinato, “Analytic solutions in non-linear massive gravity,” *Phys. Rev. Lett.* **107** (2011) 131101, [arXiv:1103.4708 \[hep-th\]](#).
- [118] A. E. Gumrukcuoglu, C. Lin, and S. Mukohyama, “Open FRW universes and self-acceleration from nonlinear massive gravity,” *J. Cosmol. Astropart. Phys.* **1111** (2011) 030, [arXiv:1109.3845 \[hep-th\]](#).
- [119] C. de Rham, G. Gabadadze, and A. J. Tolley, “Resummation of Massive Gravity,” *Phys. Rev. Lett.* **106** (2011) 231101, [arXiv:1011.1232 \[hep-th\]](#).
- [120] E. Mottola, “Particle creation in de Sitter space,” *Phys. Rev. D* **31** (1985) 754.
- [121] E. Mottola, “Thermodynamic instability of de Sitter space,” *Phys. Rev. D* **33** (1986) 1616.

- 
- [122] A. M. Polyakov, “De Sitter space and eternity,” *Nucl. Phys.* **B797** (2008) 199, arXiv:0709.2899 [hep-th].
- [123] A. M. Polyakov, “Decay of vacuum energy,” *Nucl. Phys. B* **834** (2010) 316, arXiv:0912.5503 [hep-th].
- [124] A. M. Polyakov, “Infrared instability of the de Sitter space,” arXiv:1209.4135 [hep-th].
- [125] T. Markkanen, “Decoherence Can Relax Cosmic Acceleration,” *J. Cosmol. Astropart. Phys.* **1611** 026, arXiv:1609.01738 [hep-th].
- [126] T. Markkanen, “Decoherence can relax cosmic acceleration: an example,” *J. Cosmol. Astropart. Phys.* **1709** (2017) 022, arXiv:1610.06637 [gr-qc].
- [127] T. Markkanen, “De Sitter Stability and Coarse Graining,” *Eur. Phys. J. C* **78** (2018) 97, arXiv:1703.06898 [gr-qc].
- [128] U. H. Danielsson, D. Domert, and M. E. Olsson, “Puzzles and resolutions of information duplication in de Sitter space,” *Phys. Rev. D* **68** (2003) 083508, hep-th/0210198.
- [129] S. B. Giddings, “Quantization in black hole backgrounds,” *Phys. Rev. D* **76** (2007) 064027, hep-th/0703116.
- [130] N. Arkani-Hamed, S. Dubovsky, A. Nicolis, E. Trincherini, and G. Villadoro, “A Measure of de Sitter Entropy and Eternal Inflation,” *J. High Energy Phys.* **0705** (2007) 055, arXiv:0704.1814 [hep-th].
- [131] S. B. Giddings and M. S. Sloth, “Semiclassical relations and IR effects in de Sitter and slow-roll space-times,” *J. Cosmol. Astropart. Phys.* **1101** (2011) 023, arXiv:1005.1056 [hep-th].
- [132] S. B. Giddings and M. S. Sloth, “Cosmological observables, IR growth of fluctuations, and scale-dependent anisotropies,” *Phys. Rev. D* **84** (2011) 063528, arXiv:1104.0002 [hep-th].
- [133] S. B. Giddings and M. S. Sloth, “Fluctuating geometries, q-observables, and infrared growth in inflationary spacetimes,” *Phys. Rev. D* **86** (2012) 083538, arXiv:1109.1000 [hep-th].
- [134] S. Miao, T. Prokopec, and R. Woodard, “Scalar enhancement of the photon electric field by the tail of the graviton propagator,” *Phys. Rev. D* **98** (2018) 025022, arXiv:1806.00742 [gr-qc].

- 
- [135] R. Z. Ferreira, M. Sandora, and M. S. Sloth, “Asymptotic Symmetries in de Sitter and Inflationary Spacetimes,” *J. Cosmol. Astropart. Phys.* **1704** (2017) 033, [arXiv:1609.06318 \[hep-th\]](#).
- [136] D. Flassig, A. Pritzel, and N. Wintergerst, “Black Holes and Quantumness on Macroscopic Scales,” *Phys. Rev. D* **87** (2013) 084007, [arXiv:1212.3344 \[hep-th\]](#).
- [137] R. Casadio and A. Orlandi, “Quantum Harmonic Black Holes,” *J. High Energy Phys.* **1308** (2013) 025, [arXiv:1302.7138 \[hep-th\]](#).
- [138] W. Mück, “On the number of soft quanta in classical field configurations,” *Can. J. Phys.* **92** (2014) 973, [arXiv:1306.6245 \[hep-th\]](#).
- [139] W. Mück, “Counting Photons in Static Electric and Magnetic Fields,” *Eur. Phys. J. C* **73** (2013) 2679, [arXiv:1310.6909 \[hep-th\]](#).
- [140] F. Kühnel and B. Sundborg, “Modified Bose-Einstein Condensate Black Holes in d Dimensions,” [arXiv:1401.6067 \[hep-th\]](#).
- [141] M. Chen and Y.-C. Huang, “Gas Model of Gravitons with Light Speed,” [arXiv:1402.5767 \[gr-qc\]](#).
- [142] W. Mück and G. Pozzo, “Quantum portrait of a black hole with Pöschl-Teller potential,” *J. High Energy Phys.* **1405** (2014) 128, [arXiv:1403.1422 \[hep-th\]](#).
- [143] R. Casadio, O. Micu, and P. Nicolini, “Minimum length effects in black hole physics,” *Fundam. Theor. Phys.* **178** (2015) 293, [arXiv:1405.1692 \[hep-th\]](#).
- [144] R. Casadio, A. Giugno, O. Micu, and A. Orlandi, “Black holes as self-sustained quantum states, and Hawking radiation,” *Phys. Rev. D* **90** (2014) 084040, [arXiv:1405.4192 \[hep-th\]](#).
- [145] V. F. Foit and N. Wintergerst, “Self-similar Evaporation and Collapse in the Quantum Portrait of Black Holes,” *Phys. Rev. D* **92** (2015) 064043, [arXiv:1504.04384 \[hep-th\]](#).
- [146] R. Casadio, A. Giugno, and A. Orlandi, “Thermal corpuscular black holes,” *Phys. Rev. D* **91** (2015) 124069, [arXiv:1504.05356 \[gr-qc\]](#).
- [147] D. Allahbakhshi, “Black Holes Evaporate Non-Thermally,” [arXiv:1608.04291 \[physics.gen-ph\]](#).

- [148] J. Alfaro, D. Espriu, and L. Gabbanelli, “Bose-Einstein graviton condensate in a Schwarzschild black hole,” *Class. Quant. Grav.* **35** (2016) 015001, [arXiv:1609.01639 \[gr-qc\]](#).
- [149] M. Azam, J. R. Bhatt, and M. Sami, “Manybody aspects of gravity in compact stars,” *Phys. Scripta* **93** (2018) 025001, [arXiv:1701.06189 \[gr-qc\]](#).
- [150] G. Dvali, “Black Holes and Large N Species Solution to the Hierarchy Problem,” *Fortsch. Phys.* **58** (2010) 528, [arXiv:0706.2050 \[hep-th\]](#).
- [151] G. Dvali and M. Redi, “Black Hole Bound on the Number of Species and Quantum Gravity at LHC,” *Phys. Rev. D* **77** (2008) 045027, [arXiv:0710.4344 \[hep-th\]](#).
- [152] G. Dvali and C. Gomez, “Quantum Information and Gravity Cutoff in Theories with Species,” *Phys. Lett. B* **674** (2009) 303, [arXiv:0812.1940 \[hep-th\]](#).
- [153] A. D. Linde, “A new inflationary universe scenario: A possible solution of the horizon, flatness, homogeneity, isotropy and primordial monopole problems,” *Phys. Lett. B* **108** (1982) 389.
- [154] R. Casadio, A. Giugno, and A. Giusti, “Corpuscular slow-roll inflation,” *Phys. Rev. D* **97** (2018) 024041, [arXiv:1708.09736 \[gr-qc\]](#).
- [155] V. Mukhanov, *Physical foundations of cosmology*. Cambridge University Press, 2012.
- [156] G. Obied, H. Ooguri, L. Spodyneiko, and C. Vafa, “De Sitter Space and the Swampland,” [arXiv:1806.08362 \[hep-th\]](#).
- [157] G. Dvali and C. Gomez, “On Exclusion of Positive Cosmological Constant,” *Fortschr. Phys.* **67** (2019) 1800092, [arXiv:1806.10877 \[hep-th\]](#).
- [158] A. D. Linde, “Eternally Existing Self-Reproducing Inflationary Universe,” *Phys. Scr.* **T15** (1987) 169.
- [159] A. H. Guth, “Eternal inflation and its implications,” *J. Phys. A: Math. Theor.* **40** (2007) 6811.
- [160] H. Ooguri, E. Palti, G. Shiu, and C. Vafa, “Distance and de Sitter conjectures on the Swampland,” *Phys. Lett. B* **788** (2019) 180, [arXiv:1810.05506 \[hep-th\]](#).
- [161] A. Vilenkin, “Topological inflation,” *Phys. Rev. Lett.* **72** (1994) 3137.

- [162] A. Linde, “Monopoles as big as a universe,” *Phys. Lett. B* **327** (1994) 208.
- [163] L. Boubekeur and D. H. Lyth, “Hilltop inflation,” *J. Cosmol. Astropart. Phys.* **0507** (2005) 010, [hep-ph/0502047](#).
- [164] G. Dvali and S. H. H. Tye, “Brane inflation,” *Phys. Lett. B* **450** (1999) 72, [hep-ph/9812483](#).
- [165] G. Dvali, Q. Shafi, and S. Solganik, “D-brane Inflation,” [hep-th/0105203](#).
- [166] C. Vafa, “The String landscape and the swampland,” [arXiv:hep-th/0509212](#).
- [167] E. Palti, “The Swampland: Introduction and Review,” [arXiv:1903.06239 \[hep-th\]](#).
- [168] D. Andriot, “On the de Sitter swampland criterion,” *Phys. Lett. B* **785** (2018) 570, [arXiv:1806.10999 \[hep-th\]](#).
- [169] S. K. Garg and C. Krishnan, “Bounds on Slow Roll and the de Sitter Swampland,” [arXiv:1807.05193 \[hep-th\]](#).
- [170] P. Agrawal, G. Obied, P. J. Steinhardt, and C. Vafa, “On the cosmological implications of the string Swampland,” *Phys. Lett. B* **784** (2018) 271, [arXiv:1806.09718 \[hep-th\]](#).
- [171] A. Kehagias and A. Riotto, “A Note on Inflation and the Swampland,” *Fortschr. Phys.* **66** (2018) 1800052, [arXiv:1807.05445 \[hep-th\]](#).
- [172] F. Denef, A. Hebecker, and T. Wrase, “de Sitter swampland conjecture and the Higgs potential,” *Phys. Rev. D* **98** (2018) 086004, [arXiv:1807.06581 \[hep-th\]](#).
- [173] L. Heisenberg, M. Bartelmann, R. Brandenberger, and A. Refregier, “Dark Energy in the Swampland,” *Phys. Rev. D* **98** (2018) 123502, [arXiv:1808.02877 \[astro-ph.CO\]](#).
- [174] W. H. Kinney, S. Vagnozzi, and L. Visinelli, “The Zoo Plot Meets the Swampland: Mutual (In)Consistency of Single-Field Inflation, String Conjectures, and Cosmological Data,” [arXiv:1808.06424 \[astro-ph.CO\]](#).
- [175] K. Choi, D. Chway, and C. S. Shin, “The dS swampland conjecture with the electroweak symmetry and QCD chiral symmetry breaking,” *J. High Energy Phys.* **1811** (2018) 142, [arXiv:1809.01475 \[hep-th\]](#).
- [176] U. H. Danielsson, “The quantum swampland,” [arXiv:1809.04512 \[hep-th\]](#).

- [177] M. Motaharfar, V. Kamali, and R. O. Ramos, “Warm way out of the Swampland,” *Phys. Rev. D* **99** (2018) 063513, [arXiv:1810.02816](#).
- [178] A. Ashoorioon, “Rescuing single field inflation from the swampland,” *Phys. Lett. B* **790** (2019) 568, [arXiv:1810.04001](#) [[hep-th](#)].
- [179] H. Fukuda, R. Saito, S. Shirai, and M. Yamazaki, “Phenomenological Consequences of the Refined Swampland Conjecture,” [arXiv:1810.06532](#) [[hep-th](#)].
- [180] A. Hebecker and T. Wrase, “The Asymptotic dS Swampland Conjecture - a Simplified Derivation and a Potential Loophole,” *Fortschr. Phys.* **67** (2019) 1800097, [arXiv:1810.08182](#) [[hep-th](#)].
- [181] C. G. Callan, R. F. Dashen, and D. J. Gross, “The structure of the gauge theory vacuum,” *Phys. Lett. B* **63** (1976) 334.
- [182] R. Jackiw and C. Rebbi, “Vacuum Periodicity in a Yang-Mills Quantum Theory,” *Phys. Rev. Lett.* **37** (1976) 172.
- [183] C. Vafa and E. Witten, “Parity Conservation in Quantum Chromodynamics,” *Phys. Rev. Lett.* **53** (1984) 535.
- [184] G. Dvali and A. Vilenkin, “Cosmic attractors and gauge hierarchy,” *Phys. Rev. D* **70** (2004) 063501, [hep-th/0304043](#).
- [185] G. Dvali, “Large hierarchies from attractor vacua,” *Phys. Rev. D* **74** (2006) 025018, [hep-th/0410286](#).
- [186] I. B. Zeldovich, I. I. Kobzarev, and L. B. Okun, “Cosmological consequences of a spontaneous breakdown of a discrete symmetry,” *Zh. Eksp. Teor. Fiz* **67** (1975) 3.
- [187] A. Lazanu, C. J. A. P. Martins, and E. P. S. Shellard, “Contribution of domain wall networks to the CMB power spectrum,” *Phys. Lett. B* **747** (2015) 426, [arXiv:1505.03673](#) [[astro-ph.CO](#)].
- [188] L. Sousa and P. Avelino, “Cosmic microwave background anisotropies generated by domain wall networks,” *Phys. Rev. D* **92** (2015) 083520, [arXiv:1507.01064](#) [[astro-ph.CO](#)].
- [189] B. Rai and G. Senjanovic, “Gravity and the domain-wall problem,” *Phys. Rev. D* **49** (1994) 2729.
- [190] T. W. B. Kibble, “Topology of cosmic domains and strings,” *J. Phys. A: Math. Gen.* **9** (1976) 1387.

- [191] T. W. B. Kibble, “Some implications of a cosmological phase transition,” *Phys. Rep.* **67** (1980) 183.
- [192] A. Vilenkin, “Cosmic strings and domain walls,” *Phys. Rep.* **121** (1985) 263.
- [193] C. Panagiotakopoulos and K. Tamvakis, “Stabilized NMSSM without Domain Walls,” *Phys. Lett. B* **446** (1999) 224, [arXiv:hep-ph/9809475](#).
- [194] T. D. Lee, “A Theory of Spontaneous  $T$  Violation,” *Phys. Rev. D* **8** (1973) 1226.
- [195] L. Bento and G. C. Branco, “Generation of a KM phase from spontaneous CP breaking at a high energy scale,” *Phys. Lett. B* **245** (1990) 599.
- [196] G. Dvali and M. Shifman, “Domain walls in strongly coupled theories,” *Phys. Lett. B* **396** (1997) 64, Erratum-ibid. B **407** (1997) 452.
- [197] S. Ferrara, L. Girardello, and H. P. Nilles, “Breakdown of local supersymmetry through gauge fermion condensates,” *Phys. Lett. B* **125** (1983) 457.
- [198] G. Dvali and G. Senjanovic, “Is There a Domain Wall Problem?,” *Phys. Rev. Lett.* **74** (1995) 5178.
- [199] G. Dvali, A. Melfo, and G. Senjanovic, “Nonrestoration of spontaneously broken  $P$  and  $CP$  at high temperature,” *Phys. Rev. D* **54** (1996) 7857.
- [200] S. Weinberg, “Gauge and global symmetries at high temperature,” *Phys. Rev. D* **9** (1974) 3357.
- [201] R. N. Mohapatra and G. Senjanovic, “Soft  $CP$ -Invariance Violation at High Temperature,” *Phys. Rev. Lett.* **42** (1979) 1651.
- [202] R. N. Mohapatra and G. Senjanovic, “Broken symmetries at high temperature,” *Phys. Rev. D* **20** (1979) 3390.
- [203] M. L. Mangano, “Global and Gauge Symmetries in Finite Temperature Supersymmetric Theories,” *Phys. Lett. B* **147** (1984) 307.
- [204] G. Dvali, “Critically excited states with enhanced memory and pattern recognition capacities in quantum brain networks: Lesson from black holes,” [arXiv:1711.09079](#) [quant-ph].
- [205] G. Dvali, “Black Holes as Brains: Neural Networks with Area Law Entropy,” *Fortschr. Phys.* **66** (2018) 1800007, [arXiv:1801.03918](#) [hep-th].

- [206] G. Dvali, “A Microscopic Model of Holography: Survival by the Burden of Memory,” [arXiv:1810.02336](#) [hep-th].
- [207] M. Michel, “On Critical Phenomena in Attractive Bose Gases,” Master’s thesis, Technische Universität München, 2017.
- [208] G. Dvali, “Area law micro-state entropy from criticality and spherical symmetry,” *Phys. Rev. D* **97** (2018) 105005, [arXiv:1712.02233](#) [hep-th].
- [209] G. ’t Hooft, “Dimensional Reduction in Quantum Gravity,” *Conf. Proc.* **C930308** (1993) 284.
- [210] L. Susskind, “The World as a Hologram,” *J. Math. Phys.* **36** (1995) 6377.
- [211] E. Witten, “Anti de Sitter space and holography,” *Adv. Theor. Math. Phys.* **2** (1998) 253.
- [212] L. Susskind and E. Witten, “The Holographic Bound in Anti-de Sitter Space,” [hep-th/9805114](#).
- [213] I. Bloch, J. Dalibard, and S. Nascimbène, “Quantum simulations with ultracold quantum gases,” *Nat. Phys.* **8** (2012) 267.
- [214] I. Bloch, J. Dalibard, and W. Zwerger, “Many-body physics with ultracold gases,” *Rev. Mod. Phys.* **80** (2008) 885.
- [215] C. Tsallis, “Diagonalization methods for the general bilinear hamiltonian of an assembly of bosons,” *J. Math. Phys.* **19** (1978) 277.
- [216] Wolfram Research, Inc., “Mathematica 11.3,” 2018.
- [217] Y. Tikochinsky, “On the diagonalization of the general quadratic hamiltonian for coupled harmonic oscillators,” *J. Math. Phys.* **20** (1979) 406.
- [218] S. Weinberg, “Photons and Gravitons in  $S$ -Matrix Theory: Derivation of Charge Conservation and Equality of Gravitational and Inertial Mass,” *Phys. Rev.* **135** (1964) B1049.
- [219] A. Strominger, “On BMS Invariance of Gravitational Scattering,” *J. High Energy Phys.* **1407** (2014) 152, [arXiv:1312.2229](#) [hep-th].
- [220] T. He, V. Lysov, P. Mitra, and A. Strominger, “BMS supertranslations and Weinberg’s soft graviton theorem,” *J. High Energy Phys.* **5** (2015) 151, [arXiv:1401.7026](#) [hep-th].

- [221] A. Strominger and A. Zhiboedov, “Gravitational Memory, BMS Supertranslations and Soft Theorems,” *J. High Energy Phys.* **1601** (2016) 86, [arXiv:1411.5745 \[hep-th\]](#).
- [222] S. W. Hawking, “The information paradox for black holes,” [arXiv:1509.01147 \[hep-th\]](#).
- [223] S. W. Hawking, M. J. Perry, and A. Strominger, “Soft Hair on Black Holes,” *Phys. Rev. Lett.* **116** (2016) 231301, [arXiv:1601.00921 \[hep-th\]](#).
- [224] S. W. Hawking, M. J. Perry, and A. Strominger, “Superrotation Charge and Supertranslation Hair on Black Holes,” *J. High Energy Phys.* **1705** (2017) 1, [arXiv:1611.09175 \[hep-th\]](#).
- [225] T. He, P. Mitra, A. P. Porfyriadis, and A. Strominger, “New Symmetries of Massless QED,” *J. High Energy Phys.* **1410** (2014) 112, [arXiv:1407.3789 \[hep-th\]](#).
- [226] A. Mohd, “A note on asymptotic symmetries and soft-photon theorem,” *J. High Energy Phys.* **1502** (2015) 60, [arXiv:1412.5365 \[hep-th\]](#).
- [227] M. Campiglia and A. Laddha, “Asymptotic symmetries of QED and weinberg’s soft photon theorem,” *J. High Energy Phys.* **1506** (2015) 115, [arXiv:1505.05346 \[hep-th\]](#).
- [228] D. Kapec, M. Pate, and A. Strominger, “New Symmetries of QED,” *Adv. Theor. Math. Phys.* **21** (2017) 1769, [arXiv:1506.02906 \[hep-th\]](#).
- [229] M. Mirbabayi and M. Simonović, “Weinberg Soft Theorems from Weinberg Adiabatic Modes,” [arXiv:1602.05196 \[hep-th\]](#).
- [230] A. Strominger, “Lectures on the infrared structure of gravity and gauge theory,” [arXiv:1703.05448 \[hep-th\]](#).
- [231] M. Campiglia and A. Laddha, “Asymptotic symmetries of gravity and soft theorems for massive particles,” *J. High Energy Phys.* **1512** (2015) 1, [arXiv:1509.01406 \[hep-th\]](#).
- [232] M. Mirbabayi and M. Porrati, “Shaving off black hole soft hair,” *Phys. Rev. Lett.* **117** (2016) 211301, [arXiv:1607.03120 \[hep-th\]](#).
- [233] B. Gabai and A. Sever, “Large gauge symmetries and asymptotic states in QED,” *J. High Energy Phys.* **1612** (2016) 95, [arXiv:1607.08599 \[hep-th\]](#).
- [234] C. Gomez and M. Panchenko, “Asymptotic dynamics, large gauge transformations and infrared symmetries,” [arXiv:1608.05630 \[hep-th\]](#).

- [235] R. Bousso and M. Porrati, “Soft hair as a soft wig,” *Class. Quan. Grav.* **34** (2017) 204001, [arXiv:1706.00436 \[hep-th\]](#).
- [236] R. Bousso and M. Porrati, “Observable supertranslations,” *Phys. Rev. D* **96** (2017) 086016, [arXiv:1706.09280 \[hep-th\]](#).
- [237] J. von Neumann, “On infinite direct products,” *Compositio mathematica* **6** (1939) 1.
- [238] A. S. Wightman and S. S. Schweber, “Configuration Space Methods in Relativistic Quantum Field Theory. I,” *Phys. Rev.* **98** (1955) 812.
- [239] M. Ciafaloni, D. Colferai, and G. Veneziano, “Emerging Hawking-like Radiation from Gravitational Bremsstrahlung Beyond the Planck Scale,” *Phys. Rev. Lett.* **115** (2015) 171301, [arXiv:1505.06619 \[hep-th\]](#).
- [240] M. Ciafaloni, D. Colferai, F. Coradeschi, and G. Veneziano, “Unified limiting form of graviton radiation at extreme energies,” *Phys. Rev. D* **93** (2016) 044052, [arXiv:1512.00281 \[hep-th\]](#).
- [241] T. Kinoshita, “Mass Singularities of Feynman Amplitudes,” *J. Math. Phys.* **3** (1962) 650.
- [242] C. Gomez and R. Letschka, “Memory and the Infrared,” *J. High Energy Phys.* **1710** (2017) 10, [arXiv:1704.03395 \[hep-th\]](#).
- [243] M. Panchenko, “The infrared triangle in the context of IR safe S matrices,” [arXiv:1704.03739 \[hep-th\]](#).
- [244] H.-P. Breuer and F. Petruccione, “Destruction of quantum coherence through emission of bremsstrahlung,” *Phys. Rev. A* **63** (2001) 032102.
- [245] G. Calucci, “Loss of coherence due to bremsstrahlung,” *Phys. Rev. A* **67** (2003) 042702.
- [246] G. Calucci, “Graviton emission and loss of coherence,” *Class. Quant. Grav.* **21** (2004) 2339, [arXiv:quant-ph/0312075](#).
- [247] D. Kapec, M. Perry, A.-M. Raclariu, and A. Strominger, “Infrared Divergences in QED, Revisited,” *Phys. Rev. D* **96** (2017) 085002, [arXiv:1705.04311 \[hep-th\]](#).
- [248] S. Choi and R. Akhoury, “BMS Supertranslation Symmetry Implies Faddeev-Kulish Amplitudes,” *J. High Energy Phys.* **1802** (2018) 171, [arXiv:1712.04551 \[hep-th\]](#).

- [249] D. Carney, L. Chaurette, D. Neuenfeld, and G. Semenoff, “On the need for soft dressing,” *J. High Energy Phys.* **9** (2018) 121, [arXiv:1803.02370 \[hep-th\]](#).
- [250] Y. B. Zel’dovich and A. G. Polnarev, “Radiation of gravitational waves by a cluster of superdense stars,” *Sov. Astron.* **18** (1974) 17.
- [251] R. F. Penna, “BMS invariance and the membrane paradigm,” *J. High Energy Phys.* **1603** (2016) 023, [arXiv:1508.06577 \[hep-th\]](#).
- [252] E. E. Flanagan and D. A. Nichols, “Conserved charges of the extended Bondi-Metzner-Sachs algebra,” *Phys. Rev. D* **95** (2017) 044002, [arXiv:1510.03386 \[hep-th\]](#).
- [253] L. Donnay, G. Giribet, H. A. Gonzalez, and M. Pino, “Supertranslations and Superrotations at the Black Hole Horizon,” *Phys. Rev. Lett.* **116** (2016) 091101, [arXiv:1511.08687 \[hep-th\]](#).
- [254] M. Blau and M. O’Loughlin, “Horizon Shells and BMS-like Soldering Transformations,” *J. High Energy Phys.* **1603** (2016) 29, [arXiv:1512.02858 \[hep-th\]](#).
- [255] G. Barnich, C. Troessaert, D. Tempo, and R. Troncoso, “Asymptotically locally flat spacetimes and dynamical nonspherically-symmetric black holes in three dimensions,” *Phys. Rev. D* **93** (2016) 084001, [arXiv:1512.05410 \[hep-th\]](#).
- [256] A. Averin, G. Dvali, C. Gomez, and D. Lüst, “Gravitational Black Hole Hair from Event Horizon Supertranslations,” *J. High Energy Phys.* **1606** (2016) 88, [arXiv:1601.03725 \[hep-th\]](#).
- [257] G. Compère and J. Long, “Vacua of the gravitational field,” *J. High Energy Phys.* **1607** (2016) 137, [arXiv:1601.04958 \[hep-th\]](#).
- [258] G. Compère and J. Long, “Classical static final state of collapse with supertranslation memory,” *Class. Quant. Grav.* **33** (2016) 195001, [arXiv:1602.05197 \[gr-qc\]](#).
- [259] C. Eling and Y. Oz, “On the Membrane Paradigm and Spontaneous Breaking of Horizon BMS Symmetries,” *J. High Energy Phys.* **1607** (2016) 65, [arXiv:1605.00183 \[hep-th\]](#).
- [260] A. Averin, G. Dvali, C. Gomez, and D. Lüst, “Goldstone origin of black hole hair from supertranslations and criticality,” *Mod. Phys. Lett. A* **31** (2016) 1630045, [arXiv:1606.06260 \[hep-th\]](#).

- [261] L. Donnay, G. Giribet, H. A. Gonzalez, and M. Pino, “Extended Symmetries at the Black Hole Horizon,” *J. High Energy Phys.* **1609** (2016) 100, [arXiv:1607.05703 \[hep-th\]](#).
- [262] R.-G. Cai, S.-M. Ruan, and Y.-L. Zhang, “Horizon supertranslation and degenerate black hole solutions,” *J. High Energy Phys.* **1609** (2016) 163, [arXiv:1609.01056 \[gr-qc\]](#).
- [263] S. Hollands, A. Ishibashi, and R. M. Wald, “BMS supertranslations and memory in four and higher dimensions,” *Class. Quant. Grav.* **34** (2016) 155005, [arXiv:1612.03290 \[gr-qc\]](#).
- [264] R. Penrose, “Relativistic Symmetry Groups,” in *NATO Advanced Study Institute – Group theory in non-linear problems Istanbul, Turkey, August 7 - 18, 1972*, p. 1. 1972. In R. Pensore, *Collected Works Volume II*, Oxford University Press.
- [265] P. Hayden and J. Preskill, “Black holes as mirrors: quantum information in random subsystems,” *J. High Energy Phys.* **0709** (2007) 120, [arXiv:0708.4025 \[hep-th\]](#).
- [266] Y. Sekino and L. Susskind, “Fast Scramblers,” *J. High Energy Phys.* **1810** (2008) 065, [arXiv:0808.2096 \[hep-th\]](#).
- [267] G. Dvali, “Classicalization Clearly: Quantum Transition into States of Maximal Memory Storage Capacity,” [arXiv:1804.06154 \[hep-th\]](#).
- [268] C. Gomez and R. Letschka, “Masses and electric charges: gauge anomalies and anomalous thresholds,” [arXiv:1903.01311 \[hep-th\]](#).
- [269] E. H. Lieb and W. Liniger, “Exact Analysis of an Interacting Bose Gas. I. The General Solution and the Ground State,” *Phys. Rev.* **130** (1963) 1605.
- [270] E. H. Lieb, “Exact Analysis of an Interacting Bose Gas. II. The Excitation Spectrum,” *Phys. Rev.* **130** (1963) 1616.
- [271] M. Panchenko, “The Lieb-Liniger model at the critical point as toy model for Black Holes,” [arXiv:1510.04535 \[hep-th\]](#).
- [272] M. P. Hobson, G. P. Efstathiou, and A. N. Lasenby, *General Relativity: An Introduction for Physicists*. Cambridge University Press, 2006.

# Acknowledgments

My first and foremost thanks go to Gia Dvali for the outstanding guidance, support and supervision that he has provided over the past years. I am indebted to him for giving me the opportunity to constantly explore new exciting topics and for countless discussions in which he shared his deep knowledge and intuition with me.

I am very grateful to Cesar Gomez for his generous advice and support as well as for initiating inspiring projects. It has been a great pleasure to profit from his manifold knowledge and to learn from him about some of the milestones of physics.

Many thanks go out to all my collaborators: Gia Dvali, Cesar Gomez, Marco Michel, Raoul Letschka and Lukas Eisemann. I am grateful to them for countless insights, intense collaborations and great projects.

Moreover, I am obliged to all former and current colleagues in our group for stimulating discussions on manifold topics, in particular Artem Averin, Lasha Berezhiani, Jaba Chelidze, Lukas Eisemann, Daniel Flassig, Lena Funcke, Andrea Giugno, Andrea Giusti, Lukas Gründing, Alexander Gußmann, Alexis Helou, Georgios Karananas, Marco Michel, Mischa Panchenko, Tehseen Rug, Otari Sakhelashvili, Debajyoti Sarkar, Dimitris Skliros, Max Warkentin, Nico Wintergerst and Michael Zantedeschi. Furthermore, I want to thank Henk Bart for many interesting conversations and especially for very helpful feedback on my talks.

A special word of gratitude is due to all who have supported me in finding my postdoc position, in particular Gia Dvali, Cesar Gomez and Gerhard Buchalla. Moreover, I am grateful to Lena Funcke, Claudius Krause, Alex Millar, Georg Raffelt and Nico Wintergerst for various help with my application material.

I wish to thank Roberto Emparan, Cesar Gomez, Arthur Hebecker, Jean-Luc Lehnert, Tomislav Prokopec, Antonio Riotto, Misha Shaposhnikov and Andreas Weiler for inviting me to visit their institutes and for sharing manifold valuable feedback.

It is a pleasure to thank Lena Funcke, Georgios Karananas, Marco Michel and especially Lukas Nickel for proofreading my thesis and related help. Furthermore, I am grateful to Georg Raffelt and Jochen Weller for agreeing to be on my PhD committee.

I would like to express my gratitude to Gabi Bodenmüller, Corinna Brunnlechner, Karin Gebhardt, Monika Goldammer, Frank Steffen and Herta Wiesbeck-

Yonis for helping me to overcome various bureaucratic hurdles.

Finally, I am indebted to Andreas Bluhm, Lukas Nickel and Simone Rademacher for their support and many discussions about (careers in) physics.

The final lines of this thesis are dedicated to my parents and my partner Alexandra. I owe my deepest gratitude to you for what words cannot describe and more.